INSTITUTO POTOSINO DE INVESTIGACIÓN CIENTÍFICA Y TECNOLÓGICA, A.C.

POSGRADO EN CIENCIAS AMBIENTALES

Critical factors to increase hydrogen production in continuous dark fermentation reactors

Tesis que presenta

José de Jesús Montoya Rosales

Para obtener el grado de

Doctor en Ciencias Ambientales

Director de la Tesis:

Dr. Elías Razo Flores

San Luis Potosí, S.L.P., agosto de 2022

Constancia de aprobación de la tesis

La tesis "**Critical factors to increase hydrogen production in continuous dark fermentation reactors**" presentada para obtener el Grado de Doctor en Ciencias Ambientales fue elaborada por **(José de Jesús Montoya Rosales)** y aprobada el **29 de agosto de 2022** por los suscritos, designados por el Colegio de Profesores de la División de Ciencias Ambientales del Instituto Potosino de Investigación Científica y Tecnológica, A.C.

_____

Dr. Elías Razo Flores
Director de la tesis

_____

Dra. María de Lourdes Berenice Celis García
Miembro del Comité Tutoral

_____

Dra. Claudia Etchebehere Arenas
Miembro del Comité Tutoral

_____

Dr. Vladimir Alonso Escobar Barrios
Miembro del Comité Tutoral

_____

Dr. Luis Felipe Cházaro Ruíz
Miembro del Comité Tutoral

Créditos Institucionales

Esta tesis fue elaborada en los Laboratorios de la División de Ciencias Ambientales del Instituto Potosino de Investigación Científica y Tecnológica, A.C., bajo la dirección del Dr. Elías Razo Flores.

Durante la realización del trabajo el autor recibió una beca académica del Consejo Nacional de Ciencia y Tecnología (785155) y del Instituto Potosino de Investigación Científica y Tecnológica, A. C.

Este trabajo de investigación fue financiado por el Fondo Sectorial de Investigación para la Educación SEP-CONACYT, proyecto “Barreras inhibitorias y termodinámicas de la producción de hidrógeno: Fermentación extractiva como estrategia para mejorar su producción”, A1-S-37174, cuyo responsable técnico es el Dr. Elías Razo Flores.

IPICYT

Instituto Potosino de Investigación Científica y Tecnológica, A.C.

Acta de Examen de Grado

La Secretaria Académica del Instituto Potosino de Investigación Científica y Tecnológica, A.C., certifica que en el Acta 034 del Libro Primero de Actas de Exámenes de Grado del Programa de Doctorado en Ciencias Ambientales está asentado lo siguiente:

En la ciudad de San Luis Potosí a los 29 días del mes de agosto del año 2022, se reunió a las 09:00 horas en las instalaciones del Instituto Potosino de Investigación Científica y Tecnológica, A.C., el Jurado integrado por:

Dr. Vladimir Alonso Escobar Barrios	**Presidente**	**IPICYT**
Dra. María de Lourdes Berenice Celis García	**Secretaria**	**IPICYT**
Dr. Claudia Etchebehere Arenas	**Sinodal externo**	**IIBCE**
Dr. Elías Razo Flores	**Sinodal**	**IPICYT**
Dr. Luis Felipe Cházaro Ruiz	**Sinodal**	**IPICYT**

a fin de efectuar el examen, que para obtener el Grado de:

DOCTOR EN CIENCIAS AMBIENTALES

sustentó el C.

José de Jesús Montoya Rosales

sobre la Tesis intitulada:

Critical factors to increase hydrogen production in continuous dark fermentation reactors

que se desarrolló bajo la dirección de

Dr. Elías Razo Flores

El Jurado, después de deliberar, determinó

APROBARLO

Dándose por terminado el acto a las 12:20 horas, procediendo a la firma del Acta los integrantes del Jurado. Dando fe la Secretaria Académica del Instituto.

A petición del interesado y para los fines que al mismo convengan, se extiende el presente documento en la ciudad de San Luis Potosí, S.L.P., México, a los 29 días del mes de agosto de 2022.

Dra. Lina Raquel Riego Ruiz
Secretaria Académica

Mtra. Ivonne Lizette Cuevas Vélez
Jefa del Departamento del Posgrado

IPICYT
SECRETARÍA ACADÉMICA
INSTITUTO POTOSINO DE
INVESTIGACIÓN CIENTÍFICA

Dedicatorias

Dedico el presento trabajo con todo mi cariño y admiración

A mis padres, hermanas, cuñados, sobrinos, sobrina y familiares cercanos, por motivarme y nunca dejarme solo en esta aventura.

A mis “antiguos amigos” y a los “nuevos amigos” que conocí durante esta etapa de mi vida, y que fueron un gran motor de apoyo y aliento para seguir adelante.

A todas aquellas personas que de una forma u otra me apoyaron y confiaron en mí.

Keep going

Agradecimientos

A mi director de tesis el Dr. Elías Razo, por haber creído en mí, por sus conocimientos, orientaciones, consejos y su guía que han sido fundamentales para mi formación.

A la Dra. Berenice Celis, por su invaluable apoyo y consejos en el desarrollo de este trabajo. Gracias por su paciencia, dirección y orientación.

A la Dra. Claudia Etchebehere, al Dr. Felipe Cházaro y al Dr. Vladimir Escobar, por enseñarme, aconsejarme e instruirme en el camino del buen estudiante, por darme su apoyo y su comprensión durante este trabajo.

Al M. en C. Guillermo Vidriales, al M. en C. Juan Pablo Rodas, a la Dra. Elizabeth Isaacs y a la M. en C. Ma. Carmen Rocha por su apoyo técnico y admistrativo durante la realización de este proyecto. Asímismo, agradezco al Dr. Diego Esquivel por su apoyo experto en temas de metatranscriptómica.

Al Dr. Rodolfo Palomo, por sus consejos, paciencia, disposición y motivación para trabajar. Gracias por tu amistad y por compartir tus conocimientos conmigo.

A la Dra. Aura Ontiveros, por su apoyo experto para discutir y enriquecer distintas partes de este trabajo.

Al grupo de trabajo del Dr. Elías Razo actual y a aquellos miembros que coincidieron durante mis estudios doctorales, por sus importantes aportaciones, apoyo en experimentos y análisis fundamentales para desarrollar este trabajo.

Table of contents

Constancia de aprobación de la tesis ii

Créditos institucionales iii

Acta de examen iv

Dedicatorias v

Agradecimientos vi

List of tables xii

List of figures xiv

Abreviaturas xix

Resumen xx

Abstract xxi

Chapter 1. Dark fermentative hydrogen production: state of art in continuous stirred tank reactors

1.1 Introduction 2

1.2 Basics of dark fermentation 3

1.3 Dark fermentation in continuous systems 5

1.4 Basics of the type of inhibition that can occur in dark fermentation process 9

1.5 Challenges in continuous dark fermentation process 11

1.5.1 Organic loading rate 12

1.5.2 Biomass concentration 13

1.5.3 Mass transfer conditions in a CSTR 14

1.5.4 Metabolic diversity 16

1.5.4.1 Homoacetogenesis 17

1.5.4.2 Lactic acid fermentation 18

1.6 Molecular tools for the understanding of the dark fermentation process 19

1.6.1 Microbial community diversity: Next Generation Sequencing 20

1.6.2 Microbial quantification: Quantitative-PCR 21

1.6.3 Microbial function: Metatranscriptomics 22

1.7 Scope of the thesis, hypothesis, objectives and structure of the thesis 23

Hypothesis 23

General objective 23

Specific objectives 24

Structure of the thesis 24

1.8 References 25

Chapter 2. The increase of biomass in suspended-biomass reactor as a strategy to improve the production of hydrogen and carboxylic acids

2.1 Abstract 31

2.2 Introduction 31

2.3 Materials and methods 33

2.3.1 Inoculum and substrate 33

2.3.2 Experimental setup 33

2.3.3 Analytical methods 35

2.3.4 Microbial community analysis 35

2.3.5 Calculations 36

2.3.6 Pearson's correlations 36

2.4 Results and discussion 37

2.4.1 The performance of dark fermentation is driven by the biomass concentration 37

2.4.2 The increase of biomass concentration stimulates acetate and butyrate pathways 40

2.4.3 Microbial community analysis 45

2.4.4 Implications of the discontinuous biomass recovery and recycling strategy. 48

2.5 Conclusions 49

2.6 References 49

Chapter 3. Two-phase partition reactor as a strategy to improve the productivity of dark fermentation systems

3.1 Abstract 54

3.2 Introduction 54

3.3 Materials and methods 56

3.3.1 Substrate, inoculum, mineral medium, and organic phase 56

3.3.2 Dark fermentation batch experiments 57

3.3.3 Dark fermentation continuous experiments 58

3.3.4 Microbial community analysis 59

3.3.5 Partition coefficients evaluation 59

3.3.6 Analytical methods 60

3.3.7 Calculations 60

3.3.8 Statistical analysis 61

3.4 Results and discussion 62

3.4.1 Partition coefficients relevant for H_2 and CO_2 extraction 62

3.4.2 Batch dark fermentation experiments 63

3.4.3 Continuous dark fermentation experiments 71

3.4.4 Analysis of microbial communities 74

3.4.5 H_2 and CO_2 transfer model in the two-phase partitioning bioreactor 76

3.4.6 Implications of the presence of an extractive organic phase in dark fermentation 77

3.5 Conclusions 80

3.6 References 81

Chapter 4. Microbial community structure and function in two-phase partitioning dark fermentation reactors at high organic loading rate

4.1 Abstract 85

4.2 Introduction 85

4.3 Materials and methods 87

4.3.1 Inoculum, fermentation medium, substrate, and organic phase 87

4.3.2 Bioreactors set-up and operational conditions 88
4.3.3 Analytical methods 89
4.3.4 DNA extraction and quantification of fthfs and hydA genes by qPCR 89
4.3.5 RNA extraction and transcriptome sequencing and metatranscriptome analysis 90
4.3.6 Multivariate analysis 92
4.4 Results and discussion 92
4.4.1 Dark fermentation performance 92
4.4.2 Community structure by transcriptomics 96
4.4.3 Community function by qPCR functional genes hydA and fthfs: the abundance of H_2-producing bacteria and homoacetogens 97
4.4.3.1The OLR in the prevalence of homoacetogens and H_2-producing bacteria 99
4.4.3.2 Abundance of homoacetogens and H_2-producing bacteria in two-phase partitioning reactors 101
4.4.4 Community function as analyzed by transcriptomics 101
4.5 References 113

Chapter 5. Analysis of microbial communities in continuous reactors feed with enzymatic hydrolysates.

5.1 Abstract 118
5.2 Introduction 118
5.3 Materials and methods 120
5.3.1 H_2-producing systems (source of DNA samples) 120
5.3.2 Inoculum 125
5.3.3 Agave bagasse and enzymatic hydrolysis 125
5.3.4 Analytical methods 126
5.3.5 Illumina sequencing and microbial community analysis 127
5.4 Results and discussion 127
5.4.1 Overall analysis of H_2 production from enzymatic hydrolysates of agave bagasse 127
5.4.2 Dark fermentative microbial communities and their underlying common structure 129

5.4.3 The reactor configuration as a main factor shaping microbial communities: composition and diversity 134

5.4.4 The type of hydrolysate drives the composition and diversity of microbial communities 137

5.4.5 Microbial diversity as explanatory factor of H_2 production performance 139

5.4.6 High performance H_2 production and microbial communities: final remarks 143

5.5 Conclusions 144

5.6 References 145

Chapter 6. General discussion, conclusions, and perspectives

6.1 General discussion and conclusions 149

6.2 Perspectives 154

6.3 References 156

About the author 159

List of tables

Table 1.1 Recap of steady-state hydrogen production in diverse type of reactors investigated by our group research. 5

Table 2.1 Summary of steady-states in the hydrogen production in a continuous reactor at different organic loading rates and biomass concentrations. 38

Table 2.2 Carboxylic acids produced in different configurations of continuous mesophilic reactors. 43

Table 2.3 Solids retention time values in the stages with biomass increase in the suspended-biomass reactor. 48

Table 3.1. Dimensionless partition coefficient (H) for H_2 and CO_2 in silicone oil and mineral medium. H was calculated as the ratio between the gas concentration in the gaseous and aqueous phase in the equilibrium. 62

Table 3.2. Hydrogen produced in the batch experiments (AMPTS II + H_2 desorbed from the organic phase) and kinetic parameters from the modified Gompertz modeling. 64

Table 3.3. Experimental concentrations in each batch experiments. 68

Table 3.4. COD mass balances in the batch experiments. 69

Table 3.5. Experimental concentrations in each steady state of the CSTR operation. 73

Table 3.6. COD mass balances in each steady state of the CSTR operation. 73

Table 3.7. Total hydrogen produced in the continuous experiments using silicone oil at a proportion 10% (v/v) as extractive organic phase. 74

Table 3.8 Stoichiometric reactions and Gibbs free energy values from the CSTR operation. 78

Table 3.9. Different Gibbs free energy calculated from the overall reactions reported in the Table 3.8. 79

Table 4.1. Primer Sets and Protocols Used for qPCR analyses. 90

Table 4.2. Performance of the three CSTR systems operated at different operational conditions. 95

Table 5.1. List of steady states used for the analysis of microbial communities developed during H_2 production from enzymatic hydrolysates of agave bagasse. Data was gathered from Montoya-Rosales et al. [15] and Valencia-Ojeda et al. [16]. 122

Table 5.2. Characteristics of the enzymatic hydrolysates. 126

Table 5.3. Shannon indexes and Gini coefficients of microbial communities in systems fed with enzymatic hydrolysates of agave bagasse. 141

List of figures

Figure 1.1 Metabolic pathways on the dark fermentation process. Where NFOR, is the pathway related to the enzyme NADH-Fd hydrogenase; PFOR, is the metabolic via utilized by pyruvate ferredoxin oxidoreductase enzyme. Modified from Gopalakrishnan et al., [4] 4

Figure 1.2 Summary of several issues/challenges for dark fermentation in continuous systems. 12

Figure 1.3 The H_2 mass transfer mechanism from liquid to gas phase. The molecules of H_2 or CO_2 diffuse in the liquid from high to low concentration, described by the global mass transfer rate (Q). In the interphase liquid-gas is observed an equilibrium according the Henry's law equation. 15

Figure 2.1 CSTR scheme. A) Inlet pump, B) Gas meter, C) Gas sampling port, D) Stirrer, E) redox electrode, F) pH electrode, G) Temperature sensor, H) Controller, I) Thermal jack, J) 5M NaOH pump, K) outlet pump. 34

Figure 2.2 Performance of the CSTR under different operational conditions. In stages I[a] and II[b] the loss of biomass was measured at an OLR of 90 g TC/L-d. Stages with discontinuous biomass increase: II, IV, VI, VII and VIII. VHPR: volumetric hydrogen production rate. See Table 2.1 for operational conditions under each stage. 38

Figure 2.3 Relationship between the biomass concentration and the volumetric hydrogen production rate at the steady-states with different organic loading rates. TC: total carbohydrates. 39

Figure 2.4 Concentration of the carboxylic acids produced with different organic loading rates and biomass concentrations in the CSTR. [a]=double and [b]=triple of biomass concentration than the observed in the periods without biomass recycling (*). TC: total carbohydrates. For each case, samples from the respective steady-states were considered. 41

Figure 2.5 Microbial community dynamics of the continuous stirred-tank reactor during stages I to VIII. Genera with relative abundance <1% were grouped as others. 45

Figure 2.6 Matrix of Pearson's correlations ($p < 0.05$). OLR: organic loading rate (g TC/L-d); biomass concentration (g VSS/L); sOLR: specific organic loading rate (g COD/g VSS-d); VHPR: volumetric hydrogen production rate (L H_2/L-d); H_2 yield (mol H_2/mol hexose); acetate, lactate and butyrate (mol/total moles of carboxylic acids); microorganisms were analyzed in terms of their relative abundance. COD: chemical oxygen demand; VSS: volatile suspended solids. TC: total carbohydrates. 47

Figure 3.1 Cumulative hydrogen production in the batch assays using cheese whey powder (CWP) as the substrate and silicone oil as the extractive organic phase. CWP control (■), CWP - silicone oil 2.5% (v/v) (♦), CWP - silicone oil 63

5% (v/v) (•), CWP - silicone oil 10% (v/v) (O), CWP - silicone oil 20% (v/v) (□), CWP - silicone oil 30% (v/v) (▲).

Figure 3.2 Concentration of the carboxylic acids produced in batch experiments with different proportions of silicone oil and cheese whey powder (CWP) as substrate. 67

Figure 3.3 Effect of silicone oil in continuous dark fermentation experiments added at a proportion of 10% (v/v), using cheese whey powder at an OLR of 60 g TC/L-d and 138 g TC/L-d. A) Volumetric hydrogen production rate (VHPR) and H_2 yield. B) Concentration of carboxylic acids. TC: total carbohydrates. *Stages with silicone oil. 71

Figure 3.4 Relative abundances of the microbial communities at the genus level in the continuous experiments. *Silicone oil added at a proportion of 10% (v/v). 75

Figure 3.5 Proposed mass transfer model according to the film theory. 1. Convective transport through the bulk liquid to the proximity of the gas phase and silicone oil micelles. 2. Fick's diffusion through the relatively stagnant liquid film surrounding the gas phase and silicone oil micelles. 3. Equilibrium across the interfaces (aqueous-gas and aqueous-silicone oil.). 4. Fick's diffusion through the relatively stagnant liquid film surrounding the liquid phase. 5. Convective transport from the interphases to the interior of bulk gas and the interior of silicone oil micelles. 5-9. Transport of H_2 and CO_2 absorbed in the silicone oil to the gas phase. 76

Figure 4.1 Relative abundances of the microbial communities at the species taxonomic level in CSTRs 1-3. *Silicone oil added at a proportion of 10% (v/v). 97

Figure 4.2 Correlations between the hydA gene and the fthfs gene along the VHPR (panels A and B), H2 yield (panels C and D), and the correlation of both genes (E). The circles with hatching correspond to stages with supplementation of silicone oil. 98

Figure 4.3 VHPR and abundance of *fthfs* and *hydA* gene at different OLRs (A, C, E) and for stages with and with no addition of silicone oil (B, D, F). *Silicone oil added (10 % v/v). 100

Figure 4.4 Abundance of the GO related to production of H_2, CO_2, Acetate via Wood-Ljungdahl, Acetate via pyruvate fermentation, lactate, formate, and butyrate at different organic loading rates (OLR). GO:0008861 (pyruvate formate lyase activity); GO:0008863 (formate dehydrogenase); GO:0008901(hydrogenase activity); GO:0008137 (hycE activity); GO:0004459 (lactate dehydrogenase activity); GO:0019164 (pyruvate ferredoxin oxidoreductase activity); GO:0008959 (phosphate acetyltransferase activity); GO:0008776 (acetate kinase activity). * lactate dehydrogenase activity for *Clostridium* species. ** lactate dehydrogenase activity for lactic acid bacteria. The color gradient form white to red indicates the relative expression level log2 changes at different OLR. 103

Figure 4.4 (Continued). Abundance of the GO related to production of H_2, CO_2, Acetate via Wood-Ljungdahl, Acetate via pyruvate fermentation, lactate, formate, and butyrate at different organic loading rates (OLR). GO:0003985 (acetyl-CoA C-acetyltransferase activity); GO:0008691 (3-hydroxybutyryl-CoA dehydrogenase activity); GO:0004300 (enoyl-CoA hydratase activity); GO:0016628 (N.D); GO:0050182 (phosphate butyryltransferase activity); GO:0047761 (butyrate kinase activity); GO:0008775 (acetate CoA-transferase activity). The color gradient form white to red indicates the relative expression level log2 changes at different OLR. 104

Figure 4.4 (Continued). Abundance of the GO related to production of H_2, CO_2, Acetate via Wood-Ljungdahl, Acetate via pyruvate fermentation, lactate, formate, and butyrate at different organic loading rates (OLR).GO:0008863 (formate dehydrogenase); GO:0004329 (formate-tetrahydrofolate synthetase activity); GO:0004477 (methenyltetrahydrofolate cyclohydrolase activity); GO:0004488 (methylenetetrahydrofolate dehydrogenase (NADP+) activity); GO:0004489 (methylenetetrahydrofolate reductase (NAD(P)H) activity); GO:0018492 (carbon-monoxide dehydrogenase (acceptor) activity); GO:0043884 (CO-methylating acetyl-CoA synthase activity); GO:0008776 (acetate kinase activity). The color gradient form white to red indicates the relative expression level log2 changes at different OLR. 105

Figure 4.5 Abundance of the GO related to production of H_2, CO_2, Acetate via Wood-Ljungdahl, Acetate via pyruvate fermentation, lactate, formate, and butyrate in continuous dark fermentation experiments. GO:0008861 (pyruvate formate lyase activity); GO:0008863 (formate dehydrogenase); GO:0008901(hydrogenase activity); GO:0008137 (hycE activity); GO:0004459 (lactate dehydrogenase activity); GO:0019164 (pyruvate ferredoxin oxidoreductase activity); GO:0008959 (phosphate acetyltransferase activity); GO:0008776 (acetate kinase activity). * Stages with silicone added at a proportion 10 % (v/v). The color gradient form white to red indicates the relative expression level log2 changes. 106

Figure 4.5 (Continued). Abundance of the GO related to production of H_2, CO_2, Acetate via Wood-Ljungdahl, Acetate via pyruvate fermentation, lactate, formate, and butyrate in continuous dark fermentation experiments. GO:0003985 (acetyl-CoA C-acetyltransferase activity); GO:0008691 (3-hydroxybutyryl-CoA dehydrogenase activity); GO:0004300 (enoyl-CoA hydratase activity); GO:0016628 (N.D); GO:0050182 (phosphate butyryltransferase activity); GO:0047761 (butyrate kinase activity); GO:0008775 (acetate CoA-transferase activity). * Stages with silicone added at a proportion 10 % (v/v). The color gradient form white to red indicates the relative expression level log2 changes. 107

Figure 4.5 (Continued). Abundance of the GO related to production of H_2, CO_2, Acetate via Wood-Ljungdahl, Acetate via pyruvate fermentation, lactate, formate, and butyrate in continuous dark fermentation experiments. GO:0008863 (formate dehydrogenase); GO:0004329 (formate-tetrahydrofolate synthetase activity); GO:0004477 (methenyltetrahydrofolate cyclohydrolase activity); GO:0004488 (methylenetetrahydrofolate dehydrogenase (NADP+) activity); GO:0004489 (methylenetetrahydrofolate reductase (NAD(P)H) 108

activity); GO:0018492 (carbon-monoxide dehydrogenase (acceptor) activity); GO:0043884 (CO-methylating acetyl-CoA synthase activity); GO:0008776 (acetate kinase activity). * Stages with silicone added at a proportion 10 % (v/v). The color gradient form white to red indicates the relative expression level log2.

Figure 4.6 Effect of the different OLR on the gene expression of key dark fermentation GO. The color gradient form white to red indicates the relative expression level log2 changes at different OLR. 110

Figure 4.7 Effect of the addition of silicone oil on the gene expression of key dark fermentation GO. The color gradient form white to red indicates the relative expression level log2 changes at different OLR. 111

Figure 4.8 Pearson's correlations ($p < 0.05$). OLR in g TC/L-d; VHPR in L H_2/L-d; H_2 yield in mol H_2/ mol hexose; acetate, lactate, and butyrate in mol/total moles of carboxylic acids); A/B (acetate to butyrate ratio); *pfl (*pyruvate formate lyase), *pfor* (pyruvate ferredoxin oxidoreductase), lactate dehydrogenase-LAB, lactate dehydrogenase-*Clostridium*, *fthfs (*formyl tetrahydrofolate synthetase) were analyzed in terms of their GO relative transcript abundance; qPCR-*hydA* and qPCR-*fthfs* (copies number/ng DNA); microorganisms were analyzed in terms of their relative abundance. TC: total carbohydrates. 112

Figure 5.1 Hydrogen production from different hydrolysates of agave bagasse. A) volumetric H_2 production rate (VHPR); B) H_2 yield. The dashed lines represent linear regression models, while the shaded area stands for the 95% confidence intervals. Data was gathered from Montoya-Rosales et al. and Valencia-Ojeda et al. [15,16]. 128

Figure 5.2 Structure and dynamics of H_2-producing microbial communities by using two different reactor configurations (i.e., CSTR and TBR) and four different types of hydrolysates. A) Microbial community structure depicted by an annotated heatmap. B) Non-metric multidimensional analysis (NMDS). C) Principal components analysis (PCA). 131

Figure 5.3 Pairwise Pearson's correlation analysis on H_2 production performance and microbial communities for systems fed with enzymatic hydrolysates of agave bagasse. Only significant correlations at $p<0.05$ are displayed. VHPR. Volumetric H_2 production rate; S.: substrate; OLR: organic loading rate. 134

Figure 5.4 Composition of microbial communities in CSTR and TBR systems fed with two different hydrolysates of agave bagasse. Batch 24h refers to the onset of continuous operation. Bars corresponds to relative abundance whereas circles to Shannon index. See Table 5.1 for details of reactors operational conditions. 135

Figure 5.5 Composition of microbial communities developed in CSTR systems fed with four types of hydrolysates of agave bagasse. Batch 24h refers to the onset of continuous operation. Bars corresponds to relative abundance whereas circles to Shannon index. See Table 5.1 for details of reactors operational conditions. 137

Figure 5.6 Box-plot of main microbial genera in H_2-producing systems fed with hydrolysates of agave bagasse. Microbial communities were classified as function of the achieved VHPR. The dashed line stands for the average Shannon index, while the shadow stands for ±1 standard deviation. 140

Figure 5.7 Regression analysis on the relationship between microbial diversity (assessed through the Shannon index) and H_2 production performance. Axis *Y* is shown as *ln* transformed to better represent the linear regression. The solid line represents the fitted $VHPR = e^{3.02 - 1.35 * \text{Shannon}}$ (r^2=0.57, p<0.05), while the shaded area stands for the 95% confidence intervals. The blue and red dashed lines represent the regression models for TBR (r^2=0.26) and CSTR (r^2=0.38) systems, respectively. 143

Figure 6.1 Overview of the principal results and conclusions obtained in this investigation. 149

Abreviaturas

CO_2	Carbon dioxide
COD	Chemical oxygen demand
CWP	Cheese whey powder
CSTR	Continuous stirred tank reactor
DNA	Deoxyribonucleic acid
GO	Gene Ontology
H_2	Hydrogen
HRT	Hydraulic retention time
NGS	Next generation sequencing
NADH	Nicotinamide adenine dinucleotide
OLR	Organic loading rate
PCR	Polymerase chain reaction
PFOR	Pyruvate ferredoxin oxidoreductase
PFL	Pyruvate formate lyase
qPCR	Quantitative polymerase chain reaction
RNA	Ribonucleic acid
SRT	Solids retention time
sOLR	Specific organic loading rate
TC	Total carbohydrates
TSS	Total suspended solids
TBR	Trickling bed reactor
VSS	Volatile suspended solids
VHPR	Volumetric hydrogen production rate

Resumen

Factores críticos en la fermentación oscura para incrementar la producción de hidrógeno en reactores continuos

Palabras clave: biohidrógeno, diversidad microbiana, transferencia de masa, concentración de biomasa

Actualmente la fermentación oscura es el método biológico más investigado para la producción de gas hidrógeno (H_2). Este proceso lo realizan microorganismos anaerobios y facultativos que catalizan sustratos con alto contenido de carbohidratos en H_2, CO_2 y ácidos carboxílicos. En procesos continuos, la fermentación oscura es estable y con altas productividades, particularmente en reactores de biomasa suspendida. Sin embargo, los rendimientos de H_2 reportados en la literatura son lejanos a los valores teóricos (4 mol H_2/mol hexosa). Recientemente, el tipo y concentración de sustrato, la concentración de biomasa y las condiciones de transferencia de masa han sido identificados como los parámetros operacionales clave para controlar y mejorar los rendimientos de la fermentación oscura en reactores de biomasa suspendida. Por lo tanto, en esta tesis se estudió el efecto de dichos parámetros operacionales en las comunidades microbianas, las vías metabólicas y el rendimiento general de la fermentación oscura.

Se demostró que la carga orgánica volumétrica (COV) en reactores continuos de tanque agitado alimentados con suero de leche, se relaciona directamente con la producción de H_2 a valores $\leq$ 138 g azúcares totales (AT)/L-d, y a su vez controla la composición de las comunidades microbianas de la fermentación oscura. Con COV < 90 g AT/L-d las bacterias productoras de H_2 del género *Clostridium* dominaron la comunidad microbiana en los reactores. Por otro lado a COV $\geq$ 138 g AT/L-d las bacterias ácido lácticas (LAB) surgieron como un género co-dominante con una relación máxima de abundancia de aproximadamente el 50%. En el mismo sentido, el análisis de secuenciación de seis reactores alimentados con diferentes hidrolizados enzimáticos de bagazo de agave a COV entre 10 a 65 g AT/L-d revelaron que los sistemas de producción de H_2 de alto y medio rendimiento estaban co-dominados por los géneros *Clostridium* y LAB (*Sporolactobacillus*).

Una de las limitaciones de los sistemas de biomasa suspendida es la dificultad de mantener una alta concentración de biomasa con un tiempo de retención hidráulico bajo (6 h) y una COV alta. En esta tesis, el aumento discontinuo de la concentración de biomasa mejoró con éxito la producción de H_2 y de ácidos carboxílicos a COV entre 90 y 160 g AT/L-d. En particular, se alcanzó una máxima producción de 30.8 L H_2/L-d en la COV de 138 g AT/L-d con una concentración de biomasa de 15 g de sólidos suspendidos volátiles/L.

Finalmente, se evaluaron reactores de partición bifásica utilizando aceite de silicona como fase orgánica extractiva, con el objetivo de reducir la concentración de H_2 y CO_2 en el medio de fermentación. Los resultados demostraron que la adición del aceite de silicona mejora la productividad del H_2 y de los ácidos carboxílicos en COV de 60 a 160 g AT/L-d. De estos resultados, se sugiere que la fase orgánica extractiva aumenta el área de transferencia de masa global en el reactor, causando una reducción dramática en la concentración de H_2 y CO_2 en el medio de fermentación, mejorando las vías metabólicas con mayor rendimiento de la fermentación oscura. El análisis metatranscriptómico confirmó que la adición de aceite de silicona en las COV de 138 y 160 g AT/L-d mejora la cantidad y abundancia de transcritos de los genes relacionados con la producción de H_2, acetato y butirato.

En general, se demostró que el incremento de biomasa y el uso de reactores bifásicos son estrategias efectivas y novedosas para aumentar el rendimiento de los sistemas de fermentación oscura operados a altas COV.

Abstract

Critical factors to increase hydrogen production in continuous dark fermentation reactors

Keywords: biohydrogen, microbial diversity, mass transfer, biomass concentration

The dark fermentation is currently the biological method most investigated for hydrogen (H_2) gas production, it is carried out by strict-anaerobes and facultative microorganisms that catabolize carbohydrate-rich substrates into H_2, CO_2 and carboxylic acids. In continuous processes, dark fermentative H_2 production has demonstrated to be steady and favorably productive, especially in suspended-growth reactors. Nevertheless, the reported H_2 yields stay distant from theoretical values. Recently, substrate type and concentration, biomass concentration and mass transfer conditions have been identified as key operational parameters to control and improve dark fermentation performances in suspended-growth reactors. Therefore, the aim of this thesis was to study the effect of these operational parameters on microbial communities, metabolic pathways and overall dark fermentation performance.

It was demonstrated that the organic loading (OLR). in systems fed with cheese whey powder, was directly linked to the H_2 productivity at $\leq$ OLR 138 g total carbohydrates (TC)/L-d and in turn performs a selection pressure upon the microbial community. At OLR < 90 g TC/L-d, H_2-producing bacteria from the genera *Clostridium* clearly dominates the microbial community in the systems. In contrast, at the OLR $\geq$ 138 g TC/L-d lactic acid bacteria (LAB) arose as a co-dominant genus with a maximum relative of abundance of approximately 50%. Similarly, the high-throughput sequencing analysis of six reactors fed with different enzymatic hydrolysates of agave bagasse at OLR between 10 and 65 g TC/L-d, revealed that high-performance and medium-performance H_2-producing systems were both co-dominated by *Clostridium* and LAB (*Sporolactobacillus*) genera.

One of the limitations in the suspended-growth reactors is the difficult to maintain high biomass concentration at low hydraulic retention times (6 h) and high OLR. In this thesis, the discontinuous increase of biomass concentration successfully enhanced the production of H_2 and carboxylic acids at OLR ranging from 90 to 160 g TC/L-d. In particular, a maximum H_2 production rate of 30.8 L H_2/L-d was reached at an OLR of 138 g TC/L-d with a biomass concentration of 15 g volatile suspended solids/L.

Two-phase partitioning reactors using silicone oil as an organic extractive phase, were assessed with the objective to reduce the concentration of H_2 and CO_2 in the fermentation broth. The results demonstrated that the addition of the silicone oil improves the H_2 and carboxylic acids productivity at OLR (from 60 to 160 g TC/L-d). It was hypothesized, that the organic extractive phase increases the global mass transfer area in the reactor, causing a dramatic reduction in the concentration of H_2 and CO_2 in the fermentation broth, enhancing the metabolic pathways with highest dark fermentation performance. The meta-transcriptomic analysis indeed confirms that the addition of silicone oil at both OLR of 138 and 160 g TC/L-d improves the quantity and transcripts abundance of genes related to the production of H_2, acetate and butyrate.

Overall, this thesis demonstrated that biomass augmentation and the use of two-phase partitioning reactors are effective and novel strategies to increase the performance of dark fermentation systems operated at high OLRs.

Chapter 1. *Dark fermentative hydrogen production: state of art in continuous stirred tank reactors*

Graphical abstract

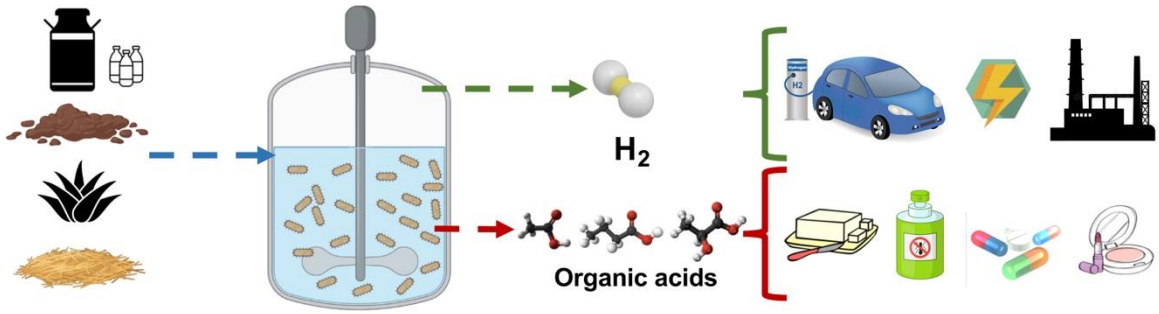

Highlights

- Dark fermentation is the most studied biotechnology to produce bioH_2.
- High concentrations of substrate and the accumulation of H_2, CO_2, and carboxylic acids can inhibit the dark fermentation process.
- Type and substrate concentration, biomass concentration, and H_2 transfer conditions are factors that rules H_2 production in CSTR systems.
- Metabolic diversity is one of the principal challenges that hinder the dark fermentation performance

1.1 Introduction

The dependency on fossil fuels and derives, and the increase of gas emissions from their combustion, currently spurs the urgent research for energy alternatives based on renewable resources. Nowadays, hydrogen gas (H_2) standouts as a potential alternative fuel, due to its attributes such as: zero CO_2 and other greenhouse gas emissions after combustion/oxidation and high energy content (122 kJ/g). The flexible production methods, positions H_2 gas as an excellent solution. Nowadays, approximately 90% of the H_2 is produced via methane gas steam reforming. In this process, steam and methane gas are heated together under high pressure to ~ 900°C over a nickel-based catalyst. The result is a mixture of carbon monoxide (CO), carbon dioxide (CO_2) and H_2 known as syngas. When both carbon-base gases are released to the atmosphere the H_2 produced is called gray H_2. In the same way, when the carbon-base gases are captured and stored, the H_2 produced is called blue H_2. The rest 10% of the H_2 are produced by methods that do not use fossil fuels as a feedstock, for example electrolysis of water powered by renewable electric energy and the use of biotechnological methods (dark fermentation and photo fermentation); the H_2 produced by such methods is called green H_2 [1].

Currently, from the biological methods, dark fermentation has the highest yields in H_2 production, it is carried out by strict-anaerobes and facultative microorganisms that catabolize carbohydrate-rich substrates into H_2, CO_2 and valuable chemicals (e.g. short-chain carboxylic acids) [2]. Moreover, dark fermentation can be included in a scheme of biorefinery and waste valorization, which highlights the potential involvement of hydrogen on the development of circular economy. However, there are still many challenges to be faced in order to achieve the best possible performance of dark fermentation in terms of hydrogen production, metabolites production, substrate utilization efficiency, among others. Therefore, this doctoral thesis studied some operational parameters control/optimization, mass transfer conditions and metabolic diversity that have been non studied in continuous reactors. This research achieved an important advance in the development of information and correlations between operational parameters, H_2 and valuable

chemicals production, and the microbial community structure/function in continuous dark fermentation reactors.

The introduction chapter presents an overview of several relevant topics on dark fermentation, which comprise basics of dark fermentation in continuous systems, types of inhibition in the dark fermentation process, the principal challenges in continuous dark fermentation systems. Afterwards, some molecular tools for the understanding the dark fermentation process also are discussed.

1.2 Basics of dark fermentation

Typically, glucose is the substrate of dark fermentation, which mainly produces butyric acid and acetic acid together with H_2 and CO_2. But complex biomass (e.g. lignocellulosic biomass) can also be used on dark fermentation process after the step of hydrolysis. The production of H_2 via dark fermentation is carried out by the metabolism of pyruvate (Figure 1.1). Glucose is metabolized to pyruvate and nicotinamide adenine dinucleotide (NADH) by the Embden-Meyerhoff-Parnas pathway (also known as glycolysis). In the dark fermentation process the pyruvic acid is used in two different ways. In the first one, it oxidizes to formic acid and acetyl-CoA (Eq. 1.1). Subsequently, by the enzyme pyruvate formate lyase (PFL), H_2 and CO_2 are produced from formate (Eq. 1.2). This pathway is accomplished by some facultative anaerobes, such as *Enterobacter* spp [3].

$$\text{Pyruvate} + \text{CoA} \rightarrow \text{acetyl–CoA} + \text{Formate} \quad (1.1)$$

$$\text{Formate} \rightarrow H_2 + CO_2 \quad (1.2)$$

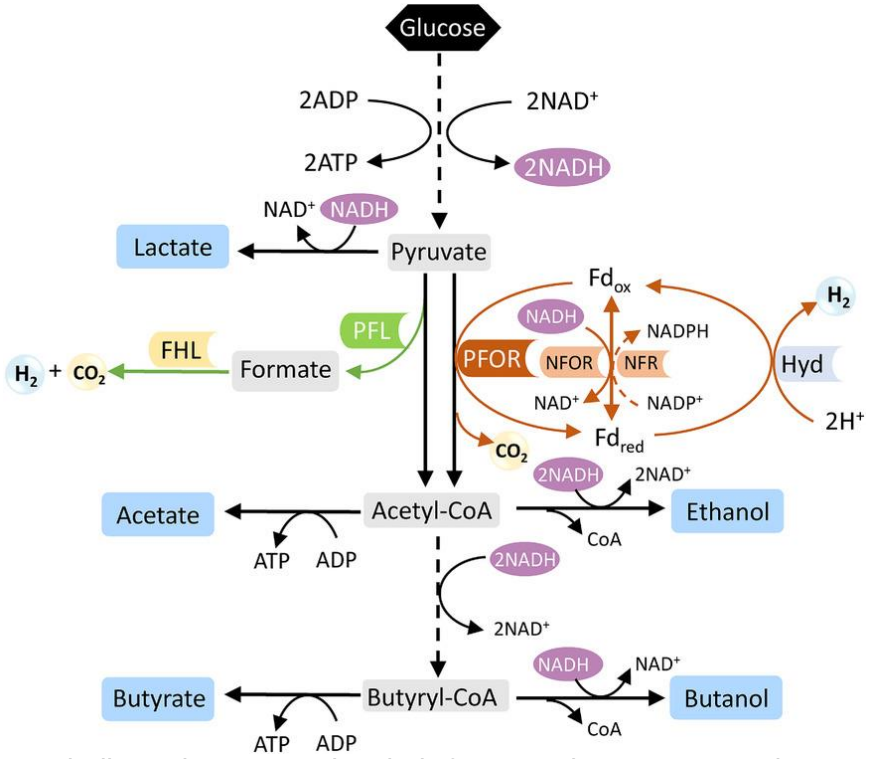

Figure 1.1 Metabolic pathways on the dark fermentation process. Where NFOR, is the pathway related to the enzyme NADH-Fd hydrogenase; PFOR, is the metabolic via utilized by pyruvate ferredoxin oxidoreductase enzyme. PFL is the metabolic via utilized by the pyruvate formate lyase. Modified from Gopalakrishnan et al., [4]

In the second pathway, accomplished by strict anaerobes (e.g. *Clostridium* spp.), pyruvic acid produces Acetyl-CoA by the activity of the enzyme pyruvate-ferredoxin oxidoreductase (PFOR). Afterwards, acetate and ATP are produced from Acetyl-CoA. The pyruvic acid conversion to acetyl-CoA requires the reduction of ferredoxin (Fd) (Eq. 1.3). The enzyme [FeFe] hydrogenase formerly oxidizes the reduced Fd and produces H_2 (Eq. 1.4). Also, the NADH produced in the glycolysis step may be utilized by the NADH-Fd hydrogenase (NFOR) generating extra production of H_2 (Eq. 1.5) [4].

$$\text{Pyruvate} + \text{CoA} + 2\,\text{Fd(ox)} \rightarrow \text{acetyl–CoA} + 2\,\text{Fd(red)} + \text{CO}_2 \quad (1.3)$$

$$2\,\text{H}^+ + \text{Fd(red)} \rightarrow \text{H}_2 + \text{Fd(ox)} \quad (1.4)$$

$$\text{NADH} + 2\,\text{Fd(red)} + 3\,\text{H}^+ \rightarrow 2\,\text{H}_2 + \text{NAD}^+ + 2\,\text{Fd(ox)} \quad (1.5)$$

The theoretical yield of H_2 production is 4 mol of H_2 per mole of glucose when pyruvate oxidizes to acetate. On the other hand, if pyruvate is converted to butyrate the H_2 theoretical yield of is only 2 mol H_2/mol of glucose.

The dark fermentation process can be carried out by a pure bacterium or by a mixture of bacteria. However, using a consortium is considered advantageous since the process is performed in unsterile environments. In the consortia it is possible the coexistence between H_2-producing bacteria and hydrolytic bacteria, allowing to degrade the complex carbohydrates into simple ones; such coexistence, upsurges the resilience ability of consortia to operational variants, e.g. substrate composition and type, modification of pH, temperature, etc. [5]. Nevertheless, the foremost bottleneck when a consortium is used in dark fermentation, is the presence of H_2-consuming bacteria in the community. Therefore, enrichment and pretreatment of the consortium is necessary for the overthrow of both groups of bacteria [6]. In a consortium two types of bacteria are present: facultative anaerobic bacteria and obligate anaerobic bacteria. *Enterobacter spp*. is the most representative facultative anaerobe that produces H_2, as they have in their genome the information for both H_2-producing enzymes [FeFe] hydrogenase and formate hydrogen lyase [7]. On the other hand, bacteria from the genus *Clostridium* is predominant in dark fermentation experiments for H_2 production. *Clostridium paraputrificum*, *Clostridium butyricum*, *Clostridium acetobutylicum*, *Clostridium beijerinckii*, are examples of such group [8].

1.3 Dark fermentation in continuous systems

The biosystem configuration and regime of operation are imperative for dark fermentation experiments. Typically, the production of H_2 via dark fermentation is carried out in continuous or batch mode. In continuous mode, the reactors are catalogued in function of biomass growth, fixed-biomass or suspended-biomass. In fixed-biomass reactors, high hydrogen yield can be achieved, due to the decoupling inside the reactors of the solids (biomass) retention time and the hydraulic retention time (HRT). Examples of reactors of fixed-biomass are the up-flow anaerobic sludge blanket reactor, agitated granular sludge bed reactor, trickling bed reactor, among others [4].

In the suspended-biomass reactors, due to the continuous stirring arrangement, bacteria are uniformly mixed within fermentation broth. In such states, there is an efficient interaction of bacteria and substrate. However, there is a constraint on suspended-biomass reactors, cell washout (loss of biomass), when the reactors are operated at lower HRT (< 6 h) [9].

The continuous stirred tank reactor (CSTR) is the most broadly used in dark fermentation, because its simple operation and construction, uniform mixing, and the likelihood of operate the system at a constant HRT [9]. The works using fixed-biomass systems reported higher volumetric H_2 production rates (VHPR), up to 78 L H_2/L-d with glucose as a substrate, in comparison with CSTR (up to 39 L H_2/L-d, galactose as a substrate) [10]. Nonetheless, as we can see in Table 1.1, with complex substrates, the volumetric hydrogen production rate (VHPR) is considerable higher in CSTR systems in comparison with fixed-biomass reactors.

Table 1.1 Recap of steady-state hydrogen production in diverse type of reactors investigated by our research group.

Category of biomass growth	Classification of reactor	Substrate	OLR (g/L-d)	VHPR (L H_2/L-d)	Reference
Suspended-biomass	CSTR	Agave bagasse enzymatic-hydrolysate	100[a]	9.9	[11]
		Agave bagasse enzymatic-hydrolysate	44[a]	6	[12]
		Agave bagasse enzymatic-hydrolysate	90[a]	13	[13]
		CWP	60[b]	7.7	[14]
		CWP	88[b]	13.9	[15]
		Agave bagasse enzymatic-hydrolysate	52.2[a]	2.5	[16]
		CWP	190[b]	25.8	[17]
		CWP	95[b]	16.1	[17]
		CWP	184[b]	24.4	[18]
		CWP	138[b]	25	[18]

		CWP	92[b]	12.5	[18]
Fixed-biomass	TBR	Agave bagasse enzymatic-hydrolysate	81[a]	5.8	[11]
	TBR	Agave bagasse enzymatic-hydrolysate	53[a]	3.5	[16]
	AFBR	Glucose	60	5.3	[19]
	EGSB	Glucose	25.6	1.3	[20]
	EGSB	Glucose	10	2.5	[21]
	TBR	Glucose	160	12	[22]
	TBR	Glucose	80	12	[22]
	TBR	Oat straw enzymatic-hydrolysate	10[a]	0.5	[22]
	UASB	CWP	48[b]	0.9	[23]
	UASB	CWP	20[b]	0.4	[24]
	TBR	Oat straw acidic-hydrolysate	6[a]	1.7	[25]

CSTR: Continuous stirred tank reactor, AFBR: Anaerobic fluidized bed reactor, UASB: Up-flow anaerobic sludge blank reactor, TBR: Trickling bed reactor, EGSB: Expanded granular sludge bed reactor, CWP: Cheese whey powder, VHPR: Volumetric H_2 production rate, [a] g chemical oxygen demand (COD), [b] g total carbohydrates (TC)

Besides the reactor configuration, the dark fermentation is decidedly reliant on process conditions such as pH, temperature, HRT, production of metabolites, type of substrate, among others. Key information of particular process conditions with the highest VHPR and H_2 yield can be obtained from the investigations carried out in our research group (Table 1.1) and the research in the field of dark fermentation. For instance, pH controls the dark fermentation process, because it upsets the activity of key dark fermentation enzymes; thus, affecting the overall performance of the dark fermentation consortium. Overall, the highest H_2 molar yields and VHPR have been reported at a pH range of 5 and 6 [26].

On the other hand, dark fermentation can be carried out at a range of temperatures in function of the type of consortium: mesophilic (25–40 ºC), thermophilic (40– 65 ºC), extreme thermophilic (65–80 ºC). According to a literature review, up-to 73% of dark fermentation lab-scale studies have been done at mesophilic temperatures [4].

Hydraulic retention time (HRT) is another essential aspect that rules the dark fermentation performance. HRT is the period of time that the liquid stays inside the reactor and it is a crucial parameter that defines the type and number of bacteria that can grow in the system. According to previous works, the specific growth rate of H_2-producing bacteria is 0.172/h. Therefore, in studies with bacterial consortia used as the inoculum, the highest VHPR and H_2 yield have been reported at HRT between 12 and 4 h [4].

In dark fermentation process not only H_2 and CO_2 are produced, metabolic end products such as acetic acid, lactic acid, butyric acid, propionic acid and some alcohols (such as butanol and ethanol) are produced. As mentioned in previous sections, theoretical H_2 yields are 4 mol H_2/mol glucose and 2 mol H_2/ mol glucose with acetate and butyrate as end products, respectively. Consequently, the concentration of acetic and butyric acid can be used as a way to determine the overall performance of the dark fermentation system. However, the substantial production/accumulation of these metabolic end products can hinder the H_2-production metabolic pathways, probably by the increases in ionic strength that leads to cellular lysis or inhibition by un-dissociated acids [4,27]. The *in situ* concentration reduction and separation of such metabolites is an eye-catching strategy to avoid a possible inhibition by soluble metabolites [27].

The nature and concentration of substrate is another basic parameter that significantly rules the dark fermentation performance. Overall, there are two types of substrates: model substrates and complex substrates. Model substrates, such as glucose, lactose, cheese whey powder and starch are the furthermost broadly substrates tested for dark fermentation [6]. Up-to date, highest VHPR were obtained with such substrates; in particular VHPR values higher than 25 L H_2/L-d were reported with cheese whey powder [17] and glucose [10].

The majority of the complex substrates are not suitable to be directly used in dark fermentation systems due to their recalcitrant characteristics. However, if such substrates are submitted to a proper pretreatment strategy, they can be suitable for H_2-producing bacteria. In the same way, considering that several complex substrates are produced in massive volume, such as the organic fraction of municipal solid

waste and agricultural residues, its use in dark fermentation is a suitable alternative to address its environmental concern [13]. As result, recently the research related to the production of H_2 from complex substrates has increased. Nonetheless, the VHPR with complex substrates is highly variable and considerably lower than that obtained with model substrates (Table 1.1).

Higher substrate concentration is preferred for energy-efficient operation of the fermentation process to minimize energy requirements for operation (primarily heating cost). However, high substrate concentrations may be unfavorable to H_2 production, since the activity of H_2-producing bacteria may be inhibited in several ways including metabolic end products, lower intracellular pH, and high H_2 partial pressure. Nevertheless, the tolerance towards high concentration of substrate and end products is one of the desirable features that an ideal H_2-producing microorganism should possess.

1.4 Basics of the type of inhibition that can occur in dark fermentation process

As mentioned in previous sections, substrate overloading, the accumulation of metabolic end products (e.g. carboxylic acids), and the accumulation of H_2 gas are the principal types of inhibition that limit the dark fermentation process. High concentrations of substrate can increase the osmolarity of the cells and cell turgor pressure causing a shift in the products spectrum, microbial community structure, and intracellular metabolic functions, such as hydrogenase activity [28].

Carboxylic acids are characterized by the presence of a carboxyl group (C(=O)OH) attached to the carbon backbone; deprotonation of this functional group produces a dissociated carboxylic acid, i.e., a negatively charged carboxylate. In terms of acidity, carboxylic acids are considered weak acids as they have pK_a values between 3.86 and 4.82 with a dissociation range from 2 to 7 on the pH scale. It is important to note that at optimum fermentation pH (5- 6) most of the carboxylic acids are in dissociated form (carboxylate) [29]. In the culture medium of dark fermentation, dissociated and undissociated forms of carboxylic acids coexist, both of which trigger cellular processes of product inhibition with increasing concentration. However, the

mechanism of inhibition depends directly on the species of carboxylic acids in solution.

In relation to the accumulation of dissociated acids in solution, the inhibition is attributed to an increase in the ionic strength of the medium. As a product of the dissociation of carboxylic acids, the concentration of cations (H^+) in the medium increases, causing the release of autolysins, which promote cell lysis of H_2-producing bacteria. Consequently, the change from acidogenesis to solventogenesis in fermentation is promoted [30]. Solvents such as ethanol and butanol cause inhibition on the cell by the degradation of biological molecules and disclosing biophysical changes to cell membranes. Furthermore, the detection of these compounds at sub-inhibitory concentrations can modify the flow of carbon and electrons causing either an stimulatory or inhibitory effects towards the production of the desired end product [28].

In contrast, carboxylic acids in their undissociated form can penetrate the bacterial membrane and alter the physiological cellular balance. Within the cytoplasm (pH≈7) the carboxylic acids dissociate, generating an excess of anions that increases the osmolarity of the cytoplasm and cell turgor pressure at the same time that the released protons decrease the intracellular pH, causing the cell to use energy intended for cell growth to restore physiological equilibrium [27]. It is even possible that the pH gradient of the membrane collapses due to excess of protons and the cell sporulates or dies.

The accumulation of H_2 gas in the culture medium of dark fermentation can cause end product inhibition. Whereas, the accumulation of H_2 in the headspace of the reactor commanding to a higher partial pressure of H_2, will increase the concentration of dissolved H_2 gas in the liquid phase. Following the Le Chatelier's principle, the production of H_2 in dark fermentation will be inhibited with the increase of H_2 gas in the liquid. At the same time, the metabolic pathways of H_2-producing bacteria may also be redirected and change for the production of other end products, such as ethanol, lactate, acetone and acetate via homoacetogenesis (the consumption of dissolved H_2 and CO_2 to producing acetate) [26].

Studies have shown, that the threshold inhibitory partial pressure of H_2 is 10^{-3} atm. If H_2 gas is not well released and generates a partial pressure higher than 10^{-3} atm in the system, the inhibition of H_2 production could arise due to thermodynamic constraint [31]. Nonetheless, it also has been described that the concentration of H_2 gas in the culture medium is not always in equilibrium with the gas phase. For instance, supersaturation phenomena of H_2 frequently appears. As a consequence, the concentration of such gas can be up to 7–80 times the equilibrium conditions [32]. Therefore, experiments concerning H_2 inhibition must be focused in the partial pressure of H_2 in the headspace of system, and also in the dissolved H_2 concentration in the culture medium.

1.5 Challenges in continuous dark fermentation process

As discussed in the previous section, several operational factors in dark fermentation such as temperature, pH, type of reactor, type and concentration of substrate have been widely studied, and general conclusions have been reached. However, there are still many challenges to be faced in order to achieve the best possible performance of dark fermentation in terms of hydrogen production, metabolites production, substrate utilization efficiency, among others. Overall, in continuous dark fermentation systems challenges in operational parameters, mass transfer conditions and metabolic diversity can be emphasized (Figure 1.2).

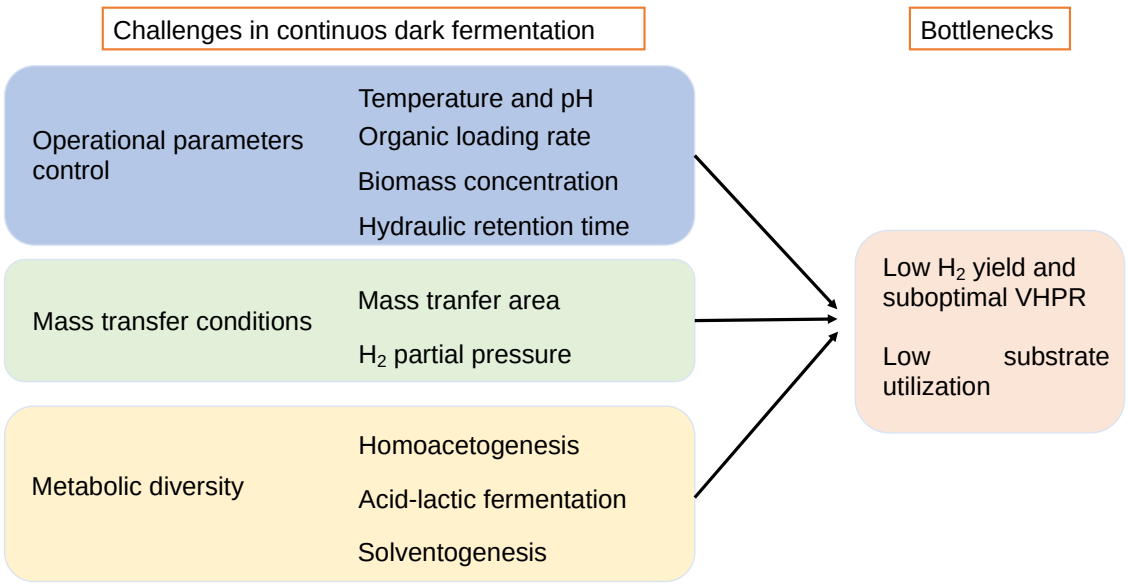

Figure 1.2 Summary of several issues/challenges for dark fermentation in continuous systems.

1.5.1 Organic loading rate

Proper substrate concentration or organic loading rate (OLR, g substrate/L-d) in continuous systems is crucial for efficient dark fermentation performance. High OLR is always desired for substrate utilization (principally for complex substrates) and energy efficiency points of view. However, high OLR might be adverse to the dark fermentation performance, since H_2 producing-bacteria are highly affected by the OLR due to they can be inhibited by substrate overloading, the accumulation of metabolic end products (e.g. carboxylic acids), and the increase of H_2 partial pressure [26]. Hence, the optimization of OLR is crucial to prevent the inhibition in continuous dark fermentation process.

In CSTR systems, the OLR controlled by increasing the concentration of the substrate in the inlet of the reactor with a constant HRT or by modifying the HRT with a fixed concentration of the substrate in the feed. Several investigations in suspended-biomass reactors have reported the highest VHPR at HRT of 6 h [18,33]. Therefore, increasing OLR by decreasing HRT to less than 6 h becomes unfeasible since there is loss of biomass (cell wash-out) and fall in the production of H_2. Consequently, the most viable option to increase OLR in a suspended biomass reactor is by modifying the concentration of substrate fed to the reactor.

Many investigations reported that in CSTR systems, OLR superior to 100 g COD/L-d typically inhibits dark fermentation performance. However, in our research group, stable H_2 production have been reached at OLR > 100 g COD/L-d (Table 1.1). In particular, using cheese whey powder as the substrate, it has been observed that the increase on the OLR from 55.4 to 138 g total carbohydrates (TC)/L-d at an HRT of 6 h, significantly increased the VHPR from 2.8 to 25 L H_2/L-d [17,18]. Conversely, a sharp fall in VHPR, but not on the fermentative process (no reduction of the substrate consumption efficiency was observed), occurred at OLR higher than 138 g TC/L-d, due to the increase on production of propionic acid and acetic acid from homoacetogenesis (metabolic route that consume H_2 and CO_2 to produce acetate) [17,18].

Aiming to overcome the OLR inhibition at high values, some strategies emerge in the recent years, such as the reduction of accumulation of metabolic ends in the reactor, the reduction of the concentration of dissolved CO_2 and H_2 in the fermentation broth, the decoupling of the HRT from the retention time of cells, bioaugmentation, co-fermentation, recirculation of CO_2, among others [17,18]. However, there is poor investigation of the OLR from the point of view of microbial communities, metabolic pathways and hydrogen production.

1.5.2 Biomass concentration

The biomass concentration is an essential parameter that rules the dark fermentation performance. One of the limitations in the CSTR systems is the difficulty to maintain high cell concentration in comparison with fixed-biomass reactors. This restriction of the CSTR is due to the equal HRT and retention time of cells, and the low specific growth rate of H_2-producing bacteria in such systems [13]. Usually, the biomass retained (as a volatile suspended solids, VSS) in the CSTR are mostly between 1 and 5 g VSS/L at HRT in the range of 12 and 4 h [4,13].

Specific organic loading rate (sOLR) is the parameter that relates the substrate concentration to the amount of biomass in continuous reactors (g substrate/g VSS-d). sOLR is an important factor that can control the dark fermentation process; at high sOLR (>20 g COD/g VSS-d) inhibition by substrate overloading can be

observed, whereas at low sOLR a major competition for the substrate is reported, producing changes in the metabolic pathways (< 5 g COD/g VSS-d) [34,35].

Recent studies propose that increasing and maintaining the biomass concentration (and constant sOLR) in suspended-biomass reactors might reduce substrate inhibition fallouts. Therefore, reactors may operate at high OLRs and relative low HRT (between 6 to 12 h), with stable conditions of H_2 productivity and substrate consumption efficiency for long period of times [10,27,36,37]. Based on this goal, many research groups are studying and designing more efficient CSTR systems. For example, recycling of biomass, membrane separation of biomass, immobilization of cells are possible solutions [4,27]. Nevertheless, to our knowledge the discontinuous biomass recycling in CSTR systems and its effect on the H_2 production and microbial community structure has not been studied.

1.5.3 Mass transfer conditions in a CSTR

The transfer of molecular H_2 from the liquid phase to the gas phase plays a critical function in the dark fermentation process. In a CSTR H_2 and CO_2 are produced in the bulk of the liquid phase (Figure 1.3). The molecules of H_2 and CO_2 move by convective transport to the nearness of the liquid transfer area. Afterward, following the film theory, transport by diffusion is present; this transport is carried out by the difference of H_2 and CO_2 concentrations between the liquid phase and the gas-liquid interphase. Such process is described by the global mass transfer rate of H_2 and CO_2 across the liquid-gas interphase (Q, g/L-m^2). The degree of the mass transfer rate is defined by 1) the difference of concentrations between the liquid phase and the interphase (ΔC, g/L), and 2) the global mass transfer coefficient (k_La, 1/h) (Eq. 1.6). The K_La links the mutually interacting parameters of specific interfacial area, the ‘a’ in the global mass transfer coefficient, and mixing intensity and efficiency [38,39].

$$Q = k_L a * (\Delta C) \quad (1.6)$$

According to the Henry’s law equation (Eq. 1.7), at the boundary gas-liquid interphase, and only there, the concentrations of the gasses dissolved in the liquid

phase and the gases in the gas phase are in equilibrium. Immediately when the H_2 and CO_2 crosses the interphase liquid-gas, the gases will diffuse to the bulk of the gas phase also driven by a change of concentration [40]. However, the Henry´s law only applies when the concentration in the liquid phase and gas phase are in equilibrium. For example, when the transfer of H_2 and CO_2 in the liquid phase to the gas phase is effective to prevent the gas accumulation. One important aspect in CSTR systems is the mass transfer limitations to transfer the dissolved H_2 and CO_2 from the liquid to the gas phase. This limitation, can cause the increase of the partial pressure by the accumulation of H_2 in the liquid phase [38].

$$CH_{2\ liquid} = He * PH_2 \quad (1.7)$$

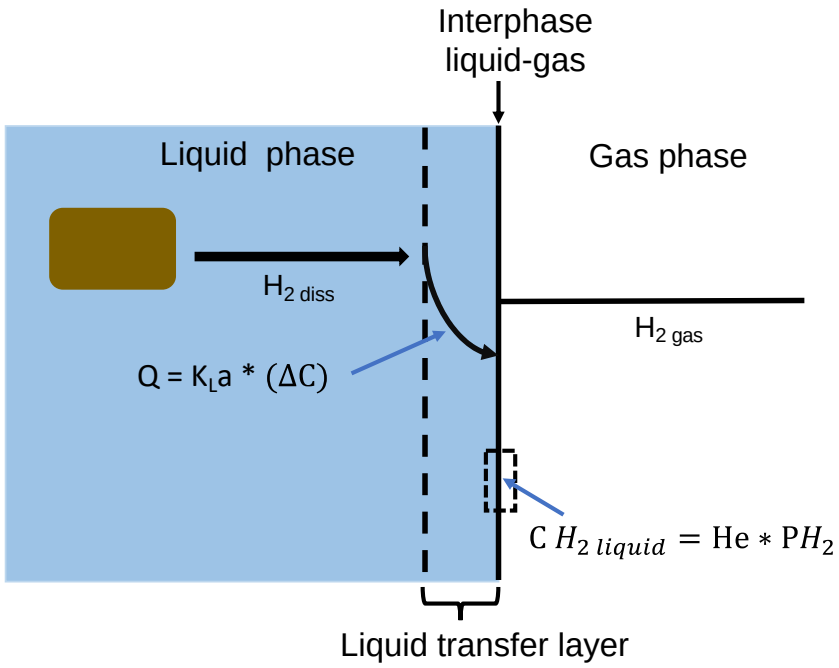

Figure 1.3 The H_2 mass transfer mechanism from liquid to gas phase. The molecules of H_2 or CO_2 diffuse in the liquid from high to low concentration, described by the global mass transfer rate (Q). In the interphase liquid-gas is observed an equilibrium according to the Henry's law equation.

Hydrogen partial pressure (PH_2) has regularly been mentioned as one the most important parameter that rules the dark fermentation performance, however it has seldom been studied. Low dissolved H_2 concentrations, and therefore, low PH_2, are

crucial to achieve high VHPR and H_2 molar yields. It has been reported that a PH_2 > 60 Pa inhibits the activity of the H_2-producing enzymes. The shift of the metabolic pathways decreases the theoretical H_2 molar yields from 4 to 2 mol H_2/mol hexose, due to the co-production of acetate and other no desired metabolites such as lactic acid, butanol, ethanol and butyric acid. Moreover, H_2 partial pressures > 600 Pa favor the homoacetogenesis pathway [41,42].

Considering the importance of the PH_2 in the dark fermentation performance, some studies focused in the study of such parameter. For instance, Beckers et al. [38] investigated the influence of stirring speed and gas sparging on dissolved H_2 concentration and mass transfer conditions for the *Clostridium butyricum* CWBI1009, they found that H_2 yield increased from 1.58 to 3.09 mol H_2/mol glucose when K_La changed from 0.08 to 4.55/h. In the same way, Palomo-Briones et al. [14] studied the effect of different stirring speeds on the concentration of dissolved H_2 in CSRT systems, they reported the maximum VHPR of 7.66 L H_2/L-d with a H_2 yield of 1.1 mol H_2/mol hexose at a k_La of 4.23/h. Alternatively, the mass transfer of H_2 and CO_2 to the gas phase could be increased with the use of two-phase partitioning bioreactors. These systems imply the addition of an extractive organic phase to the aqueous phase where fermentative microorganisms are contained. The extractive organic phase increases the total mass transfer area, leading to higher global mass transfer rates [15]. Nevertheless, to our information two-phase partitioning bioreactors have not been evaluated on dark fermentation process.

1.5.4 Metabolic diversity

Continuous H_2 production processes with suspended mixed cultures generally show a low diversity of carboxylic acids; mainly acetate and butyrate. However, the production of 1 mole of butyrate involves, in any case, the virtual loss of 2 moles of H_2. Therefore, a higher ratio acetate (fermentative) of butyrate involves higher H_2 yield. However, considering that H_2 transfer to the gas is limited in CSTR systems, a considerable part of the electron equivalents generated from the carbohydrates catabolism are usually redirected toward the synthesis of butyrate and other

compounds (propionate, lactate, ethanol, valerate or caproate), reducing directly or indirectly the amount of H_2 recovered.

H_2 can be consumed in two ways: as reducing equivalents ($NADH_2$; potential H_2) and as molecular H_2. The former way of consumption avoids the production of Fd(red) and formic acid which both lead to H_2 formation (Eq 1.2, 1.4 and 1.5). The reactions that produces metabolites such as lactic acid, propionic acid, butyric acid, valeric acid, and alcohols (ethanol and propanol) use $NADH_2$ as the electron donor [42,43]. On the other hand, molecular H_2 is consumed in the production of acetate via homoacetogenesis. In the same way, molecular H_2 at high PH_2 can be consumed in the production of acetic acid from ethanol. [44]. Two principal metabolic pathways have been recognized as a major H_2 sink: homoacetogenesis and lactic acid fermentation.

1.5.4.1 Homoacetogenesis

The homoacetogenesis is carried out by acetogenic microorganisms (homoacetogens) that produce acetate via the consumption of CO_2 and H_2 by the Wood- Ljungdahl pathway (WLP) according to Eq. 1.8 [44].

$$4\ H_2 + 2\ CO_2 \rightarrow \text{Acetate} + 2\ H_2O \qquad (1.8)$$

Homoacetogens are strict anaerobes, fast growing, and someone of these bacteria have the ability of sporulate. *Acetobacterium*, *Butyribacterium*, *Clostridium*, *Eubacterium*, are examples of homoacetogens. Homoacetogens can grow by two ways: Autotrophically when they use the H_2 as the electron donor and CO_2 or CO as the carbon source, and the heterotrophic way when using organic substrates, such as carbohydrates, alcohols, metabolites (e.g. formic acid) as sources of energy and carbon [42].

Operational parameters such as HRT, substrate concentration or OLR and reactor configuration might also influence homoacetogenesis. In particular, a recent study of 19 different dark fermentative reactors reported that H_2-producing bacteria were favored over homoacetogens in conditions of high substrate availability (high OLR)

[2]. Montoya-Rosales et al. [13] studied the homoacetogenesis in two reactor configurations, CSTR and a fixed-biomass reactor; they found that in CSTR (that interestingly reported higher VHPR than the fixed-biomass reactor) the homoacetogenic acetate production rates were up to three times higher in comparison with the fixed biomass reactor. This difference is because the CSTR has inherent low liquid-gas mass transfer conditions in comparison with fixed-biomass reactor. Poor mass transfer conditions induce the accumulation of dissolved H_2 in the liquid phase and, hence, leads to higher PH_2. Dinamarca and Bakke [45] studied the effect of HRT and homoacetogenesis in CSTR systems, they reported that probably the consumption of H_2 was faster with increasing HRT from 6 to 40 h.

Different methodologies have been explored to diminish the impact of homoacetogenesis in H_2 production, including the operation at thermophilic or alkaline conditions, variation of HRT and OLR, the decrease of dissolved H_2 concentration, among others [42]. However, the avoidance/decrease of homoacetogenesis is specially challenging, since most of homoacetogens related to dark fermentative systems belong to the genus *Clostridium*, which can also perform H_2 production.

1.5.4.2 Lactic acid fermentation

Lactic acid fermentation is the production of lactate with the pyruvate and NADH produced in the glycolysis step (Eq. 1.9) or/and by the direct consumption of substrates, such as glucose (Eq. 1.10). Commonly, lactic acid bacteria (LAB) are considered detrimental for the dark fermentation performance because they compete with the H_2-producing bacteria for the substrate and sub-products such as pyruvate and NADH. In the same way, some LAB, e.g. *Lactococcus* have the capacity to inhibit other group of bacteria by the production/release of anti-microbial substances (bacteriocins) [9,46].

$$\text{Pyruvate} + \text{NADH} + H^+ \rightarrow \text{Lactate} + NAD^+ \quad (1.9)$$

$$\text{Glucose} + 2\ \text{ADP} + 2\ \text{Pi} \rightarrow 2\ \text{Lactate} + 2\ \text{ATP} \quad (1.10)$$

Genera such as *Lactobacillus, Enterococcus*, *Sporolactobacillus*, *Streptococcus* have been reported as co-dominant bacterial genera in continuous dark fermentation systems with low VHPR and H_2 molar yields [46–48]. Palomo-Briones et al. [15] evaluated different HRT in a CSTR and its relationship with the abundance of LAB and H_2-producing bacteria; at high HRT (18-24 h) they reported the increase of the abundance of LAB (*Sporolactobacillaceae* and *Streptococcaceae*) and a considerable fall of H_2 production.

On the other hand, many reports discussed the positive role of LAB in dark fermentation systems. This positive effect is because LAB provide an extra substrate (lactic acid) to produce H_2. This secondary fermentation is called “lactate-acetate pathway”, which consists in the consumption of lactate and acetate to produce H_2 and butyrate (Eq. 1.11) [49]. *Clostridium acetobutylicum*, *Clostridium beijerinckii*, and *Clostridium tyrobutyricum* have proved the capacity to ferment lactate and acetate as a carbon source [50]. Garcia-Depraect et al. [50] studied the community dynamic in the co-fermentation of tequila vinasses and nixtamalization wastewater in batch experiments; they reported the primary fermentation with the co-production of acetate and lactate from the consume of the fermentable carbohydrates, and a secondary fermentation with the consume of lactate and acetate after the 100 h of the fermentation. From these results they concluded that the H_2-producing bacteria and LAB are in a coordinated dynamic behavior in the dark fermentation process.

$$\text{Lactic acid} + 0.5\ \text{Acetic acid} \rightarrow 0.75\ \text{Butyric acid} + CO_2 + 0.5\ H_2 + 0.5\ H_20 \qquad (1.11)$$

From current reports, there is a debate if the acid lactic fermentation is detrimental or positive in dark fermentation, causing an increase of the discussion and interest to study the exact role of LAB in the dark fermentation process.

1.6 Molecular tools for the understanding of the dark fermentation process

Molecular tools are technologies and methodologies that provide information about the microbial composition and its function in a particular biological process. In recent years, the development of more powerful and economically accessible technologies triggered the use of molecular tools in dark fermentation studies. Several molecular

tools may be used in function of the question formulated: What microorganisms are there? How many microorganisms are there? and What is their function or role in the microbial community?

1.6.1 Microbial community diversity: Next Generation Sequencing

Cloning and sequencing by Sanger, DNA microarrays and next generation sequencing (NGS) of PCR amplicons are the principal tools used to identify the microorganisms present in a sample. However, in the last decade, NGS is the most used technology to identify microbial diversity in environmental samples, specially, by the platform Illumina and 454 pyrosequencing genomes. NGS in comparison with the other techniques has the advantages to be faster and cheaper, providing millions of reads (sequences) that can be obtained in a single analysis [51].

The phylogenetic identification of microorganisms through NGS is carried out by the PCR amplification and sequencing of a conserved gen. The 16S rRNA gen is the most used housekeeping genetic marker, because it exists in generally all bacteria and archaea, has not changed over the time and has a proper length (1500 bp) to be successfully used in NGS methods [52]. Once the sequences are obtained, the posterior bacteria identification is carried out by a bioinformatic pipeline, e.g. QIIME, Mothur. In the bioinformatic step the sequences are clustered into taxa. For example, Operational Taxonomic Units (OTU) and Amplicon sequence variant (ASV). In particular, one OTU is when two strains from the same specie share more than 97% of homology in their 16S rRNA gene sequence. Finally, to achieve the identification of the taxa generated in the bioinformatic step, such taxa are compared with the sequences already reported in massive databases, e.g. NCBI, SILVA, National DNA Index System, among others. One way to present the sequencing results are in relative abundance (%). For example, Arellano-García et al. [53] studied the microbial community diversity over the time from the CSTR feed with tequila vinasses; they reported in the day 104 of operation that the microbial community was dominated by the genera *Sporolactobacillus* (~ 75%) and *Clostridium* (~ 20%). From these results they concluded that the apparent antagonism between abundances of relevant bacterial genera such as *Clostridium* and *Sporolactobacillus* more than

portraying competition may represent an underlying governing probably related to the substrate composition.

1.6.2 Microbial quantification: Quantitative-PCR

The FISH method and quantitative polymerase chain reaction (q-PCR) are the main molecular tools used to quantify and detect specific rRNA genes. Nowadays, the FISH method is less used because it has disadvantages such as the relatively low detection limit (from 10^3 to 10^4 cells or copies/mL), the low cell permeability, is a time-consuming process. On the other hand, q-PCR has the advantages to be highly specific with wide detection range and it is possible to analyze numerous samples at the same time [51].

q-PCR is a molecular technique used to simultaneously amplify and quantify the amplification product absolutely. This technique consists in the amplification of a template DNA with specific primers and the products of the amplification are detected in each PCR-cycle of the exponential phase. The SYBR Green I is the fluorescent-dye most used to detect a target DNA-region in environmental samples. The quantification of fluorescent signals can be absolute or relative. The first one is actually the most used in environmental samples and consists in the use of standard curve constructed by amplifying known amounts of target DNA [54]. Usually, the results are reported in number of copies/mL of sample, number of copies/ng DNA, among others.

Conserved genes, such as 16S rRNA, or specific genes can be amplified and quantified. In the case of dark fermentation, specific genes have been identified that encode enzymes to perform a particular function in the process. This is the case of the Fe-Fe hydrogenase (*hydA*) gene found in H_2-producing bacteria [3]. On the other hand, for homoacetogenic bacteria, formyltetrahydrofolate synthetase (*fthfs*) has been identified as the main marker gene to quantify this group of bacteria [55]. In recent years, the quantification of particular genes involved in fermentation has become very relevant, since it allows quantitative estimation of the abundance of these genes and its relation to aspects such as H_2 production, percentage of homoacetogenesis, H_2 molar yield, among others. Fuentes et al. [2] quantified by q-

PCR the genes *hydA* and *fthfs* in 70 samples of 19 different continuous dark fermentation systems; they reported the presence of both genes in all samples at values of 10^3 to 10^{12} *hydA* copies/ng DNA and 1.92 to 10^4 *fthfs* copies/ng DNA. They concluded that the population dynamics is influenced by the inoculum used, the substrate, and the operating conditions.

1.6.3 Microbial function: Metatranscriptomics

In recent years, several molecular tools have been developed and used to study the metabolic activities of microbial communities in environmental process, such as, anaerobic digestion and dark fermentation. Examples of such molecular tools are the meta-omics techniques, functional microarrays, microautoradiography combined with FISH, raman microspectroscopy combined with FISH, among others.

Omics tools are used to study microbial functionalities in an environmental process. Metagenomics studies the genic material of all organisms contained in a sample, metabolomics studies metabolic fluxes, metatranscriptomics studies gene expression and metaproteomics is used for protein identification. Metatranscriptomics is a molecular tool that provides information about possible changes in the expression of genes that have a specific function in a given biological process. For the particular case of dark fermentation, for example, it can be determined whether genes involved in H_2 production (by the PFL and PFOR pathways (e.g. Fe-H_2-ase, formate hydrogen lyase)), in H_2 consumption, in the production of other compounds (e.g. lactate, alcohols, etc.), are expressed in higher or lower abundance when some operational condition is changed.

Some studies reported the interactions and changes in gene expression in dark fermentation [56,57]. However, works dealing with metatranscriptomics in dark fermentation are very scarce. Hongyuan et al., [56] studied the transcriptomic responses (gene expression) in a co-culture of *Clostridium cellulovorans* and *Rhodopseudomonas palustris*; they reported that in the co-culture a downregulation of the genes pyruvate ferredoxin/flavodoxin oxidoreductase and hydrogenase exists in *C. cellulovorans* and an upregulation of the genes related to synthesis of metabolites (acetate, butyrate and lactate, principally).

1.7 Scope of the thesis, hypothesis, objectives and structure of the thesis

The dark fermentation process standouts as the most suitable biological process for the production of H_2 gas and also valuable chemicals (e.g. carboxylic acids). However as revised above there are a number of challenges that still need to be studied/evaluated in order to achieve the best possible dark fermentation performance. Type and substrate concentration, the biomass concentration, and H_2 transfer conditions have been identified as key operational parameters to control and improve dark fermentation performances in suspended-growth reactors. Nevertheless, there are scarce information of the role of these key operational parameters in the production of hydrogen as well as in the microbial community function and structure. Therefore, this doctoral thesis studied the discontinuous biomass increase, the addition of an organic extractive phase and the modification of the organic loading rates and it is relationship with the key operational parameters mentioned above from the point of view of the microbial community, metabolic pathways and overall dark fermentation performance.

Hypothesis

The discontinuous biomass increase, the addition of an organic extractive phase and the modification of the organic loading rates in suspended-biomass reactors will increase the production of hydrogen and valuable chemicals and will modify the microbial community structure. Furthermore, the addition of an organic extractive phase in suspended-biomass reactors will stimulate the dark fermentation metabolic pathways.

General objective

Evaluate the type and substrate concentration, the biomass concentration, and H_2 transfer conditions in the microbial community, metabolic pathways and overall dark fermentation performance.

Specific objectives

- To determine the effect of decoupling the hydraulic retention time and cells retention time by the discontinuous increase and maintaining of recycled biomass in a suspended-biomass reactor.
- To implement and evaluate a novel two-phase partitioning bioreactor in the production of H_2 and carboxylic acids and evaluate the effect on the composition of microbial communities in such dark fermentation system.
- To evaluate the prevalence of homoacetogens and H_2-producing bacteria, and to investigate the expression changes of genes involved in continuous dark fermentation systems.
- To investigate the composition of microbial communities developed in H_2-producing reactors fed with lignocellulosic enzymatic hydrolysates and unveil general relationships between diversity, structure and performance of H_2-producing systems

Structure of the thesis

The **Chapter two**, reports the effect of decoupling the hydraulic retention time and cells retention time in a suspended-biomass reactor in the production of H_2 and carboxylic acids. Besides the microbial community structure was also investigated.

In the **Chapter three**, the modification of the mass transfer conditions by the addition of an organic extractive phase (silicone oi) in batch and continuous experiments was investigated. From the microbial community structure results reported in the chapter three, in **Chapter four**, the impact of the operation of suspended-biomass reactors at high OLR (> 90 g TC/L-d) and with the addition of silicone oil on the expression of dark fermentation key genes was investigated using the molecular tools of meta-transcriptomic and genes quantification.

In the chapters two, three and four a model substrate was used as a feedstock in the suspended-biomass reactors. However, the use of complex substrates (e.g. agricultural residues) is one the aspects that highlights the dark fermentation as a

suitable option for the production of green H_2. For instance, in **Chapter five**, the effect of type and concentration of complex substrates on H_2 production performance and microbial community structure and diversity was evaluated. Finally, the **Chapter six** presents a general discussion of the principal results and conclusions obtained in the investigation.

1.8 References

[1] P. Sivagurunathan, G. Kumar, A. Mudhoo, E.R. Rene, G.D. Saratale, T. Kobayashi, K. Xu, S.H. Kim, D.H. Kim, Fermentative hydrogen production using lignocellulose biomass: An overview of pre-treatment methods, inhibitor effects and detoxification experiences, Renew. Sustain. Energy Rev. 77 (2017) 28–42. doi:10.1016/j.rser.2017.03.091.

[2] L. Fuentes, R. Palomo-Briones, J. de Jesús Montoya-Rosales, L. Braga, E. Castelló, A. Vesga, E. Tapia-Venegas, E. Razo-Flores, C. Ecthebehere, Knowing the enemy: homoacetogens in hydrogen production reactors, Appl. Microbiol. Biotechnol. (2021). doi:10.1007/s00253-021-11656-6.

[3] L. Cabrol, A. Marone, E. Tapia-Venegas, J.-P. Steyer, G. Ruiz-Filippi, E. Trably, Microbial ecology of fermentative hydrogen producing bioprocesses: useful insights for driving the ecosystem function, FEMS Microbiol. Rev. 41 (2017) 158–181. doi:10.1093/femsre/fuw043.

[4] B. Gopalakrishnan, N. Khanna, D. Das, Dark-Fermentative Biohydrogen Production, in: Biohydrogen, second, Elsevier, 2019: pp. 79–122. doi:10.1016/B978-0-444-64203-5.00004-6.

[5] R. Moscoviz, E. Trably, N. Bernet, H. Carrère, The environmental biorefinery: State-of-the-art on the production of hydrogen and value-added biomolecules in mixed-culture fermentation, Green Chem. 20 (2018) 3159–3179. doi:10.1039/c8gc00572a.

[6] J. Wang, W. Wan, Factors influencing fermentative hydrogen production: A review, Int. J. Hydrogen Energy. 34 (2009) 799–811. doi:10.1016/j.ijhydene.2008.11.015.

[7] C. Zhang, F.-X. Lv, X.-H. Xing, Bioengineering of the Enterobacter aerogenes strain for biohydrogen production, Bioresour. Technol. 102 (2011) 8344–8349. doi:https://doi.org/10.1016/j.biortech.2011.06.018.

[8] C. Xue, J. Zhao, L. Chen, S.T. Yang, F. Bai, Recent advances and state-of-the-art strategies in strain and process engineering for biobutanol production by Clostridium acetobutylicum, Biotechnol. Adv. 35 (2017) 310–322. doi:10.1016/j.biotechadv.2017.01.007.

[9] E. Castelló, L. Braga, L. Fuentes, C. Etchebehere, Possible causes for the instability in the H2 production from cheese whey in a CSTR, Int. J. Hydrogen Energy. 43 (2018) 2654–2665. doi:10.1016/j.ijhydene.2017.12.104.

[10] J.H. Park, K. Chandrasekhar, B.H. Jeon, M. Jang, Y. Liu, S.H. Kim, State-of-the-art technologies for continuous high-rate biohydrogen production, Bioresour. Technol. 320 (2021) 124304. doi:10.1016/j.biortech.2020.124304.

[11] C. Valencia-Ojeda, J. de J. Montoya-Rosales, R. Palomo-Briones, V. Montiel-Corona, L.B. Celis, E. Razo-Flores, Saccharification of agave bagasse with Cellulase 50 XL is an effective alternative to highly specialized lignocellulosic enzymes for continuous hydrogen production, J. Environ. Chem. Eng. 9 (2021) 105448. doi:10.1016/j.jece.2021.105448.

[12] V. Montiel Corona, E. Razo-Flores, Continuous hydrogen and methane production

from Agave tequilana bagasse hydrolysate by sequential process to maximize energy recovery efficiency, Bioresour. Technol. 249 (2018) 334–341. doi:10.1016/j.biortech.2017.10.032.
[13] J. de J. Montoya-Rosales, D.K. Olmos-Hernández, R. Palomo-Briones, V. Montiel-Corona, A.G. Mari, E. Razo-Flores, Improvement of continuous hydrogen production using individual and binary enzymatic hydrolysates of agave bagasse in suspended-culture and biofilm reactors, Bioresour. Technol. 283 (2019) 251–260. doi:https://doi.org/10.1016/j.biortech.2019.03.072.
[14] R. Palomo-Briones, L.B. Celis, H.O. Méndez-Acosta, N. Bernet, E. Trably, E. Razo-Flores, Enhancement of mass transfer conditions to increase the productivity and efficiency of dark fermentation in continuous reactors, Fuel. 254 (2019) 115648. doi:10.1016/j.fuel.2019.115648.
[15] R. Palomo-Briones, E. Trably, N.E. López-Lozano, L.B. Celis, H.O. Méndez-Acosta, N. Bernet, E. Razo-Flores, Hydrogen metabolic patterns driven by Clostridium-Streptococcus community shifts in a continuous stirred tank reactor, Appl. Microbiol. Biotechnol. 102 (2018) 2465–2475. doi:10.1007/s00253-018-8737-7.
[16] C.A. Contreras-Dávila, H.O. Méndez-Acosta, L. Arellano-García, F. Alatriste-Mondragón, E. Razo-Flores, Continuous hydrogen production from enzymatic hydrolysate of Agave tequilana bagasse: Effect of the organic loading rate and reactor configuration, Chem. Eng. J. 313 (2017) 671–679. doi:10.1016/j.cej.2016.12.084.
[17] C.B. Cota-Navarro, J. Carrillo-Reyes, G. Davila-Vazquez, F. Alatriste-Mondragón, E. Razo-Flores, Continuous hydrogen and methane production in a two-stage cheese whey fermentation system, Water Sci. Technol. 64 (2011) 367–374. doi:10.2166/wst.2011.631.
[18] G. Davila-Vazquez, C.B. Cota-Navarro, L.M. Rosales-Colunga, A. de León-Rodríguez, E. Razo-Flores, Continuous biohydrogen production using cheese whey: Improving the hydrogen production rate, Int. J. Hydrogen Energy. 34 (2009) 4296–4304. doi:10.1016/j.ijhydene.2009.02.063.
[19] C. Cisneros-Pérez, C. Etchebehere, L.B. Celis, J. Carrillo-Reyes, F. Alatriste-Mondragón, E. Razo-Flores, Effect of inoculum pretreatment on the microbial community structure and its performance during dark fermentation using anaerobic fluidized-bed reactors, Int. J. Hydrogen Energy. 42 (2017) 9589–9599. doi:10.1016/J.IJHYDENE.2017.03.157.
[20] C.D. Bárcenas-Ruiz, J. Carrillo-Reyes, L. Arellano-García, L.B. Celis, F. Alatriste-Mondragón, E. Razo-Flores, Pretreatment and upward liquid velocity effects over granulation in hydrogen producing EGSB reactors, Biochem. Eng. J. 107 (2016) 75–84. doi:10.1016/J.BEJ.2015.12.010.
[21] C. Cisneros-Pérez, J. Carrillo-Reyes, L.B. Celis, F. Alatriste-Mondragón, C. Etchebehere, E. Razo-Flores, Inoculum pretreatment promotes differences in hydrogen production performance in EGSB reactors, Int. J. Hydrogen Energy. 40 (2015) 6329–6339. doi:10.1016/J.IJHYDENE.2015.03.048.
[22] J. Arreola-Vargas, F. Alatriste-Mondragón, L.B. Celis, E. Razo-Flores, A. López-López, H.O. Méndez-Acosta, Continuous hydrogen production in a trickling bed reactor by using triticale silage as inoculum: Effect of simple and complex substrates, J. Chem. Technol. Biotechnol. 90 (2015) 1062–1069. doi:10.1002/jctb.4410.
[23] J. Carrillo-Reyes, L.B. Celis, F. Alatriste-Mondragón, L. Montoya, E. Razo-Flores, Strategies to cope with methanogens in hydrogen producing UASB reactors: Community dynamics, Int. J. Hydrogen Energy. 39 (2014) 11423–11432. doi:10.1016/j.ijhydene.2014.05.099.
[24] J. Carrillo-Reyes, L.B. Celis, F. Alatriste-Mondragón, E. Razo-Flores, Different start-up strategies to enhance biohydrogen production from cheese whey in UASB

reactors, Int. J. Hydrogen Energy. 37 (2012) 5591–5601. doi:10.1016/j.ijhydene.2012.01.004.
[25] S. Arriaga, I. Rosas, F. Alatriste-Mondragón, E. Razo-Flores, Continuous production of hydrogen from oat straw hydrolysate in a biotrickling filter, Int. J. Hydrogen Energy. 36 (2011) 3442–3449. doi:10.1016/j.ijhydene.2010.12.019.
[26] P. Sivagurunathan, G. Kumar, P. Bakonyi, S.H. Kim, T. Kobayashi, K.Q. Xu, G. Lakner, G. Tóth, N. Nemestóthy, K. Bélafi-Bakó, A critical review on issues and overcoming strategies for the enhancement of dark fermentative hydrogen production in continuous systems, Int. J. Hydrogen Energy. 41 (2016) 3820–3836. doi:10.1016/j.ijhydene.2015.12.081.
[27] E. Elbeshbishy, B.R. Dhar, G. Nakhla, H.S. Lee, A critical review on inhibition of dark biohydrogen fermentation, Renew. Sustain. Energy Rev. 79 (2017) 656–668. doi:10.1016/j.rser.2017.05.075.
[28] A. Ciranna, R. Ferrari, V. Santala, M. Karp, Inhibitory effects of substrate and soluble end products on biohydrogen production of the alkalithermophile Caloramator celer: Kinetic, metabolic and transcription analyses, Int. J. Hydrogen Energy. 39 (2014) 6391–6401. doi:10.1016/j.ijhydene.2014.02.047.
[29] M.A.Z. Bundhoo, R. Mohee, Inhibition of dark fermentative bio-hydrogen production: A review, Int. J. Hydrogen Energy. 41 (2016) 6713–6733. doi:10.1016/j.ijhydene.2016.03.057.
[30] Y. Chen, Y. Yin, J. Wang, Recent advance in inhibition of dark fermentative hydrogen production, Int. J. Hydrogen Energy. 46 (2021) 5053–5073. doi:10.1016/J.IJHYDENE.2020.11.096.
[31] A. Noblecourt, G. Christophe, C. Larroche, G. Santa-Catalina, E. Trably, P. Fontanille, High hydrogen production rate in a submerged membrane anaerobic bioreactor, Int. J. Hydrogen Energy. 42 (2017) 24656–24666. doi:10.1016/j.ijhydene.2017.08.037.
[32] G. Dreschke, S. Papirio, P.N.L. Lens, G. Esposito, Influence of liquid-phase hydrogen on dark fermentation by Thermotoga neapolitana, Renew. Energy. 140 (2019) 354–360. doi:10.1016/J.RENENE.2019.02.126.
[33] R. Palomo-Briones, E. Razo-Flores, N. Bernet, E. Trably, Dark-fermentative biohydrogen pathways and microbial networks in continuous stirred tank reactors: Novel insights on their control, Appl. Energy. 198 (2017) 77–87. doi:10.1016/j.apenergy.2017.04.051.
[34] M. Del Pilar Anzola-Rojas, S.G. Da Fonseca, C.C. Da Silva, V.M. De Oliveira, M. Zaiat, The use of the carbon/nitrogen ratio and specific organic loading rate as tools for improving biohydrogen production in fixed-bed reactors, Biotechnol. Reports. 5 (2015) 46–54. doi:10.1016/J.BTRE.2014.10.010.
[35] S.D. Gomes, L.T. Fuess, E.D. Penteado, S.D.M. Lucas, J.T. Gotardo, M. Zaiat, The application of an innovative continuous multiple tube reactor as a strategy to control the specific organic loading rate for biohydrogen production by dark fermentation, Bioresour. Technol. 197 (2015) 201–207. doi:10.1016/J.BIORTECH.2015.08.077.
[36] M. Saleem, M.C. Lavagnolo, A. Spagni, Biological hydrogen production via dark fermentation by using a side-stream dynamic membrane bioreactor: Effect of substrate concentration, Chem. Eng. J. 349 (2018) 719–727. doi:10.1016/j.cej.2018.05.129.
[37] Z. Trad, J. Akimbomi, C. Vial, C. Larroche, M.J. Taherzadeh, J.P. Fontaine, Development of a submerged anaerobic membrane bioreactor for concurrent extraction of volatile fatty acids and biohydrogen production, Bioresour. Technol. 196 (2015) 290–300. doi:10.1016/j.biortech.2015.07.095.
[38] L. Beckers, J. Masset, C. Hamilton, F. Delvigne, D. Toye, M. Crine, P. Thonart, S. Hiligsmann, Investigation of the links between mass transfer conditions, dissolved

hydrogen concentration and biohydrogen production by the pure strain Clostridium butyricum CWBI1009, Biochem. Eng. J. 98 (2015) 18–28. doi:10.1016/j.bej.2015.01.008.
[39] B. Chezeau, J.P. Fontaine, C. Vial, Analysis of liquid-to-gas mass transfer, mixing and hydrogen production in dark fermentation process, Chem. Eng. J. 372 (2019) 715–727. doi:10.1016/j.cej.2019.04.191.
[40] J.T. Kraemer, D.M. Bagley, Supersaturation of Dissolved H2 and CO2 During Fermentative Hydrogen Production with N2 Sparging, Biotechnol. Lett. 2006 2818. 28 (2006) 1485–1491. doi:10.1007/S10529-006-9114-7.
[41] S. De Kok, J. Meijer, M.C.M. Van Loosdrecht, R. Kleerebezem, Impact of dissolved hydrogen partial pressure on mixed culture fermentations, Appl. Microbiol. Biotechnol. 97 (2013) 2617–2625. doi:10.1007/S00253-012-4400-X/FIGURES/2.
[42] N.M.C. Saady, Homoacetogenesis during hydrogen production by mixed cultures dark fermentation: Unresolved challenge, Int. J. Hydrogen Energy. 38 (2013) 13172–13191. doi:10.1016/j.ijhydene.2013.07.122.
[43] H.S. Lee, M.B. Salerno, B.E. Rittmann, Thermodynamic evaluation on H2 production in glucose fermentation, Environ. Sci. Technol. 42 (2008) 2401–2407. doi:10.1021/ES702610V/SUPPL_FILE/ES702610V-FILE003.PDF.
[44] S.R. Shanmugam, S.R. Chaganti, J.A. Lalman, D.D. Heath, Statistical optimization of conditions for minimum H2 consumption in mixed anaerobic cultures: Effect on homoacetogenesis and methanogenesis, Int. J. Hydrogen Energy. 39 (2014) 15433–15445. doi:10.1016/j.ijhydene.2014.07.143.
[45] C. Dinamarca, R. Bakke, Apparent hydrogen consumption in acid reactors: observations and implications, Water Sci. Technol. 59 (2009) 1441–1447. doi:10.2166/WST.2009.135.
[46] E. Castelló, A.D. Nunes Ferraz-Junior, C. Andreani, M. del P. Anzola-Rojas, L. Borzacconi, G. Buitrón, J. Carrillo-Reyes, S.D. Gomes, S.I. Maintinguer, I. Moreno-Andrade, R. Palomo-Briones, E. Razo-Flores, M. Schiappacasse-Dasati, E. Tapia-Venegas, I. Valdez-Vázquez, A. Vesga-Baron, M. Zaiat, C. Etchebehere, Stability problems in the hydrogen production by dark fermentation: Possible causes and solutions, Renew. Sustain. Energy Rev. 119 (2019). doi:10.1016/j.rser.2019.109602.
[47] T. Noike, H. Takabatake, O. Mizuno, M. Ohba, Inhibition of hydrogen fermentation of organic wastes by lactic acid bacteria, Int. J. Hydrogen Energy. 27 (2002) 1367–1371. doi:10.1016/S0360-3199(02)00120-9.
[48] S.D. Gomes, L.T. Fuess, T. Mañunga, P.C. Feitosa de Lima Gomes, M. Zaiat, Bacteriocins of lactic acid bacteria as a hindering factor for biohydrogen production from cassava flour wastewater in a continuous multiple tube reactor, Int. J. Hydrogen Energy. 41 (2016) 8120–8131. doi:10.1016/j.ijhydene.2015.11.186.
[49] O. García-Depraect, E. León-Becerril, Fermentative biohydrogen production from tequila vinasse via the lactate-acetate pathway: Operational performance, kinetic analysis and microbial ecology, Fuel. 234 (2018) 151–160. doi:10.1016/j.fuel.2018.06.126.
[50] O. García-Depraect, I. Valdez-Vázquez, E.R. Rene, J. Gómez-Romero, A. López-López, E. León-Becerril, Lactate- and acetate-based biohydrogen production through dark co-fermentation of tequila vinasse and nixtamalization wastewater: Metabolic and microbial community dynamics, Bioresour. Technol. 282 (2019) 236–244. doi:10.1016/j.biortech.2019.02.100.
[51] A. Cabezas, J.C. de Araujo, C. Callejas, A. Galès, J. Hamelin, A. Marone, D.Z. Sousa, E. Trably, C. Etchebehere, How to use molecular biology tools for the study of the anaerobic digestion process?, Rev. Environ. Sci. Bio/Technology. 14 (2015) 555–593. doi:10.1007/s11157-015-9380-8.

[52] C. Etchebehere, E. Castelló, J. Wenzel, M. del Pilar Anzola-Rojas, L. Borzacconi, G. Buitrón, L. Cabrol, V.M. Carminato, J. Carrillo-Reyes, C. Cisneros-Pérez, L. Fuentes, I. Moreno-Andrade, E. Razo-Flores, G.R. Filippi, E. Tapia-Venegas, J. Toledo-Alarcón, M. Zaiat, Microbial communities from 20 different hydrogen-producing reactors studied by 454 pyrosequencing, Appl. Microbiol. Biotechnol. 100 (2016) 3371–3384. doi:10.1007/s00253-016-7325-y.

[53] L. Arellano-García, J.B. Velázquez-Fernández, M. Macías-Muro, E.N. Marino-Marmolejo, Continuous hydrogen production and microbial community profile in the dark fermentation of tequila vinasse: Response to increasing loading rates and immobilization of biomass, Biochem. Eng. J. 172 (2021) 108049. doi:10.1016/j.bej.2021.108049.

[54] C. Panuzzo, A. Jovanovski, M.S. Ali, D. Cilloni, B. Pergolizzi, Revealing the Mysteries of Acute Myeloid Leukemia: From Quantitative PCR through Next-Generation Sequencing and Systemic Metabolomic Profiling, J. Clin. Med. 11 (2022). doi:10.3390/jcm11030483.

[55] G. Henderson, S.C. Leahy, P.H. Janssen, Presence of novel, potentially homoacetogenic bacteria in the rumen as determined by analysis of formyltetrahydrofolate synthetase sequences from ruminants, Appl. Environ. Microbiol. 76 (2010) 2058–2066. doi:10.1128/AEM.02580-09.

[56] L. Hongyuan, J. Chen, Y. Jia, M. Cai, P.K.H. Lee, Transcriptomic responses of the interactions between Clostridium Cellulovorans 743b and Rhodopseudomonas Palustris CGA009 in a cellulose-grown coculture for enhanced hydrogen production, Appl. Environ. Microbiol. 82 (2016) 4546–4559. doi:10.1128/AEM.00789-16.

[57] A. Detman, D. Laubitz, A. Chojnacka, E. Wiktorowska-Sowa, J. Piotrowski, A. Salamon, W. Kaźmierczak, M.K. Błaszczyk, A. Barberan, Y. Chen, E. Łupikasza, F. Yang, A. Sikora, Dynamics and Complexity of Dark Fermentation Microbial Communities Producing Hydrogen From Sugar Beet Molasses in Continuously Operating Packed Bed Reactors, Front. Microbiol. 11 (2021) 1–19. doi:10.3389/fmicb.2020.612344.

Chapter 2. *The increase of biomass in suspended-biomass reactor as a strategy to improve the production of hydrogen and carboxylic acids*

Graphical abstract

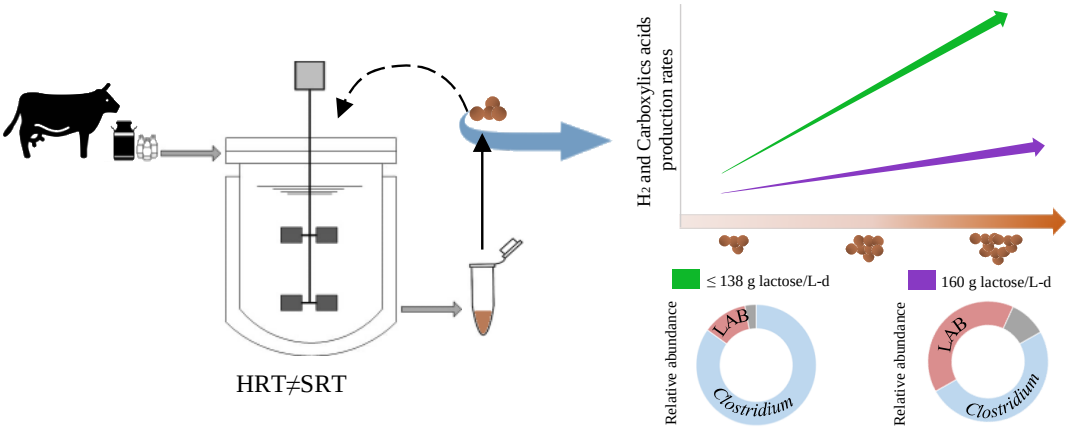

Highlights

- Up to 30.8 L H_2/L-d were produced in a CSTR with biomass recycling.
- The increase of biomass concentration enhances H_2 production rates by 19-25%.
- *Clostridium* and lactic acid bacteria co-dominated the continuous H_2 production.
- The discontinuous increase of biomass improved the carboxylic acids production by 8-23%.
- A maximum VHPR was found at specific OLR lower than 23 g COD/g VSS-d.

The present chapter is a modified version of the article:
J. de J. Montoya-Rosales, R. Palomo-Briones, L.B. Celis, C. Etchebehere, E. Razo-Flores, 2020. Discontinuous biomass recycling as a successful strategy to enhance continuous hydrogen production at high organic loading rates, *International Journal of Hydrogen Energy*, 45, 17260-17269.

2.1 Abstract

A novel strategy to discontinuously increase the biomass concentration in a continuous stirred-tank reactor was evaluated to enhance the performance of dark fermentation. Different concentrations of biomass were evaluated at organic loading rates (OLR) ranging from 90 to 160 g total carbohydrates (TC)/L-d with a hydraulic retention time (HRT) of 6 h. The study revealed that the discontinuous increase of biomass enhanced the hydrogen (H_2) production rates and carboxylic acids concentrations by 19-25% and 8-23%, respectively. In particular, a maximum H_2 production rate of 30.8 L H_2/L-d with carboxylic acids concentration of 20 g/L was reached at an OLR of 138 g TC/L-d with a biomass concentration of 15 g volatile suspended solids/L. The analysis of microbial communities showed the co-dominance of *Clostridium* and lactic acid bacteria. Overall, the discontinuous increase of biomass was an effective strategy to improve the performance of suspended-biomass reactors operated at high OLR and low HRT.

2.2 Introduction

In pursuit of sustainable and clean energy sources, hydrogen (H_2) has gained attention as a relevant actor in the future energy sector. H_2 is a gaseous chemical element with the highest energy content (142 kJ/g), its combustion is free of CO_2, and it can be produced from a wide diversity of methods [1]. Among biological methods, H_2 production via dark fermentation can be highlighted due to i) its potential to directly use wastewater and organic residues, ii) its high rate of H_2 production, and iii) its ease of operation, in comparison with photo-fermentative processes [2]. Furthermore, dark fermentation also produces carboxylic acids and other reduced end-products, such as alcohols, that can be used either as feedstock of diverse industrial processes (e.g. plastics, solvents, food, cosmetics, polymers, among others) or liquid biofuels [3].

Most of the studies about continuous H_2 production through dark fermentation have been conducted in continuous stirred-tank reactors (CSTR) with suspended-biomass, which are characterized by keeping uniform and steady concentrations of substrate, biomass, metabolic products, etc. [4]. Additionally, the highest volumetric

H_2 production rates (VHPR) have been attained mostly with CSTR systems. For instance, Cota-Navarro et al. [5] reported up to 25.8 L H_2/L-d in a CSTR fed with cheese whey. However, the H_2 production performance in a CSTR is limited by the relatively low concentration of biomass that can be maintained in the reactor in comparison with fixed-biomass systems. This is a consequence of the low specific growth rate of H_2-producing bacteria and the solids retention time (SRT) being equal to the hydraulic retention time (HRT). Specifically, at HRT between 12-4 h, required for high-performance H_2 production, the biomass concentrations in common CSTR are generally below 5 g volatile suspended solids (VSS)/L [6,7]. Therefore, to increase the H_2 production rate, the substrate consumption rate, and the substrate consumption efficiency of CSTR systems, the biomass concentration must also be increased while maintaining the HRT at relatively short times.

The increase of the biomass within the reactor can be achieved by using different cell-retention technologies, including membranes, biomass immobilization and biomass settling; such technologies also lead to more stable H_2 production at relatively low HRT (<8 h) [8–10]. In particular, biomass settling and recycling are simple to design and operate, preventing biomass from being washed-out from the reactor and allow to reach the relatively short HRT required for efficient performance [11]. For instance, Hafez et al. [2] coupled a continuous gravity settler to a common CSTR to attain HRT and SRT values of 8 and 48 h, respectively. In this manner, they found that the VHPR was about 5.3 fold the obtained without the gravity settler (9.6 L H_2/L-d vs 1.8 L H_2/L-d). Nevertheless, an important drawback of the CSTR and biomass settler configuration is that the SRT is usually above 48 h, which not only increases the reactor volume required to process a fixed wastewater flowrate but also can lead to the appearance of microbial species detrimental to H_2 production. Moreover, large volumes of the settling tank are required to efficiently separate the suspended solids from the reactor. In practice, the volume of a continuous clarification system is between 1.5 and 2 times bigger than the volume of the production tank [2,12].

In this work, a novel strategy to discontinuously increase the biomass concentration to enhance the H_2 production performance was proposed and evaluated. With this

new approach, the biomass concentration in the CSTR can be substantially increased while maintaining the SRT values similar to the HRT. In this manner, the VHPR, H_2 yields, and production of carboxylic acids are expected to improve without hindering the fermentation performance.

2.3 Materials and methods

2.3.1 Inoculum and substrate

Anaerobic granular sludge from a full-scale UASB reactor treating tequila vinasses (Casa Herradura, Mexico) was used as inoculum. The sludge was thermally treated at 105 ºC for 24 h to promote H_2-producing spore-forming microorganisms [7]. The dry inoculum was grinded and added to the reactor to obtain a final concentration of 4.5 g VSS/L. Cheese whey powder (CWP) (Darigold, USA) was used as the substrate at concentrations ranging from 22.5 to 40 g total carbohydrates (TC)/L. Each gram of CWP corresponded to 1.06 g chemical oxygen demand (COD) and 0.76 g TC. The mineral medium contained (mg/L) [6]: NH_4Cl, 2100; MgCl2·6H2O, 100; CuCl2·H2O, 1.25; MnCl2·4H2O, 7; FeCl2·4H2O, 19.1; NiCl2·6H2O, 102.5; KH2PO4, 0.125; Na2HPO4, 0.635.

2.3.2 Experimental setup

A CSTR system (Applikon Biotechnologies, USA) with a working volume of 1 L and 0.3 L of headspace was used (Figure 2.1). The reactor was started up in batch mode for 24 h using CWP at a concentration of 22 g TC/L. Afterward, the reactor was shifted to continuous operation at pH 5.9, 37 ºC, 300 rpm, and constant HRT of 6 h (flow rate = 2.8 mL/min). Different organic loading rates (OLR), ranging from 90 to 160 g TC/L-d, were evaluated at different concentrations of biomass (Table 2.1). Each OLR condition was maintained for at least 20 HRT and steady-state conditions were considered when the VHPR showed a variation lower than 10% for at least three consecutive days.

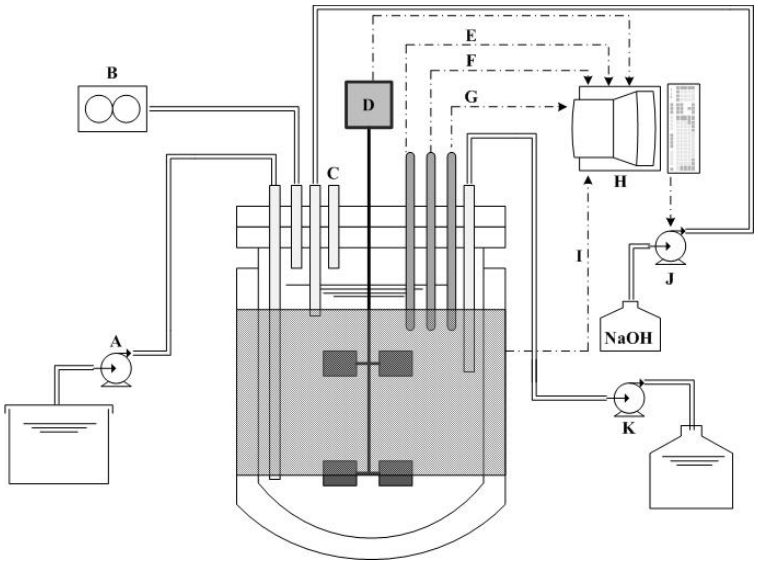

Figure 2.1 CSTR scheme. A) Inlet pump, B) Gas meter, C) Gas sampling port, D) Stirrer, E) redox electrode, F) pH electrode, G) Temperature sensor, H) Controller, I) Thermal jack, J) 5M NaOH pump, K) outlet pump.

Before increasing the biomass concentration in the CSTR at the different OLR, VSS were calculated at steady-states with no biomass increase (stages I, III, V). Once the VSS were known, a defined volume of effluent biomass was harvested and added to the reactor to reach biomass concentrations in the reactor that doubled or tripled the concentrations observed without biomass addition. To harvest the biomass, enough reactor effluent from the steady-states was collected in sealed ice-cold centrifuge bottles (500 mL) and immediately concentrated by centrifugation at 3200 rpm for 10 minutes [13]. Recovered biomass was collected and re-suspended in mineral medium to obtain 20 mL approximately of concentrated biomass. In order to avoid (as much as possible) the contact of biomass with atmospheric oxygen, the biomass was handled for a short period of time (15 to 20 min approximately, including the centrifugation step) at gentle conditions.

The addition of harvested biomass was carried out every 48 hours to sustain the desired biomass concentration. This time interval was defined from the assessment of the biomass loss profile in the CSTR evaluated in the complementary stages I^a and I^b (Figure 2.2). The harvested biomass was added by the CSTR inlet pump at a rate of 4 mL/min for 5 minutes.

2.3.3 Analytical methods

The concentration of COD and VSS was determined according to the standard methods [14] and the TC concentration by the phenol-sulfuric method [15]. The gas production and its composition (H_2 and CO_2) were measured by a liquid displacement device (SEV, Mexico) and gas chromatography with TCD detector 6890N (Agilent Technologies, Germany), respectively [16]. Carboxylic acids were quantified from filtered (0.22 μm) samples by capillary electrophoresis 1600A (Agilent Technologies, Germany) as reported previously [6]. All the gas volumes are reported at 1 atm and 273.15 K. Results are in general reported as an average value ± 1 standard deviation considering a minimum of three consecutive samples obtained from steady states.

2.3.4 Microbial community analysis

Biomass samples from the last day of each steady-state were collected from the effluent of the reactor (4 mL). Then, the biomass was harvested by centrifugation (10 min at 3200 rpm) and stored at -20 ºC until their use. The DNA was extracted using the Fungal/Bacterial DNA MiniPrep kit (Zymo Research, USA) according to the manufacturer's instructions. The V3-V4 regions of the 16S rRNA gene (~ 450 bp) were amplified with primers f-341 (CCTACGGGNGGCWGCAG) and r-785 (GACTACHVGGGTATCTAATCC) and sequenced with Illumina MiSeq and MiSeq v3 reagent kit (600 cycles) by ZymoBIOMICS laboratories (Zymo Research Corp., USA). The downstream processing was carried out with the Quantitative Insights into Microbial Ecology 2 (QIIME 2) software. Unique amplicon sequences were inferred from raw reads using the DADA2 pipeline. Chimeric sequences were also removed with the DADA2 pipeline [17]. Afterward, closed-reference OTU picking at a 97% sequence identity was achieved using BLAST+ consensus taxonomy classifier [18] with the SILVA rRNA database (release 132) as a reference (https://www.arb silva.de/download/archive/qiime/). The sequences were deposited in the NCBI BioProject PRJNA603837.

2.3.5 Calculations

The theoretical acetate produced from homoacetogenic activity was estimated from a mass balance on H_2, acetate, butyrate, and propionate using Eq. (2.1) as reported by Luo et al. (2011):

$$\text{Homoacetogenic acetate} = (2[\text{Butyrate}] + 2[\text{Acetate}] - [\text{Propionate}] - [H_2])/6 \quad (2.1)$$

Where all compounds are given in volumetric molar productivities (mole compound/L-d). The SRT in the stages where the biomass was discontinuously increased was calculated using the following equation [4]:

$$SRT = \frac{V X_a}{Q (X_a - X_c)} \quad (2.2)$$

Where V is the working volume of the reactor (L), Q is the effluent flow rate (L/d), Xa is the biomass concentration in the reactor (g VSS/L) and Xc is the concentration of biomass (g VSS/L) to be recycled from the effluent to keep the biomass concentration steady in the CSTR system. Xc was calculated as follows:

$$X_c = \frac{M_x}{(f^*V)/HRT} \quad (2.3)$$

Where Mx is the mass of biomass harvested each recycling event (g VSS), f is the time interval between two recycling events (d) and HRT is given in days.

2.3.6 Pearson's correlations

Pearson's correlation analysis was carried out using the relative abundances of most abundant bacteria, VHPR, H_2 yield, OLR, specific organic loading rate (sOLR, g COD/g VSS-d), molar fractions of carboxylic acids, and biomass concentration to gain insights on the different interactions occurring in the system. The analysis was performed in R software using the factoextra package [20].

2.4 Results and discussion

2.4.1 The performance of dark fermentation is driven by the biomass concentration

The CSTR system was operated for 74 days at different OLR and biomass concentrations as detailed in Table 2.1 and Figure 2.2. The performance results showed that VHPR was directly linked with the OLR and biomass concentration as shown in Figure 2.3. At the OLR of 90 g TC/L-d, the VHPR increased from 13.1 L H_2/L-d (stage I) to 16.3 L H_2/L-d (stage II) as a result of increasing the biomass concentration from 2.8 g VSS/L to 6.1 g VSS/L (Figure 2.3), which was equivalent to 20.2% improvement. A similar behavior of the VHPR was observed at the OLR of 138 g TC/L-d, where H_2 production increased 15.3% (from 24.7 L H_2/L-d to 29.2 L H_2/L-d) when the biomass was recycled into the system. This increase of VHPR was associated to the change of biomass concentration from 5.1 g VSS/L to 11.2 g VSS/L. In stage V, an OLR of 160 g TC/L-d resulted in a VHPR of 14.4 L H_2/L-d, which was remarkably lower than expected (Table 2.1, Figure 2.2 and Figure 2.3). In this stage, biomass concentrations also decreased to 2.5 g VSS/L. At the same OLR in stage VI, the biomass concentration was increased to 5.3 g VSS/L; however, this action did not affect the VHPR. Only when the biomass concentration was increased to 10.6 g VSS/L (stage VII), the VHPR increased by 15.3% in comparison to stage V. Finally, in stage VIII, the OLR was set back to 138 g TC/L-d and the biomass concentration was fixed to 15.1 g VSS/L (about 3-fold the biomass concentration in stage III). At such conditions, a maximum VHPR of 30.8 L H_2/L-d was obtained.

In sum, the results indicated that the discontinuous increase of biomass concentration had a positive effect on the VHPR at the OLR of 90 and 138 g TC/L-d. This behavior, has been also reported by Hafez et al. [2] in suspended biomass reactors; they observed that increasing the biomass concentration from 0.75 g VSS/L to 4.2 g VSS/L resulted in an increase of the glucose consumption efficiency from 50 to 99% with a maximum H_2 gas production of 9.6 L H_2/L-d.

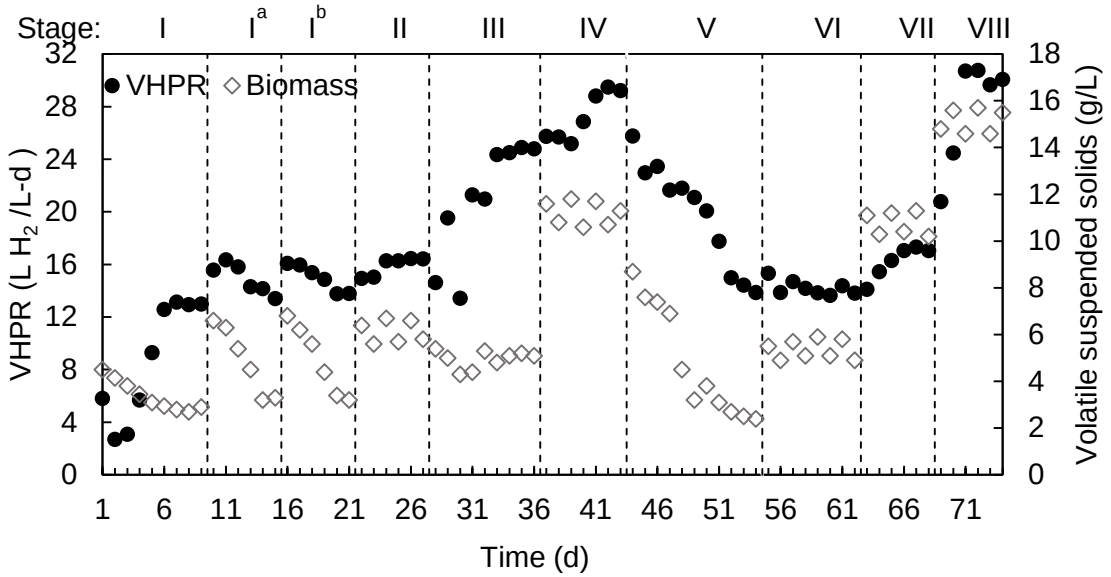

Figure 2.2 Performance of the CSTR under different operational conditions. In stages I[a] and II[b] the loss of biomass was measured at an OLR of 90 g TC/L-d. Stages with discontinuous biomass increase: II, IV, VI, VII and VIII. VHPR: volumetric hydrogen production rate. See Table 2.1 for operational conditions under each stage.

Table 2.1 Summary of steady-states in the hydrogen production in a continuous reactor at different organic loading rates and biomass concentrations.

Stage	OLR (g TC/ L-d)	Biomass concentration (g VSS/L)	sOLR (g COD/ g VSS-d)	Carbohydrates removal (%)	VHPR (L H_2/L-d)	H_2 yield[a] (mol H_2/mol hexose)	SRT (h)
I	90*	2.8 ± 0.1	44.2	92 ± 1	13.1 ± 0.1	1.28 ± 0.1	6
II	90	6.1 ± 0.5	20.3	97 ± 1	16.3 ± 0.1	1.42 ± 0.2	6.13
III	138*	5.1 ± 0.2	37.5	91 ± 2	24.7 ± 0.2	1.56 ± 0.2	6
IV	138	11.2 ± 0.5	17.1	98 ± 1	29.2 ± 0.3	1.72 ± 0.1	6.08
V	160*	2.5 ± 0.2	95.8	78 ± 3	14.4 ± 0.6	1.04 ± 0.3	6
VI	160	5.3 ± 0.4	41.6	80 ± 2	13.9 ± 0.4	1.12 ± 0.2	6.17
VII	160	10.6 ± 0.2	22.9	86 ± 2	17.2 ± 0.2	1.22 ± 0.1	6.11
VIII	138	15.1 ± 0.5	12.7	99 ± 1	30.8 ± 0.5	1.85 ± 0.2	6.07

Number of samples retrieved from the steady-states = 4, 4, 4, 3, 3, 4, 3 and 3 for stages I–VIII, respectively. [a]Calculated as equivalents of consumed hexose. *Stages without biomass increase. OLR: organic loading rate; VSS: volatile suspended solids; sOLR: specific organic loading rate; COD: chemical oxygen demand; VHPR: volumetric hydrogen production rate; STR: solids retention time.TC: total carbohydrates. Response variables are shown in the form "average ± 1 standard deviation".

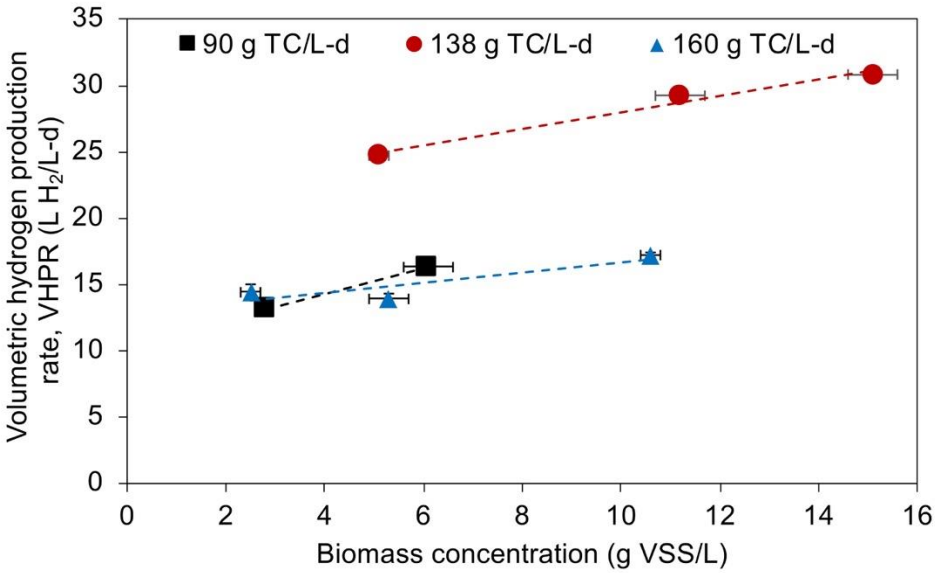

Figure 2.3 Relationship between the biomass concentration and the volumetric hydrogen production rate at the steady-states with different organic loading rates. TC: total carbohydrates.

In regard with observations of stages V-VII (OLR = 160 g TC/L-d), where the VHPR was in the range of 14.4 and 17.2 L H_2/L-d, it was clear that the high value of OLR (> 138 g TC/L-d) was detrimental for H_2 production regardless the increase of the biomass. This is possibly the result of substrate overload. For instance, Davila-Vazquez et al. [21] reported that the VHPR decreased abruptly when the OLR changed from 138 to 180 g TC/L-d in a CSTR; they also reported an increase of acetate and propionate productivities. In the present contribution, an increase of acetate concentrations (approximately 23%) were also observed when the OLR was shifted from 138 to 160 g TC/L-d.

In terms of H_2 yield, a maximum value of 1.85 mol H_2/mol hexose was found at 138 g TC/L-d and a concentration of biomass of 15.1 g VSS/L (stage VIII). In general, the H_2 yields varied from 1.04 to 1.85 mol H_2/mol hexose and also showed a clear relationship with the concentration of biomass (Table 2.1). However, when focusing on the effect of OLR, the behavior of H_2 yield was parallel to VHPR observations discussed above, which sustains the hypothesis of substrate overload at OLR > 138 g TC/L-d.

To further evaluate and understand the behavior of the CSTR at the different conditions of biomass concentration, the sOLR was calculated (Table 2.1). The results obtained for the sOLR present a direct relationship with H_2 productivities (VHPR and H_2 yield). For example, at the OLR of 138 g TC/L-d the decrease of the sOLR (controlled by the increase of biomass) is accompanied by an increase of the VHPR (stage III sOLR= 37.5 g COD/g VSS-d, VHPR= 24.7 L H_2/L-d; stage IV sOLR= 17.1 g COD/g VSS-d, VHPR= 29.2 L H_2/L-d; stage VIII sOLR= 12.7 g COD/g VSS-d, VHPR 30.8 L H_2/L-d). This finding strongly suggests that the improvement of H_2 production was probably due to the increase of the carbohydrates consumption rate in the system, which in turn is governed by the biomass concentration. Indeed, the increase of the VHPR at the different OLR values was accompanied by a decrease of the sOLR and an improvement of the carbohydrates consumption rate (Table 2.1). Interestingly, the maximum VHPR values at the different OLR were all found at sOLR lower than 23 g COD/g VSS-d. These observations are consistent with different studies that reported a decrease of H_2 production at sOLR > 20 g COD/g VSS-d [21–23].

2.4.2 The increase of biomass concentration stimulates acetate and butyrate pathways

During the CSTR operation, acetate and butyrate were the main carboxylic acids produced (Figure 2.4). In case of acetate, the concentration of such compound was quite stable in stages with OLR < 138 g TC/L-d. However, at an OLR of 160 g TC/L-d, acetate concentrations increased approximately 23% with respect to stages I to IV and VIII, while the proportion of acetate produced via homoacetogenesis (consumption of H_2 and CO_2) reached up to 50-70% (Figure 2.4). This could explain the low VHPR obtained at such OLR. In this regard, similar relationships between the production of acetate from homoacetogenesis and OLR in a CSTR have been previously reported [6,7]. Likewise, the butyrate production was improved by an average of 30% when the biomass concentration was increased at the OLR of 90 and 138 g TC/L-d. However, at the OLR of 160 g TC/L-d, the concentration of butyrate showed no major changes (Figure 2.4). Overall, the VHPR increase

observed at the OLR of 90 and 138 g TC/L-d is possibly explained by the stimulation of H_2 production via acetate-butyrate that are the fermentation pathways directly linked to higher H_2 production.

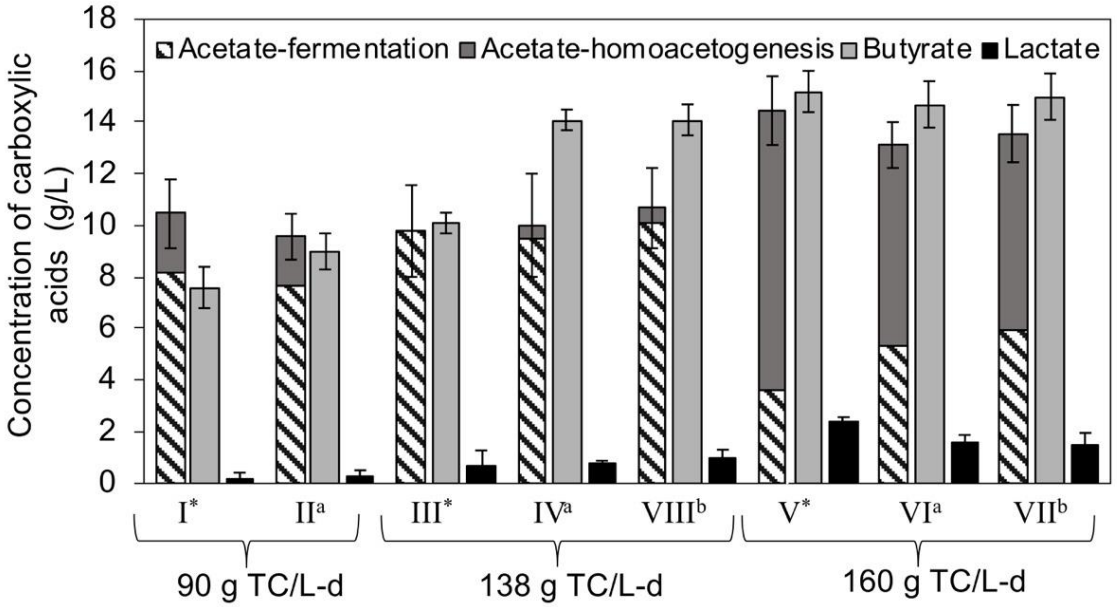

Figure 2.4 Concentration of the carboxylic acids produced with different organic loading rates and biomass concentrations in the CSTR. [a]=double and [b]=triple of biomass concentration than the observed in the periods without biomass recycling (*). TC: total carbohydrates. For each case, samples from the respective steady-states were considered.

Lactate was observed in all stages at concentrations between 0.2 to 2.4 g/L; major concentrations were found in stages V, VI and VII (at 160 g TC/L-d) and stage VIII (90 g TC/L-d) at values ranging from 1 to 2.4 g/L. This carboxylic acid has been associated with low to none H_2 production; this is because microorganisms that perform lactic acid fermentation compete with H_2-producing microorganisms for the substrate and can produce growth-inhibitory compounds. Conversely, it was reported recently that high concentrations of lactate (5 g/L) are associated to high values of VHPR and H_2 yield [6].

Different lab-scale strategies to enhance the production of carboxylic acids in dark fermentation have been evaluated elsewhere (Table 2.2); however, most of them have showed operational issues that can limit their application. For instance, the use of membranes at long-term operation present a significant decrease in its efficiencies due to fouling by biomass accumulation, being necessary to wash or change the

membrane [10]. On the other hand, the long start-up time for UASB reactors and problems with particle granulation are challenging for H_2 production in these reactors [22]. It is worth to note that the substrate concentration (48.9 g COD/L, stage VIII) used in the present work was remarkably higher than those reported elsewhere. The high substrate concentration in combination with the increase of the biomass concentration, resulted in similar yields of carboxylic acids production. However, our strategy to discontinuously increase the biomass concentration differs from others due to its simple operation and stable performance at higher OLR.

Finally, it is worth to remark that the core of the proposed strategy is the discontinuous increase of biomass concentration by recycling it from effluents. It is by no means suggested the use of centrifugation at large scale for recovery of biomass. This mechanism was selected and used in this research only for its practicality at lab-scale conditions; however, at pilot-scale or full-scale conditions, other mechanisms for the recovery of biomass (e.g. settling) could be more practical and cost-effective.

Table 2.2 Carboxylic acids produced in different configurations of continuous mesophilic reactors.

Substrate	Operational conditions	Yield of main carboxylic acids (g COD/ g COD_{feed})[a]	Carboxylic acids distribution (%)				Main drawbacks	References
			Acetate	Butyrate	Lactate	Others		
Glucose	pH 5.5, HRT 8 h, 8.5 g COD/L, integrated biohydrogen reactor clarifier system	0.69	54	34	0	12	Performance decrease at substrate concentrations (>17 g COD/L) due to competition from non H_2-producers.	[2]
Tuna waste	pH 8, HRT 10 d, 17 g COD/L, CSTR	0.73	48	28	1	23	Presence of undesired bacteria due to higher solids retention time (20 days).	[24]
Glucose	pH 5.5, HRT 6h, 16 g COD/L, CSTR with external membrane	0.47	33	54	1	12	Decrease of efficiencies due to fouling by biomass accumulation.	[25]
Galactose	No pH control, HRT 6 h, 22 g COD/L, UASB	0.48	20	71	1	7	Long start-up time for UASB reactors and problems with particle granulation.	[26]
Glucose	pH 4, HRT 2 h, 2.13 g COD/L, anaerobic	0.43	51	40	0	9	Low substrate conversion due to high OLR (> 96 g glucose/L-d)	[27]

	packed-bed reactor							
Cheese whey powder	pH 5.9, HRT 6 h, 48.9 g COD/L, CSTR with discontinuous biomass addition (Stage VIII)	0.59	35	59	6	0	Decrease in H_2 production at OLR higher than 138 g TC/L-d	This study

[a]Main carboxylic acids are acetate, butyrate, and lactate.
COD: chemical oxygen demand; HRT: hydraulic retention time; UASB: up-flow anaerobic sludge blanket reactor CSTR: continuous stirred tank reactor; OLR: organic loading rate; TC: total carbohydrates.

2.4.3 Microbial community analysis

The 16S-rRNA sequencing resulted in 53,260 ± 13,030 high-quality reads per sample that were grouped in 290 OTUS. In general, the sequencing analysis revealed that H_2 production was performed by a microbial community dominated by organisms from the genera *Clostridium*, *Sporolactobacillus* and *Lactobacillus* that accounted for about 90% of the relative abundance during all reactor operation (Figure 2.5). Bacteria of the genus *Clostridium* are commonly considered as the most abundant and efficient H_2-producing bacteria in dark-fermentative systems since they are usually dominant during the periods of highest H_2 production efficiency [28]. On the other hand, *Sporolactobacillus* and *Lactobacillus* are lactic acid bacteria (LAB) considered as the main competitors (for substrate) of H_2-producing bacteria [29]. LAB can also cause inhibition by producing high amounts of lactate and bacteriocins [30]. Nevertheless, their effects on dark fermentative systems remain under discussion [31]. Other genera such as *Klebsiella* (< 1%), *Lactococcus* (< 4%), *Caproiciproducens* (< 11%), *Leuconostoc* (< 3.6%) and *Robinsoniella* (< 11%) were also found at low levels of relative abundance.

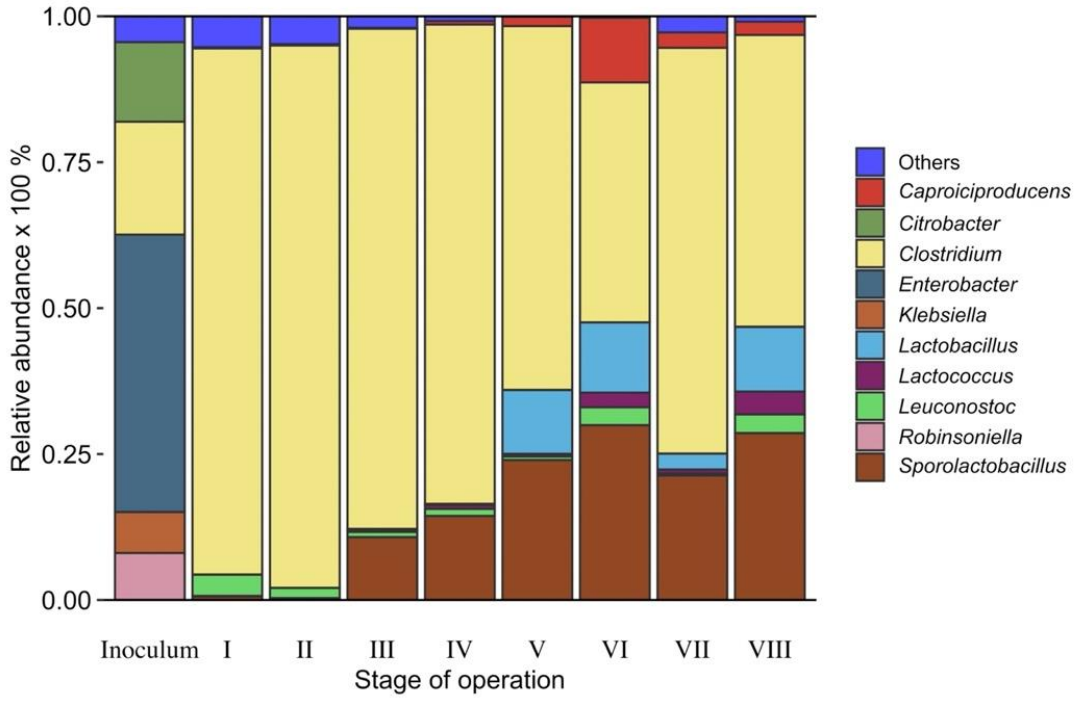

Figure 2.5 Microbial community dynamics of the continuous stirred-tank reactor during stages I to VIII. Genera with relative abundance <1% were grouped as others.

As shown in Figure 2.5 the relative abundance of the dominant genera was similar in stages with the same OLR regardless of the biomass concentration. In stages I and II (OLR of 90 g TC/L-d), the system was dominated by the *Clostridium* genus that accounted up to 91% of relative abundance in the fermentation broth. At the OLR of 138 g TC/L-d in stages III and IV, *Clostridium* genus displayed dominance of approximately 83% of relative abundance, while *Sporolactobacillus* genus was detected with a dominance of less than 13% of relative abundance. In stages V, VI and VII (OLR of 160 g TC/L-d), the relative abundance of *Clostridium* genus decreased to about 50% with the concomitant increase of the proportions of the genera *Sporolactobacillus* and *Lactobacillus* (25% and 10%, respectively). Finally, in stage VIII (OLR = 138 g TC/L-d) the relative abundance of the *Clostridium* genus was 50%, with the presence of the genera *Sporolactobacillus* and *Lactobacillus* in relative abundance of 28% and 11%, respectively. It was observed that an OLR $\geq$ 138 TC/L-d the presence of *Lactobacillus* and *Sporolactobacillus* is concomitant to H_2-producers, therefore we hypothesized that members of these genera could be directly involved in H_2 production, by providing extra substrate to H_2-producing bacteria in the form of lactate, or by directly converting lactate to H_2 and butyrate [28]. Nevertheless, at the OLR of 160 g TC/L-d the relative abundance of LAB increased, this increase can be linked to the abundance of substrate that enhance the competence between H_2-producing bacteria and LAB [32], causing a considerable drop of the H_2 production in our system. According to our results, the role of LAB as detrimental for H_2 production should not be taken for granted, since in certain conditions they only compensate the *Clostridium* inability to consume all the substrate that is being fed into the reactor.

To further investigate the relationships between the microbial community and dark fermentation performance, a Pearson´s correlation analysis was carried out (Figure 2.6.). The relative abundance of the *Clostridium* genus was correlated positively with the acetate production via fermentation ($r = 0.85$, $p < 0.01$). Meanwhile, the relative abundance of *Clostridium* was correlated negatively with the lactate concentration ($r = 0.85$, $p < 0.01$). On the other hand, the analysis confirmed that LAB (*Lactobacillus* and *Sporolactobacillus*) were correlated with the production of lactate ($r = 0.72$, p

=0.04 and r=0.90, p<0.01). The lactic acid fermentation and homoacetogenesis could be a response to the accumulation of H_2 in the fermentation broth that was probably taking place at high OLR.

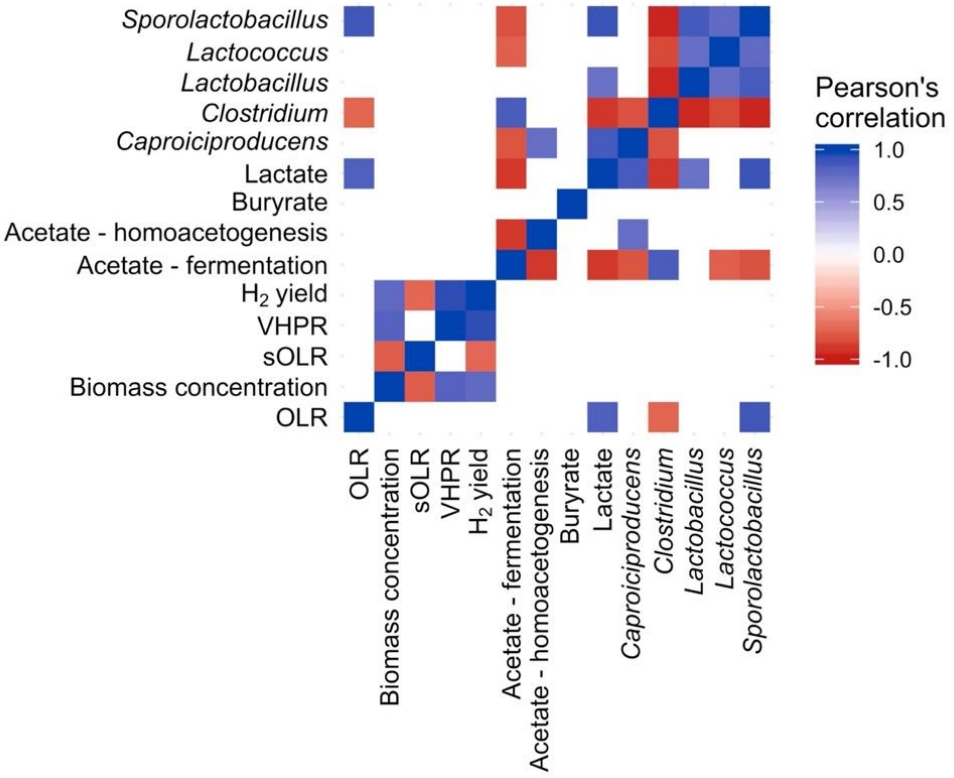

Figure 2.6 Matrix of Pearson's correlations ($p < 0.05$). OLR: organic loading rate (g TC/L-d); biomass concentration (g VSS/L); sOLR: specific organic loading rate (g COD/g VSS-d); VHPR: volumetric hydrogen production rate (L H_2/L-d); H_2 yield (mol H_2/mol hexose); acetate, lactate and butyrate (mol/total moles of carboxylic acids); microorganisms were analyzed in terms of their relative abundance. COD: chemical oxygen demand; VSS: volatile suspended solids. TC: total carbohydrates.

Although no significant correlation was observed between the relative abundance of the *Clostridium* genus and acetate produced by homoacetogenesis ($p = 0.15$), it has been widely reported that different microbial species belonging to the *Clostridium* genus are able to produce H_2 via dark fermentation but also to consume H_2 via homoacetogenesis (e.g. C. *ljungdahili*, C. *acetobutylicum*) [28,32,33]. This is the most probable explanation behind the lack of correlation. In this way, other techniques such as gene-specific qPCR can be used [34].

Interestingly, at the OLR of 160 g TC/L-d, the increase of biomass concentration resulted in a slight decrease of both lactate and acetate-homoacetogenesis (Figure

2.4); however, the low H_2 productivities observed at such OLR indicated that LAB were probably present in high abundance and that the productivity of homoacetogenic acetate was still at high levels (approximately 60% of the total acetate produced). The production of acetate by homoacetogenesis (that represented about 50% of the total acetate observed) has been widely reported as one of the principal causes of CSTR instability at OLR > 30 g COD/L-d [32,35]. For instance, more experiments will be required to confidently determine if the biomass recycling has any effect on homoacetogenesis and the presence of LAB.

2.4.4 Implications of the discontinuous biomass recovery and recycling strategy.

As shown in Table 2.1 and Table 2.3, in all the cases with biomass recycling (stages II, IV, VI, VII, and VIII) the SRT values were quite close to the HRT used in the reactor (SRT ranged from 6.07 to 6.17 h). The proximity of the SRT and the HRT could sound counterintuitive since the concentrations of biomass were substantially increased from one stage to another; however, this is due to the fact that small amounts (between 1.1 to 1.5 g VSS) of biomass were required (added every 48 hours) to maintain the concentration at the desired value.

Table 2.3 Solids retention time values in the stages with biomass increase in the suspended-biomass reactor.

Stage	OLR (g TC/L-d)	M_x (g VSS)	f (d)	X_c [a] (g VSS/L)	X_a (g VSS/L)	SRT[b] (h)
II	90	1.1	2	0.137	6.1	6.13
IV	138	1.2	2	0.150	11.2	6.08
VI	160	1.2	2	0.150	5.3	6.17
VII	160	1.4	2	0.175	9.6	6.11
VIII	138	1.5	2	0.187	15.1	6.07

[a] X_c was calculated according equation (2.2) presented in section 2.3.5
[b] SRT was calculated according equation (3) presented in section 2.5
M_x: mass of biomass harvested in each recycling event (g VSS); f: time interval between two recycling events (d); X_c: concentration of biomass recycled from the effluent to keep the biomass concentration (g VSS/L) steady in the continuous stirred-tank reactor; X_a: biomass concentration in the reactor (g VSS/L); SRT: solids retention time (h). TC: total carbohydrates.

The discontinuous increase of biomass concentration by means of recycling biomass from fermentation effluents was similar to bioaugmentation, which is the addition of specialized microorganisms to improve a given process [36]. Nonetheless, the strategy followed in this work did not aim to augment the relative abundance of any particular microbial species. Still, the addition of biomass collected from the effluent demonstrated an improvement in the production of carboxylic acids and H_2, which is the principal objective in a bioaugmentation strategy. At the same time, the use of this strategy, allowed the use of low values of SRT (similar to HRT) that limited the increase of non H_2-producing bacteria.

2.5 Conclusions

The discontinuous increase of biomass concentration by means of biomass recycling successfully enhanced the production of H_2 and carboxylic acids at OLR $\leq$ 138 g TC/L-d. Following such strategy, a maximum VHPR of 30.8 L H_2/L-d and total carboxylic acids concentrations of 20 g/L, were obtained at an OLR of 138 g TC/L-d with a biomass concentration of 15.1 g VSS/L. The microbial community was dominated by *Clostridium* and lactic acid bacteria that could promote H_2 production through a beneficial symbiosis between them at OLR lower than 138 g TC/L-d. In deep analysis of results showed that the specific OLR is a key factor that controls the performance in continuous dark fermentative systems while avoiding substrate overload. Overall, the discontinuous biomass recycling was proposed for the first time as a successful strategy to enhance continuous H_2 production performance at high OLR.

2.6 References

[1] P. Sivagurunathan, G. Kumar, A. Mudhoo, E.R. Rene, G.D. Saratale, T. Kobayashi, K. Xu, S.H. Kim, D.H. Kim, Fermentative hydrogen production using lignocellulose biomass: An overview of pre-treatment methods, inhibitor effects and detoxification experiences, Renew. Sustain. Energy Rev. 77 (2017) 28–42. doi:10.1016/j.rser.2017.03.091.

[2] H. Hafez, B. Baghchehsaraee, G. Nakhla, D. Karamanev, A. Margaritis, H. El Naggar, Comparative assessment of decoupling of biomass and hydraulic retention times in hydrogen production bioreactors, Int. J. Hydrogen Energy. 34 (2009) 7603–7611. doi:10.1016/j.ijhydene.2009.07.060.

[3] D.Y. Lee, Y.Y. Li, T. Noike, Influence of solids retention time on continuous H2

production using membrane bioreactor, Int. J. Hydrogen Energy. 35 (2010) 52–60. doi:10.1016/j.ijhydene.2009.10.010.
[4] B.E. Rittmann, P.L. McCarty, Environmental Biotechnology: Principles and Applications, 2001.
[5] C.B. Cota-Navarro, J. Carrillo-Reyes, G. Davila-Vazquez, F. Alatriste-Mondragón, E. Razo-Flores, Continuous hydrogen and methane production in a two-stage cheese whey fermentation system, Water Sci. Technol. 64 (2011) 367–374. doi:10.2166/wst.2011.631.
[6] R. Palomo-Briones, E. Trably, N.E. López-Lozano, L.B. Celis, H.O. Méndez-Acosta, N. Bernet, E. Razo-Flores, Hydrogen metabolic patterns driven by Clostridium-Streptococcus community shifts in a continuous stirred tank reactor, Appl. Microbiol. Biotechnol. 102 (2018) 2465–2475. doi:10.1007/s00253-018-8737-7.
[7] J. de J. Montoya-Rosales, D.K. Olmos-Hernández, R. Palomo-Briones, V. Montiel-Corona, A.G. Mari, E. Razo-Flores, Improvement of continuous hydrogen production using individual and binary enzymatic hydrolysates of agave bagasse in suspended-culture and biofilm reactors, Bioresour. Technol. 283 (2019) 251–260. doi:https://doi.org/10.1016/j.biortech.2019.03.072.
[8] S.E. Oh, P. Iyer, M.A. Bruns, B.E. Logan, Biological hydrogen production using a membrane bioreactor, Biotechnol. Bioeng. 87 (2004) 119–127. doi:10.1002/bit.20127.
[9] D.Y. Lee, Y.Y. Li, T. Noike, Continuous H2 production by anaerobic mixed microflora in membrane bioreactor, Bioresour. Technol. 100 (2009) 690–695. doi:10.1016/j.biortech.2008.06.056.
[10] M. Saleem, M.C. Lavagnolo, A. Spagni, Biological hydrogen production via dark fermentation by using a side-stream dynamic membrane bioreactor: Effect of substrate concentration, Chem. Eng. J. 349 (2018) 719–727. doi:10.1016/j.cej.2018.05.129.
[11] H. Liu, Y. Wang, B. Yin, Y. Zhu, B. Fu, H. Liu, Improving volatile fatty acid yield from sludge anaerobic fermentation through self-forming dynamic membrane separation, Bioresour. Technol. 218 (2016) 92–100. doi:10.1016/j.biortech.2016.06.077.
[12] J.C. Zemor, W. Wasielesky, G.K. Fóes, L.H. Poersch, The use of clarifiers to remove and control the total suspended solids in large-scale ponds for production of Litopenaeus vannamei in a biofloc system, Aquac. Eng. 85 (2019) 74–79. doi:https://doi.org/10.1016/j.aquaeng.2019.03.001.
[13] G. Dreschke, G. d'Ippolito, A. Panico, P.N.L. Lens, G. Esposito, A. Fontana, Enhancement of hydrogen production rate by high biomass concentrations of Thermotoga neapolitana, Int. J. Hydrogen Energy. 43 (2018) 13072–13080. doi:10.1016/j.ijhydene.2018.05.072.
[14] APHA/AWWA/WEF, Standard Methods for the Examination of Water and Wastewater, Stand. Methods. (2012). doi:ISBN 9780875532356.
[15] M. Dubois, K.A.Gilles, J.K.Hamilton, P.A.Rebers, Fred.Smith, Colorimetric Method for Determination of Sugars and Related Substances, Anal. Chem. 28 (1956) 350–356. doi:10.1021/ac60111a017.
[16] C.A. Contreras-Dávila, H.O. Méndez-Acosta, L. Arellano-García, F. Alatriste-Mondragón, E. Razo-Flores, Continuous hydrogen production from enzymatic hydrolysate of Agave tequilana bagasse: Effect of the organic loading rate and reactor configuration, Chem. Eng. J. 313 (2017) 671–679. doi:10.1016/j.cej.2016.12.084.
[17] B.J. Callahan, P.J. McMurdie, M.J. Rosen, A.W. Han, A.J.A. Johnson, S.P. Holmes, DADA2: High-resolution sample inference from Illumina amplicon data, Nat. Methods. 13 (2016) 581. https://doi.org/10.1038/nmeth.3869.
[18] C. Camacho, G. Coulouris, V. Avagyan, N. Ma, J. Papadopoulos, K. Bealer, T.L. Madden, BLAST+: architecture and applications, BMC Bioinformatics. 10 (2009) 421.

doi:10.1186/1471-2105-10-421.
[19] G. Luo, D. Karakashev, L. Xie, Q. Zhou, I. Angelidaki, Long-term effect of inoculum pretreatment on fermentative hydrogen production by repeated batch cultivations: Homoacetogenesis and methanogenesis as competitors to hydrogen production, Biotechnol. Bioeng. 108 (2011) 1816–1827. doi:10.1002/bit.23122.
[20] R. Palomo-Briones, E. Razo-Flores, N. Bernet, E. Trably, Dark-fermentative biohydrogen pathways and microbial networks in continuous stirred tank reactors: Novel insights on their control, Appl. Energy. 198 (2017) 77–87. doi:10.1016/j.apenergy.2017.04.051.
[21] E. Elbeshbishy, B.R. Dhar, G. Nakhla, H.S. Lee, A critical review on inhibition of dark biohydrogen fermentation, Renew. Sustain. Energy Rev. 79 (2017) 656–668. doi:10.1016/j.rser.2017.05.075.
[22] N. Nasr, E. Elbeshbishy, H. Hafez, G. Nakhla, M.H. El Naggar, Bio-hydrogen production from thin stillage using conventional and acclimatized anaerobic digester sludge, Int. J. Hydrogen Energy. 36 (2011) 12761–12769. doi:10.1016/j.ijhydene.2011.07.032.
[23] G. Davila-Vazquez, C.B. Cota-Navarro, L.M. Rosales-Colunga, A. de León-Rodríguez, E. Razo-Flores, Continuous biohydrogen production using cheese whey: Improving the hydrogen production rate, Int. J. Hydrogen Energy. 34 (2009) 4296–4304. doi:10.1016/j.ijhydene.2009.02.063.
[24] N. Bermúdez-Penabad, C. Kennes, M.C. Veiga, Anaerobic digestion of tuna waste for the production of volatile fatty acids, Waste Manag. 68 (2017) 96–102. doi:10.1016/j.wasman.2017.06.010.
[25] J.H. Park, J.H. Park, Y.B. Sim, S.H. Kim, H.D. Park, Formation of a dynamic membrane altered the microbial community and metabolic flux in fermentative hydrogen production, Bioresour. Technol. 282 (2019) 63–68. doi:10.1016/j.biortech.2019.02.124.
[26] P. Sivagurunathan, P. Anburajan, G. Kumar, J.H. Park, S.H. Kim, Recovering hydrogen production performance of upflow anaerobic sludge blanket reactor (UASBR) fed with galactose via repeated heat treatment strategy, Bioresour. Technol. 240 (2017) 207–213. doi:10.1016/j.biortech.2017.03.062.
[27] J.A.C. Leite, B.S. Fernandes, E. Pozzi, M. Barboza, M. Zaiat, Application of an anaerobic packed-bed bioreactor for the production of hydrogen and organic acids, Int. J. Hydrogen Energy. 33 (2008) 579–586. doi:10.1016/j.ijhydene.2007.10.009.
[28] L. Cabrol, A. Marone, E. Tapia-Venegas, J.P. Steyer, G. Ruiz-Filippi, E. Trably, Microbial ecology of fermentative hydrogen producing bioprocesses: Useful insights for driving the ecosystem function, FEMS Microbiol. Rev. 41 (2017) 158–181. doi:10.1093/femsre/fuw043.
[29] Y. Rafrafi, E. Trably, J. Hamelin, E. Latrille, I. Meynial-Salles, S. Benomar, M.T. Giudici-Orticoni, J.P. Steyer, Sub-dominant bacteria as keystone species in microbial communities producing bio-hydrogen, Int. J. Hydrogen Energy. 38 (2013) 4975–4985. doi:10.1016/j.ijhydene.2013.02.008.
[30] T. Noike, H. Takabatake, O. Mizuno, M. Ohba, Inhibition of hydrogen fermentation of organic wastes by lactic acid bacteria, Int. J. Hydrogen Energy. 27 (2002) 1367–1371. doi:10.1016/S0360-3199(02)00120-9.
[31] S. Morra, M. Arizzi, P. Allegra, B. La Licata, F. Sagnelli, P. Zitella, G. Gilardi, F. Valetti, Expression of different types of [FeFe]-hydrogenase genes in bacteria isolated from a population of a bio-hydrogen pilot-scale plant, Int. J. Hydrogen Energy. 39 (2014) 9018–9027. doi:10.1016/j.ijhydene.2014.04.009.
[32] R. Palomo-Briones, L.B. Celis, H.O. Méndez-Acosta, N. Bernet, E. Trably, E. Razo-Flores, Enhancement of mass transfer conditions to increase the productivity and

efficiency of dark fermentation in continuous reactors, Fuel. 254 (2019) 115648. doi:10.1016/j.fuel.2019.115648.
[33] E. Castelló, A.D. Nunes Ferraz-Junior, C. Andreani, M. del P. Anzola-Rojas, L. Borzacconi, G. Buitrón, J. Carrillo-Reyes, S.D. Gomes, S.I. Maintinguer, I. Moreno-Andrade, R. Palomo-Briones, E. Razo-Flores, M. Schiappacasse-Dasati, E. Tapia-Venegas, I. Valdez-Vázquez, A. Vesga-Baron, M. Zaiat, C. Etchebehere, Stability problems in the hydrogen production by dark fermentation: Possible causes and solutions, Renew. Sustain. Energy Rev. 119 (2019). doi:10.1016/j.rser.2019.109602.
[34] O. Okonkwo, A.M. Lakaniemi, V. Santala, M. Karp, R. Mangayil, Quantitative real-time PCR monitoring dynamics of Thermotoga neapolitana in synthetic co-culture for biohydrogen production, Int. J. Hydrogen Energy. 43 (2018) 3133–3141. doi:10.1016/j.ijhydene.2017.12.002.
[35] E. Castelló, L. Braga, L. Fuentes, C. Etchebehere, Possible causes for the instability in the H2 production from cheese whey in a CSTR, Int. J. Hydrogen Energy. 43 (2018) 2654–2665. doi:10.1016/j.ijhydene.2017.12.104.
[36] Z. Yang, R. Guo, X. Shi, S. He, L. Wang, M. Dai, Y. Qiu, X. Dang, Bioaugmentation of Hydrogenispora ethanolica LX-B affects hydrogen production through altering indigenous bacterial community structure, Bioresour. Technol. 211 (2016) 319–326. doi:10.1016/j.biortech.2016.03.097.

Chapter 3. *Two-phase partition reactor as a strategy to improve the productivity of dark fermentation systems*

Graphical abstract

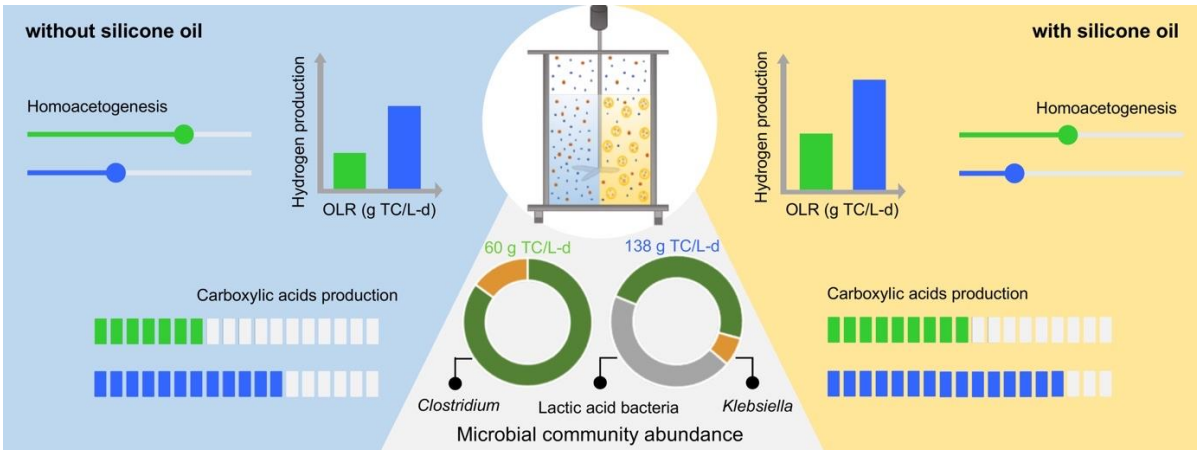

Highlights

- Two-phase system reduces inhibition caused by dissolved H_2.
- Organic extractive phase increases the interfacial area available for mass transfer.
- Enhancement of mass transfer promotes the metabolic dark fermentation pathways.
- Up to 27.6 L H2/L-d were produced in a CSTR with 10% v/v silicone oil.
- 10 % v/v silicone oil in a CSTR improved the carboxylic acids production by 13–66%.

The present chapter is a modified version of the article:
J. de J. Montoya-Rosales, R. Palomo-Briones, L.B. Celis, C. Etchebehere, L.F. Cházaro-Ruiz, V. Escobar-Barrios, E. Razo-Flores, 2022. Coping with mass transfer constrains in dark fermentation using a two-phase partitioning bioreactor, *Chemical Engineering Journal*, 445, 136749.

3.1 Abstract

In dark fermentation systems, the accumulation of byproducts (i.e., carboxylic acids, hydrogen) in the aqueous phase can cause the inhibition of key metabolic pathways. Two-phase partitioning reactors are an alternative solution for reducing the concentration of hydrogen (H_2) and CO_2 in the aqueous phase by improving the mass transfer of these gases to the organic phase. From batch reactors, it was found that silicone oil at a proportion of 10% (v/v) led to the highest volumetric H_2 production rate (VHPR, 4.1 L H_2/L-d). The results in continuous reactors showed that using silicon oil the VHPR and carboxylic acids production increased up to 13% and 24%, respectively (i.e., VHPR = 27.6 L H_2/L-d and 29.8 g/L of carboxylic acids at a substrate loading of 138 g total carbohydrates/L-d). These results could be explained by the enhancement of the following mass-transfer mechanisms: i) H_2 and CO_2 transfer from microorganisms to the extractive organic phase, ii) Diffusion of dissolved H_2 and CO_2 into the extractive organic phase, and iii) Transfer by convection of dissolved H_2 and CO_2 to the gas phase. Furthermore, the thermodynamic analysis revealed that the addition of silicone oil also improved the feasibility of the fermentation process by increasing the Gibbs free energy up to 27% compared to the control without silicone oil (i.e., –172.6 kJ/mol vs –219.23 kJ/mol, at a substrate loading of 60 g total carbohydrates/L-d). Overall, the use of an organic extractive phase is a novel and effective strategy to increase the performance of dark fermentation systems for biofuel production.

3.2 Introduction

Facultative and strict anaerobic microorganisms can perform dark fermentation converting carbohydrate-rich substrates into hydrogen (H_2), CO_2, and carboxylic acids. Dark fermentation can take place via two main metabolic routes: the pyruvate formate lyase and the pyruvate ferredoxin oxidoreductase pathway [1], with maximum theoretical H_2 yields of 2 and 4 mol H_2 per mol of consumed hexose, respectively.

Typically, in H_2-producing continuous reactors, the volumetric H_2 production rates (VHPR) have a positive correlation with the organic loading rate (OLR) [2,3].

However, it has been reported that the H_2 yield and VHPR decrease at OLR > 100 g of chemical oxygen demand (COD)/L-d [4,5]. In general, the VHPR and H_2 yield depend on multiple factors, including the substrate and operational conditions (e.g., temperature, pH, mixing, hydraulic retention time), the composition of the microbial communities, and the concentrations of H_2, CO_2, and carboxylic acids in the aqueous phase. In particular, the accumulation of fermentation byproducts (i.e., carboxylic acids, H_2) in the aqueous phase could lead to inhibition of metabolic pathways of dark fermentation. Such inhibition can be tracked through the change of Gibbs free energy (ΔG). When the change of ΔG is negative, the reaction under study proceeds spontaneously in the written direction, without the need for external energy input [6]. On the contrary, positive values of ΔG indicate that the reaction under study cannot proceed spontaneously in the written direction, and can be considered a bottleneck. Regarding dark fermentation systems, the increase in the concentrations of dissolved H_2 increases the Gibbs free energy values, affecting the efficiency of product formation in the system [7].

In H_2-producing reactors, the control of mass transfer bottlenecks ultimately depends on the global mass transfer rate of H_2 and CO_2 across the liquid–gas interphase (Q, g/L-m^2). The magnitude of the mass transfer rate is defined by 1) the concentration gradient between the fermentation bulk and the interphase (ΔC, g/L), and 2) the global mass transfer coefficient (k_La, 1/h) (Eq. (3.1)).

$$Q = k_L a * (\Delta C) \quad (3.1)$$

From Equation 3.1, improving the H_2 and CO_2 mass transfer rates can be attained by increasing the value of k_La. For that matter, different strategies such as the increase of stirring velocity, selective separation of gases by membranes, gas sparging, and gas recirculation have been evaluated to improve H_2 and CO_2 mass transfer rates [8, 9, 10, 11, 12, 13]. Nevertheless, these strategies have led to low biomass concentrations (due to physiological changes caused by vigorous mixing), H_2 dilution, among other problems, affecting the dark fermentation performance [14],

and highlighting the need to evaluate different strategies to enhance dark fermentation.

Alternatively, the mass transfer of H_2 and CO_2 to the gas phase could be increased with the use of two-phase partitioning bioreactors. These systems imply the addition of an extractive organic phase to the aqueous phase where fermentative microorganisms are contained. The extractive organic phase increases the total mass transfer area, leading to higher global mass transfer rates. Ultimately, this can also decrease the aqueous phase concentration of substances that could be inhibitory to microorganisms [15]. To be applied in biological systems, the extractive organic phase must be biocompatible and non-biodegradable, in addition to having a high affinity for the target gas or gases, low cost, insoluble in water, etc. [16]. The affinity of the extractive organic phase toward the target gaseous substrate can be quantified through the partition coefficient (H, dimensionless). In particular, silicone oil has been widely reported as an excellent compound for extracting volatile compounds (e.g. hexane, toluene, BTEX, among others) in gas-treatment biotechnologies [15]. However, the addition of an extractive organic phase in dark fermentation processes has not been explored up to date. In this work, we hypothesized that adding an extractive organic phase to dark fermentation processes could improve the mass transfer of H_2 and CO_2 from the aqueous phase to either the gas phase or the extractive organic phase, reducing the concentration of dissolved H_2 and CO_2. Therefore, the objective was to implement a novel two-phase partitioning bioreactor to enhance the production of H_2 and carboxylic acids and evaluate the effect on the composition of microbial communities in such dark fermentation system.

3.3 Materials and methods

3.3.1 Substrate, inoculum, mineral medium, and organic phase

Cheese whey powder (CWP, Chilchota Alimentos S.A de C.V, Mexico) was used as the substrate for the H_2 production experiments. Each gram of CWP contains 1.06 g COD and 0.77 g of total carbohydrates (TC). The granular seed sludge was obtained from a full-scale up-flow anaerobic sludge bed reactor treating tequila vinasses

(Casa Herradura, Mexico), and was thermally treated at 105 °C for 24 h according to Contreras-Davila et al. [17]. After pretreatment, the sludge contained 0.94 g of total suspended solids (TSS)/g sludge and 0.87 g of volatile suspended solids (VSS)/g sludge.

The mineral medium was modified from Palomo-Briones et al. [11] to contain (mg/L): NH_4Cl, 2100; $MgCl_2 \cdot 6H_2O$, 100; $CuCl_2 \cdot H_2O$, 1.25; $MnCl_2 \cdot 4H_2O$, 7; $FeCl_2 \cdot 4H_2O$, 19.1; $NiCl_2 \cdot 6H_2O$, 102.5.KH_2PO_4. In addition, a phosphate buffer (KH_2PO_4-Na_2HPO_4) was added to reach a final concentration of 50 mM. Silicone oil (CHEM SIL, Mexico) with a viscosity of 100 centistokes was used as the extractive organic phase.

3.3.2 Dark fermentation batch experiments

To evaluate the effect of silicone oil on hydrogen and carboxylic acids production by dark fermentation, a series of batch experiments were performed with different proportions of silicone oil (2.5, 5, 10, 20, and 30% v/v). An additional experiment without silicone oil was used as control, while another one with silicone oil (10% v/v) but without substrate was used to evaluate the stability of silicone oil.

The batch experiments were carried out in an automatic methane potential test system (AMPTS II, Bioprocess Control, Sweden) following the methodology described elsewhere [18]. In brief, 600 mL glass bottles (360 mL of working volume) were prepared with a substrate concentration of 5 g TC/L and inoculated at a substrate/inoculum (S/I) ratio of 2.7 g TC/g volatile solids (VS). The initial pH of all experiments was adjusted to 7.5. The incubation conditions were set at 37 °C and intermittent stirring (1 min stirring at 120 rpm with 3 min pause between stirring). All fermentation experiments were conducted by triplicate. The proportion of silicone oil that showed the highest H_2 productivity was selected to conduct further continuous dark fermentation experiments. The H_2 production was modeled with the modified Gompertz equation (Eq. 3.2) using the *solver* tool of Microsoft Excel (2019).

$$H(t) = H_{max} \exp\left\{ - \exp\left[\frac{2.71828 * R_{max}}{H_{max}} (\lambda - t) + 1\right]\right\} \quad (3.2)$$

where H (t) stands for the cumulative H_2 volume (L H_2/L) across time t (d), H_{max} is the maximum cumulative H_2 volume (L H_2/L), R_{max} is the maximum H_2 production rate (L H_2/L-d), and λ is the lag time (d).

To quantify the H_2 and CO_2 absorbed in the silicone oil at the end of the batch experiments, the silicone oil was separated from the fermentation broth (of each bottle) using a 1 L separation funnel. The silicone oil recovered was transferred to 120 mL glass bottles, which were sealed and heated (50–60 °C) on a hot plate for 10 min. The desorption of gases by increasing the temperature of silicone oil, is a gas-desorption strategy with recovery percentages between 90 and 95% [19]. The gas volume released was measured by liquid displacement using an inverted burette immersed in acidified water (pH 2). The gas composition was determined by gas chromatography.

3.3.3 Dark fermentation continuous experiments

To evaluate the effect of silicone oil on the continuous H_2 production, a continuous stirred tank reactor (CSTR, Applikon model Z310210011, The Netherlands) of 1.3 L total volume (1 L working volume) was set and operated at organic loading rates (OLR) of 60 and 138 g TC/L-d. The reactor was started up in batch mode for 24 h with 4.5 g VSS/L of heat-treated anaerobic sludge and 22 g TC/L of CWP. Thereafter, the reactor was shifted to continuous operation at a fixed hydraulic retention time (HRT) of 6 h (input flow rate of 2.8 mL/min). Temperature (37 °C), pH (5.9), and stirring velocity (300 rpm) were automatically controlled. The CSTR was operated during four stages: Stages I and III served as control stages without the addition of extractive organic phase. In stages II and IV, silicone oil was added at the proportion that showed the highest H_2 productivity in the batch experiments. Each stage was maintained for at least 10 HRT (60 h), and steady-state conditions were considered when the VHPR showed a variation lower than 10% for at least three consecutive quantifications.

To maintain the continuous regime in stages II and IV, while continuously adding silicone oil, the input flow rates of the substrate and the silicone oil pumps were adjusted to keep the desired proportion of silicone oil and constant HRT of 6 h. It is

worth mentioning that, between stages II and III, the reactor was operated for two days at an OLR of 60 g TC/L-d without extractive organic phase to flush out the silicone oil from the previous stage as much as possible. Finally, the silicone oil was recovered to quantify the absorbed H_2 and CO_2 during the steady states at stages II and IV, as described in Section 3.3.2

3.3.4 Microbial community analysis

To elucidate the effect of silicone oil on the microbial community dynamics of the CSTR, biomass samples (6 mL) from the last day of each steady-state were collected from the effluent. Subsequently, the biomass was harvested by centrifugation (10 min at 3200 rpm) and stored at −20 °C until use. The DNA was extracted from the biomass samples using the Fungal/Bacterial DNA Miniprep kit (Zymo Research, USA) according to the manufacturer's instructions. The Illumina MiSeq and MiSeq v3 reagent kits (600 cycles) were used for sequencing the V3-V4 regions of the 16S-rRNA gene. Sequencing was carried out at ZymoBIOMICS laboratories (Zymo Research Corp., USA). The downstream processing was performed with the Quantitative Insights Into Microbial Ecology 2 (QIIME 2) software, following the methodology previously reported [4]. The sequences were deposited in the NCBI Bioproject PRJNA742404.

3.3.5 Partition coefficients evaluation

To determine the partition coefficient (H, dimensionless) of H_2 and CO_2 in the silicone oil, different quantities of the gas (0.2, 0.3, 0.6, 1.0, and 1.3 mmol of H_2 or CO_2) were placed in previously sealed serological glass bottles (60 mL) containing 20 mL of silicone oil. Afterward, the bottles were placed in a rotatory shaker at 37 °C and 150 rpm. Gas samples (from each condition) were taken every 12 h to quantify the H_2 or CO_2 concentration by gas chromatography [20]. The CO_2 and H_2 partition coefficients were calculated as the ratio of the concentration in the gaseous and liquid phases using Eqs. 3.3 and 3.4.

$$H = C_s^g / C_s^l \quad (3.3)$$

$$C_s^l = C_s^i - C_s^g \quad (3.4)$$

where H is the partition coefficient (dimensionless), C_s^g is the equilibrium concentration in the gas phase (g/m^3), C_s^l is the equilibrium concentration in the aqueous phase (g/m^3), and C_s^i is the initial concentration in the gas phase (g/m^3). For comparative purposes, the same experimental procedure was carried out with mineral medium instead of silicone oil. All experiments were conducted in triplicate.

3.3.6 Analytical methods

COD and VSS concentrations were determined according to the standard methods [21]. The concentration of TC was determined by the phenol–sulfuric method [22]. Carboxylic acids were quantified from filtered (0.22 mm) samples by capillary electrophoresis 1600A (Agilent Technologies, Germany), as reported elsewhere [5]. In the continuous experiments, the gas production and its composition (H_2 and CO_2) were measured by a liquid displacement device (SEV, Mexico) and gas chromatography with TCD detector 6890 N (Agilent Technologies, Germany), respectively [17]. All the gas volumes are reported at standard conditions (1 atm and 273.15 K). The results are reported as an average value ± standard deviation from: a) the triplicates of the batch and coefficient partition experiments or b) three consecutive samples obtained from steady states in the CSTR assays.

3.3.7 Calculations

To estimate the COD balances in both batch and continuous dark fermentation experiments, the carboxylic acids, biomass production, H_2 production, and residual carbohydrates were considered. The COD mass balances were calculated in g COD/L for the batch experiments and g COD/L-d for the continuous experiments, following the methodology reported by Rittmann and McCarty [23] and equation 3.5

COD_{in} = COD (carboxylic acids) + COD (biomass)+ COD (hydrogen) + COD (residual TC) (3.5)

Where COD_{in} is the COD of the substrate fed; *COD (carboxylic acids)* is the COD of the mean carboxylic acids produced; *COD (biomass)* is the COD of the biomass measured as VSS, assuming that the chemical formula of biomass is $C_5H_7O_2N$; *COD (hydrogen)* is the COD of the hydrogen produced; and *COD (residual TC)* is the COD of the total sugars remaining, considering total sugars as glucose.

The Gibbs free energy at steady-state (only for the CSTR results) was calculated for dark fermentative reactions in two steps: i) Generation of the overall reactions in each stage of the CSTR, following the methodology described by Lee and Rittmann [24], ii) From the overall reactions and following the methodology described by Kleerebezem and Van Loosdrecht [6]. Three values of Gibbs free energy were calculated as follows: 1) $\Delta G°$: considering all standard conditions, 2) $\Delta G'^{t}$: 37 °C, pH 7, and standard concentrations (1 M) of glucose, acetate, and butyrate, and 3) ΔG^{r}: 37 °C, pH 5.5, and experimental concentrations of the compounds.

3.3.8 Statistical analysis

In the batch dark fermentation experiments, Spearman correlation analysis was carried out with the total H_2 produced and the different proportions of silicone oil (control, 2.5, 5, 10, 20, and 30% v/v). Also, a one-way analysis of variance (non-parametric test of Kruskal-Wallis) was used to evaluate the effects of silicone oil addition on the total H_2 production and TC consumption. The Dunn test was carried out to compare the effects of the different treatments. Additionally, the Kruskal-Wallis test was used to elucidate if the differences in the Gibbs free energies were significant at the same OLR with and without silicone oil. In all the analyses, the results were considered to be significant at a *p*-value lower than 0.05. The statistical analysis was carried out in R software [25].

3.4 Results and discussion

3.4.1 Partition coefficients relevant for H_2 and CO_2 extraction

For the purposes of this work, the partition coefficient is the ratio of the concentrations of H_2 or CO_2 between the gas and liquid phases in the equilibrium. Table 3.1 shows the values of the partition coefficients for H_2 and CO_2 in silicone oil and mineral medium, compared with the previously reported for water [26]. According to the partition coefficient in mineral medium, it can be observed that the values for both gases were very similar to those reported for water, being H_2 about 42 times less soluble compared to CO_2. Despite the low solubility of H_2 in mineral medium, it has been reported that the accumulation of trace concentrations (~20 mmol/L) of this gas in the aqueous phase promotes metabolic pathways not favorable for the production of H_2, such as homoacetogenesis [27]. In contrast, with silicone oil, partition coefficients were approximately 50 and 9 times lower than the partition coefficient in the mineral medium for H_2 and CO_2, respectively, indicating a higher affinity of both gases to diffuse in silicone oil than in mineral medium (Table 3.1).

Table 3.1. Dimensionless partition coefficient (H) for H_2 and CO_2 in silicone oil and mineral medium. H was calculated as the ratio between the gas concentration in the gaseous and aqueous phase in the equilibrium.

Compound	$H_{\text{Silicone Oil}}$	$H_{\text{mineral medium}}$	H_{water} [26]
H_2	0.92 ± 0.15	46.5 ± 0.4	51.7
CO_2	0.12 ± 0.03	1.1 ± 0.14	1.22

In a typical dark fermentation, the gas produced is composed of 55% H_2 and 45% CO_2. Considering, as an example, this composition in a headspace of 40 mL, the theoretical concentrations of H_2 and CO_2 dissolved in the mineral medium can be estimated as 1.8×10^{-4} mol/L and 1.3×10^{-2} mol/L, respectively. In contrast, the theoretical dissolved concentrations of H_2 and CO_2 in the silicone oil can be estimated as 9.5×10^{-3} mol/L and 1.2×10^{-2} mol/L, respectively. These theoretical calculations, together with the partition coefficient values (Table 3.1), showed that there is a high affinity of the silicone oil to absorb H_2 and CO_2; however, this affinity

is more evident with H_2, indicating that H_2 and CO_2 will tend to be absorbed into the extractive organic phase, decreasing the concentrations of both gases in the mineral medium.

3.4.2 Batch dark fermentation experiments

To determine the most appropriate proportion of silicone oil to be added to the medium, the cumulative H_2 production was determined in batch assays with proportions of silicone oil ranging from 2.5 to 30% (v/v) (Figure 3.1). The H_2 production behavior was similar in all the experiments, reaching the steady states in approximately 1.2 days. The differences among the experiments became clearer when looking at the total H_2 produced (H_2 potential + H_2 desorbed), where the highest value was observed with 10% (v/v) silicone oil, as shown in Table 3.2. Overall, considering the amount of H_2 desorbed from the extractive organic phase, the total H_2 production increased approximately between 6% and 15% in all the experiments. It is worth noting that H_2 and carboxylic acids were not produced in the control of silicone oil 10% (v/v) + biomass without substrate. Nonetheless, several reports established the ability of microorganisms to adhere to the surface of the micelles of the silicone oil, without observing the presence of microorganisms within the micelles [28].

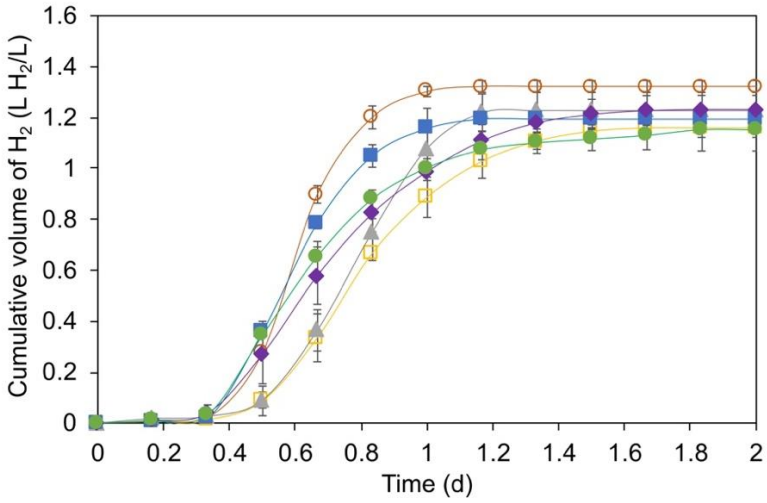

Figure 3.1. Cumulative hydrogen production in the batch assays using cheese whey powder (CWP) as the substrate and silicone oil as the extractive organic phase. CWP control (■), CWP - silicone oil 2.5% (v/v) (♦), CWP - silicone oil 5% (v/v) (●), CWP - silicone oil 10% (v/v) (O), CWP - silicone oil 20% (v/v) (□), CWP - silicone oil 30% (v/v) (▲).

Table 3.2. Hydrogen produced in the batch experiments (AMPTS II + H_2 desorbed from the organic phase) and kinetic parameters from the modified Gompertz modeling.

Experiment	TC consumption (%)	Kinetic parameters*			H_2 production in AMPTS II			Desorbed H_2			Total H_2 produced (L H_2/L)
		λ (d)	H_{max} (L H_2/L)	R_{max} (L H_2/L-d)	H_2 potential (L H_2/L)	% H_2	% CO_2	H_2 desorbed (L H_2/L)	% H_2	% CO_2	
CWP control no silicone oil	97	0.38 ± 0.04	1.23 ± 0.3	3.32 ± 0.2	1.19 ± 0.4	52 ± 2	48 ± 1	N.A.	N.A.	N.A.	1.19 ± 0.4[a]
CWP - silicone oil 2.5% (v/v)	94	0.37 ± 0.02	1.24 ± 0.1	3.10 ± 0.3	1.22 ± 0.2	54 ± 1	46 ± 3	0.08 ± 0.03	45 ± 2	55 ± 2	1.30 ± 0.07[a]
CWP - silicone oil 5% (v/v)	94	0.36 ± 0.04	1.15 ± 0.2	3.15 ± 0.4	1.13 ± 0.3	52 ± 3	48 ± 1	0.10 ± 0.02	42 ± 1	58 ± 1	1.23 ± 0.08[a]
CWP - silicone oil 10% (v/v)	94	0.41 ± 0.04	1.39 ± 0.2	4.05 ± 0.3	1.32 ± 0.2	65 ± 1	35 ± 2	0.21 ± 0.04	30 ± 1	70 ± 2	1.53 ± 0.1[b]
CWP - silicone oil 20% (v/v)	92	0.52 ± 0.02	1.15 ± 0.1	2.01 ± 0.5	1.15 ± 0.3	59 ± 1	41 ± 2	0.10 ± 0.04	31 ± 1	69 ± 2	1.25 ± 0.1[a]
CWP - silicone oil 30% (v/v)	91	0.56 ± 0.02	1.22 ± 0.1	2.69 ± 0.2	1.22 ± 0.3	60 ± 2	40 ± 3	0.10 ± 0.06	33 ± 4	66 ± 3	1.32 ± 0.08[a]

CWP: cheese whey powder, TC: total carbohydrates, λ: lag time, H_{max}: maximum cumulative production of hydrogen, R_{max}: maximum hydrogen production rate. *Coefficient of determination, $R^2 > 0.98$ in all cases. [a,b] Dunn test result: Only the total H_2 production of CWP - silicone oil 10% (v/v) was statistically different from the other experiments.

Table 3.2 also summarizes the performance and main kinetic parameters obtained from the batch experiments with different proportions of silicone oil. The consumption of total carbohydrates was similar for all the experiments (>90%, Kruskal-Wallis test $p = 0.12$), suggesting that the silicone oil was not inhibitory to the microorganisms and the fermentation process progressed as expected.

As for the H_2 production rate, no clear relationship was observed between the proportion of silicone oil and total H_2 produced (Spearman correlation, $R^2 = 0.55$, $p = 0.14$). However, the silicone oil had a statistically significant effect on the total H_2 production (Kruskal-Wallis test, $p < 0.05$). Only the total H_2 production value (1.53 ± 0.1 L H_2/L) using silicone oil 10% (v/v) was statistically different from the CWP control and the other proportions of silicone oil (Dunn test, $p < 0.05$, Table 3.2). On the other hand, when the proportions of silicone oil were ≥ 20% (v/v), the R_{max} decreased considerably compared to the CWP control. This decrement could be explained by the increase of viscosity resulting from the higher proportion of silicone oil, which possibly leads to problems on mass transport, reduction of specific transfer area due to bigger droplets, and dark fermentation metabolism [13], [29]. In dark fermentation experiments, it has been reported that the increase of viscosity impairs the development of the bacterial community due to the resulting higher hydro-mechanical shear stress applied to microorganisms [13]. In addition, higher viscosity could decrease the transfer rate of nutrients to microorganisms as well as the liquid-to-gas mass transfer rate, which results from the reduction of the diffusivity of soluble species according to the penetration theory of Higbie [30].

All these problems could favor hydrogen inhibition, contributing to slow down the hydrogen production rate. Similar results have been reported for volatile organic compounds (VOC) treatment and biogas purification, where proportions of silicone oil near 30% (v/v) caused the drop of the removal efficiency of VOC due to problems related to mass transport [28], [30]. On the other hand, in the experiments with silicone oil < 10% (v/v), total H_2 produced values were very similar to the CWP control (Dunn test, $p > 0.05$ in all cases). Low proportions of silicone oil may reflect minimal changes in the mass transfer conditions and, therefore, in the total H_2 production. For instance, Chezeu et al. [13] investigated the influence of digestate viscosity and

agitation on H_2 production potential; the authors estimated that liquid to gas mass transfer experiments, with polyalkylene glycol lower than 10% v/v, presented similar K_La values to the control (0.030 1/s vs. 0.028 1/s).

Interestingly, it was also found that the percentage of H_2 in the gas was higher when using silicone oil 10% (v/v) in the batch experiments (Table 3.2). This outcome probably results from the fact that CO_2 is absorbed in higher proportion than H_2 in the organic extractive phase, which is ultimately related to the differences of CO_2 and H_2 affinities for silicone oil (Table 3.1). In agreement, the composition of the desorbed gas from the extractive organic phase showed considerably higher CO_2 concentrations than those found in the gas produced in the batch assays without the addition of the extractive organic phase. These results were consistent with the higher affinity of CO_2 for the extractive organic phase. The silicone oil also helped to reduce the acidification of the medium. In aqueous systems, dissolved CO_2 leads to increasing the H^+ ions with the consequent decrease of pH. According to the results of this research, the extractive organic phase decreases the concentration of CO_2 and H_2 dissolved in the aqueous phase, causing to a lower formation of carbonic acid and, therefore, lower acidification of the aqueous phase. However, such effect was compensated by the expected production of carboxylic acids, leading to a pH change from 7.5 to 4 – 4.4.

Few changes were also observed in the concentration of the carboxylic acids produced in the batch experiments; it is worth noting that carboxylic acids were not detected in the silicone oil collected at the end of each experimental condition. In general, the fermentation was essentially acetate-butyrate type with the presence of formate and lactate in experiments with proportions of silicone oil higher than 10% (v/v) (Figure 3.2 and Table 3.3). This outcome was consistent with the COD balances, which showed that most of the COD from the substrate was directed toward acetate and butyrate (Table 3.4). At the end of the batch experiments, the identified COD recovery was between 63 and 70%, while the unidentified COD could correspond to alcohols (i.e., ethanol, butanol) and/or other metabolites (i.e., pyruvate, succinate, valerate, acetone) that were not analyzed [24].

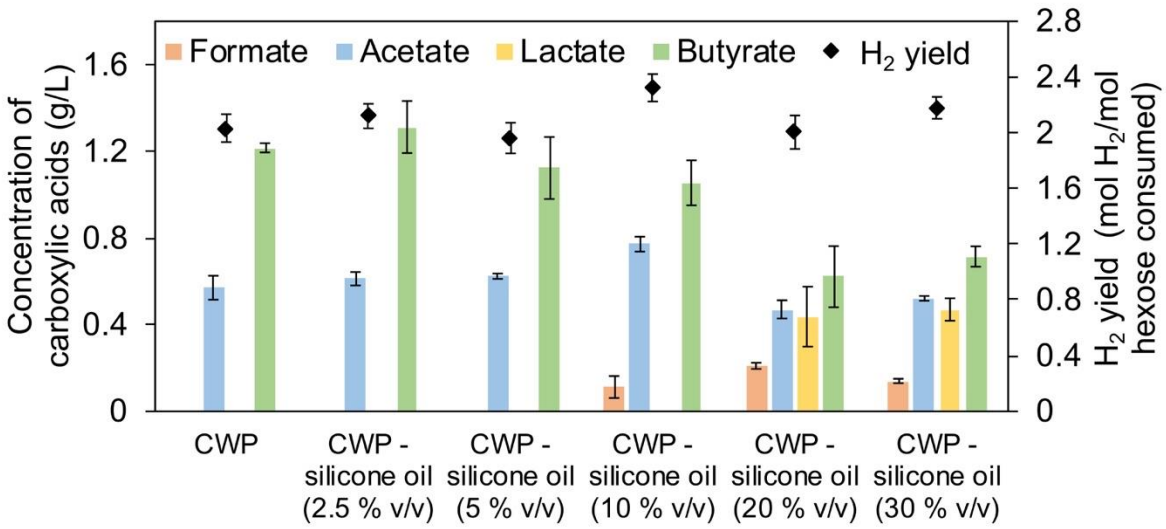

Figure 3.2. Concentration of the carboxylic acids produced in batch experiments with different proportions of silicone oil and cheese whey powder (CWP) as substrate.

Table 3.3. Experimental concentrations in each batch experiments.

Experiment	Compound (g/L)						
	Acetate	**Butyrate**	**Lactate**	**Formate**	**Biomass**	**Residual TC**	**Total H_2***
CWP	0.57 ± 0.05	1.21 ± 0.05	ND	N.D.	2.1 ± 0.2	0.15 ± 0.01	0.055 ± 0.01
CWP - silicone oil 2.5% (v/v)	0.61 ± 0.06	1.31 ± 0.1	ND	N.D.	1.9 ± 0.2	0.3 ± 0.01	0.062 ± 0.01
CWP - silicone oil 5% (v/v)	0.62 ± 0.06	1.12 ± 0.2	ND.	N.D	2.3 ± 0.3	0.3 ± 0.01	0.055 ± 0.02
CWP - silicone oil 10% (v/v)	0.77 ± 0.03	1.05 ± 0.1	N.D.	0.11 ± 0.05	2.1 ± 0.3	0.3 ± 0.01	0.051 ± 0.01
CWP - silicone oil 20% (v/v)	0.47 ± 0.04	0.62 ± 0.1	0.43 ± 0.1	0.21 ± 0.01	2.3 ± 0.2	0.4 ± 0.01	0.054 ± 0.02
CWP - silicone oil 30% (v/v)	0.52 ± 0.05	0.71 ± 0.1	0.47 ± 0.05	0.14 ± 0.01	2.4 ± 0.3	0.45 ± 0.02	0.051 ± 0.02

CWP: cheese whey powder, TC: total carbohydrates. ND: no detected, *mol H_2/L

Table 3.4. COD mass balances in the batch experiments.

Experiment	COD_{in} (g COD/L)	Compound (g COD/L)							COD out	COD_{out}/COD_{in}
		Acetate	Butyrate	Lactate	Formate	Biomass[a]	Residual TC	Total H_2		
CWP	6.5	0.62	2.22	0	0.00	0.34	0.16	0.88	4.22	0.65
CWP - silicone oil 2.5% (v/v)	6.5	0.66	2.41	0	0.00	0.06	0.32	0.99	4.44	0.68
CWP - silicone oil 5% (v/v)	6.5	0.67	2.06	0	0.00	0.62	0.32	0.88	4.55	0.70
CWP - silicone oil 10% (v/v)	6.5	0.84	1.93	0	0.04	0.34	0.32	0.82	4.28	0.66
CWP - silicone oil 20% (v/v)	6.5	0.51	1.14	0.46	0.07	0.62	0.43	0.86	4.10	0.63
CWP - silicone oil 30% (v/v)	6.5	0.56	1.30	0.51	0.05	0.76	0.48	0.82	4.49	0.69

CWP: cheese whey powder, COD: chemical oxygen demand, TC: total carbohydrates, COD_{in}: estimated inlet concentration, COD_{out}: estimated outlet concentration. [a] Biomass = final biomass – initial biomass.

In the experiments with silicone oil proportions below 10% (v/v), the concentrations of acetate (on average 0.6 ± 0.03 g/L) and butyrate (on average 1.2 ± 0.1 g/L) were similar to the assay with no silicone oil, this result was expected because the R_{max} values were also similar (see Table 3.2). In the experiment with silicone oil 10% (v/v), with the highest obtained R_{max}, the concentration of acetate increased by about 33% and reflected in the increase of the H_2 yield from 2.07 mol H_2/mol glucose consumed (CWP control) to 2.37 mol H_2/mol glucose consumed (Figure 3.2). These results suggest that using silicone oil 10% (v/v) favors the production of H_2 by the acetate route because the lower CO_2 dissolved in the aqueous medium, which is theoretically associated with the highest H_2 yield [31].

In the experiments with>10% (v/v) of silicone oil, the formate concentrations were between 0.1 and 0.3 g/L. The production of this carboxylic acid has been associated with low activity of the enzyme formate-lyase [32], which is involved in the transformation of formate to H_2 and CO_2. However, it seems that the concentration of formate produced in the batch experiments was not an indicative of an inefficient metabolism in dark fermentation processes since the highest R_{max} was obtained at a silicon oil proportion of 10% (v/v).

In the experiments with 20 and 30% (v/v) of silicone oil, lactate was specifically found at concentrations of 0.45 ± 0.02 g/L. Lactate has been associated with low or no production of H_2. Microorganisms that perform lactic acid fermentation compete for the substrate with H_2-producing microorganisms and can produce inhibitory compounds [33]. However, previous investigations (in batch experiments) reported the production of H_2 by converting lactate into butyrate and H_2. Some authors also suggest that lactate could be an additional substrate for H_2-producing bacteria [1, 34]. In our experiments, the presence of lactate, accompanied by a decrease in acetate and butyrate, could be a possible explanation of the low productivity of H_2 obtained in the experiments with silicone oil 20 and 30% (v/v). On the other hand, the outgassing of H_2 and CO_2 from the aqueous to the gas phase is reduced with silicone oil at proportions higher than 10% (v/v), and therefore, H_2 stays longer in the liquid favoring its consumption by other metabolic routes, such as homoacetogenesis.

3.4.3 Continuous dark fermentation experiments

As expected, a positive effect of the silicone oil was also observed in the continuous experiments ($p < 0.05$ for both OLR). In particular, using silicone oil increased the H_2 productivity equivalent to 29% and 13% at the OLR of 60 and 138 TC/L-d, respectively (Figure 3.3 A). Such increase resulted in average VHPR values of 8.4 and 27.1 L H_2/L-d, respectively. The VHPR values were similar to those reported in previous investigations intended to improve dark fermentation performance [4, 11, 35, 36]. For instance, Palomo-Briones et al. [11] reported that the increase of the stirring velocity in a CSTR enhanced the VHPR from 4.4 L H_2/L-d (100 rpm) to 7.6 L H_2/L-d (400 rpm) at an OLR of 60 g TC/L-d. Montoya-Rosales et al. [4] reported a VHPR increase of 23% in a CSTR operated at an OLR of 138 g TC/L-d, by the recycling and discontinuous increase of biomass concentration in the reactor.

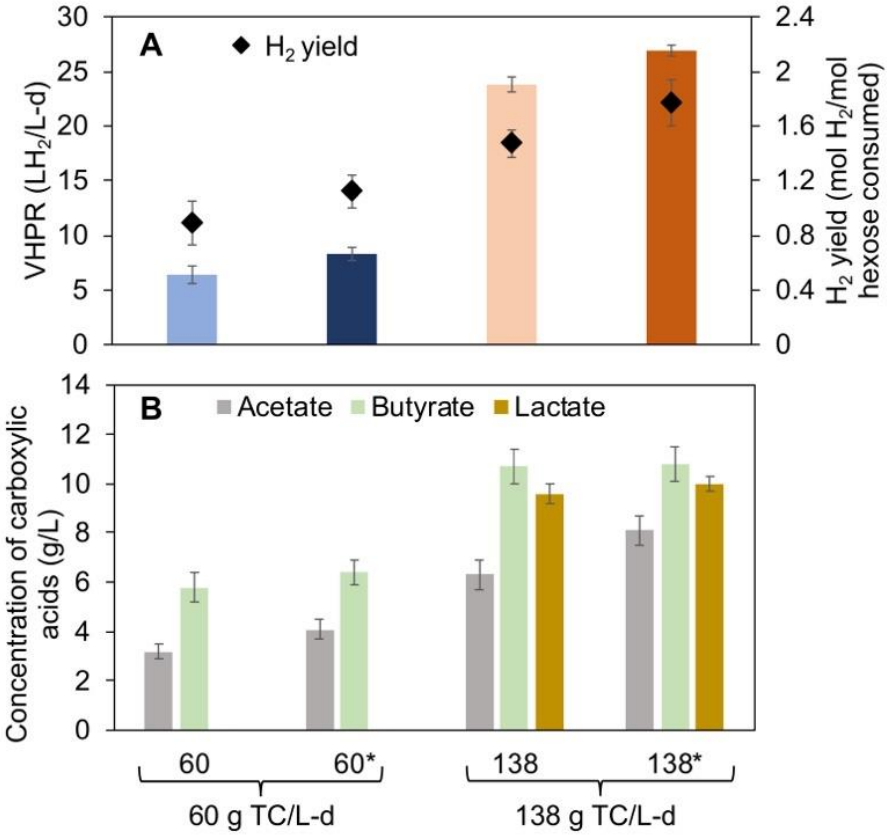

Figure 3.3. Effect of silicone oil in continuous dark fermentation experiments added at a proportion of 10% (v/v), using cheese whey powder at an OLR of 60 g TC/L-d and 138 g TC/L-d. A) Volumetric hydrogen production rate (VHPR) and H_2 yield. B) Concentration of carboxylic acids. TC: total carbohydrates. *Stages with silicone oil.

From the analysis of the carboxylic acids (Table 3.5 and Figure 3.3 B), acetate and butyrate were the main metabolic products in both conditions of OLR. As shown for the batch experiments, COD balances also showed that most of the COD (65–88%) from the substrate was transformed into biomass, acetate, and butyrate (Table 3.6). Overall, the use of silicone oil led to an increase of the acetate and butyrate concentrations compared with the stages with no addition of silicone oil (stages I and III). The butyrate concentrations increased approximately 13% in the stages with silicone oil at both OLR. In the same way, at both OLR the acetate concentration increased approximately 29%.

Moreover, at the OLR of 138 g TC/L-d, lactate was observed at concentrations between 9.6 and 10.3 g/L (Figure 3.3 B). The production of lactate at concentrations higher than 5 g/L in CSTR systems has been associated to high VHPR values and H_2 yields [4]. In contrast to the batch experiments, it was observed that the production of lactate did not affect the production either of acetate or butyrate, being possible that lactate could be an additional substrate for H_2 production. Similar results have been reported previously for CSTR systems operated at high OLR [4, 31]. The experiments carried out in the CSTR did not allow ensuring that lactate consumption produced H_2 (if lactate is indeed used for H_2 production). Thus, the consumption of lactate for H_2 production in continuous systems will be considered in future works. These observations suggest a controversial role of lactic acid bacteria on the production of H_2. Most probably, the interaction between lactic acid bacteria and H_2-producing bacteria also depends on the operational conditions, such as, substrate concentration, reactor configuration, partial pressure, among others [27].

Table 3.5. Experimental concentrations in each steady state of the CSTR operation.

OLR (g TC/L-d)	Compound (g/L)					
	Acetate	**Butyrate**	**Lactate**	**Biomass**	**Residual TC**	**VHPR**[**]
60	3.2 ± 0.3	5.8 ± 0.6	N.D.	2.8 ± 0.4	0.9 ± 0.2	0.28 ± 0.05
60[*]	4.1 ± 0.4	6.4 ± 0.5	N.D.	3 ± 0.3	0.6 ± 0.1	0.37 ± 0.02
138	6.3 ± 0.6	10.7 ± 0.7	9.6 ± 0.4	3.1 ± 0.4	1.7 ± 0.3	1.06 ± 0.02
138[*]	8.1 ± 0.6	10.8 ± 0.7	10 ± 0.3	3.2 ± 0.3	1.1 ± 0.3	1.2 ± 0.02

OLR: organic loading rate, N.D.: no detected, TC: total carbohydrates, [*]silicone oil 10% (v/v) added, [**] mol H_2/L-d

Table 3.6. COD mass balances in each steady state of the CSTR operation.

OLR (g TC/L-d)	COD_{in} (g COD/L-d)	Compound (g COD/L-d)						COD out	COD_{out}/COD_{in}
		Acetate	**Butyrate**	**Lactate**	**Biomass**	**Residual TC**	**VHPR**		
60	82.60	13.88	42.61	0	15.86	3.84	4.48	80.68	0.98
60*	82.60	17.79	47.02	0	16.99	2.56	5.92	90.28	1.09
138	189.97	27.34	78.61	41.42	17.56	7.38	16.96	189.27	1.00
138*	189.97	35.15	79.35	43.15	18.12	4.44	19.20	199.40	1.05

OLR: organic loading rate, COD: chemical oxygen demand, TC: total carbohydrates, VHPR: volumetric hydrogen production rate, COD_{in}: estimated inlet concentration, COD_{out}: estimated outlet concentration. [*]silicone oil 10% (v/v) added

Finally, it was observed that the concentration of H_2 in the produced gas was slightly higher in the stages where silicone oil was added, which contrasted with the higher CO_2 concentration in the desorbed gas than in the gas produced in the reactor, as shown in Table 3.7. These results were similar to those observed in the batch experiments.

Table 3.7. Total hydrogen produced in the continuous experiments using silicone oil at a proportion 10% (v/v) as extractive organic phase.

OLR (g TC/L-d)	H_2 production in CSTR			Desorbed H_2			Total H_2 produced (L H_2/L-d)
	VHPR (L H_2/L-d)	% H_2	% CO_2	H_2 desorbed (L H_2/L-d)	% H_2	% CO_2	
60	6.4 ± 0.8	56 ± 2	44 ± 1	N.A.	N.A.	N.A.	6.4 ± 0.8
60*	8.3 ± 0.6	60 ± 1	40 ± 1	0.1 ± 0.03	30 ± 3	70 ± 3	8.4 ± 0.5
138	23.8 ± 0.7	53 ± 2	47 ± 2	N.A.	N.A.	N.A.	23.8 ± 0.6
138*	26.9 ± 0.5	59 ± 2	41 ± 3	0.13 ± 0.06	32 ± 2	68 ± 3	27.1 ± 0.5

VHPR: volumetric hydrogen production rate, OLR: organic loading rate, TC: total carbohydrates. *Silicone oil added.

3.4.4 Analysis of microbial communities

To determine the effect of the OLR and the addition of silicone oil on the microbial communities, 16S rRNA gene sequence analysis was performed in samples taken at the end of each operation phase and from the inoculum. The applied OLR clearly influenced the microbial composition, while the effect of the silicone oil addition was not so clear. When the CSTR operated at an OLR of 60 g TC/L-d, the relative abundance of the dominant genera was similar regardless of adding silicone oil; more than 97 % of the relative abundance was represented by H_2-producing bacteria (genera *Clostridium* and *Klebsiella*) (Figure 3.4). Microorganisms belonging to the *Clostridium* genus are considered the most efficient H_2 producers; these versatile microorganisms can produce H_2 via acetate-type fermentation and butyrate-type

fermentation [34]. The genus *Klebsiella* includes facultative anaerobic microorganisms that produce alcohols (2,3 butanediol, isopropanol, and ethanol) as well as H_2 and CO_2 [37], the theoretical H_2 yield reported for members of the *Klebsiella* genus are in general lower than those reported for *Clostridium* [38].

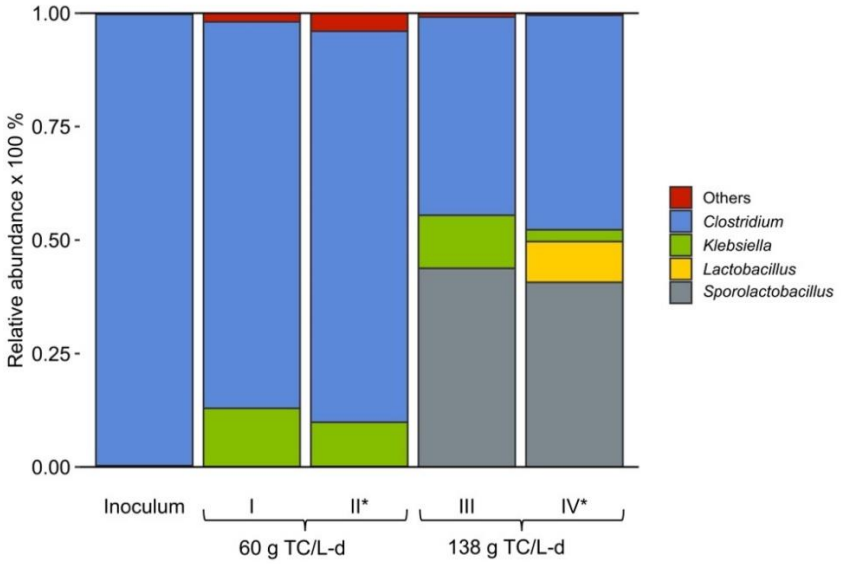

Figure 3.4. Relative abundances of the microbial communities at the genus level in the continuous experiments. *Silicone oil added at a proportion of 10% (v/v).

When increasing the OLR to 138 g TC/L-d, a co-dominance between the H_2-producing bacteria and acid-lactic bacteria (*Lactobacillus* and *Sporolactobacillus*) was observed. Previous studies in CSTR systems at OLR > 90 g TC/L-d reported that members of lactic acid bacteria could be directly involved in H_2 production by providing extra substrate to H_2-producing bacteria in the form of lactate [1, 4, 32]. Overall, it was observed that the change of the OLR exerted a selection on the microbial community composition and the performance of the CSTR. Considering that the addition of silicone oil to the CSTR does not modify the composition of the microbial communities substantially, we hypothesized that the increase of the H_2 and carboxylic acids productivities in the presence of silicone oil was due to the stimulation of key microorganisms that carry out the crucial metabolic pathways to achieve efficient dark fermentation.

3.4.5 H_2 and CO_2 transfer model in the two-phase partitioning bioreactor

Three interphases are formed in the presence of silicone oil (aqueous-gas, aqueous-silicone oil, and silicone oil–gas) as shown in Figure 3.5. At such molecular level, the mass transport of H_2 and CO_2 across any of these interphases can be described according to the film theory [39]. The film theory states that the transport rate of solutes across two immiscible phases is dominated by Fick's diffusion at the proximity of the interphase, as already shown in Equation (3.1). At such interphases, the mass transfer rate (Q) is proportional to the difference of concentrations between the aqueous phase and the phase boundary (ΔC), but also to the transfer coefficient (k_L) and the area available for the mass transfer (a). At the boundary, and only there, the concentrations at each side are assumed to be correlated by Henry's law (Eq. (3.3)).

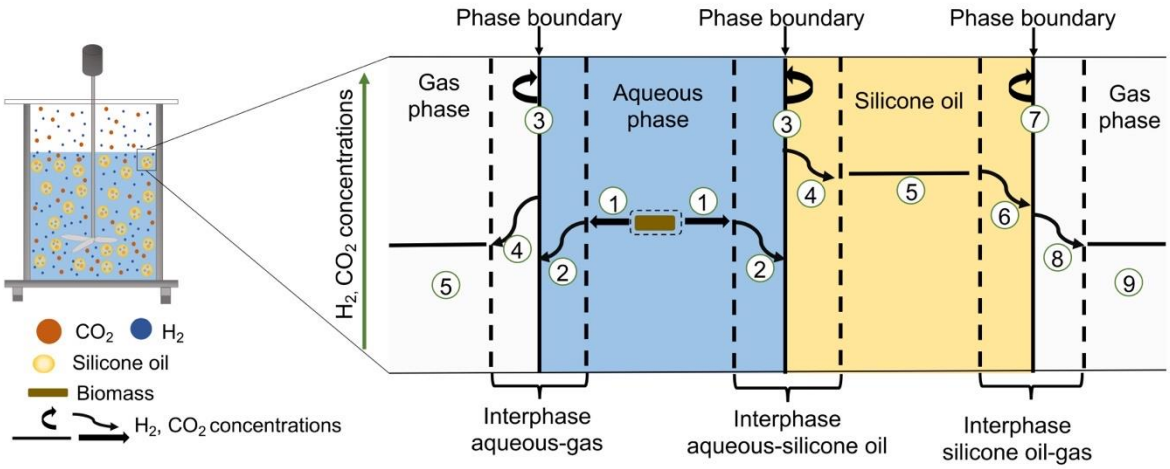

Figure 3.5. Proposed mass transfer model according to the film theory. 1. Convective transport through the bulk liquid to the proximity of the gas phase and silicone oil micelles. 2. Fick's diffusion through the relatively stagnant liquid film surrounding the gas phase and silicone oil micelles. 3. Equilibrium across the interfaces (aqueous-gas and aqueous-silicone oil.). 4. Fick's diffusion through the relatively stagnant liquid film surrounding the liquid phase. 5. Convective transport from the interphases to the interior of bulk gas and the interior of silicone oil micelles. 5-9. Transport of H_2 and CO_2 absorbed in the silicone oil to the gas phase.

When considering the film theory and the different interphases as depicted in Figure 3.5, the complete model for H_2 and CO_2 transfer from H_2-producing bacteria to the gas and silicone oil phases would include the following steps: 1) Convective

transport through the bulk liquid to the proximity of the gas phase and silicone oil micelles. 2) Fick's diffusion through the relatively stagnant liquid film surrounding the gas phase and silicone oil micelles. 3) Equilibrium across the interfaces (aqueous-gas and aqueous-silicone oil.). 4) Fick's diffusion through the relatively stagnant liquid film surrounding the liquid phase. 5) Convective transport from the interphases to the interior of bulk gas and the interior of silicone oil micelles. Additionally, the H_2 and CO_2 absorbed in the silicone oil can also be transported to the gas phase following the steps 5 to 9 (Figure 3.5).

Based on the film theory and the whole mass transfer model described above, the addition of silicone oil meant an increase of the transfer area (provided by the silicone oil micelles), which in conjunction with to the high affinity (k_L) of H_2 and CO_2 for the silicone oil, led to higher H_2 transfer rates. Moreover, in a continuous reactor, the silicone oil micelles would serve as an unsaturated reservoir for H_2 and CO_2. This scenario translated into a substantial and time-wise sustained increase of H_2 and carboxylic acids productivities.

3.4.6 Implications of the presence of an extractive organic phase in dark fermentation

As shown in Table 3.2 and Figure 3.3, the use of silicone oil, especially at a proportion of 10% (v/v), led to a considerable increase in the production of H_2 and carboxylic acids. These results can be explained by the improvement of the mass transfer conditions, due to the higher dissolution of H_2 and CO_2 in the silicone oil compared with the aqueous media (Section 3.4.5). Such mass transfer improvement probably impacts on three different phenomena identified as the main drivers: i) changes in the Gibbs free energy values, ii) changes in the concentration of H_2 and CO_2 in the aqueous phase, and iii) changes in the microbial composition or metabolic pathways, or both.

Theoretically, the decrease in the concentrations of dissolved H_2 could yield more negative Gibbs free energy values. To demonstrate these phenomena, first, the stoichiometric reactions obtained from the compounds reported in each steady state of the CSTR operation were generated (Table 3.8). Once these reactions were

obtained, the calculation of the Gibbs free energy at the experimental concentrations was possible (Table 3.9). In general, it was observed that the ΔG^r values are considerably more positive at the OLR of 138 g TC/L-d (Table 3.8). These results can be associated with the increased concentrations of dissolved H_2 and CO_2 in the aqueous phase. However, at the same OLR, the ΔG^r becomes more negative when silicone oil is added to the system, at the same OLR. At the OLR of 60 g TC/L-d, 27% more free energy was obtained due to the addition of silicone oil to the reactor (Kruskal-Wallis test, $p < 0.05$). In the same way, at the OLR of 138 g TC/L-d, the ΔG^r changed from –107.3 ± 3.2 to –119.78 ± 5.4 kJ/mol (12% more free energy, Kruskal-Wallis test, $p < 0.05$). This thermodynamic approach demonstrates that the addition of silicone oil improves the capacity of the microorganisms to catalyze the substrate and reduce a possible inhibition caused by the accumulation of H_2.

Table 3.8 Stoichiometric reactions and Gibbs free energy values from the CSTR operation.

OLR (g TC/L-d)	**Overall reactions with cell synthesis**	**ΔG^r (kJ/mol)**
60	$C_6H_{12}O_6 + 0.24NH_4^+ = 2.33H_2 + 0.44C_2H_3O_2^- + 0.48C_4H_7O_2^- + 0.24C_5H_7O_2N + 2CO_2 + 0.12\ H_2O + 1.16\ H^+$	–172.60 ± 8.8
60*	$C_6H_{12}O_6 + 0.21NH_4^+ = 2.67H_2 + 0.49C_2H_3O_2^- + 0.52C_4H_7O_2^- + 0.21C_5H_7O_2N + 1.89CO_2 + 0.18\ H_2O + 1.22\ H^+$	–219.23 ± 9.7
138	$C_6H_{12}O_6 + 0.13NH_4^+ + 1.03\ H_2O = 3.42H_2 + 0.33C_2H_3O_2^- + 0.39C_4H_7O_2^- + 0.13C_5H_7O_2N + 2.11CO_2 + 0.34C_3H_5O_3^- + 1.19\ H^+$	–107.30 ± 3.2
138*	$C_6H_{12}O_6 + 0.12NH_4^+ + 1.01\ H_2O = 3.52H_2 + 0.43C_2H_3O_2^- + 0.36C_4H_7O_2^- + 0.12C_5H_7O_2N + 2.05CO_2 + 0.35C_3H_5O_3^- + 1.25\ H^+$	–119.78 ± 5.4

Number of samples retrieved from the steady-states = 3 in each operational condition.
OLR: organic loading rate, TC: total carbohydrates, ΔG^r: Gibbs free energy calculated at 37 ºC, pH 5.5, and experimental concentrations of the compounds. $C_6H_{12}O_6$: glucose, NH_4^+: ammonium, $C_2H_3O_2^-$: acetate, $C_4H_7O_2^-$: butyrate, $C_5H_7O_2N$: biomass, $C_3H_5O_3^-$: lactate.
*Silicone oil added.

Table 3.9. Different Gibbs free energy calculated from the overall reactions reported in the Table 3.8.

OLR (g TC/L-d)	$\Delta G°$ (kJ/mol)	$\Delta G'^{t}$ (kJ/mol)	ΔG^{r} (kJ/mol)
60	–173.59 ± 9.9	–123.54 ± 10.3	–172.60 ± 8.8
60*	–199.33 ± 8.1	–150.33 ± 8. 4	–219.23 ± 9.7
138	–117.05 ± 3.2	–72.00 ± 3.4	–107.30 ± 3.2
138*	–120.98 ± 4.6	–69.05 ± 4.8	–119.78 ± 5.4

Number of samples retrieved from the steady-states = 3 in each operational condition.
OLR: organic loading rate, TC: total carbohydrates, *Silicone oil 10% (v/v) added, $\Delta G°$: considering all standard conditions, $\Delta G'^{t}$: 37 ºC, pH 7, and standard concentrations (1 M) of glucose, acetate, and butyrate, and ΔG^{r}: 37 ºC, pH 5.5, and experimental concentrations of the compounds reported in the Table 3.5

The decrease of gas concentrations in the aqueous phase is another explanation for the improvement of H_2 production. The 1.3 L CSTR used in the present research has a specific transfer area from liquid to gas of approximately 75.42 cm^2 (considering the internal diameter of the reactor of 9.8 cm). Considering the same gas transfer area and operational conditions, dissolved H_2 concentrations of approximately 3.4 mmol/L were reported [11]. The addition of silicone oil was expected to increase the mass transfer area due to the formation of micelles. With this hypothetical increase of total transfer area, the k_La values should increase while the concentration of dissolved CO_2 and H_2 in the aqueous phase should reduce, favoring the metabolic routes with higher H_2 productivity. From the CSTR results (Section 3.4.3), silicone oil would reduce the percentage of acetate from homoacetogenesis, which can be explained by the reduction of both dissolved CO_2 and H_2 in the aqueous phase.

The reduction of gas concentrations in the aqueous phase is also justified from the gas composition point of view. As shown in Table 3.7, the CO_2 percentage in the gas phase desorbed from the silicone oil is considerably higher than the gas released from the CSTR (69% vs 40%, on average with the two OLR). These observations demonstrate the high affinity of silicone oil to absorb dissolved CO_2 from the aqueous phase, consequently reducing the possibility to be used for the production of acetate by homoacetogenesis. In the end, the reduction of H_2 and CO_2 concentrations from the aqueous phase enhanced the dark fermentation performance and the reduction

of non-desired metabolic pathways, e.g., homoacetogenesis. From the perspective of microbial community analysis, the results showed that the composition of the microbial communities differed due to the OLR applied but not due to the addition of silicone oil (Figure 3.4). These results indicated that probably adding silicone oil stimulated the metabolic pathways with the highest dark fermentation performance. For example, in species of the *Clostridium* genus with the dual capacity to produce and consume H_2, the reduction of the concentrations of H_2 and CO_2 in the aqueous phase could stimulate the pyruvate formate lyase and the pyruvate ferredoxin oxidoreductase pathways while hindering the homoacetogenesis pathway. Nevertheless, more investigation about gene expression in dark fermentation systems is needed.

3.5 Conclusions

This investigation showed that the addition of silicone oil stimulates the metabolic pathways achieving the highest dark fermentation performance (acetate and butyrate), improving hydrogen productivity, and hindering undesired metabolisms, such as homoacetogenesis. In particular, silicone oil at the proportion of 10% (v/v) was the condition in batch assays with the highest increase in VHPR (22%) and acetate production (33%), compared with the assay without silicone oil. In the same way, in the continuous experiments with silicone oil 10% (v/v), the improvement on the VHPR was on average 29% and 13% higher at the OLR of 60 and 138 g TC/L-d, respectively. The calculations of the Gibbs free energy demonstrated that in the stages with silicone oil added to the CSTR, the reaction is thermodynamically more favorable. The diversity of the microbial community in the CSTR appeared to be ruled by the substrate loading rate rather than by the addition of silicone oil. At the OLR of 60 g TC/L-d, the microbial community was clearly dominated by H_2-producing bacteria (*Clostridium* and *Klebsiella*), whereas at 138 g TC/L-d H_2-producing bacteria and lactic acid bacteria co-dominated in the reactor. Overall, the addition of silicone oil proved to be an efficient strategy to increase the production of hydrogen and carboxylic acids in dark fermentation systems.

3.6 References

[1] L. Cabrol, A. Marone, E. Tapia-Venegas, J.-P. Steyer, G. Ruiz-Filippi, E. Trably, Microbial ecology of fermentative hydrogen producing bioprocesses: useful insights for driving the ecosystem function, FEMS Microbiol. Rev. 41 (2017) 158–181. doi:10.1093/femsre/fuw043.

[2] H. Hafez, G. Nakhla, M.H. El. Naggar, E. Elbeshbishy, B. Baghchehsaraee, Effect of organic loading on a novel hydrogen bioreactor, Int. J. Hydrogen Energy. 35 (2010) 81–92. doi:10.1016/j.ijhydene.2009.10.051.

[3] W. Han, Y. Hu, S. Li, Q. Nie, H. Zhao, J. Tang, Effect of organic loading rate on dark fermentative hydrogen production in the continuous stirred tank reactor and continuous mixed immobilized sludge reactor from waste pastry hydrolysate, Waste Manag. 58 (2016) 335–340. doi:10.1016/j.wasman.2016.09.019.

[4] J. de J. Montoya-Rosales, R. Palomo-Briones, L.B. Celis, C. Etchebehere, E. Razo-Flores, Discontinuous biomass recycling as a successful strategy to enhance continuous hydrogen production at high organic loading rates, Int. J. Hydrogen Energy. 45 (2020) 17260–17269. doi:10.1016/j.ijhydene.2020.04.265.

[5] G. Davila-Vazquez, C.B. Cota-Navarro, L.M. Rosales-Colunga, A. de León-Rodríguez, E. Razo-Flores, Continuous biohydrogen production using cheese whey: Improving the hydrogen production rate, Int. J. Hydrogen Energy. 34 (2009) 4296–4304. doi:10.1016/j.ijhydene.2009.02.063.

[6] R. Kleerebezem, M.C.M. Van Loosdrecht, A generalized method for thermodynamic state analysis of environmental systems, Crit. Rev. Environ. Sci. Technol. 40 (2010) 1–54. doi:10.1080/10643380802000974.

[7] W. Buckel, R.K. Thauer, Energy conservation via electron bifurcating ferredoxin reduction and proton/Na+ translocating ferredoxin oxidation, Biochim. Biophys. Acta - Bioenerg. 1827 (2013) 94–113. doi:10.1016/j.bbabio.2012.07.002.

[8] I. Ullah Khan, M. Hafiz Dzarfan Othman, H. Hashim, T. Matsuura, A.F. Ismail, M. Rezaei-DashtArzhandi, I. Wan Azelee, Biogas as a renewable energy fuel – A review of biogas upgrading, utilisation and storage, Energy Convers. Manag. 150 (2017) 277–294. doi:10.1016/j.enconman.2017.08.035.

[9] P. Bakonyi, G. Buitrón, I. Valdez-Vazquez, N. Nemestóthy, K. Bélafi- Bakó, A novel gas separation integrated membrane bioreactor to evaluate the impact of self-generated biogas recycling on continuous hydrogen fermentation, Appl. Energy. 190 (2017) 813–823. doi:10.1016/j.apenergy.2016.12.151.

[10] A.L. Popov, I.S. Michie, J.R. Kim, R.M. Dinsdale, A.J. Guwy, S.R. Esteves, G.C. Premier, Enrichment strategy for enhanced bioelectrochemical hydrogen production and the prevention of methanogenesis, Int. J. Hydrogen Energy. 41 (2016) 4120–4131. doi:10.1016/j.ijhydene.2016.01.014.

[11] R. Palomo-Briones, L.B. Celis, H.O. Méndez-Acosta, N. Bernet, E. Trably, E. Razo-Flores, Enhancement of mass transfer conditions to increase the productivity and efficiency of dark fermentation in continuous reactors, Fuel. 254 (2019) 115648. doi:10.1016/j.fuel.2019.115648.

[12] G. Dreschke, S. Papirio, G. d'Ippolito, A. Panico, P.N.L. Lens, G. Esposito, A. Fontana, H2-rich biogas recirculation prevents hydrogen supersaturation and enhances hydrogen production by Thermotoga neapolitana cf. capnolactica, Int. J. Hydrogen Energy. 44 (2019) 19698–19708. doi:10.1016/j.ijhydene.2019.06.022.

[13] B. Chezeau, J.P. Fontaine, C. Vial, Analysis of liquid-to-gas mass transfer, mixing and hydrogen production in dark fermentation process, Chem. Eng. J. 372 (2019) 715–727. doi:10.1016/j.cej.2019.04.191.

[14] P. Sivagurunathan, C.-Y. Lin, Enhanced biohydrogen production from beverage wastewater: process performance during various hydraulic retention times and their microbial insights, RSC Adv. 6 (2016) 4160–4169. doi:10.1039/C5RA18815F.
[15] R. Muñoz, A.J. Daugulis, M. Hernández, G. Quijano, Recent advances in two-phase partitioning bioreactors for the treatment of volatile organic compounds, Biotechnol. Adv. 30 (2012) 1707–1720. doi:10.1016/j.biotechadv.2012.08.009.
[16] D. Mosca Angelucci, V. Stazi, A.J. Daugulis, M.C. Tomei, Treatment of synthetic tannery wastewater in a continuous two-phase partitioning bioreactor: Biodegradation of the organic fraction and chromium separation, J. Clean. Prod. 152 (2017) 321–329. doi:10.1016/j.jclepro.2017.03.135.
[17] C.A. Contreras-Dávila, H.O. Méndez-Acosta, L. Arellano-García, F. Alatriste-Mondragón, E. Razo-Flores, Continuous hydrogen production from enzymatic hydrolysate of Agave tequilana bagasse: Effect of the organic loading rate and reactor configuration, Chem. Eng. J. 313 (2017) 671–679. doi:10.1016/j.cej.2016.12.084.
[18] J. Carrillo-Reyes, A. Tapia-Rodríguez, G. Buitrón, I. Moreno-Andrade, R. Palomo-Briones, E. Razo-Flores, O. Aguilar Juárez, J. Arreola-Vargas, N. Bernet, A.F. Maluf Braga, L. Braga, E. Castelló, L. Chatellard, C. Etchebehere, L. Fuentes, E. León-Becerril, H.O. Méndez-Acosta, G. Ruiz-Filippi, E. Tapia-Venegas, E. Trably, J. Wenzel, M. Zaiat, A standardized biohydrogen potential protocol: An international round robin test approach, Int. J. Hydrogen Energy. 44 (2019) 26237–26247. doi:10.1016/j.ijhydene.2019.08.124.
[19] J. Huang, A. Riisager, R.W. Berg, R. Fehrmann, Tuning ionic liquids for high gas solubility and reversible gas sorption, J. Mol. Catal. A Chem. 279 (2008) 170–176. doi:10.1016/J.MOLCATA.2007.07.036.
[20] S. Arriaga, R. Muñoz, S. Hernández, B. Guieysse, S. Revah, Gaseous hexane biodegradation by Fusarium solani in two liquid phase packed-bed and stirred-tank bioreactors, Environ. Sci. Technol. 40 (2006) 2390–2395. doi:10.1021/es051512m.
[21] APHA/AWWA/WEF, Standard Methods for the Examination of Water and Wastewater, Stand. Methods. (2012). doi:ISBN 9780875532356.
[22] M. DuBois, K.A. Gilles, J.K. Hamilton, P.A. Rebers, F. Smith, Colorimetric Method for Determination of Sugars and Related Substances, Anal. Chem. 28 (1956) 350–356. doi:10.1021/ac60111a017.
[23] B.E. Rittmann, P.L. McCarty, Environmental Biotechnology: Principles and Applications, 2001.
[24] H. Lee, B.E. Rittmann, Evaluation of Metabolism Using Stoichiometry in Fermentative Biohydrogen, Biotechnol. Bioeng. 102 (2009) 749–758. doi:10.1002/bit.22107.
[25] R.C. Team, R: A language and environment for statistical computing, R Found. Stat. Comput. Vienna, Austria. (2020).
[26] R. Sander, Compilation of Henry's law constants (version 4.0) for water as solvent, Atmos. Chem. Phys. 15 (2015) 4399–4981. doi:10.5194/acp-15-4399-2015.
[27] E. Castelló, L. Braga, L. Fuentes, C. Etchebehere, Possible causes for the instability in the H2 production from cheese whey in a CSTR, Int. J. Hydrogen Energy. 43 (2018) 2654–2665. doi:10.1016/j.ijhydene.2017.12.104.
[28] R. Muñoz, S. Villaverde, B. Guieysse, S. Revah, Two-phase partitioning bioreactors for treatment of volatile organic compounds, Biotechnol. Adv. 25 (2007) 410–422. doi:10.1016/j.biotechadv.2007.03.005.
[29] C.V. B. Chezeau, Combined effects of digestate viscosity and agitation conditions on the fermentative biohydrogen production, Biochem. Eng. J. 142 (2018) 105–116. doi:10.1016/j.bej.2018.11.016.

[30] Z. Trad, C. Vial, J.P. Fontaine, C. Larroche, Mixing and liquid-to-gas mass transfer under digester operating conditions, Chem. Eng. Sci. 170 (2017) 606–627. doi:10.1016/j.ces.2017.01.056.
[31] E. Tapia-Venegas, J.E. Ramirez-Morales, F. Silva-Illanes, J. Toledo-Alarcón, F. Paillet, R. Escudie, C.H. Lay, C.Y. Chu, H.J. Leu, A. Marone, C.Y. Lin, D.H. Kim, E. Trably, G. Ruiz-Filippi, Biohydrogen production by dark fermentation: scaling-up and technologies integration for a sustainable system, Rev. Environ. Sci. Biotechnol. 14 (2015) 761–785. doi:10.1007/s11157-015-9383-5.
[32] A. Tapia-Rodríguez, E. Ibarra-Faz, E. Razo-Flores, Hydrogen and methane production potential of agave bagasse enzymatic hydrolysates and comparative technoeconomic feasibility implications, Int. J. Hydrogen Energy. 44 (2019) 17792–17801. doi:10.1016/j.ijhydene.2019.05.087.
[33] R. Palomo-Briones, E. Trably, N.E. López-Lozano, L.B. Celis, H.O. Méndez-Acosta, N. Bernet, E. Razo-Flores, Hydrogen metabolic patterns driven by Clostridium-Streptococcus community shifts in a continuous stirred tank reactor, Appl. Microbiol. Biotechnol. 102 (2018) 2465–2475. doi:10.1007/s00253-018-8737-7.
[34] E. Castelló, A.D. Nunes Ferraz-Junior, C. Andreani, M. del P. Anzola-Rojas, L. Borzacconi, G. Buitrón, J. Carrillo-Reyes, S.D. Gomes, S.I. Maintinguer, I. Moreno-Andrade, R. Palomo-Briones, E. Razo-Flores, M. Schiappacasse-Dasati, E. Tapia-Venegas, I. Valdez-Vázquez, A. Vesga-Baron, M. Zaiat, C. Etchebehere, Stability problems in the hydrogen production by dark fermentation: Possible causes and solutions, Renew. Sustain. Energy Rev. 119 (2019). doi:10.1016/j.rser.2019.109602.
[35] H. Hafez, B. Baghchehsaraee, G. Nakhla, D. Karamanev, A. Margaritis, H. El Naggar, Comparative assessment of decoupling of biomass and hydraulic retention times in hydrogen production bioreactors, Int. J. Hydrogen Energy. 34 (2009) 7603–7611. doi:10.1016/j.ijhydene.2009.07.060.
[36] Á. Robles, M. Victoria Ruano, A. Charfi, G. Lesage, M. Heran, J. Harmand, A. Seco, J.-P. Steyer, D.J. Batstone, J. Kim, J. Ferrer, A review on anaerobic membrane bioreactors (AnMBRs) focused on modelling and control aspects, Bioresour. Technol. (2018). doi:10.1016/j.biortech.2018.09.049.
[37] S. Pattra, C.-H. Lay, C.-Y. Lin, S. O-Thong, A. Reungsang, Performance and population analysis of hydrogen production from sugarcane juice by non-sterile continuous stirred tank reactor augmented with Clostridium butyricum, Int. J. Hydrogen Energy. 36 (2011) 8697–8703. doi:https://doi.org/10.1016/j.ijhydene.2010.05.120.
[38] C. Etchebehere, E. Castelló, J. Wenzel, M. del Pilar Anzola-Rojas, L. Borzacconi, G. Buitrón, L. Cabrol, V.M. Carminato, J. Carrillo-Reyes, C. Cisneros-Pérez, L. Fuentes, I. Moreno-Andrade, E. Razo-Flores, G.R. Filippi, E. Tapia-Venegas, J. Toledo-Alarcón, M. Zaiat, Microbial communities from 20 different hydrogen-producing reactors studied by 454 pyrosequencing, Appl. Microbiol. Biotechnol. 100 (2016) 3371–3384. doi:10.1007/s00253-016-7325-y.
[39] P. Doran, Bioprocess Engineering Principles, in: Acad. Press, 2nd ed., Chapter 10, 2012: p. 926.

Chapter 4. *Microbial community structure and function in two-phase partitioning dark fermentation reactors at high organic loading rate*

Graphical abstract

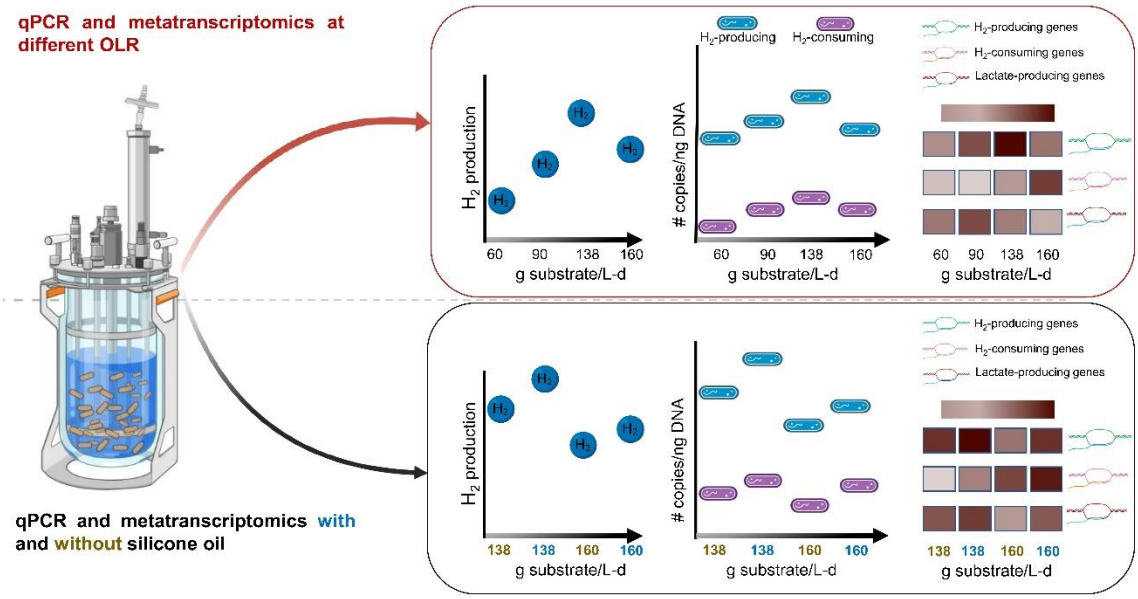

Highlights

- Secuencing results showed the co-dominance of H_2-producing bacteria, H_2-consuming bacteria and lactic acid bacteria.
- qPCR results revealed that the quantity of genes *hydA* and *fthfs* are strongly associated to H_2 production and the OLR.
- The increase of the OLR strongly influenced the expression of genes related to H_2 production and homoacetogenesis.
- Extractive organic phase improves H_2 production, quantity of *fthfs* and *hydA* genes and the expression of H_2 production and homoacetogenesis genes.
- Two-phase partitioning reactors promote the dark fermentative metabolic pathways.

In preparation to be submitted to *Environmental Science and Technology*

4.1 Abstract

In dark fermentation the structure and dynamics of the microbial community in continuous systems are affected by factors such as substrate type and concentration, products accumulation (i.e. H_2 and CO_2) and type of reactor. Here, metatranscriptomics and quantitative PCR (qPCR) were applied to assess the impacts of high substrate concentration on microbial community diversity and expression of key dark fermentative genes. The analysis of microbial communities showed the co-dominance of H_2-producing bacteria (*Clostridium butyricum*), homoacetogens (*Clostridium luticellari*) and lactic acid bacteria (*Enteroccocus gallinarum* and *Leuconostoc mesenteroides)*. Quantification through qPCR showed that the abundance of genes encoding for the formyltetrahydrofolate synthetase (*fthfs*, homoacetogens) and hydrogenase (*hydA*, H_2-producing bacteria) were strongly associated by the organic loading rate (OLR) and H_2 production performance. Similarly, the increase of the OLR strongly influenced the abundance of the transcripts of genes responsible for H_2 production and homoacetogenesis. In particular, the highest abundance of genes conferring H_2 production were detected at the OLR of 138 total carbohydrates (TC)/L-d that also reported the highest H_2 productivity of 23.5 L H_2/L-d. In the same way, the addition of an extractive organic phase (to enhance gas mass transfer rate) at both OLR of 138 and 160 g TC/L-d improved the production of H_2, the copy numbers of the *fthfs* and *hydA* genes and the abundance of transcripts of the genes related to H_2 production and homoacetogenesis. Overall, the results revealed that the applied operational parameters clearly modified the abundance of genes that play a key role in H_2 production via dark fermentation and H_2 consumption via homoacetogenesis.

4.2 Introduction

Hydrogen (H_2) production via dark fermentation is a developing technology for energy production and management of organic carbohydrate-rich substrates. In dark fermentation, carbohydrates are metabolized by two main routes: the pyruvate formate lyase (PFL) and the pyruvate ferredoxin oxidoreductase (PFOR) pathways. These routes are associated with maximum theoretical metabolic yields of 2 and 4

mol H_2/mol hexose consumed, respectively [1]. However, most studies report H_2 yields below such thresholds. In continuous H_2-producing reactors, the volumetric hydrogen production rate (VHPR) is positively correlated with the organic loading rate (OLR) of substrate fed. However, it has been reported that the H_2 yield and VHPR decrease at OLR > 140 g of total carbohydrates (TC)/L-d [2–4]. The changes in H_2 yields and VHPR at high OLR depend on multiple factors, such as the accumulation of fermentation products (mainly H_2, CO_2 and carboxylic acids), the composition of the microbial communities, the substrate concentrationm, OLR, and operational conditions (e.g., temperature, pH, mixing, hydraulic retention time) [5]. These factors may inhibit the metabolic activity of H_2-producing bacteria and favor the development of undesirable metabolisms such as homoacetogenesis (consumption of H_2 and CO_2 to produce acetic acid).

In recent years, the in-situ extraction of fermentation products has been evaluated to improve dark fermentation systems. In particular, modification of stirring velocity, use of membranes for the selective separation of gases, gas sparging, and gas recirculation have been evaluated to reduce H_2 and CO_2 concentrations in the fermentation broth [6–8]. Recent studies carried out by our research group have shown that the use of silicone oil as an extractive organic phase, for enhancing the gas mass transfer rate in batch and continuous systems, improved the production of H_2 and carboxylic acids. In such investigation, the diversity of the microbial community in the continuous stirred tank reactors (CSTR) appeared to be ruled by the substrate loading rate rather than by the addition of silicone oil. At the OLR of 60 g TC/L-d, the microbial community was dominated by H_2-producing bacteria (*Clostridium* and *Klebsiella*), whereas at 138 g TC/L-d H_2-producing bacteria and lactic acid bacteria (LAB, *Lactobacillus* and *Sporolactobacillus*) co-dominated in the reactor [9]. Therefore, based on the positive effect of silicone oil on H_2 and carboxylic acids production, we hypothesized that the addition of such organic phase may stimulate metabolic pathways with better dark fermentation performance (e.g. PFL and PFOR pathways).

The microbial community function in dark fermentation bioreactors has been assessed by a variety of analysis and tools [1,10,11]. Quantitative PCR (qPCR) is a

molecular technique capable of quantifying marker genes, such as 16S rRNA [12]. In the case of dark fermentation, specific genes such as the Fe-Fe hydrogenase (*hydA*) gene found in H_2-producing bacteria and the formyltetrahydrofolate synthetase (*fthfs*) gene for homoacetogenic bacteria have been identified as main markers of interest [12,13] because it is possible to evaluate the influence of specific parameters (i.e. substrate concentration, temperature, HRT, among others) in the population dynamics of H_2-producing bacteria and H_2-consuming bacteria.

Transcriptomics studies RNA transcripts that are produced by the genome under specific circumstances by using high-throughput methods such as Illumina seq. The comparison of transcriptomes allows the identification of genes that are differentially expressed in different microbial communities or in response to different treatments [14,15]. For the particular case of dark fermentation, it can be determined whether genes involved in: i) H_2 production by the PFL and PFOR pathways (e.g. *hydA*, formate hydrogen lyase [*fhl*]), ii) H_2 consumption (*fthfs*), and iii) production of other compounds (e.g. lactate dehydrogenase) are expressed in higher or lower proportion. The combination of advanced molecular tools provide insight on the microbial community structure and function of dark fermentation systems. In this work, several OLR were applied in a CSTR with or without silicone oil as an extractive organic phase to improve the H_2 yields and VHPR. Functional gene analysis by qPCR and transcriptomics were utilized to evaluate the prevalence of homoacetogens and H_2-producing bacteria, and to investigate the expression changes of the genes involved in continuous dark fermentation systems.

4.3 Materials and methods

4.3.1 Inoculum, fermentation medium, substrate, and organic phase

Anaerobic granular seed sludge from a full-scale up-flow anaerobic sludge blanket reactor treating wastewater from a tequila factory (Casa Herradura, Mexico) was used as the inoculum for the start-up of CSTR1 (Section 4.3.2). Before its use, the sludge was heat-treated at 105 °C for 24 h, powdered in a mortar, and sieved through 0.5 mm mesh [16]. The fermentation medium was supplemented with the following minerals as described previously (mg/L) [9]: NH_4Cl, 2100; $MgCl_2 \cdot 6H_2O$,

100; $CuCl_2 \cdot H_2O$, 1.25; $MnCl_2 \cdot 4H_2O$, 7; $FeCl_2 \cdot 4H_2O$, 19.1; $NiCl_2 \cdot 6H_2O$, 102.5; KH_2PO_4. Furthermore, a phosphate buffer (KH_2PO_4-Na_2HPO_4) was added to reach a final concentration of 50 mM.

In all dark fermentation experiments, cheese whey powder (CWP, Chilchota Alimentos S.A de C.V, Mexico) containing 72% TC was used as the substrate at concentrations ranging 15 to 40 g TC/L. Silicone oil (CHEM SIL, Mexico) with a viscosity of 100 centistokes was used as the extractive organic phase in the reactors.

4.3.2 Bioreactors set-up and operational conditions

Three CSTR (Applikon Biotechnologies, USA) were operated independently. In all cases, the reactors had a working volume of 1 L. CSTR1 was operated with the main objective of producing seed-biomass for subsequent experiments. CSTR1 was inoculated with 4.5 g volatile suspended solids (VSS)/L of heat-treated inoculum and started-up in batch mode during 24 h at an initial substrate concentration of 15 g TC/L. Thereafter, the reactor was switched to continuous mode at a hydraulic retention time (HRT) of 6 h and an OLR of 60 g TC/L-d. CSTR1 operated at a constant agitation (300 rpm), temperature (37 ºC) and pH (5.9). The reactor operated for at least 20 HRT (5 days) and until steady state was reached in terms of VHPR. The steady state was stated as the period where the variation of three consecutive values of VHPR was < 10%. During steady-state conditions, ~ 4.5 L of effluent was recovered and centrifuged at 3500 rpm for 10 min at 4 °C. The resulting pellets were re-suspended in mineral medium without substrate, characterized in terms of VSS and stored at −4 °C until their use as inoculum in reactors CSTR2 and CSTR3.

CSTR2 and CSTR3 were inoculated with the recovered biomass from CSTR1 at a concentration of 4.5 g VSS/L. The reactors start-up conditions and operational parameters were the same as those defined for the CSTR1. These reactors were also operated for at least 20 HRT at each of the assessed stages, and the change of stage was performed until a steady state of VHPR was observed. The stages of the reactors with and without silicone oil were operated according to the methodology proposed by Montoya-Rosales et al. [9].

4.3.3 Analytical methods

Liquid samples were collected on a regular basis and used to determine the concentrations of biomass, total carbohydrates and carboxylic acids. The concentration of VSS was determined according to the standard methods [17], and the concentration of TC by the phenol-sulfuric method [18]. Carboxylic acids were quantified from filtered (0.22 mm) samples by capillary electrophoresis 1600A (Agilent Technologies, Germany), as reported elsewhere [19]. The gas production and its composition (i.e., H_2 and CO_2) were measured by a liquid displacement device (SEV, Mexico) and gas chromatography with TCD detector 6890 N (Agilent Technologies, Germany), respectively [6]. All the gas volumes are reported at standard conditions (1 atm and 273.15 K). The results are reported as averages ± standard deviation from three consecutive samples obtained from steady states in the CSTR assays.

4.3.4 DNA extraction and quantification of *fthfs* and *hydA* genes by qPCR

Ten milliliters samples from the last three measurements of each steady state were collected in 15 mL falcon tubes from the effluent of the three CSTR. Then, the biomass was harvested by centrifugation (10 min at 3200 rpm) and stored at - 20 ºC until their use. Prior to DNA extraction, the three biomass samples from the same steady state were pooled. The DNA was extracted using the Fungal/Bacterial DNA MiniPrep kit (Zymo Research, USA) according to the manufacturer's instructions.

The quantification of *fthfs* and *hydA* genes across the different experimental conditions of CSTR1-3 was determined through qPCR by sybr green following the methodology reported by Fuentes et al. [12]. The qPCR procedure was carried out at the Microbial Ecology Laboratory - Clemente Estable Biological Research Institute, Uruguay. In brief, the copy number of *hydA* gene was measured in all the samples. This gene codifies the enzyme Ferredoxin hydrogenase that catalyzes the reversible oxidation of molecular H_2. To construct the standard curve for the quantification of the gene *hydA*, a clone of the hydrogenase enzyme gene A10 was used [20]. To quantify the gene *fthfs* codifying for formyltetrahydrofolate synthetase

enzyme, plasmids from strain *Acetobacter woodii* DSMZ 1030 containing target fragments of the functional gene *fthfs* were used to construct the calibration curve. The qPCR conditions and melting curve were performed according to Xu et al. [21]. The standard curves for both genes were prepared by making successive dilutions 1:10. Table 4.1 summarizes the primers used for this study and the qPCR protocols. DNA from *Pseudomonas sp*. and *Raoultella sp.* were used as negative controls. Finally, all reactions were made by triplicate and the qPCR results were expressed in copy number/ng DNA.

Table 4.1. Primer Sets and Protocols Used for qPCR Analyses

Target gene	Primer name	Sequence	PCR protocol	Calibration curve	
				E	R^2
hydA	M13F M13R	5´ -CAGGAAACAGCTATGAC-3´ 5 -GTTTGATCCTGGCTCAG-3´	95 °C 10 min 50 cycles 95 °C 30 s 52 °C 30 s 72 °C 30 s 72 °C 5 min	1.71	0.99
fthfs	FTHFS-f FTHFS-r	5′-TTYACWGGHGAYTTCCATGC-3′ 5′-GTATTGDGTYTTRGCCATACA-3´	94 °C 4 min 30 cycles 94 °C 45 s 55 °C 45 s 72 °C 1 min 72 °C 5 min	1.06	0.99

4.3.5 RNA extraction and transcriptome sequencing and metatranscriptome analysis

To elucidate the expression of the genes involved in continuous dark fermentation systems, biomass samples (30 mL) from the last three measurements of each steady state (except CSTR2-I, Table 4.2) were collected in 50 mL falcon tubes from the effluent of the three CSTR. Formerly and following the company's specifications

(Zymo Research, USA), the biomass was harvested by centrifugation at 3500 rpm by 10 min. RNAlater (to avoid RNA degradation) was immediately added to each centrifuged tube containing the biomass pellets. The samples with RNAlater were stored at -20 ºC until use. Prior to RNA extraction, the harvested biomass from the three falcon tubes of each stage were pooled. RNA extraction was performed using the commercial ZymoBIOMICS RNA Mini Kit (Zymo Research, USA) by following the manufacturer's instructions. The RNA was quantified by a NanoDrop. RNA samples were sent to the Arizona State University Genomics Core facility (USA) for transcriptomic analysis.

The following steps were made at Arizona State University's Genomics Core facility: the complementary DNA (cDNA) synthesis was performed using Ovation® RNA-Seq System V2 (Tecan Genomics, Inc. USA) and random hexamers primers following manufacturer's instructions. cDNA was sheared to approximately 300-base-pair fragments with Covaris M220 system (Woburn, MA) prior to library construction. The construction proceeded with an Apollo 324™ Library Prep System, including sheared cDNA repair and a bead cleanup. Following post-enhancement PCR for libraries, the average fragment size and rough quantity of each library were evaluated using an Agilent 4200 TapeStation.

Once quality control was attained with TapeStation, the samples were assessed by quantitative PCR (qPCR) for exact quantification of Illumina adapters, which had been attached during library construction. The nanomolar quantities of the library were based upon the qPCR results combined with the average fragment size from TapeStation. The libraries were then pooled equimolar for sequencing on 1 × 75 flow cells on the NextSeq500 platforms (Illumina) at Arizona State University Genomics Core facility. All sample sequences were deposited at the NCBI/Sequence Read Archive (SRA) under project PRJNA 742404.

All the metatranscriptomi analysis were performed according to microbiome RNA-seq data by Jagtap et al. [22] and Batut et al. [23]. Briefly, RNA reads were trimmed and filtered for length and quality using Cutadapt [24]. Reads passing a quality control (QC) value of 30 were mapped to contigs produced by assembly of Illumina sequences. To make the downstream functional annotation, the rRNA sequences

were sorted by using SortMeRNA to remove all sequences cataloged as ribosomal RNAs. To analyze the structure of the communities, a taxonomic profiling was performed with MetaPhlAn [25]. This tool uses a database of ~1M unique clade-specific marker genes (not only the rRNA genes) identified from ~17,000 reference (i.e., bacterial, archaeal, viral, and eukaryotic) genomes. As rRNAs reads are good marker genes, the quality-controlled files were directly used (output of Cutadapt) with all reads (not only the non-rRNAs which were obtained with SortMeRNA).

To analyze the functional information, HUMAnN was used to identify genes and their functions, and to build metabolic pathways in the microbial community [26]. Furthermore, HUMAnN is a pipeline developed for efficient and accurate profiling of the presence/absence and abundance of microbial pathways in a community from metagenomic or metatranscriptomic sequencing data [26]. Lastly, taxonomic and functional information was combined to offer insights into taxonomic contribution to a function or functions expressed by a particular taxon.

4.3.6 Multivariate analysis

Pearson's correlation (ρ) analysis was carried out with the information of abundance of transcripts from the metatranscriptome analysis, qPCR values for gene *hydA* and *fthfs*, fermentation performance (i.e., VHPR, H_2 yield, and carboxylic acids production) and the OLR to provide better insight on the diverse microbial ecological interactions within the CSTR. This analysis was performed in R software [27], using the corrplot package.

4.4 Results and discussion

4.4.1 Dark fermentation performance

The operational conditions and the performance of the reactors are summarized in Table 4.2. The CSTR1 was operated for 10 days at an OLR of 60 g TC/L-d. The performance of CSTR1 was stable with an average VHPR of 6.1 ± 0.6 L H_2/L-d and total carboxylic acids production of 12.5 g/L (Table 4.2). VHPR values were similar to those reported in previous investigations at similar OLR [6,9]. The constant H_2

production agrees with former reports and showed an effective establishment of the dark fermentative H_2-producing microbial community. Consequently, the biomass was then recovered to serve as inoculum for CSTR2 and CSTR3.

In the first three operational conditions of the CSTR2 the effect of the increment in the OLR was studied (Table 4.2). The increase of OLR from 90 to 138 g TC/L-d had a direct effect on the VHPR and H_2 yield. In particular, the VHPR increased from 12.7 to 23.2 L H_2/L-d. However, a drop in the H_2 production was observed when the OLR was increased to 160 g TC/L-d. This drop in the performance of CSTR2 was expected since previous works reported a decrease in H_2 productivity at OLR >140 g TC/L-d possibly as a consequence of substrate overloading and inhibition by products (e.g., H_2, CO_2 and carboxylic acids) accumulation [3,4]. As estimated, a positive effect of the silicone oil was observed in the CSTR2-stage IV. In particular, silicone oil increased the H_2 productivity equivalent to 15% in comparison with the stage III without silicone oil, resulting in an average VHPR of 19.8 $\pm$ 0.4 L H_2/L-d. This behavior was reported previously by Montoya-Rosales et al. [9] who found that adding and maintaining a proportion of 10% v/v of silicone oil within a CSTR enhanced the VHPR from 23.8 to 26.9 L H_2/L-d at an OLR of 138 g TC/L-d.

CSTR3 was operated for 27 days, in this reactor the effect of adding silicone oil at the OLR of 138 g TC/L-d was evaluated. Overall, when silicone oil was added an increase in the VHPR and H_2 yield of 16% and 24% were observed. Such increase resulted in average VHPR value of 27.1 L H_2/L-d and a H_2 yield of 1.8 mol H_2/mol glucose consumed and were in accordance to previous studies [9].

From the analysis of the carboxylic acids (Table 4.2), acetate and butyrate were the main metabolic products at OLR < 138 g TC/L-d. On the other hand, at OLR ≥ 138 g TC/L-d, acetate-butyrate fermentation and lactic acid fermentation occurred simultaneously. In lactic acid fermentation (production of lactate as a by-product), H_2 is not produced, because LAB competes directly with H_2-producing bacteria for the available substrate (i.e. lactose in cheese whey) [28]. Nonetheless, some studies reported that lactate produced during lactic fermentation can serve as substrate to produce more H_2 and butyrate [29,30]. The role of lactic acid fermentation in dark fermentation is not yet considered as beneficial or detrimental, and must be analyzed

on a case-by-case basis. For this investigation, it appears that at 138 g TC/L-d the production of lactate did not affect the concentrations of neither acetate, butyrate, nor H_2. Similarly, at the OLR of 160 g TC/L-d, acetate and butyrate concentrations did not decrease in comparison with lower OLR. On the contrary, the concentration of both carboxylic acids was higher than OLR from 60 to 138 g TC/L-d (Table 4.2). Therefore, the CSTR apparently did not show competition for substrate between lactic acid bacteria and H_2-producing bacteria. In consequence, substrate overloading and accumulation of carboxylic acids, H_2, and CO_2 appear as the most probably factors that caused the decrease in the VHPR in the CSTR2

Table 4.2. Performance of the three CSTR systems at different operational conditions.

Reactor	Stage	OLR (g TC/L-d)	VHPR (L H_2/L-d)	H_2 yield (mol H_2/mol hexose consumed)	TC removal (%)	Carboxylic acids concentration (g/L)		
						Acetate	Butyrate	Lactate
CSTR1	I	60	6.1 ± 0.6	0.78 ± 0.2	92 ± 1	3.9 ± 0.3	8.6 ± 0.4	N.D.
CSTR2	I	90	12.7 ± 0.6	1.09 ± 0.1	92 ± 2	4.7 ± 0.4	9.6 ± 0.5	N.D.
	II	138	22.1 ± 0.7	1.42 ± 0.1	91 ± 2	6.6 ± 0.6	10.4 ± 0.7	8.6 ± 0.4
	III	160	17.2 ± 0.5	1.12 ± 0.2	80 ± 3	8.7 ± 0.6	11.8 ± 0.7	9.3 ± 0.3
	IV	160*	19.8 ± 0.4	1.19 ± 0.1	86 ± 2	9.1 ± 0.2	11.1 ± 0.6	9.1 ± 0.2
CSTR3	I	90	13.1 ± 0.4	1.10 ± 0.1	93 ± 1	4.9 ± 0.2	8.9 ± 0.3	N.D
	II	138	23.5 ± 0.5	1.45 ± 0.1	92 ± 2	6.2 ± 0.3	9.7 ± 0.4	8 ± 0.3
	III	138*	27.2 ± 0.3	1.81 ± 0.1	96 ± 2	7.8 ± 0.4	10.8 ± 0.4	9.7 ± 0.3

Number of samples retrieved from the steady-states was 3 in all cases.
OLR: organic loading rate; TC: total carbohydrates; VHPR: volumetric hydrogen production rate; N.D.: not detected
*Silicone oil added at a proportion 10% (v/v).

4.4.2 Community structure by transcriptomics

The mRNA-sequencing results showed that the applied OLR clearly influenced the microbial composition in the reactors, while the effect of the silicone oil addition was not clear. Figure 4.1 illustrates that the microbial community in all the CSTRs were dominated by organisms from the genera *Clostridium*, *Enteroccocus*, and *Leuconostoc* that accounted for about 98% of the relative abundance for all the reactors. In CSTR1 and CSTR2-I, *C. butyricum* was the species that showed the highest relative abundance of detected mRNA (> 92 %). *C. butyricum* belongs to the genus *Clostridium* sensu stricto 1 and has been intensively detected among dark fermentative reactors as a strict H_2-producing bacterium with the co-production of butyrate, acetate, and ethanol [31,32]. Another *Clostridium* detected in all the CSTR was *Clostridium luticellari*, its mRNA relative abundance ranged from 1% to 7%. *C. luticellari* fits in the *Clostridim* sensu stricto 12 and has been widely classified as a homoacetogenic (capable to consume dissolved H_2 and CO_2) and chain elongating bacterium (from acetate to n- and iso-butyrate). Interestingly, higher abundance percentages of *C. luticellari* were detected in the stages with higher VHPR that also were the stages with more calculated dissolved H_2 and CO_2, making these gases available for homoacetogenic bacteria. *C. luticellari* was not dominant in the communities but present at low proportions, its presence becomes relevant as this bacterium can compete and use H_2 and CO_2 generated by other dominant H_2-producing microorganisms which not have the capacity to carry out homoacetogenesis.

At the OLR of 138 g TC/L-d (CSTR2-II, CSTR3-II and III), *C. butyricum* displayed dominance of approximately 70% of relative abundance, while *Enteroccocus gallinarum* and *Leuconostoc mesenteroides* were detected with a dominance of about 13% and 6%, respectively. *E. gallinarum* and *L. mesenteroides* are LAB that consume substrate (e.g. pyruvate produced in the glycolysis step) to produce lactate [33]. The distribution of the mRNA relative abundance at the OLR of 138 g TC/L-d together with the VHPR and H_2 yield, suggest that the presence of *E. gallinarum* and *L. mesenteroides* is concomitant to H_2-producers that even can provide extra substrate by converting lactate to H_2 and butyrate. For instance, *C. butyricum* has

been reported as a *Clostridium* bacteria that belongs to the diverse group of the lactate-fermenting hydrogen producing bacteria (LF-HPB) that in a second fermentation consume lactate and acetate to produce H_2 and butyrate [30]. Nevertheless, at the OLR of 160 g TC/L-d (CSTR2-III) the relative abundance of LAB increased, this increase can be linked to the abundance of substrate that enhance the competence between H_2-producing bacteria and LAB [33], and caused a considerable drop of the H_2 production in the system (Table 4.2). Nonetheless, when silicone oil was added at the system in the CSTR2-IV, an increase of the mRNA relative abundance for *C. butyricum* (73%) was observed. This result, combined with the increase of the VHPR in comparison with the CSTR2-III condition, implies that the addition of silicone oil stimulated the prevalence of H_2 producing bacteria over non-H_2 producing bacteria, enhancing the metabolic pathways to improve the dark fermentation performance (i.e., acetate and butyrate production).

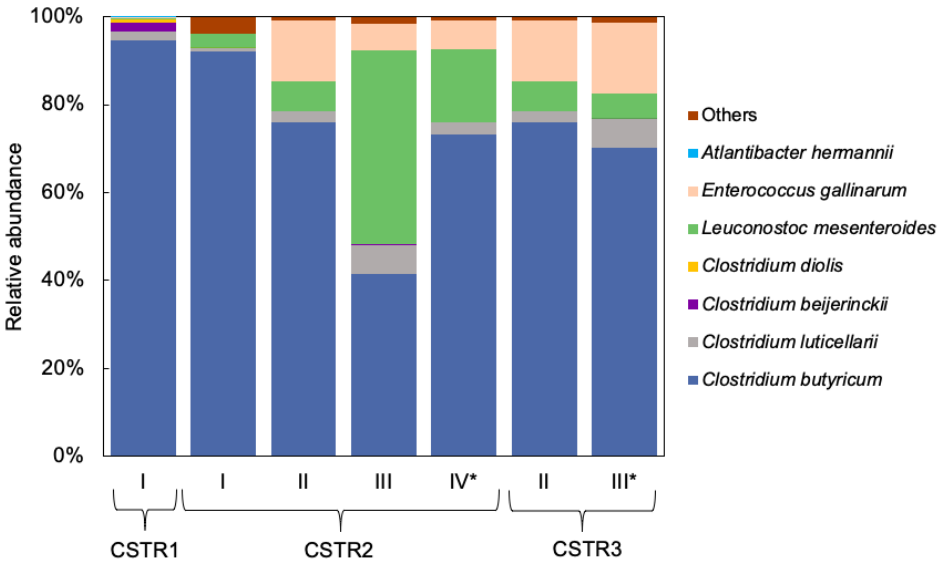

Figure 4.1. Relative abundances of the microbial communities at the species taxonomic level in CSTRs 1-3. *Silicone oil added at a proportion of 10% (v/v). See Table 4.2 for operational conditions details.

4.4.3 Community function by qPCR functional genes *hydA* and *fthfs*: the abundance of H_2-producing bacteria and homoacetogens

The quantitative analysis of the gene *fthfs* showed that homoacetogenic microorganisms were present in all dark fermentation reactors (Figure 4.2). The

abundance of the *fthfs* gene ranged from 6.38 E +01 and 2.45 E +03 copies/ng DNA, and was positively correlated with the VHPR (ρ= 0.49, $p<0.05$) and H_2 yield (ρ=0.74, $p<0.05$) (Figures 4.2-B and 4.2-D). The *hydA* gene was also found to have a positive correlation with VHPR (ρ= 0.63, $p<0.05$) and H_2 yield (ρ=0.83, $p<0.05$) (Figures 4.2-A and 4.2-C). The relationship between *fthfs* and *hydA* gene with operational parameters has been also reported by Fuentes et al. [12] in a study of 19 continuous dark fermentation reactors. They reported that the abundance of both genes was strongly dependent of the type of substrate, the OLR, and the VHPR. In our case, a positive relationship between both *ftfhs* and *hydA* genes was clearly observed as seen in Figure 4.2-E (ρ= 0.78, $p<0.05$). Higher VHPR and therefore higher H_2 and CO_2 dissolved concentrations in the fermentation broth led to an increase of microorganisms performing homoacetogenesis through the Wood-Ljungdahl pathway [34].

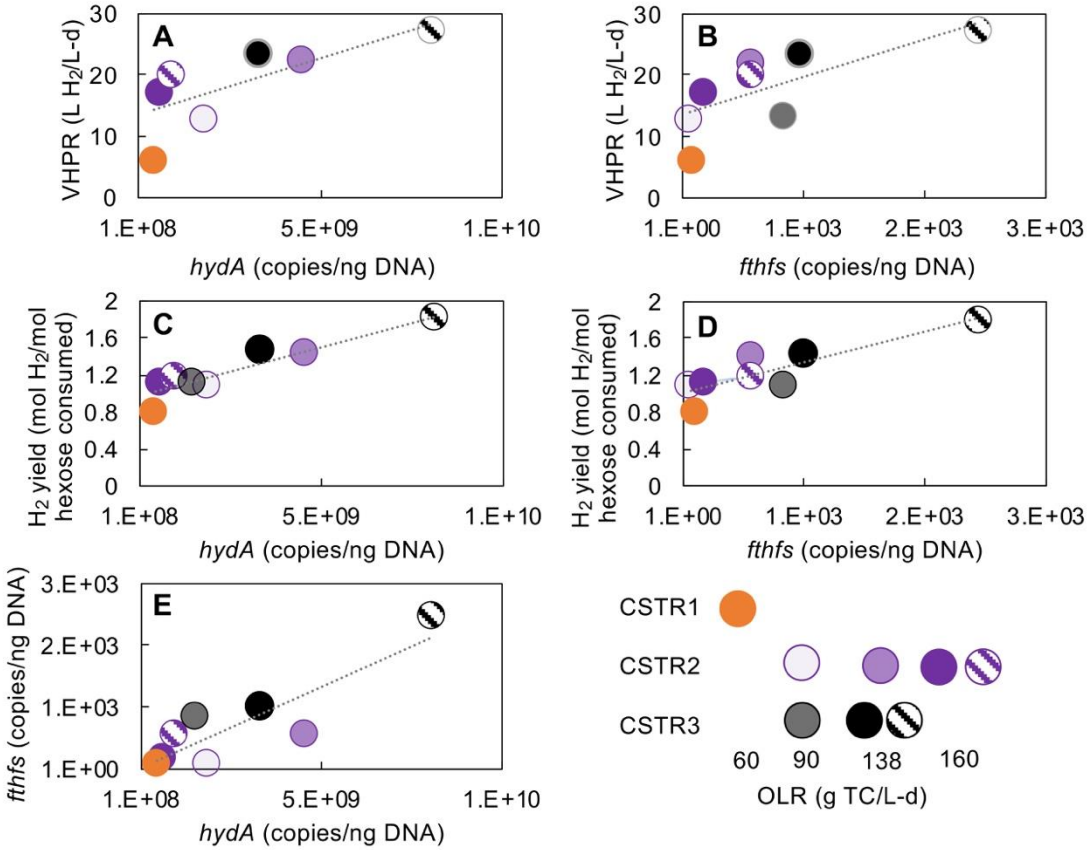

Figure 4.2. Correlations between the *hydA* gene and the *fthfs* gene along the VHPR (panels A and B), H_2 yield (panels C and D), and the correlation of both genes (E). The circles with hatching correspond to stages with silicone oil.

4.4.3.1 The OLR in the prevalence of homoacetogens and H_2-producing bacteria

The effect of OLR on dark fermentation was evaluated for CSTR2. As the OLR was increased (as seen from Figures 4.3-A, 4.3-C and 4.3-E), a relationship between the VHPR, the abundance of H_2-producing bacteria (measured by the *hydA* gene) and homoacetogens was observed (measured by the *ftfhs* gene). When the OLR was changed from 90 to 138 g TC/L-d, the VHPR increased from 12.7 to 23.2 L H_2/L-d. Likewise the abundance of H_2-producing bacteria and homoacetogens increased from 1.93 E+ 09 to 4.64 E +09 copies/ng DNA and 6.38 E +01 a 5.71 E +02 copies/ng DNA, respectively (Figures 4.3-A and 4.3-C). Interestingly, at the OLR of 160 g TC/L-a decline in the abundance of both genes was observed, which coincides with the drop of the VHPR. From these results, it can be inferred that at an OLR of 90 and 138 g TC/L-d, the high availability of substrate allows the enrichment of both bacterial groups without compromising the performance of the reactor for the production of H_2 and carboxylic acids. Likewise, the decline of H_2 production at the OLR of 160 g TC/L-d are in agreement with previous studies proposing that at high OLR homoacetogenesis was favored by the possible accumulation of H_2 and CO_2 in the aqueous phase of the reactor [12]. However, at the OLR of 160 g AT/L-d, such hypothesis does not seem to hold true, as a decrease in the abundance of H_2-producing and homoacetogenic bacteria was reported [12]. In this particular case, the decrease of both groups of bacteria may be due to a possible substrate overload in the reactor, which inhibited their growth.

It is important to mention that some groups of bacteria can have a dual capacity to produce and consume H_2. *Clostridium carboxydivorans* and *Acetobacterium woodii* have both genes (i.e., *fthfs* and *hydA*) in their genome and some explames. As qPCR amplifies and quantifies particular genes which may be in the same bacterium, a second hypothesis can be established: The abundance of both genes as a function of the OLR and VHPR may be due to a change in the prevalence of bacterial groups with dual capacity and not necessarily to a change in the predominance of both H_2-producing and homoacetogenic bacteria. Previous works in continuous reactors operated at high OLR have identified dual-capacity bacteria (i.e., *C. carboxidivorans*

and *A, woodii*), strictly H_2-producing bacteria (e.g., *Clostridum acetobutylicum*, *Enterobacter spp*) and homoacetogenic bacteria (e.g., *Blautia coccoides*, *Eubacterium limosum*, *Oscillibacter valericigenes*) [12,35,36]. However, mRNA-sequencing results (Figure 4.1) shows that the microbial community structure in all CSTR was composed by strict H_2-producing bacteria (i.e., *C. butyricum*, *C. diolis*), and homoacetogenic bacteria (i.e., *C. luticellari*). Nonetheless, the abundance of dual-capacity bacteria which may be at such low abundances cannot be ruled out. In the same way, the considerably lower mRNA relative abundance in all the CSTR of *C. luticellari* in comparison with *C. butyricum* and LAB (Figure 4.1), likely explain the remarkable difference of gene copies between hydrogen-producing bacteria (i.e., *hydA* gene) and homoacetogenic bacteria (i.e., *fthfs* gene). This might respond to the slow-growing mechanism of homoacetogens such as *C. luticellari*, as their ability to produce energy from H_2 and CO_2 is very limited due to the low free energy of the reaction ($\Delta G^{\prime o}$ = -104 kJ) [12].

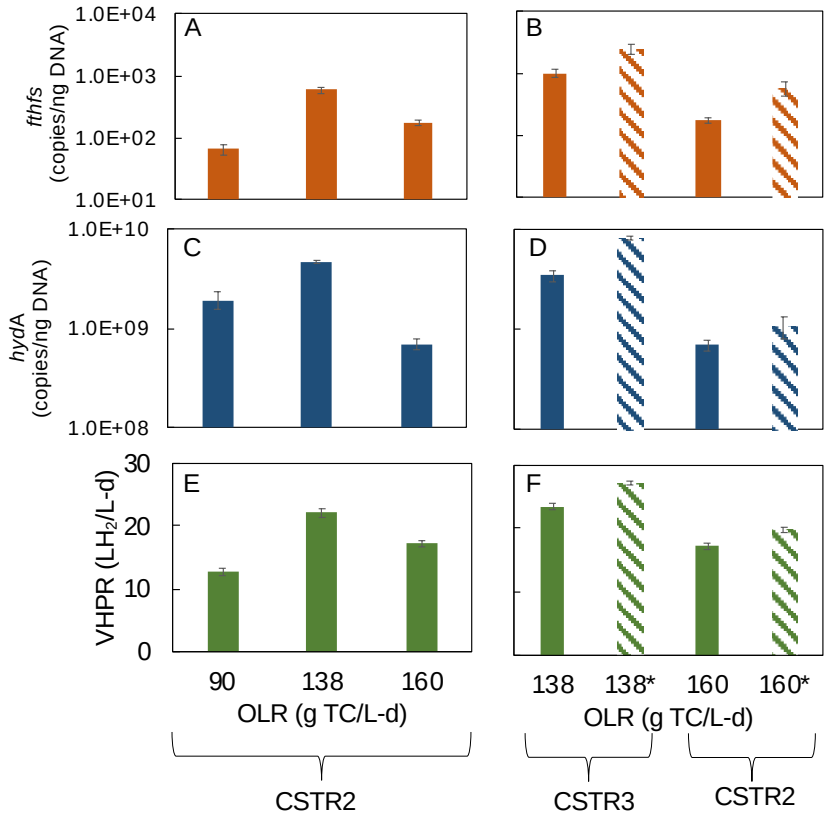

Figure 4.3. VHPR and abundance of *fthfs* and *hydA* genes at different OLRs (A, C, E) and for stages with and without silicone oil (B, D, F). *Silicone oil added at 10 % v/v.

4.4.3.2 Abundance of homoacetogens and H_2-producing bacteria in two-phase partitioning reactors

Figures 4.3-B, 4.3-D and 4.3-F show the qPCR results for the hydA and fthfs gene, as well as the VHPR at the OLR of 138 and 160 g TC/L-d with and without silicone oil. For the OLR of 138 g TC/L-d, silicone oil increased the VHPR with the concomitant increase in the abundance of H_2-producing bacteria as compared to the same OLR without silicone oil (3.42 E +09 vs. 8.19 E +09 hydA copies/ng DNA). Similar results were observed at the OLR of 160 g TC/L-d, where the abundance of H_2-producing bacteria increases from 6.92 E +08 to 1.07 E +09 copies/ng DNA. The positive effect of adding an extractive organic phase in fermentative reactors may be due to a stimulation of H_2-producing metabolic pathways and then a possible change in the abundance of H_2-producing bacteria.

In the case of homoacetogenic bacteria, similar results to the previous section were observed, i.e., the abundance of this group increased in the same way that the abundance of H_2-producing bacteria and VHPR. Considering these results, it can be inferred that supplementing with silicone oil a H_2-producing reactor incremented the abundance of both H_2-producing and homoacetogenic bacteria (and/or bacteria with dual capacity). The increase of the abundance of such bacteria caused higher VHPR as compared to the controls (samples with the same OLR without silicone oil). A possible explanation for this positive relationship between the addition of silicone oil and bacterial abundance is that the increase of the liquid-gas transfer area, and therefore the reduction of the partial pressure in the system by the addition of silicone oil decreased the possibility of an inhibition of H_2-producing bacteria, homoacetogenic bacteria, and dual-capacity bacteria.

4.4.4 Community function as analyzed by transcriptomics

To understand the molecular response of several dark fermentation genes at different OLR, the transcriptomes of the CSTR1 and CSTR2 microbial biomass were examined and compared. The identified transcripts were classified according to gene ontology (GO) terms. The category of molecular function was used to identify the GO that carried out the activities for producing H_2 via the PFOR and PFL

pathways. In the same way, the GO that participate in the production of fermentative metabolites such as acetate via homoacetogenesis (Wood- Ljungdahl metabolism), acetate via Acetyl-CoA, butyrate, and lactate were also identified (Figures 4.4 and Figure 4.5). In dark fermentation, pyruvate ferredoxin oxidoreductase (*pfor*, GO:0019164), pyruvate formate lyase (*pfl*, GO:0008861), and hydrogenase (*hydA*, GO:0008901) are known to play critical roles in catalyzing H_2 evolution during dark fermentation [37]. In such processes, pyruvate is oxidized to acetyl-coenzyme A (acetyl-CoA) by ferredoxin oxidoreductase and simultaneously electrons are donated to convert the oxidized ferredoxin to its reduced form. Subsequently, the reduced ferredoxin is oxidized by hydrogenase (*hydA*) to generate H_2 by using protons as terminal electron acceptors [38]. Pyruvate also is oxidized to acetyl-CoA and formate by the pyruvate formate lyase. Afterward, the formate can be converted to CO_2 and H^+ by the formate dehydrogenase (*fdh*, GO:0008863) while the H^+ are used by the hydrogenase (*hydA* and *hycE*) to produce H_2 [39] (see diagram in Figure 4.4).

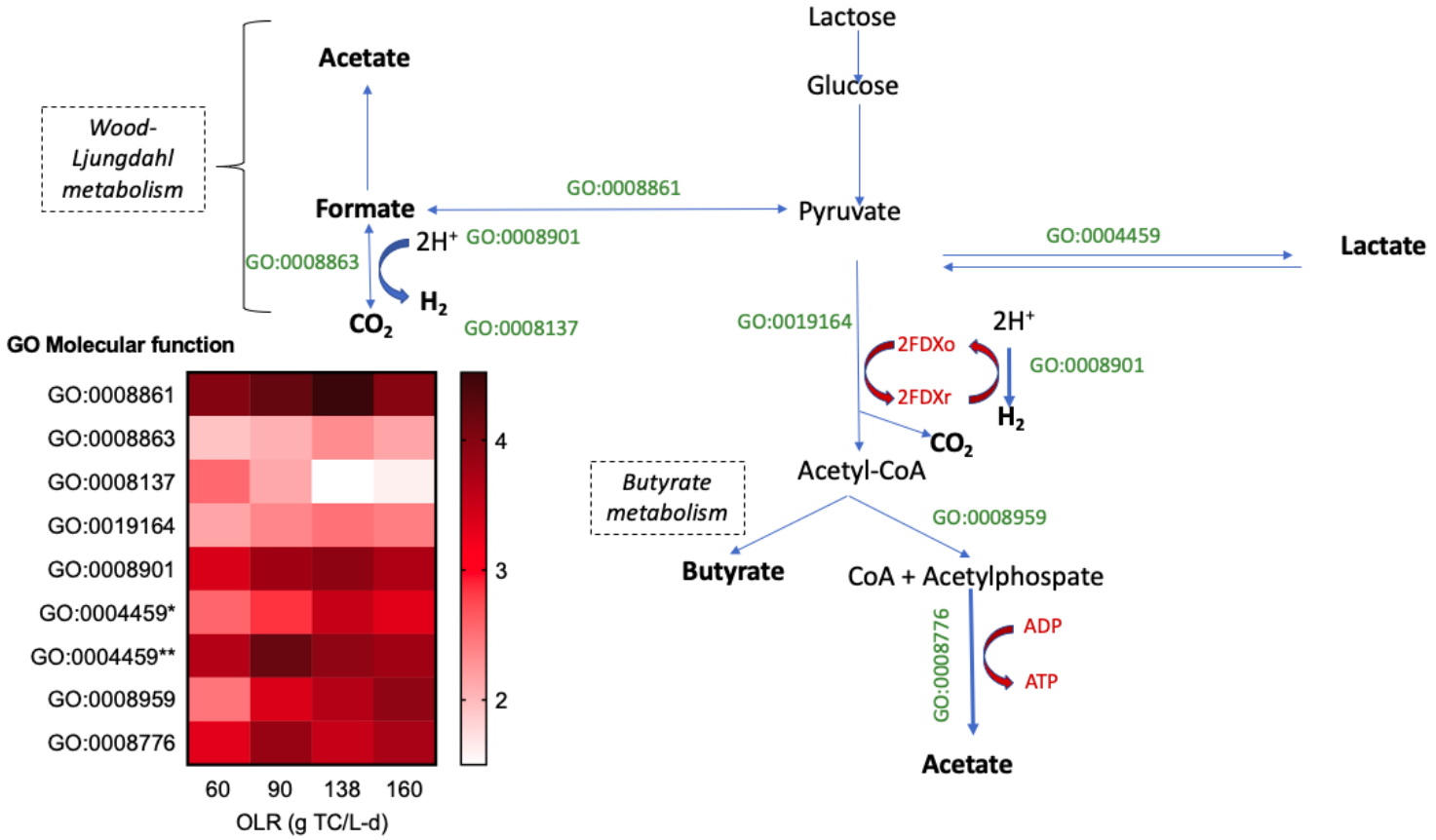

Figure 4.4. Abundance of the gene ontology (GO) related to production of H_2, CO_2, acetate via Wood-Ljungdahl, acetate via pyruvate fermentation, lactate, formate, and butyrate at different organic loading rates (OLR). GO:0008861 (pyruvate formate lyase activity); GO:0008863 (formate dehydrogenase); GO:0008901(hydrogenase activity); GO:0008137 (hycE activity); GO:0004459 (lactate dehydrogenase activity); GO:0019164 (pyruvate ferredoxin oxidoreductase activity); GO:0008959 (phosphate acetyltransferase activity); GO:0008776 (acetate kinase activity). *lactate dehydrogenase activity for *Clostridium* species. **lactate dehydrogenase activity for lactic acid bacteria. The color gradient from white to red indicates the relative expression level log2 changes at different OLR.

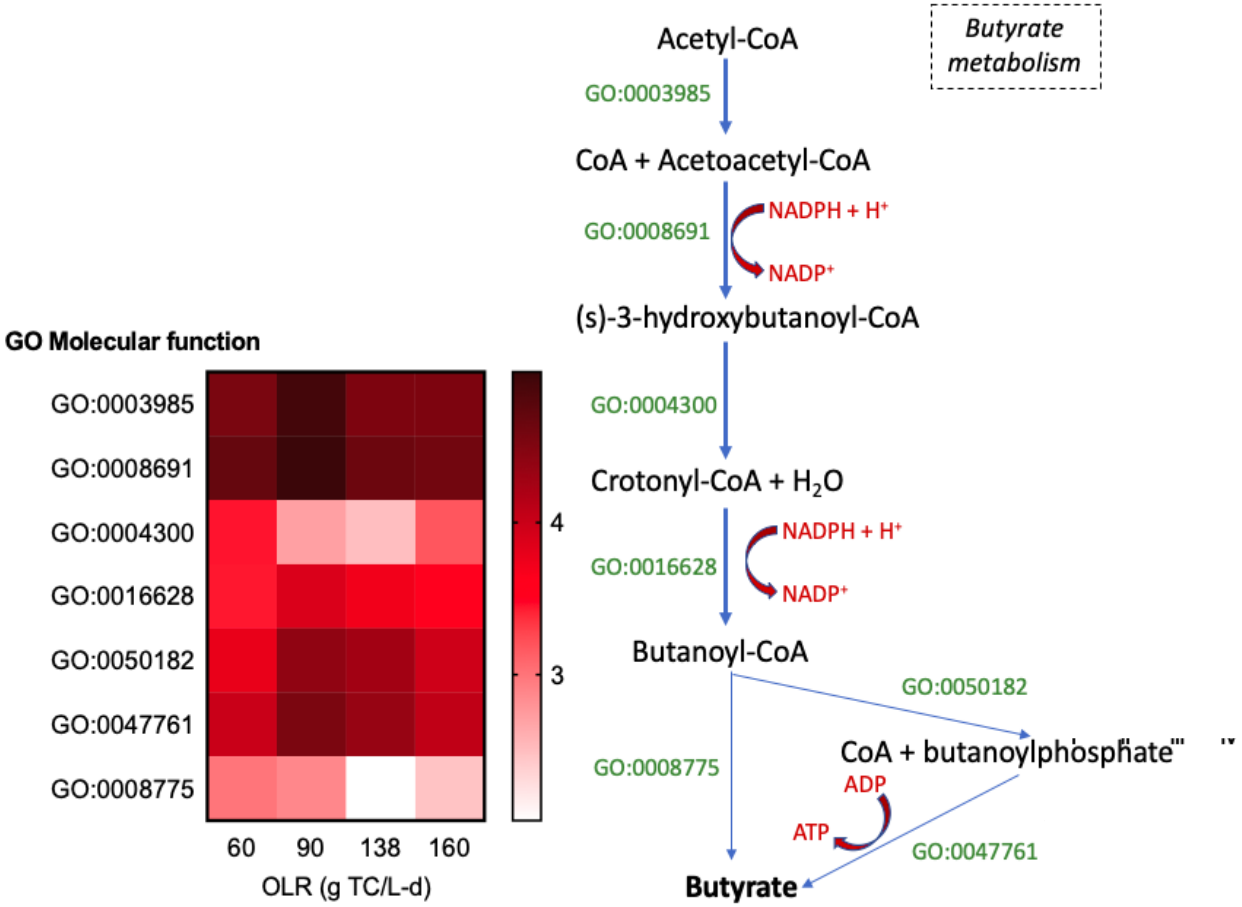

Figure 4.4 (Continued). Abundance of the gene ontology (GO) related to production of H_2, CO_2, acetate via Wood-Ljungdahl, acetate via pyruvate fermentation, lactate, formate, and butyrate at different organic loading rates (OLR). GO:0003985 (acetyl-CoA C-acetyltransferase activity); GO:0008691 (3-hydroxybutyryl-CoA dehydrogenase activity); GO:0004300 (enoyl-CoA hydratase activity); GO:0016628 (N.D); GO:0050182 (phosphate butyryltransferase activity); GO:0047761 (butyrate kinase activity); GO:0008775 (acetate CoA-transferase activity). The color gradient from white to red indicates the relative expression level log2 changes at different OLR.

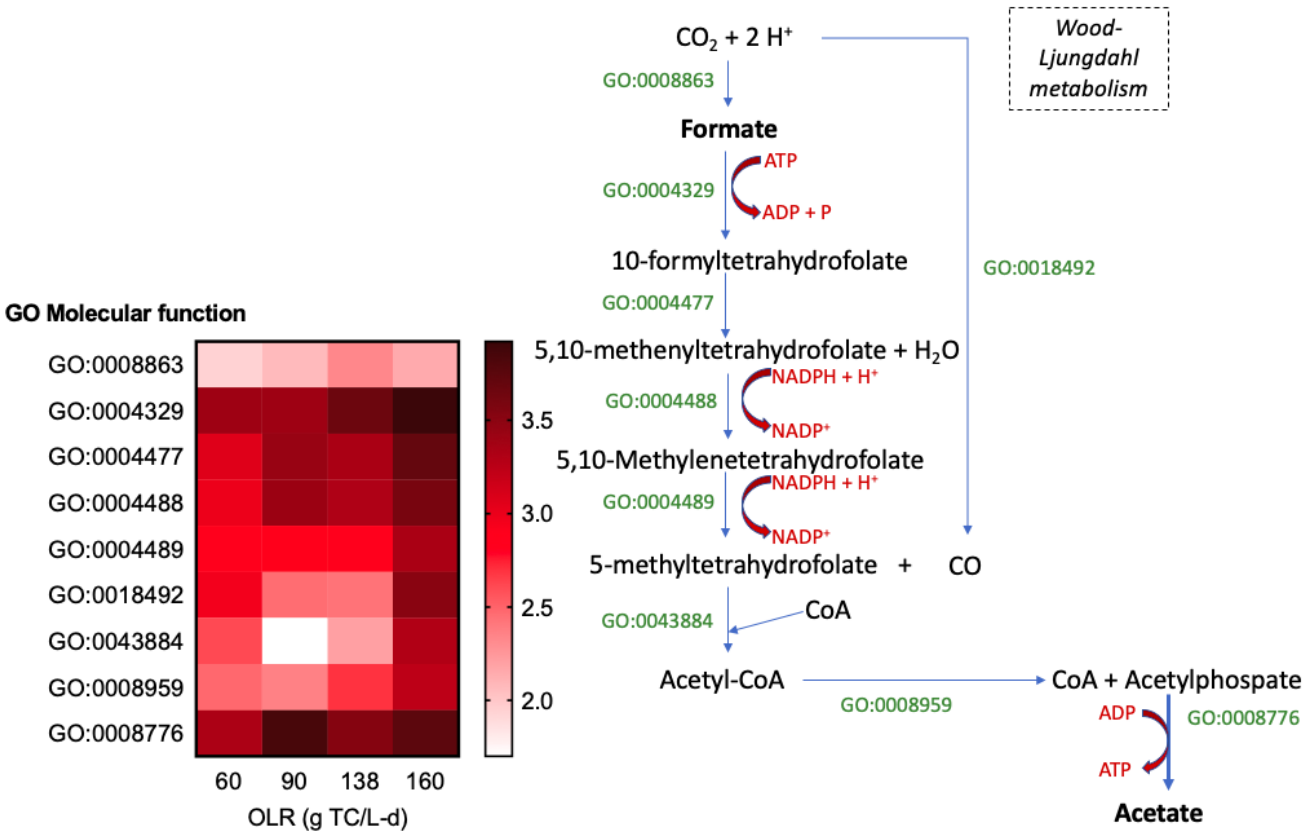

Figure 4.4 (Continued). Abundance of the gene ontology (GO) related to production of H_2, CO_2, acetate via Wood-Ljungdahl, acetate via pyruvate fermentation, lactate, formate, and butyrate at different organic loading rates (OLR). GO:0008863 (formate dehydrogenase); GO:0004329 (formate-tetrahydrofolate synthetase activity); GO:0004477 (methenyltetrahydrofolate cyclohydrolase activity); GO:0004488 (methylenetetrahydrofolate dehydrogenase (NADP+) activity); GO:0004489 (methylenetetrahydrofolate reductase (NAD(P)H) activity); GO:0018492 (carbon-monoxide dehydrogenase (acceptor) activity); GO:0043884 (CO-methylating acetyl-CoA synthase activity); GO:0008776 (acetate kinase activity). The color gradient from white to red indicates the relative expression level log2 changes at different OLR.

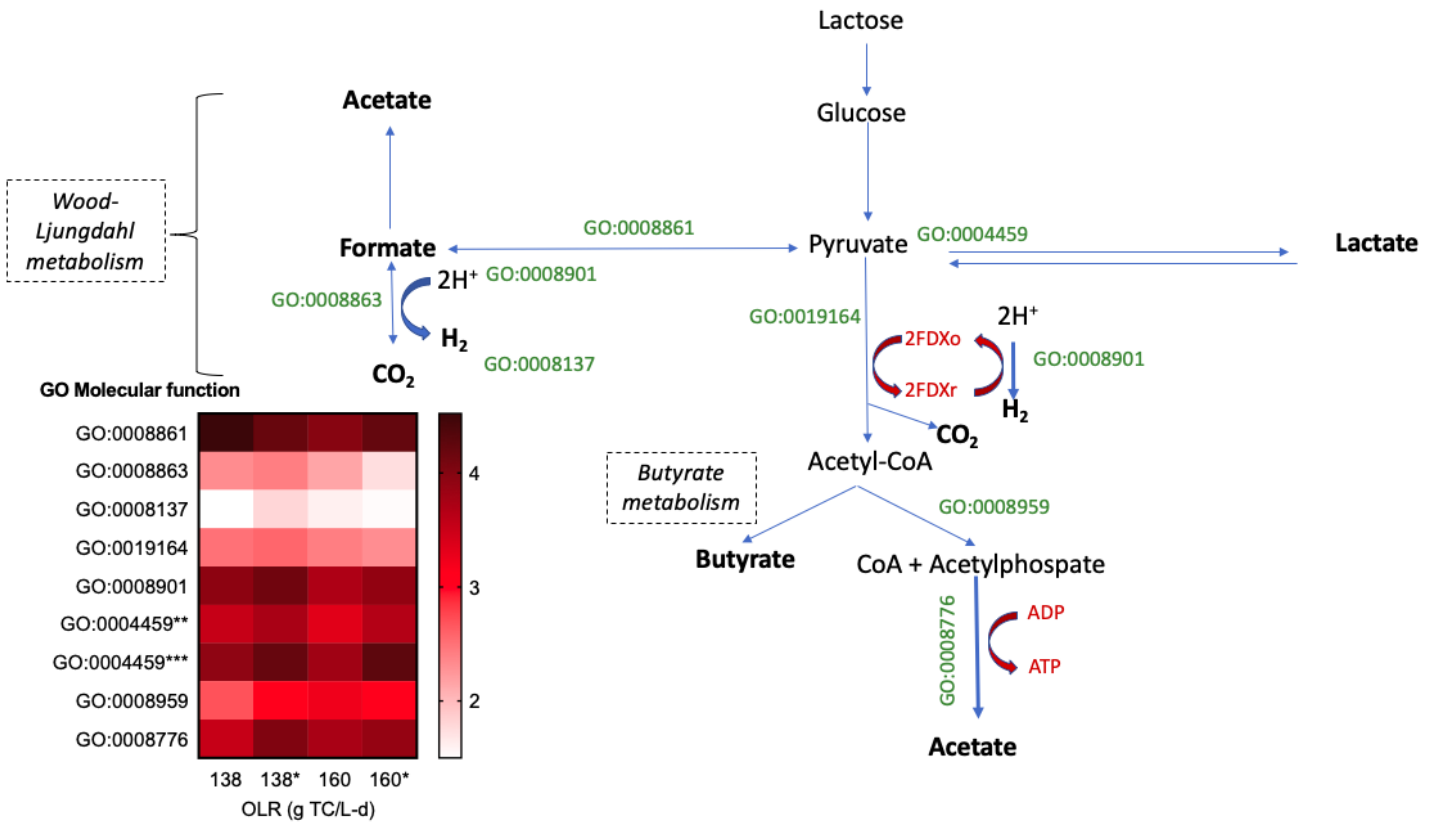

Figure 4.5. Abundance of the gene ontology (GO) related to production of H_2, CO_2, acetate via Wood-Ljungdahl, acetate via pyruvate fermentation, lactate, formate, and butyrate in continuous dark fermentation reactors. GO:0008861 (pyruvate formate lyase activity); GO:0008863 (formate dehydrogenase); GO:0008901(hydrogenase activity); GO:0008137 (hycE activity); GO:0004459 (lactate dehydrogenase activity); GO:0019164 (pyruvate ferredoxin oxidoreductase activity); GO:0008959 (phosphate acetyltransferase activity); GO:0008776 (acetate kinase activity). *Stages with silicone added at a proportion 10% (v/v). **lactate dehydrogenase activity for *Clostridium* species. ***lactate dehydrogenase activity for lactic acid bacteria. The color gradient from white to red indicates the relative expression level log2 changes.

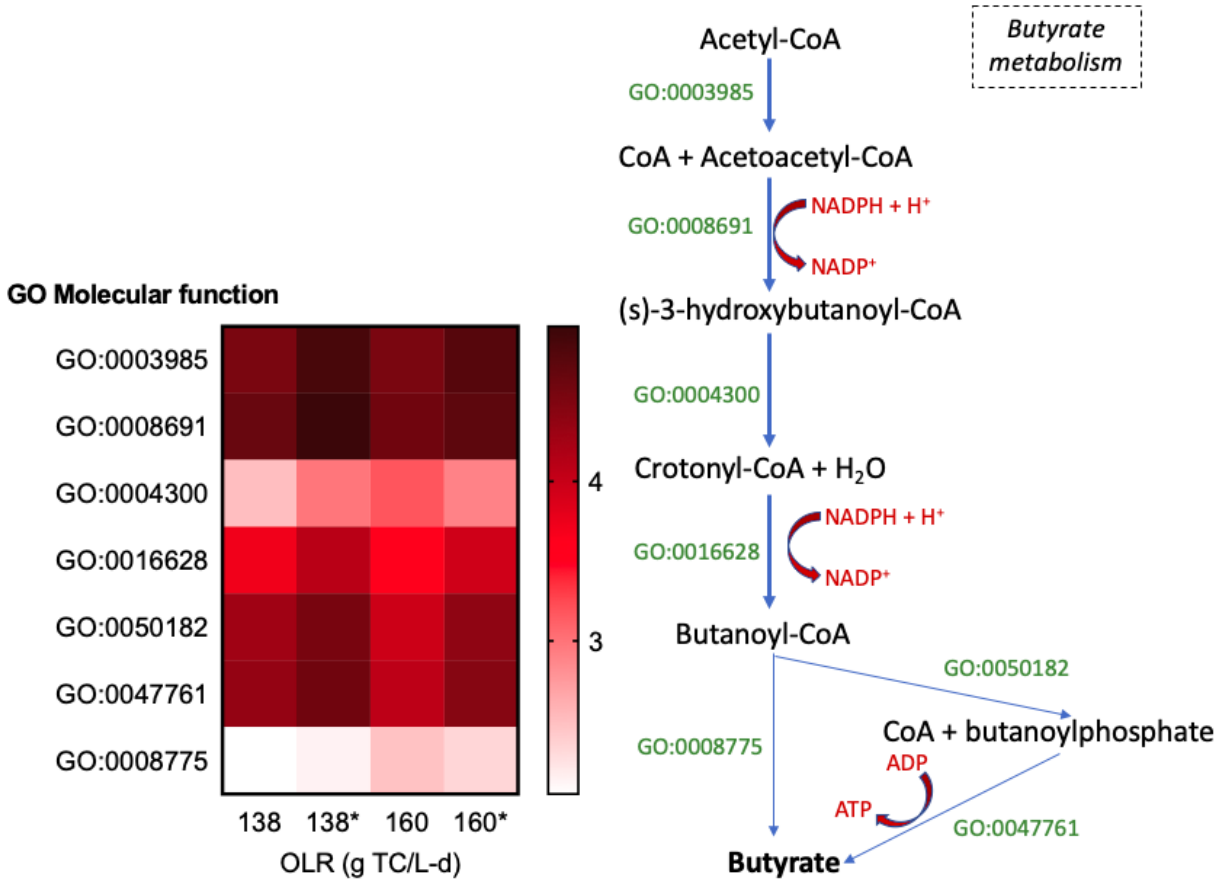

Figure 4.5 (Continued). Abundance of the gene ontology (GO) related to production of H_2, CO_2, acetate via Wood-Ljungdahl, acetate via pyruvate fermentation, lactate, formate, and butyrate in continuous dark fermentation reactors. GO:0003985 (acetyl-CoA C-acetyltransferase activity); GO:0008691 (3-hydroxybutyryl-CoA dehydrogenase activity); GO:0004300 (enoyl-CoA hydratase activity); GO:0016628 (N.D); GO:0050182 (phosphate butyryltransferase activity); GO:0047761 (butyrate kinase activity); GO:0008775 (acetate CoA-transferase activity). *Stages with silicone added at a proportion 10% (v/v). The color gradient from white to red indicates the relative expression level log2 changes.

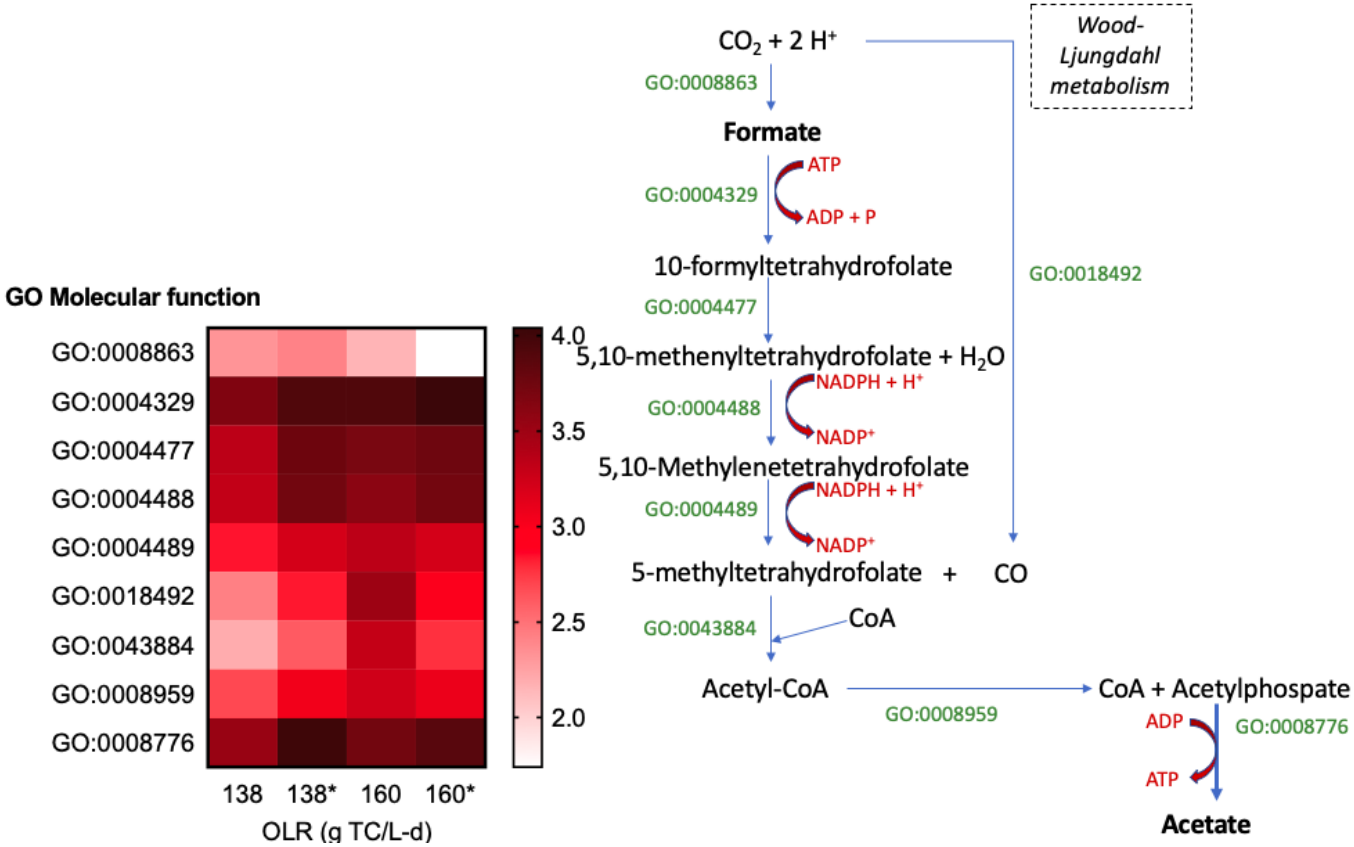

Figure 4.5 (Continued). Abundance of the gene ontology (GO) related to production of H_2, CO_2, acetate via Wood-Ljungdahl, acetate via pyruvate fermentation, lactate, formate, and butyrate in continuous dark fermentation reactors. GO:0008863 (formate dehydrogenase); GO:0004329 (formate-tetrahydrofolate synthetase activity); GO:0004477 (methenyltetrahydrofolate cyclohydrolase activity); GO:0004488 (methylenetetrahydrofolate dehydrogenase ($NADP^+$) activity); GO:0004489 (methylenetetrahydrofolate reductase (NAD(P)H) activity); GO:0018492 (carbon-monoxide dehydrogenase (acceptor) activity); GO:0043884 (CO-methylating acetyl-CoA synthase activity); GO:0008776 (acetate kinase activity). *Stages with silicone added at a proportion 10% (v/v). The color gradient from white to red indicates the relative expression level log2.

In this study, the increase of the OLR from 90 to 138 g TC/L-d led to an augmentation in the abundance of the transcripts of the GO *pfor*, *pfl*, *hydA* and *fdh* (Figure 4.6) and agreed with the observation that the maximum VHPR and H_2 yield was reached at the OLR of 138 g TC/L-d. Meanwhile, a lower abundance of the GO *pfor*, *pfl*, *hydA* and *fdh* at the OLR 160 g TC/L-d than those ones at OLR 138 g TC/L-d (Figure 4.6) was observed. This result, together with the drop of VHPR and H_2 yield at the OLR of 160 g TC/L-d, indicate that the possible substrate overload in the reactor inhibited the metabolic activity of the GO that plays a key role in H_2 production via the pyruvate transformation.

In lactic acid fermentation, pyruvate is reduced to produce lactate or inversely by lactate dehydrogenase (*ldh*, GO:0004459). From the metatranscriptomic analysis it was possible to identify that the activity of the GO *ldh* is performed by both *Clostridium* species and LAB (Figure 4.6). However, according to some reports, *Clostridium* does not have the metabolic capacity to produce lactate [30,40], therefore we hypothesize that the activity of the GO *ldh*-*Clostridium* is in the direction of pyruvate production from the consumption of lactate. The abundance of the transcripts from the GO *ldh*-*Clostridium* suppose that the production of H_2 and butyrate via the acetate-lactate pathway could be possible in suspended-biomass reactors operated at low HRT (6 h). Furthermore, the highest abundance of the transcripts for GO *ldh*-LAB were observed at OLR 138 g TC/L-d, which coincides with the highest concentration of residual lactate (not consumed for pyruvate production). Overall, the metatranscriptomic analysis suggested that the acetate-butyrate fermentation and lactic acid fermentation occurred simultaneously at all OLR conditions, despite the no detection of residual lactate at OLR 138 g TC/L-d.

The production of acetate via the Wood-Ljungdahl pathway is composed of two linear branches: 1) the methyl branch which forms the methyl group of acetate and 2) the carbonyl branch which forms the carboxyl group. The methyl group is synthesized through a series of reactions, which uses formate and reduces C1 intermediates, and is catalyzed by several genes [34]. From such genes, the *fthfs* (GO: 0004329) has been identified as potential marker for homoacetogens. The GO *fthfs* catalyzes the ATP- dependent activation of formate in the acetyl-CoA pathway

of acetogenesis [41]. In our study, the metatranscriptomic analysis shows that transcripts for the GO *fthfs* were present at all OLR (Figure 4.3); however, the abundance of such gene increased with the increments of the OLR. Remarkably, the OLR of 160 g TC/L-d reported the highest abundance of transcripts related to the GO *fthfs* and all the GO that had a role in the Wood-Ljungdahl metabolism (Figure 4.4). These results and the drop of VHPR and H_2 yield at such OLR suggest that a possible substrate overloading reduced the transcripts abundance of key H_2-producing GO and favored the improvement of homoacetogenesis.

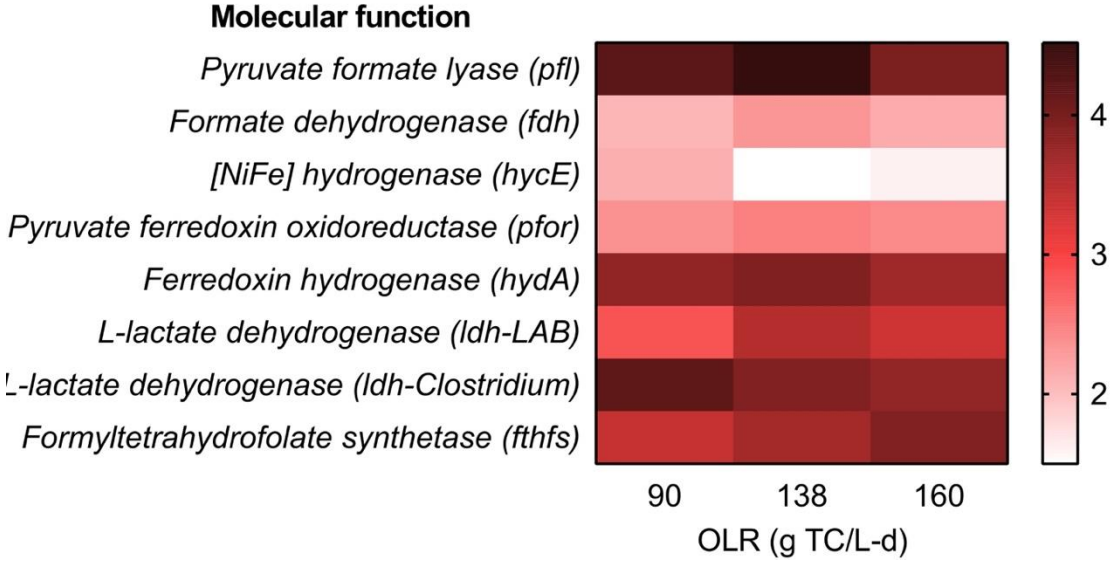

Figure 4.6 Effect of the different organic loading rates (OLR) on the gene expression of key dark fermentation gene ontology. The color gradient form white to red indicates the relative expression level log2 changes at different OLR.

The transcriptomes of microbial biomass from the stages III and IV of CSTR2 and stages II and III of CSTR3 were assessed and compared to evaluate the effect of the addition of silicone oil on the expression of GO keys in the dark fermentation process. As seen in Figure 4.7, the increase of the abundance of the GOs *pfor, pfl, hydA* and *fdh* in the stages with silicone oil as compared with the samples with no addition of silicone oil was observed. These results connected with the observation that silicone oil improved the VHPR and H_2 yield confirmed the hypothesis that the addition of silicone oil stimulated the metabolic activity of crucial H_2-producing GO by dark fermentation. In the same way, the abundance of the GO *ldh* LAB and *Clostridium* increased in the stages with silicone oil. These results coupled with the

statement that the latter enhanced the transcripts abundance of crucial H_2-producing GO, suggests that the addition of silicone oil simultaneously promoted the acetate-butyrate fermentation, the lactic acid fermentation, and the lactic acid consumption. One of the hypotheses stated in the chapter 3 (section 3.4.6) was that the improvement of the H_2 production in two-phase partitioning reactors is related to the reduction in the concentration of H_2 and CO_2 in the aqueous phase favoring the metabolic routes with higher H_2 productivity and probably reducing the homoacetogenesis pathway activity. Nonetheless, the metatranscriptomic analysis showed the presence of transcripts for the GO *fthfs* in all conditions at similar relative expression levels regardless the addition of silicone oil. These results are congruent with the qPCR results for the gene *fthfs*, and suggest that homoacetogenesis is a coexistent phenomenon of H_2 production in mixed culture dark fermentations even in extractive fermentation systems (i.e. two-phase partitioning reactors).

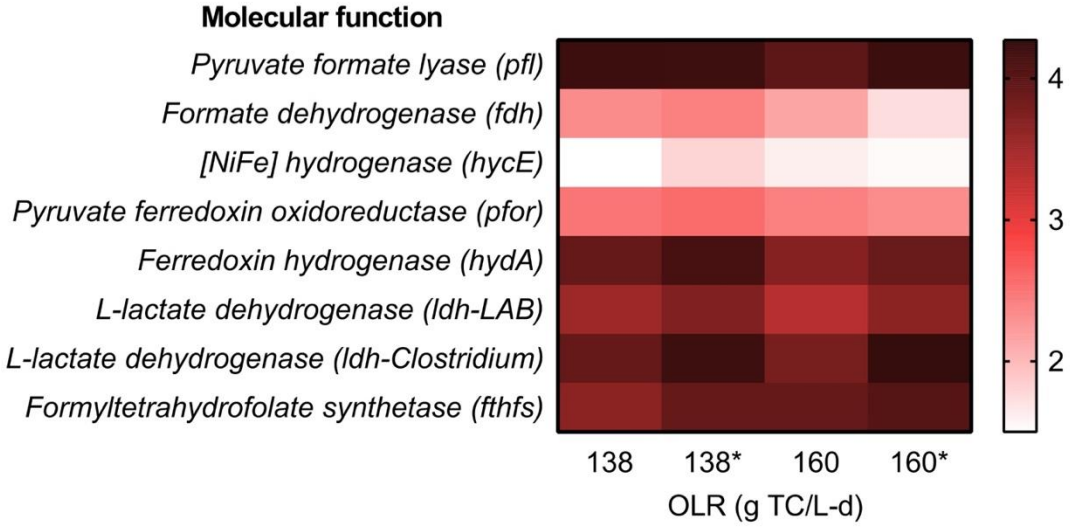

Figure 4.7. Effect of the addition of silicone oil on the gene expression of key dark fermentation gene ontology. The color gradient from white to red indicates the relative expression level log2 changes at different organic loading rates (OLR).

To further investigate the relationships between the transcripts abundance, qPCR values and dark fermentation performance, a Pearson's correlation analysis was carried out (Figure 4.8). The abundance of GO *hydA* transcripts was correlated positively with the VHPR (ρ= 0.52, $p<0.05$), H_2 yield (ρ= 0.68, $p<0.05$), GO *pfor* (ρ= 0.48, $p<0.05$), and GO *pfl* (ρ= 0.57, $p<0.05$). In the same way, the abundance of

qPCR-*hydA* was strongly correlated with the VHPR (ρ= 0.63, p <0.05), H_2 yield (ρ=0.83, p <0.05), and the abundance of GO *hydA* (ρ=0.79, p <0.05). In general, these results confirmed that abundance of gene *hydA* (by qPCR and transcriptomics) was a crucial factor for the production of H_2. Interestingly, no significant correlation was observed between the abundance of GO *ldh-Clostridium* and any other parameter. However, the abundance of GO *ldh*-LAB was positively correlated with the VHPR (ρ=0.57, p <0.05), lactate concentration (ρ=0.47, p <0.05), and abundance of *hydA* GO (ρ=0.34, p <0.05). These results imply that lactate type fermentation and dark fermentation simultaneously occurred without compromising the performance of the reactor for the production of H_2 and carboxylic acids.

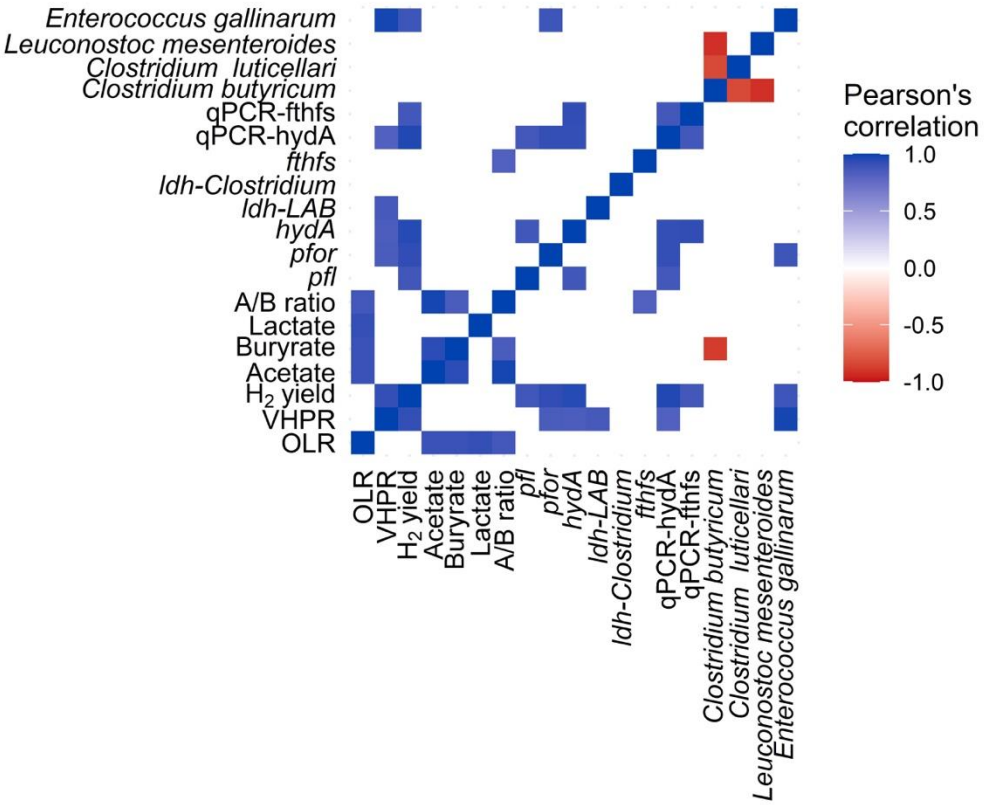

Figure 4.8. Pearson's correlations (p < 0.05). OLR in g TC/L-d; VHPR in L H_2/L-d; H_2 yield in mol H_2/ mol hexose; acetate, lactate, and butyrate in mol/total moles of carboxylic acids; A/B (acetate to butyrate ratio); *pfl (*pyruvate formate lyase), *pfor* (pyruvate ferredoxin oxidoreductase), lactate dehydrogenase-LAB, lactate dehydrogenase-*Clostridium*, *fthfs (*formyl tetrahydrofolate synthetase) were analyzed in terms of their gene ontology relative transcript abundance; qPCR-*hydA* and qPCR-*fthfs* (copies number/ng DNA); microorganisms were analyzed in terms of their relative abundance. TC: total carbohydrates.

Overall, this study is an important step toward characterizing dark fermentation and its metabolic pathways. Although transcriptome is not an exact prediction of metabolic activity, it is a closer approximation of metabolism than 16S rRNA genome-based predictions that have been reported previously for dark fermentation investigations. Other approaches including proteomics or metabolomics may aid in the understanding of dark fermentation metabolism. A comprehensive analysis of our results revealed that OLR and the addition of an extractive organic phase such as silicone oil clearly modifies the abundance of GO that play a key role in H_2 production via the dark fermentation, including H_2 consumption via homoacetogenesis.

4.5 References

[1] L. Cabrol, A. Marone, E. Tapia-Venegas, J.P. Steyer, G. Ruiz-Filippi, E. Trably, Microbial ecology of fermentative hydrogen producing bioprocesses: Useful insights for driving the ecosystem function, FEMS Microbiol. Rev. 41 (2017) 158–181. doi:10.1093/femsre/fuw043.

[2] C.B. Cota-Navarro, J. Carrillo-Reyes, G. Davila-Vazquez, F. Alatriste-Mondragón, E. Razo-Flores, Continuous hydrogen and methane production in a two-stage cheese whey fermentation system, Water Sci. Technol. 64 (2011) 367–374. doi:10.2166/wst.2011.631.

[3] G. Davila-Vazquez, C.B. Cota-Navarro, L.M. Rosales-Colunga, A. de León-Rodríguez, E. Razo-Flores, Continuous biohydrogen production using cheese whey: Improving the hydrogen production rate, Int. J. Hydrogen Energy. 34 (2009) 4296–4304. doi:10.1016/j.ijhydene.2009.02.063.

[4] J. de J. Montoya-Rosales, R. Palomo-Briones, L.B. Celis, C. Etchebehere, E. Razo-Flores, Discontinuous biomass recycling as a successful strategy to enhance continuous hydrogen production at high organic loading rates, Int. J. Hydrogen Energy. 45 (2020) 17260–17269. doi:10.1016/j.ijhydene.2020.04.265.

[5] E. Elbeshbishy, B.R. Dhar, G. Nakhla, H.S. Lee, A critical review on inhibition of dark biohydrogen fermentation, Renew. Sustain. Energy Rev. 79 (2017) 656–668. doi:10.1016/j.rser.2017.05.075.

[6] R. Palomo-Briones, L.B. Celis, H.O. Méndez-Acosta, N. Bernet, E. Trably, E. Razo-Flores, Enhancement of mass transfer conditions to increase the productivity and efficiency of dark fermentation in continuous reactors, Fuel. 254 (2019) 115648. doi:10.1016/j.fuel.2019.115648.

[7] P. Bakonyi, G. Buitrón, I. Valdez-Vazquez, N. Nemestóthy, K. Bélafi- Bakó, A novel gas separation integrated membrane bioreactor to evaluate the impact of self-generated biogas recycling on continuous hydrogen fermentation, Appl. Energy. 190 (2017) 813–823. doi:10.1016/j.apenergy.2016.12.151.

[8] I. Ullah Khan, M. Hafiz Dzarfan Othman, H. Hashim, T. Matsuura, A.F. Ismail, M. Rezaei-DashtArzhandi, I. Wan Azelee, Biogas as a renewable energy fuel – A review of biogas upgrading, utilisation and storage, Energy Convers. Manag. 150 (2017) 277–294. doi:10.1016/j.enconman.2017.08.035.

[9] J. de J. Montoya-Rosales, R. Palomo-briones, L.B. Celis, V. Escobar-barrios, E. Razo-flores, C. Etchebehere, L.F. Cházaro, Coping with mass transfer constrains in dark fermentation using a two-phase partitioning bioreactor, Chem. Eng. J. 445 (2022) 1–9. doi:10.1016/j.cej.2022.136749.
[10] M.-Y. Wang, Y.-L. Tsai, B.H. Olson, J.-S. Chang, Monitoring dark hydrogen fermentation performance of indigenous Clostridium butyricum by hydrogenase gene expression using RT-PCR and qPCR, (2008). doi:10.1016/j.ijhydene.2008.06.048.
[11] R. Palomo-Briones, E. Razo-Flores, N. Bernet, E. Trably, Dark-fermentative biohydrogen pathways and microbial networks in continuous stirred tank reactors: Novel insights on their control, Appl. Energy. 198 (2017) 77–87. doi:10.1016/j.apenergy.2017.04.051.
[12] L. Fuentes, R. Palomo-Briones, J. de Jesús Montoya-Rosales, L. Braga, E. Castelló, A. Vesga, E. Tapia-Venegas, E. Razo-Flores, C. Ecthebehere, Knowing the enemy: homoacetogens in hydrogen production reactors, Appl. Microbiol. Biotechnol. (2021). doi:10.1007/s00253-021-11656-6.
[13] G. Henderson, S.C. Leahy, P.H. Janssen, Presence of novel, potentially homoacetogenic bacteria in the rumen as determined by analysis of formyltetrahydrofolate synthetase sequences from ruminants, Appl. Environ. Microbiol. 76 (2010) 2058–2066. doi:10.1128/AEM.02580-09.
[14] S. Yang, M.T. Guarnieri, S. Smolinski, M. Ghirardi, P.T. Pienkos, De novo transcriptomic analysis of hydrogen production in the green alga Chlamydomonas moewusii through RNA-Seq, (2013). doi:10.1186/1754-6834-6-118.
[15] C. Grimmler, C. Held, W. Liebl, A. Ehrenreich, Transcriptional analysis of catabolite repression in Clostridium acetobutylicum growing on mixtures of d-glucose and d-xylose, J. Biotechnol. 150 (2010) 315–323. doi:10.1016/j.jbiotec.2010.09.938.
[16] C.A. Contreras-Dávila, H.O. Méndez-Acosta, L. Arellano-García, F. Alatriste-Mondragón, E. Razo-Flores, Continuous hydrogen production from enzymatic hydrolysate of Agave tequilana bagasse: Effect of the organic loading rate and reactor configuration, Chem. Eng. J. 313 (2017) 671–679. doi:10.1016/j.cej.2016.12.084.
[17] APHAA/WWA/WEF, Standar Methods for examination of water & wastewater, (2012). www.standardmethods.org.
[18] M. Dubois, K.A.Gilles, J.K.Hamilton, P.A.Rebers, Fred.Smith, Colorimetric Method for Determination of Sugars and Related Substances, Anal. Chem. 28 (1956) 350–356. doi:10.1021/ac60111a017.
[19] G. Davila-Vazquez, F. Alatriste-Mondragón, A. de León-Rodríguez, E. Razo-Flores, Fermentative hydrogen production in batch experiments using lactose, cheese whey and glucose: Influence of initial substrate concentration and pH, Int. J. Hydrogen Energy. 33 (2008) 4989–4997. doi:10.1016/j.ijhydene.2008.06.065.
[20] V. Perna, E. Castelló, J. Wenzel, C. Zampol, D.M. Fontes Lima, L. Borzacconi, M.B. Varesche, M. Zaiat, C. Etchebehere, Hydrogen production in an upflow anaerobic packed bed reactor used to treat cheese whey, Int. J. Hydrogen Energy. 38 (2013) 54–62. doi:10.1016/J.IJHYDENE.2012.10.022.
[21] K. Xu, H. Liu, G. Du, J. Chen, Real-time PCR assays targeting formyltetrahydrofolate synthetase gene to enumerate acetogens in natural and engineered environments, Anaerobe. 15 (2009) 204–213. doi:https://doi.org/10.1016/j.anaerobe.2009.03.005.
[22] P. Jagtap, S. Mehta, R. Sajulga, B. Batut, E. Leith, P. Kumar, S. Hiltemann, Metatranscriptomics analysis using microbiome RNA-seq data (Galaxy Training Materials), (2021). https://training.galaxyproject.org/training-material/topics/metagenomics/tutorials/metatranscriptomics/tutorial.html (accessed May 12, 2022).

[23] B. Batut, S. Hiltemann, A. Bagnacani, D. Baker, V. Bhardwaj, C. Blank, A. Bretaudeau, L. Brillet-Guéguen, M. Čech, J. Chilton, D. Clements, O. Doppelt-Azeroual, A. Erxleben, M.A. Freeberg, S. Gladman, Y. Hoogstrate, H.-R. Hotz, T. Houwaart, P. Jagtap, D. Larivière, G. Le Corguillé, T. Manke, F. Mareuil, F. Ramírez, D. Ryan, F.C. Sigloch, N. Soranzo, J. Wolff, P. Videm, M. Wolfien, A. Wubuli, D. Yusuf, J. Taylor, R. Backofen, A. Nekrutenko, B. Grüning, Community-Driven Data Analysis Training for Biology., Cell Syst. 6 (2018) 752-758.e1. doi:10.1016/j.cels.2018.05.012.
[24] M. Martin, Cutadapt removes adapter sequences from high-throughput sequencing reads, EMBnet.Journal. 17 (2011) 10–12. doi:10.14806/EJ.17.1.200.
[25] D.T. Truong, E.A. Franzosa, T.L. Tickle, M. Scholz, G. Weingart, E. Pasolli, A. Tett, C. Huttenhower, N. Segata, MetaPhlAn2 for enhanced metagenomic taxonomic profiling, Nat. Methods. 12 (2015) 902–903. doi:10.1038/nmeth.3589.
[26] E.A. Franzosa, L.J. McIver, G. Rahnavard, L.R. Thompson, M. Schirmer, G. Weingart, K.S. Lipson, R. Knight, J.G. Caporaso, N. Segata, C. Huttenhower, Species-level functional profiling of metagenomes and metatranscriptomes, Nat. Methods. 15 (2018) 962–968. doi:10.1038/s41592-018-0176-y.
[27] R. R Development Core Team, R: A Language and Environment for Statistical Computing, 2011. doi:10.1007/978-3-540-74686-7.
[28] E. Castelló, L. Braga, L. Fuentes, C. Etchebehere, Possible causes for the instability in the H2 production from cheese whey in a CSTR, Int. J. Hydrogen Energy. 43 (2018) 2654–2665. doi:10.1016/j.ijhydene.2017.12.104.
[29] O. García-Depraect, I. Valdez-Vázquez, E.R. Rene, J. Gómez-Romero, A. López-López, E. León-Becerril, Lactate- and acetate-based biohydrogen production through dark co-fermentation of tequila vinasse and nixtamalization wastewater: Metabolic and microbial community dynamics, Bioresour. Technol. 282 (2019) 236–244. doi:10.1016/j.biortech.2019.02.100.
[30] O. García-Depraect, R. Castro-Muñoz, R. Muñoz, E.R. Rene, E. León-Becerril, I. Valdez-Vazquez, G. Kumar, L.C. Reyes-Alvarado, L.J. Martínez-Mendoza, J. Carrillo-Reyes, G. Buitrón, A review on the factors influencing biohydrogen production from lactate: the key to unlocking enhanced dark fermentative processes, Bioresour. Technol. 324 (2020) 124595. doi:10.1016/j.biortech.2020.124595.
[31] S. Pattra, C.-H.H. Lay, C.-Y.Y. Lin, S. O-Thong, A. Reungsang, Performance and population analysis of hydrogen production from sugarcane juice by non-sterile continuous stirred tank reactor augmented with Clostridium butyricum, Int. J. Hydrogen Energy. 36 (2011) 8697–8703. doi:10.1016/j.ijhydene.2010.05.120.
[32] A. Pugazhendhi, P. Anburajan, J.H. Park, G. Kumar, P. Sivagurunathan, S.H. Kim, Process performance of biohydrogen production using glucose at various HRTs and assessment of microbial dynamics variation via q-PCR, Int. J. Hydrogen Energy. 42 (2017) 27550–27557. doi:10.1016/j.ijhydene.2017.06.184.
[33] M.A.Z. Bundhoo, R. Mohee, Inhibition of dark fermentative bio-hydrogen production: A review, Int. J. Hydrogen Energy. 41 (2016) 6713–6733. doi:10.1016/j.ijhydene.2016.03.057.
[34] N.M.C. Saady, Homoacetogenesis during hydrogen production by mixed cultures dark fermentation: Unresolved challenge, Int. J. Hydrogen Energy. 38 (2013) 13172–13191. doi:10.1016/j.ijhydene.2013.07.122.
[35] M. Del Pilar Anzola-Rojas, S.G. Da Fonseca, C.C. Da Silva, V.M. De Oliveira, M. Zaiat, The use of the carbon/nitrogen ratio and specific organic loading rate as tools for improving biohydrogen production in fixed-bed reactors, Biotechnol. Reports. 5 (2015) 46–54. doi:10.1016/J.BTRE.2014.10.010.
[36] S.G. Santiago, E. Trably, E. Latrille, G. Buitrón, I. Moreno-Andrade, The hydraulic retention time influences the abundance of Enterobacter, Clostridium and

Lactobacillus during the hydrogen production from food waste, Lett. Appl. Microbiol. 69 (2019) 138–147. doi:10.1111/lam.13191.
[37] H.S. Lee, M.B. Salerno, B.E. Rittmann, Thermodynamic evaluation on H2 production in glucose fermentation, Environ. Sci. Technol. 42 (2008) 2401–2407. doi:10.1021/ES702610V/SUPPL_FILE/ES702610V-FILE003.PDF.
[38] L. Hongyuan, J. Chen, Y. Jia, M. Cai, P.K.H. Lee, Transcriptomic responses of the interactions between Clostridium Cellulovorans 743b and Rhodopseudomonas Palustris CGA009 in a cellulose-grown coculture for enhanced hydrogen production, Appl. Environ. Microbiol. 82 (2016) 4546–4559. doi:10.1128/AEM.00789-16.
[39] F. Oswald, I.K. Stoll, M. Zwick, S. Herbig, J. Sauer, N. Boukis, A. Neumann, Formic acid formation by Clostridium ljungdahlii at elevated pressures of carbon dioxide and hydrogen, Front. Bioeng. Biotechnol. 6 (2018). doi:10.3389/fbioe.2018.00006.
[40] J.-H. Park, D.-H. Kim, J.-H. Baik, J.-H. Park, J.-J. Yoon, C.-Y. Lee, S.-H. Kim, Improvement in H2 production from Clostridium butyricum by co-culture with Sporolactobacillus vineae, Fuel. 285 (2021) 119051. doi:https://doi.org/10.1016/j.fuel.2020.119051.
[41] C.R. Lovell, A. Przybyla, L.G. Ljungdahl, Primary structure of the thermostable formyltetrahydrofolate synthetase from Clostridium thermoaceticum, Biochemistry. 29 (1990) 5687–5694. doi:10.1021/bi00

Chapter 5. *Analysis of microbial communities in continuous reactors feed with enzymatic hydrolysates.*

Graphical abstract

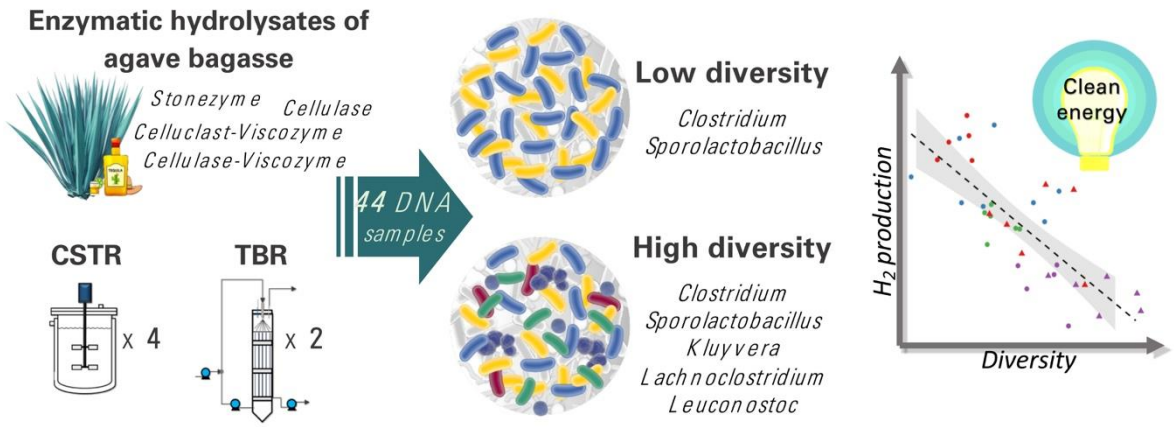

Highlights

- Microbial communities performed hydrolysis, primary and secondary fermentation.
- *Clostridium* and *Lachnoclostridium* perform H_2 production from enzymatic hydrolysates.
- Controlled environments in CSTR favored low diverse microbial communities.
- Trickling bed reactors lead to high diversity microbial communities.
- H_2 production rate was inversely related to the microbial diversity.

The present chapter is a modified version of the article:
R. Palomo-Briones, J. de J. Montoya-Rosales, E. Razo-Flores, 2021. Advances towards the understanding of microbial communities in dark fermentation of enzymatic hydrolysates: Diversity, structure and hydrogen production performance, *International Journal of Hydrogen Energy*, 46, 27459-27472.

5.1 Abstract

Microbial communities involved in hydrogen (H_2) production from enzymatic hydrolysates of agave bagasse were analyzed through 16S-rRNA sequencing. Two types of reactor configurations and four different enzymatic hydrolysates were evaluated. Trickling bed reactors led to highly-diverse microbial communities, but low volumetric H_2 production rates (VHPR, maximum: 5.8 L H_2/L-d). On the contrary, well-controlled environments of continuous stirred-tank reactors favored the establishment of low diverse microbial communities composed by *Clostridium*-*Sporolactobacillus* leading to high-performance H_2-production (VHPR maximum: 13 L H_2/L-d). Cellulase-Viscozyme and Celluclast-Viscozyme hydrolysates led to the co-dominance of *Clostridium* and *Sporolactobacillus*, possibly due to the presence of xylose and hemicellulose-derived carbohydrates. Cellulase hydrolysates were linked to communities dominated by *Clostridium*, while maintaining low abundance of *Sporolactobacillus*. Stonezyme hydrolysates favored microbial communities co-dominated by *Clostridium-Lachnoclostridium-Leuconostoc*. Moreover, contrary to the prevailing theory, it was demonstrated that H_2 production performance was inversely related to microbial diversity.

5.2 Introduction

Hydrogen (H_2) has been referred to as "the fuel of the future" because of its high energy content (142 kJ/g), the possibility to produce it from renewable sources, the high conversion efficiency into electricity, and the near-zero carbon emissions associated to its utilization [1]. Beyond its role as energy source and storage, H_2 is considered a central molecule to produce building block chemicals for the synthesis of high-value products [2]. Among the multiple methods available for H_2 production, dark fermentation is gaining attention due to its potential to use a wide diversity of organic residues, the ease of its operation, its high performance in terms of H_2 production rates, and the less energy required compared to electrolysis [1,3]. Moreover, dark fermentation can be easily adapted and integrated into biorefinery chains fed with renewable complex organic matrices [4]. Nevertheless, dark fermentative H_2 production is susceptible to instability and failure due to multiple

factors, including inefficient mass transfer, suboptimal operating conditions (temperature, pH, substrate concentration, etc.), presence of inhibitory chemicals, changes in microbial communities, presence of detrimental microorganisms [5]. Thus, appropriate understanding of its microbiology and operation is required to assure efficient performance in H_2 production through dark fermentation.

In dark fermentation, anaerobic microorganisms use carbohydrate-rich substrates to produce H_2 and carboxylic acids. Regularly, dark fermentation is performed using mixed cultures due to multiple reasons, including [6]: i) the circumvention of using pure cultures as an inoculum, ii) the avoidance of sterilization and antibiotic addition; and iii) the resilience to complex and variable organic waste substrates, among others. In mixed-culture dark fermentation, the performance of H_2 production depends largely on the composition, diversity and structure of the microbial community [7].

It is widely accepted that highly-efficient microbial communities in dark fermentation are dominated by *Clostridium* species, spore-forming obligate anaerobes commonly found during high H_2 production [8]. However, facultative anaerobes as well as non-spore-forming bacteria are also frequently found in dark-fermentative systems; these secondary microorganisms can be directly involved in H_2 production, but also in other positive or negative roles, ranging from depleting oxygen in the media and maintaining anaerobic conditions to competing for the substrate uptake and H_2 consumption [5, 8, 9]. In general, the composition, diversity and structure of microbial communities found in H_2 production is expected to be influenced by operating conditions, inoculum source and pretreatment, type of reactor, and type of substrate [7,10]. Nonetheless, it is still unknown how these parameters influence the composition, diversity and structure of microbial communities.

In the case of H_2 production from lignocellulosic hydrolysates, few studies have approached the characterization of microbial communities [11, 12, 13, 14]. It has been reported that such microbial communities were also dominated by *Clostridium* species, while the community composition was affected by the type of hydrolysate as well as the presence of inhibitory compounds (e.g., furan derivatives, phenolic compounds and lignin). Still, conclusions are often circumscribed to narrow

experimental designs (limited number of reactors, substrate, conditions, etc.) and engineering-centered objectives. Therefore, general conclusions about the links between microbial diversity, community structure and reactor performance have been insufficient.

Therefore, the first objective of the present study was to investigate the composition of microbial communities developed in H_2-producing reactors fed with lignocellulosic enzymatic hydrolysates. The second objective was to unveil general relationships between diversity, structure and performance of H_2-producing systems. Through the development of this work, new insights on the diversity-functionality discussion are also presented.

5.3 Materials and methods

5.3.1 H_2-producing systems (source of DNA samples)

A total of six independent reactors were previously set up and operated to evaluate different enzymatic hydrolysates of agave bagasse for H_2 production (Table 5.1) [15, 16]. Four of them were configured as continuous stirred-tank reactors (CSTR), where operating conditions (pH, temperature) and the concentrations of substrate and byproducts were uniformly distributed. In general, CSTR are known for sustaining suspended growth of biomass (planktonic biomass). On the other hand, two systems were configured as trickling bed reactors (TBR) using polyvinyl ethylene tubes as packing material. In TBR systems, biomass grows as a biofilm, which is not flooded but sprinkled with fermentation media. TBR systems are characterized by high liquid-gas transfer area compared to submerged conventional reactors. It is important to recall that, in suspended growth systems, theoretically all microbial cells can sense the same substrate concentration, products concentration, and operating conditions. In contrast, in biofilm systems, the micro-environmental conditions change from the surface to the bottom of the biofilm. Therefore, the control not only of environmental conditions, but also of microbial communities is expected to be more efficient in suspended-growth than biofilm-growth. All reactors were set up and operated at different values of organic loading rate (OLR) ranging from 34.6 to 120 g chemical

oxygen demand (COD)/L-d. The hydraulic retention time (HRT), temperature and pH were automatically controlled at 6 h, 37 °C and 5.5, respectively.

The performance of both reactor configurations was characterized in terms of volumetric H_2 production rate (VHPR), H_2 yield, carboxylic acids production and other relevant parameters as shown in Table 5.1 [15, 16]. For the analysis of reactor performance and in order to facilitate the discussion, steady states were classified based on VHPR into low performance (VHPR < 4 L H_2/L-d), medium performance (VHPR = 4–8 L H_2/L-d) and high performance (VHPR > 8 L H_2/L-d). To define these groups, the complete range of observed VHPR (0–12.9 L H_2/L-d) was considered and divided into three groups. However, for convenient purposes, the limits of the groups were rounded to 4 and 8 L H_2/L-d. Similar classification approaches have been conducted previously to evaluate H_2 production performance (e.g. Ref. [7]) and make intuitive discussion.

To investigate the links between these parameters and the composition, diversity and structure of microbial communities, biomass samples were collected from steady states (where H_2 production variation remained < 10% for three consecutive days). In general, biomass samples were taken at the end of the steady state, as indicated in Table 5.1. Afterwards, genomic DNA was extracted and the V3–V4 region of the 16S-rRNA gene was amplified and sequenced through the Illumina platform (details in section Illumina sequencing and microbial community analysis).

Table 5.1. List of steady states used for the analysis of microbial communities developed during H_2 production from enzymatic hydrolysates of agave bagasse. Data was gathered from Montoya-Rosales et al. [15] and Valencia-Ojeda et al. [16].

Reactor No.	Reactor configuration	Type of hydrolysate	Stage (days)	OLR (g COD/L-d)	VHPR (L H_2/L-d)	H_2 yield (L H_2/kg bagasse)	Acetate (g/L)	Butyrate (g/L)	Lactate (g/L)
1	CSTR	Celluclast + Viscozyme	I (23 – 29)	52.0	7.66 ± 0.04	117.86 ± 0.61	3.13 ± 0.12	3.21 ± 0.26	N.D.
	CSTR	Celluclast + Viscozyme	II (30 – 41)	60.0	7.72 ± 0.06	101.94 ± 0.74	2.33 ± 0.30	2.72 ± 0.35	N.D.
	CSTR	Celluclast + Viscozyme	III (42 – 47)	70.0	9.51 ± 0.03	108.63 ± 0.29	3.28 ± 0.59	3.47 ± 0.67	N.D.
	CSTR	Celluclast + Viscozyme	IV (48 – 52)	80.0	10.25 ± 0.10	102.51 ± 1.04	3.51 ± 0.47	4.45 ± 0.48	N.D.
	CSTR	Celluclast + Viscozyme	V (53 – 57)	90.0	12.99 ± 0.13	107.95 ± 12.89	4.44 ± 0.43	4.49 ± 0.29	N.D.
2	CSTR	Stonezyme	I (1 – 10)	44.0	0.72 ± 0.04	11.77 ± 0.61	1.63 ± 0.18	1.99 ± 0.35	0.25 ± 0.10
	CSTR	Stonezyme	II (11 – 16)	52.0	1.10 ± 0.02	15.25 ± 0.28	1.10 ± 0.06	1.62 ± 0.21	N.D.
	CSTR	Stonezyme	III (17 – 23)	60.0	1.70 ± 0.02	20.44 ± 0.21	1.69 ± 0.13	2.48 ± 0.53	N.D.
	CSTR	Stonezyme	IV (24 – 30)	80.0	2.01 ± 0.09	18.16 ± 0.81	2.05 ± 0.46	3.70 ± 0.28	N.D.
	CSTR	Stonezyme	V (31 – 35)	100.0	2.25 ± 0.04	16.26 ± 0.15	6.57 ± 0.91	4.72 ± 0.47	N.D.
	CSTR	Stonezyme	VI (36 – 39)	100.0	2.23 ± 0.06	16.15 ± 0.42	5.64 ± 0.24	5.07 ± 0.21	N.D.
3	TBR	Celluclast + Viscozyme	I (1 – 12)	34.6	1.78 ± 0.03	49.01 ± 0.69	3.41 ± 0.54	2.44 ± 0.38	0.24 ± 0.21

	TBR	Celluclast + Viscozyme	II (13 – 21)	43.2	2.57 ± 0.02	55.81 ± 0.43	3.55 ± 0.44	3.46 ± 0.48	0.27 ± 0.47
	TBR	Celluclast + Viscozyme	III (22 – 28)	52.9	3.61 ± 0.08	65.69 ± 1.50	2.88 ± 0.32	3.44 ± 0.60	0.97 ± 0.21
	TBR	Celluclast + Viscozyme	IV (40 – 46)	60.5	4.09 ± 0.03	62.63 ± 0.39	3.59 ± 0.65	2.97 ± 1.03	0.52 ± 0.22
	TBR	Celluclast + Viscozyme	V (47 – 52)	69.1	5.43 ± 0.10	72.43 ± 1.38	3.40 ± 0.28	4.36 ± 0.33	0.26 ± 0.09
	TBR	Celluclast + Viscozyme	VI (53 – 59)	81.0	5.76 ± 0.03	67.82 ± 0.35	2.97 ± 0.10	4.85 ± 0.12	0.85 ± 0.10
4	TBR	Stonezyme	I (1 – 6)	43.2	1.23 ± 0.03	19.88 ± 0.47	2.92 ± 0.53	5.03 ± 0.71	0.52 ± 0.16
	TBR	Stonezyme	II (7 – 13)	52.9	1.31 ± 0.04	17.75 ± 0.56	3.26 ± 0.10	4.28 ± 0.56	1.34 ± 0.03
	TBR	Stonezyme	III (14 – 22)	60.5	1.61 ± 0.02	18.78 ± 0.28	3.03 ± 0.26	3.30 ± 0.06	1.51 ± 0.35
	TBR	Stonezyme	IV (23 – 29)	69.0	1.78 ± 0.04	18.06 ± 0.39	3.44 ± 0.43	3.93 ± 0.07	1.27 ± 0.11
	TBR	Stonezyme	V (30 –36)	81.0	1.98 ± 0.07	16.91 ± 0.60	2.02 ± 0.10	3.36 ± 0.14	1.20 ± 0.05
	TBR	Stonezyme	VI (37 – 40)	81.0	1.96 ± 0.05	16.76 ± 0.45	2.05 ± 0.04	3.72 ± 0.14	1.23 ± 0.06
5	CSTR	Cellulase	I (1 – 9)	44.0	3.73 ± 0.18	25.71 ± 1.21	2.14 ± 0.26	0.69 ± 0.10	N.D.
	CSTR	Cellulase	II (10 – 18)	52.0	4.67 ± 0.13	23.47 ± 0.67	4.15 ± 0.22	2.46 ± 0.46	N.D.
	CSTR	Cellulase	III (19 – 27)	60.0	4.47 ± 0.08	23.52 ± 0.41	4.06 ± 0.53	2.93 ± 0.30	N.D.
	CSTR	Cellulase	IV (28 – 32)	80.0	6.31 ± 0.07	22.76 ± 0.74	5.43 ± 0.48	3.70 ± 0.16	N.D.
	CSTR	Cellulase	V (33 –41)	100.0	9.94 ± 0.03	32.51 ± 0.10	4.58 ± 0.67	4.41 ± 0.12	N.D.
	CSTR	Cellulase	VI (42– 48)	120.0	11.62 ± 0.32	29.45 ± 0.81	4.95 ± 0.28	4.32 ± 0.18	N.D.
	CSTR	Cellulase	VII (49– 54)	60.0	5.34 ± 0.12	27.46 ± 0.59	4.71 ± 0.35	2.22 ± 0.17	N.D.

	CSTR	Cellulase	VIII (55– 62)	72.0	4.67 ± 0.06	20.00 ± 0.27	3.18 ± 0.31	2.04 ± 0.05	N.D.
	CSTR	Cellulase + Viscozyme	I (1 – 5)	44.0	3.46 ± 0.08	33.91 ± 0.83	1.48 ± 0.22	0.87 ± 0.24	N.D.
6	CSTR	Cellulase + Viscozyme	II (6 – 10)	52.0	3.43 ± 0.07	28.47 ± 0.57	1.74 ± 0.34	1.31 ± 0.11	N.D.
	CSTR	Cellulase + Viscozyme	III (11 – 15)	60.0	4.57 ± 0.04	32.89 ± 0.28	2.11 ± 0.36	1.41 ± 0.24	0.61 ± 0.70
	CSTR	Cellulase + Viscozyme	IV (1 – 5)	60.0	3.99 ± 0.06	25.23 ± 0.37	2.22 ± 0.20	1.50 ±0.29	1.69 ± 0.09
	CSTR	Cellulase + Viscozyme	V (6 –11)	70.0	4.15 ± 0.03	22.52 ± 0.14	2.62 ± 0.35	2.42 ± 0.14	2.29 ± 0.29
	CSTR	Cellulase + Viscozyme	VI (12– 17)	80.0	2.86 ± 0.58	13.58 ± 2.73	2.67 ± 0.18	1.72 ± 0.22	2.14 ± 0.04
	CSTR	Cellulase + Viscozyme	VII (18– 22)	52.0	1.78 ± 0.04	13.01 ± 0.31	2.17 ± 0.28	1.39 ± 0.30	1.37 ± 0.08
	CSTR	Cellulase + Viscozyme	VIII (23– 27)	70.0	3.14 ± 0.09	17.01 ± 0.49	2.37 ± 0.17	1.57 ± 0.17	1.23 ± 0.16
	CSTR	Cellulase + Viscozyme	IX (28– 35)	80.0	2.10 ± 0.07	9.98 ± 0.32	0.96 ± 0.14	1.00 ± 0.08	0.73 ± 0.16

OLR: organic loading rate; COD: chemical oxygen demand; VHPR: volumetric H_2 production rate; CSTR: continuous stirred-tank reactor; TBR: trickling bed reactor; N.D.: not detected. Hydraulic retention time (HRT) was 6 h for all cases, except stage VIII in CSTR fed with Cellulase hydrolysates (reactor 5) that was 10 h.

5.3.2 Inoculum

In all reactors, anaerobic granular sludge from a full scale up-flow anaerobic sludge blanket reactor treating tequila vinasses (Casa Herradura. Jalisco, Mexico) was used as inoculum. The sludge was heat-treated at 105 °C for 24 h to select spore-forming bacteria. The dried sludge was then milled and mesh-sieved through a #20-mesh in accordance with Carrillo-Reyes et al. [17]. For all cases, the heat-treated sludge was added to fermentation reactors at an initial concentration of 4.5 g volatile solids (VS)/L.

5.3.3 Agave bagasse and enzymatic hydrolysis

Agave bagasse was collected from a tequila distillery (Casa Herradura. Jalisco, Mexico). Right after receiving the agave bagasse, it was sun-dried to reduce its biological decomposition. Then, the bagasse was milled with a knife mill to get fibers of manageable size. The resulting material was washed to eliminate any residues from the distillery processing to later be sun-dried and sieved to obtain fibers of 0.5–4.0 cm large.

The processed agave bagasse was used as feedstock in four different types of hydrolyses that were conducted with the following enzymatic preparations: 1) Celluclast 1.5L (Novozymes, Bagsværd, Denmark) + Viscozyme L (Novozymes, Bagsværd, Denmark), 2) Cellulase 50XL (ENZIQUIM, Mexico City, Mexico), 3) Cellulase 50XL + Viscozyme L, and 4) Stonezyme (Banner Química, Tultitlán, Mexico). The conditions of each enzymatic hydrolysis were detailed in previous works [15,16]. The resulting hydrolysates (hereinafter referred to as Stonezyme, Celluclast-Viscozyme, Cellulase, and Cellulase-Viscozyme hydrolysates) were filtered through an absorbent cloth and characterized in terms of soluble COD and carbohydrates concentration (Table 5.2). The CSTR systems (reactors 1, 2, 5 and 6 in Table 5.1) were fed with the four types of hydrolysates, while TBR systems (reactors 3 and 4 in Table 1) were fed only with two types of hydrolysates (Cellulase and Cellulase-Viscozyme hydrolysates). It should be noted that not all hydrolysates were used for the two reactor configurations. This is because the comparison of

reactor configurations, conducted by Montoya-Rosales et al. [15], concluded that the use of TBR showed multiple disadvantages for H_2 production, mainly related to the poor control of environmental conditions within biofilms. Therefore, in the following study conducted by Valencia-Ojeda et al. [16], H_2 production from Cellulase and Cellulase-Viscozyme hydrolysates was evaluated only in CSTR.

Table 5.2. Characteristics of the enzymatic hydrolysates

Type of hydrolysate	CODs (g/L)	TC (g/L)	TC to COD ratio	TSS (g/L)	VSS (g/L)	Reference
Celluclast + Viscozyme	39.7 ± 1.7	12.6 ± 1.0	0.32	39.6 ± 0.5	29.1 ± 0.2	[15]
Stonezyme	59.1 ± 2.2	17.5 ± 1.3	0.27	45.9 ± 1.4	36.3 ± 0.4	[15]
Cellulase	30.2 ± 2	15.8 ± 1	0.52	18.5 ± 2.8	15.2 ± 1.6	[16]
Cellulase + Viscozyme	36.9 ± 2	20.3 ± 0.8	0.55	21.8 ± 1.4	18.7 ± 1.3	[16]

CODs: soluble chemical oxygen demand; TC: total carbohydrates; TSS: total suspended solids; VSS: Volatile suspended solids

5.3.4 Analytical methods

As detailed in previous reports [15, 16], liquid samples were taken during steady states of operation in order to determine the concentrations of soluble carbohydrates, soluble COD, and carboxylic acids. The carbohydrates concentrations were analyzed through the phenol-sulfuric method [18], the COD was determined through the standard method [19], and carboxylic acids concentrations were determined with a capillary electrophoresis (CE) instrument equipped with a fused silica capillary column and an UV detector (1600A, Agilent Technologies, Germany) as reported elsewhere [20]. The gas production rate was measured with a liquid-displacement device (Prendo, Puebla, Mexico) and its composition was determined with a gas chromatograph (6890 N, Agilent Technologies, Germany) equipped with a packed column (HayeSep D, Alltech, USA) and a thermal conductivity detector [20]. All volumes of gas were reported at 273.15 K and 1 atm.

5.3.5 Illumina sequencing and microbial community analysis

The genomic DNA was extracted from biomass samples collected during steady states using the ZR Fungal/Bacterial DNA MiniPrep extraction kit, in accordance with manufacturer's instructions (Zymo Research, USA). The Illumina MiSeq platform (paired-end, 2 by 250 bp) was used for sequencing of the V3–V4 regions of the 16S-rRNA gene. In the case of samples from CSTR and TBR fed with Celluclast-Viscozyme and Stonezyme hydrolysates, the sequencing work was carried out by the Unidad Universitaria de Secuenciación Masiva y Bioinformática, Instituto de Biotecnología (UNAM, Mexico). On the other hand, samples from CSTR fed with Cellulase and Cellulase-Viscozyme hydrolysates were sequenced by the ZymoBiomics laboratories (Zymo Research, Irvin, USA). The downstream sequencing processing was performed using the Quantitative Insights into Microbial Ecology (QIIME) software [21] following the pipeline described elsewhere [22]. The analysis included the quality filter, chimera check, and taxonomy assignment using the SILVA RNA database (132 release) as reference. The sequencing data was classified into operational taxonomic units (OTUs) to the genus level and expressed as relative abundance. The sequences were deposited in the NCBI Bioproject PRJNA684758.

5.4 Results and discussion

5.4.1 Overall analysis of H_2 production from enzymatic hydrolysates of agave bagasse

In previous reports, four different types of enzymatic hydrolysates of agave bagasse were tested for H_2 production in two reactor configurations. Briefly herein, we report on the performance highlights in terms of H_2 production during dark fermentation microbial processes. In terms of H_2 production rate, the CSTR fed with Celluclast-Viscozyme hydrolysates outperformed the rest of H_2-producing systems with a maximum VHPR of 12.9 L H_2/L-d at an OLR of 90 g COD/L-d (Figure 5.1-A). The second highest VHPR of 11.6 L H_2/L-d was achieved at an OLR of 120 g COD/L-d in a CSTR fed with Cellulase hydrolysates. The lowest VHPR was achieved with Stonezyme hydrolysates and it was ≤ 2.25 L H_2/L-d regardless of the use of OLR up

to 100 g COD/L-d. As shown in Figure 5.1-B, the CSTR fed with Celluclast-Viscozyme hydrolysates also showed the highest H_2 yield (108–118 L H_2/kg bagasse) regardless of the type of reactor. On the other hand, the lowest H_2 yield were observed mainly with Stonezyme hydrolysates (13–34 L H_2/kg bagasse), although the minimum of 10 L H_2/kg bagasse was found with Cellulase-Viscozyme hydrolysates. In previous reports, the mode of growth has been reported as an important factor affecting H_2 production performance; being suspended-growth more advantageous than biofilm-growth due to the adequate control of environmental conditions and (therefore) microbial communities [15,23]. On the other hand, the composition of carbohydrates and other compounds used for preservation of enzymes, altogether referred to as "quality" of the hydrolysate have been also referred to as main drivers of H_2 production performance [15, 16].

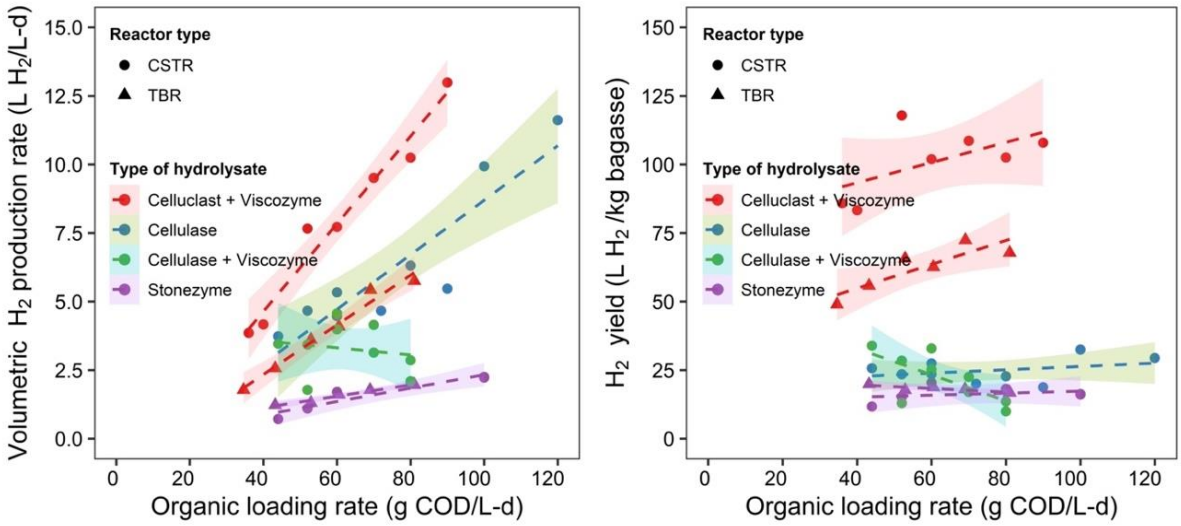

Figure 5.1. Hydrogen production from different hydrolysates of agave bagasse. A) volumetric H_2 production rate (VHPR); B) H_2 yield. The dashed lines represent linear regression models, while the shaded area stands for the 95% confidence intervals. Data was gathered from Montoya-Rosales et al. and Valencia-Ojeda et al. [15,16].

The changes of the quality of hydrolysates and reactor configuration have been hypothetically associated to changes on the composition, diversity and structure of microbial communities. In the following sections, evidence showing that microbial communities were indeed affected by both the type of hydrolysate and reactor configuration are presented.

5.4.2 Dark fermentative microbial communities and their underlying common structure

The 16S-rRNA sequencing analysis revealed that microbial communities were mainly composed by microorganisms belonging to the genera *Clostridium*, *Sporolactobacillus*, *Lachnoclostridium*, *Kluyvera*, and *Leuconostoc* (Figure 5.2-A). The dominance of *Clostridium* was mainly observed in CSTR systems fed with Cellulase or Celluclast-Viscozyme hydrolysates. A maximum *Clostridium* relative abundance of 90.1% was found in the CSTR fed with Cellulase hydrolysates at an OLR of 80 g COD/L-d. At such conditions, an average VHPR of 6.3 L H_2/L-d was obtained. *Clostridium* species are largely referred to as the main microbial group responsible for H_2 production [5, 7, 8]. This is due to their unique theoretical metabolic capacity for producing up to 4 mol H_2/mol hexose consumed. The *Clostridium* genus is integrated by a wide number of species, including C. *acetobutylicum*, C. *butyricum*, C. *saccharobutylicum*, C. *tyrobutyricum*, C. *pasteurianum*, and C. *beijerinckii*, among others. Their dominance in most of the systems was a clear indicator of the inoculation effectiveness and the selective pressure of operational conditions (i.e., pH and temperature) to increment spore-forming H_2-producing microorganisms.

The *Sporolactobacillus* genus, on the other hand, was mainly found in systems fed with Celluclast-Viscozyme and Cellulase-Viscozyme hydrolysates, although its relationship with H_2 production performance was unclear. *Sporolactobacillus* is a representative genus of lactic acid bacteria (LAB) which are characterized by their capacity to conduct lactic acid fermentation. The appearance of LAB in stages of high-performance H_2 production (i.e., CSTR fed with Celluclast-Viscozyme hydrolysates) can be associated to the previously suggested phenomenon of inhibition of H_2-producing bacteria [22]. In brief, such inhibition occurs when there is a high rate of H_2 production and an inefficient release of H_2 from the fermentation broth to the reactor headspace. These issues lead to the accumulation of dissolved H_2, which inhibits H_2-producing bacteria and, therefore, make an opportunity for LAB to better compete for the substrate uptake. An alternative explanation to the co-dominance of *Sporolactobacillus* relies on its role to sustain lactate-driven H_2

production, which is the conversion of lactate and acetate into butyrate and H_2 [24]. In dark fermentative systems, the lactate-driven H_2 production is based on the mutualistic interaction of LAB and some species of *Clostridium* that can perform lactate fermentation. LAB could consume carbohydrates and produce lactate, while *Clostridium* species could then use lactate as a substrate to produce butyrate and additional H_2. It is worth to note that carbohydrates fermentation and the lactate-driven H_2 production could take place at the same time, which could quite well explain the co-dominance of LAB and *Clostridium* during high-performance H_2 production. Nevertheless, although *Sporolactobacillus* has been previously reported in high-performance H_2-producing systems (e.g. Refs. [7, 22, 25]), their exact role in H_2 production remains unclear since they have been also identified in low-performance reactors [7, 26].

In regard with *Kluyvera*, *Lachnoclostridium* and *Leuconostoc*, these genera were found in systems with low performance H_2 production (i.e., VHPR < 2.5 L H_2/L-d), mainly in reactors fed with Stonezyme hydrolysates. *Kluyvera* was observed only in the TBR systems, at relative abundances up to 42% at the OLR of 60.5 g COD/L-d. *Kluyvera* is a facultative anaerobic bacteria that has been reported to be sub-dominant and not directly related to H_2 production [27, 28], but possibly implied in secondary metabolic functions, such as the fermentation of glucose, xylose, and cellobiose [29]. *Lachnoclostridium* was found in both systems fed with Stonezyme hydrolysates, although it was mainly present in the CSTR system at relative abundances up to 57.8% at an OLR of 100 g COD/L-d. Finally, the *Leuconostoc* genus was found across all systems investigated; however, its relative abundance was >10% only in reactors fed with hydrolysates prepared with Stonezyme, with a maximum relative abundance of 46.8% in the TBR fed at an OLR of 81 g COD/L-d. *Leuconostoc* is a heterofermentative LAB capable of producing acetate and lactate from pentoses, and ethanol and lactate from hexoses [30]. From a wider perspective, it is worth to note that *Lachnoclostridium*, *Kluyvera*, and *Leuconostoc* are microorganisms with reported capacities to metabolize oligomers derived from cellulose and hemicellulose. *Lachnoclostridium* and *Kluyvera* have been reported to produce extracellular hydrolytic enzymes that depolymerize plant cell wall

polysaccharides into fermentable sugars [31, 32, 33, 34], while some *Leuconostoc* strains have been found to be capable of using hydrolyzed xylan (xylose, xylobiose, xylotriose, xylotetraose, etc.) as carbon source [35]. Therefore, the presence of these bacteria could be associated to the type of substrate, a phenomenon broader explored in following sections.

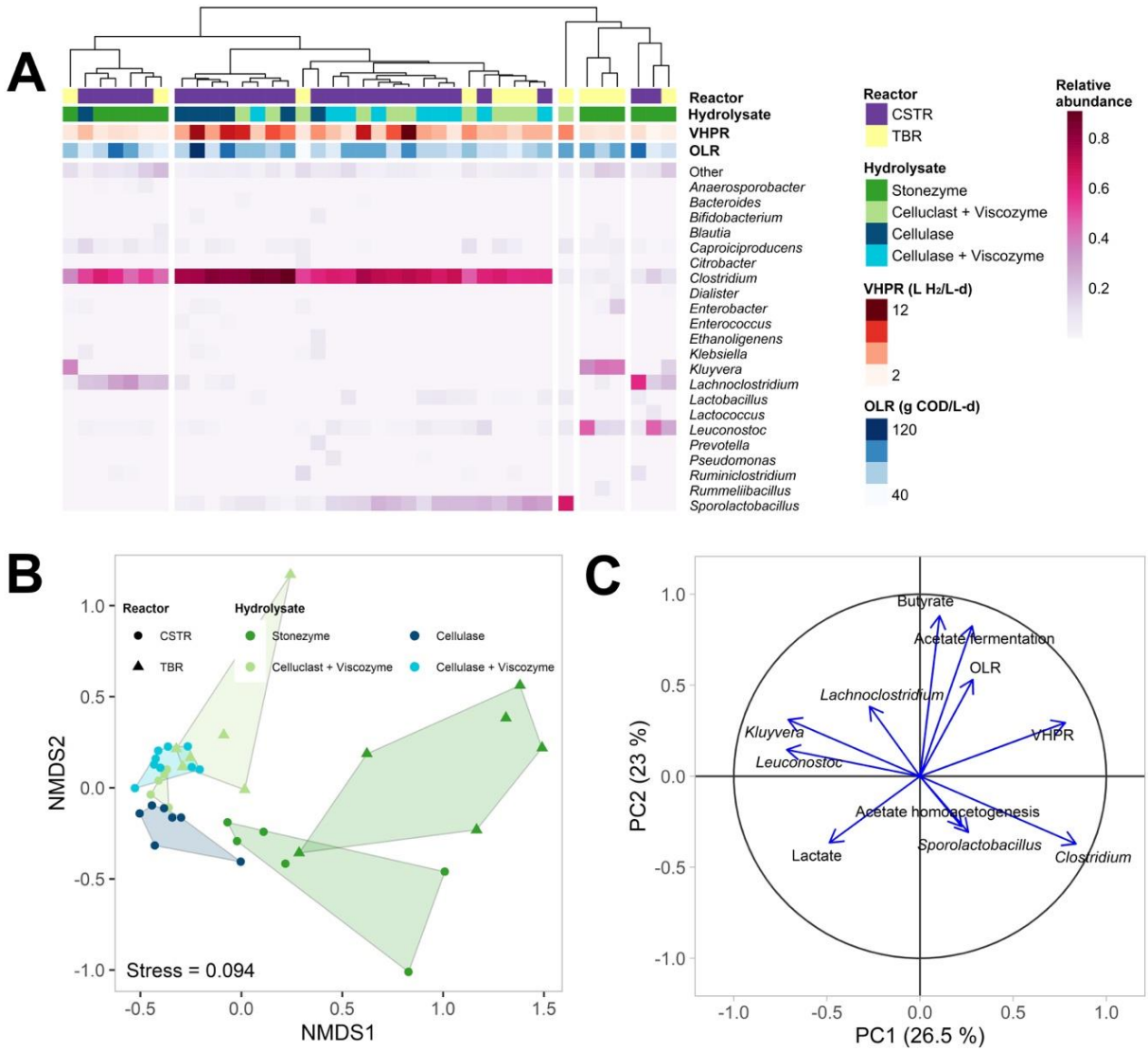

Figure 5.2. Structure and dynamics of H_2-producing microbial communities by using two different reactor configurations (i.e., CSTR and TBR) and four different types of hydrolysates. A) Microbial community structure depicted by an annotated heatmap. B) Non-metric multidimensional analysis (NMDS). C) Principal components analysis (PCA).

Other microorganisms including *Caproiciproducens*, *Lactobacillus*, and *Lactococcus*, were found at lower relative abundances (<15%). *Caproiciproducens*

was found in all systems, but mainly in the TBR systems fed with Celluclast-Viscozyme (relative abundances: 6.5 ± 4%) and Stonezyme hydrolysates (relative abundances: 3.2 ± 2%). *Lactobacillus* was found in the CSTR fed with Cellulase-Viscozyme hydrolysates (relative abundances: 3.6 ± 3.4%) and in the TBR fed with Celluclast-Viscozyme hydrolysates (relative abundances: 2.7 ± 2.7%). Finally, *Lactococcus* was found only in the CSTR fed with Stonezyme hydrolysates (relative abundances: 1.9 ± 4%). Microorganisms belonging to the *Caproiciproducens* genus are known for performing reverse β-oxidation to produce medium-chain carboxylic acids from ethanol-acetate or lactate-acetate pairs [36]. *Lactobacillus* and *Lactococcus* are LAB genera, they were present regardless of the reactor configuration and hydrolysate type (Figure 5.2-A).

The presence of *Caproiciproducens*, *Lactobacillus*, and *Lactococcus* seemed to be unrelated to the reactor configuration, the hydrolysate type, or operating conditions. Therefore, it is suggested that they could be contributing to the stability of the process by either 1) providing a functional reservoir that stabilizes the fermentation performance in case of disturbances or 2) maintaining equilibrium of metabolic fluxes. The first point refers to the idea that subdominant microorganisms can be seen as microbial replacements that can arise when dominant microorganisms are either inhibited or washed-out due to changes of operating conditions. The second point refers to the idea that some species in the microbial community use either the carbohydrates or byproducts left by dominating species (as a substrate); in this form, the sub-dominating species contribute to keep byproducts concentrations low and favor the overall fermentation due to the avoidance of thermodynamic bottlenecks.

Non-metric multidimensional analysis (NMDS) confirmed that the composition of microbial communities was affected by the type of hydrolysate and reactor configuration (Figure 5.2-B); most of microbial communities fed with Celluclast-Viscozyme, Cellulase, and Cellulase-Viscozyme hydrolysates were relatively similar to each other in terms of the NMDS distance, and were clearly separated (different) from communities developed in systems fed with Stonezyme hydrolysates (Figure 5.2-B). Moreover, microbial communities in the systems fed with Stonezyme showed high variability across stages. In contrast, CSTR systems fed with Cellulase,

Cellulase-Viscozyme, and Celluclast-Viscozyme, showed a relatively low variability measured as the inter stage distances.

Furthermore, the relationships between operating conditions, H_2-production performance, and the relative abundance of main genera in microbial communities were assessed through a PCA analysis. The two main principal components of the PCA analysis only described 49.5% of variance (Figure 5.2-C). In such analysis, the presence of*Clostridium* was positively associated to VHPR. In contrast, microorganisms belonging to the *Kluyvera* and *Leuconostoc* genera were negatively associated to VHPR. Interestingly, VHPR and the lactate production rate were negatively but strongly associated to each other, suggesting both metabolisms were mutually exclusive in systems under study. Besides, it is worth to note that other relationships between identified microbial genera, H_2 production and other factors (e.g., substrate concentration, OLR, and carboxylates production rate) were not observed. A pairwise Pearson correlation analyses was therefore performed to verify such observation. Results confirmed the relationships already observed in the PCA while other possible relationships were not relevant and not statistically significant (Figure 5.3).

Beyond the specific composition of microbial communities and their relationship with the type of hydrolysate and reactor, it was observed that most microbial communities shared common characteristics and could be organized in accordance with three metabolic functions: 1) hydrolysis, 2) primary fermentation, and 3) secondary fermentation. The first group would be integrated by microorganisms that perform the hydrolysis of oligomers remaining from the enzymatic hydrolysis step. This group was probably conformed of *Lachnoclostridium*, *Kluyvera* and *Leuconostoc*, which have been reported to perform hydrolysis of lignocellulosic biomass [31, 32, 33, 34]. The second group would be integrated by strict and facultative anaerobes capable to carry out H_2 production from simple carbohydrates; this group possibly included microorganisms belonging to *Clostridium* and *Lachnoclostridium* [5, 7, 8]. The third group would be composed by microorganisms that use carbohydrates not utilized by the primary fermenters as well as reduced byproducts; this group could include *Sporolactobacillus*, *Lactobacillus*, and *Leuconostoc* [22, 35].

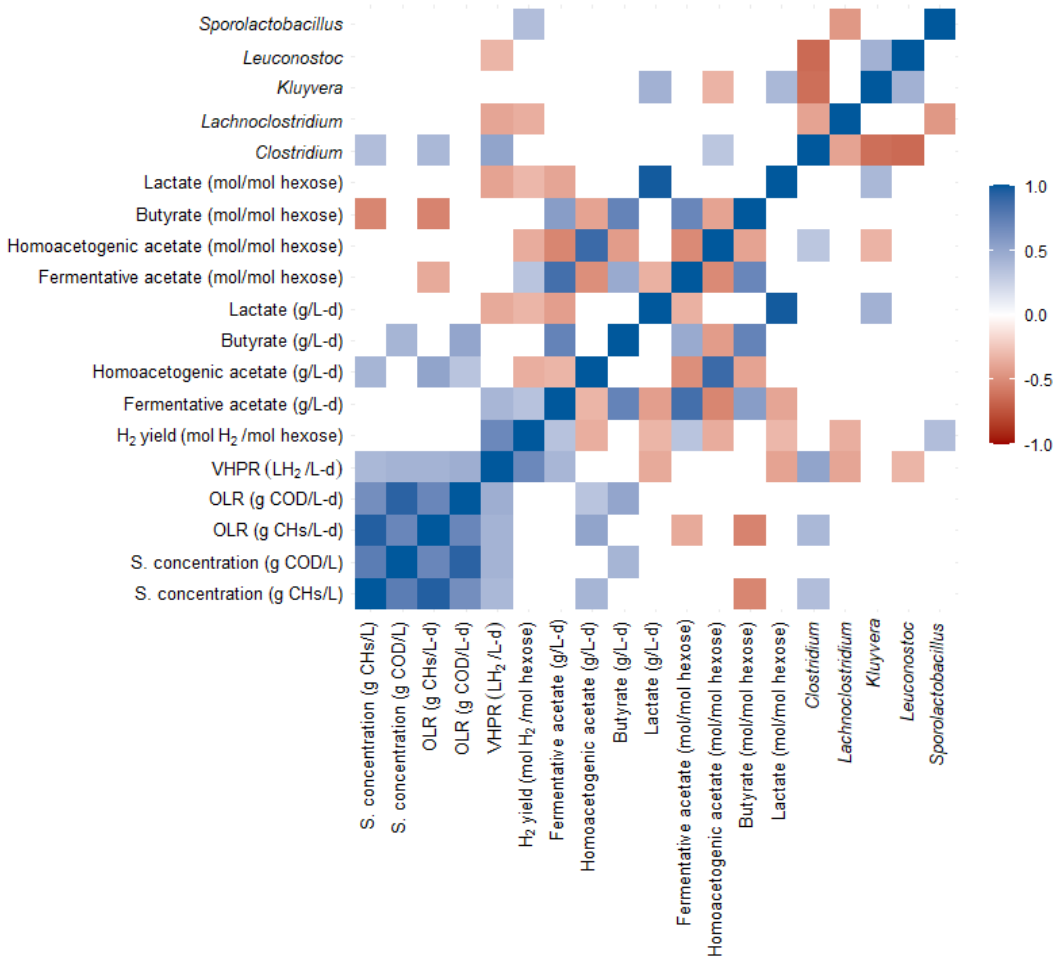

Figure 5.3. Pairwise Pearson's correlation analysis on H_2 production performance and microbial communities for systems fed with enzymatic hydrolysates of agave bagasse. Only significant correlations at $p<0.05$ are displayed. VHPR. Volumetric H_2 production rate; S.: substrate; OLR: organic loading rate.

5.4.3 The reactor configuration as a main factor shaping microbial communities: composition and diversity

The effect of the reactor configuration on the microbial community composition and diversity was evaluated in CSTR and TBR systems fed with Stonezyme and Celluclast-Viscozyme hydrolysates; microbial communities from these systems are displayed and directly compared in Figure 5.4. CSTR systems were co-dominated by microorganisms belonging to *Clostridium*, *Sporolactobacillus*, and *Lachnoclostridium* genera. Although none of these was exclusively found in CSTR systems, their presence was in all cases more intense in CSTR than in TBR. In

CSTR systems, *Clostridium* was found at a relative abundance of 56.8 ± 2.5%, while in TBR systems the *Clostridium* abundance was 32.1 ± 25%. In regard with the *Sporolactobacillus* genus, this lactic-acid bacterium accounted for 13.7 ± 8% of relative abundance in CSTR systems, while in TBR systems their relative abundance was 28.2 ± 19.6%. In third instance, *Lachnoclostridium* accounted for 29.9 ± 15% of the microbial abundance in CSTR systems, while in TBR, such organisms remained at 9.2 ± 9.8%.

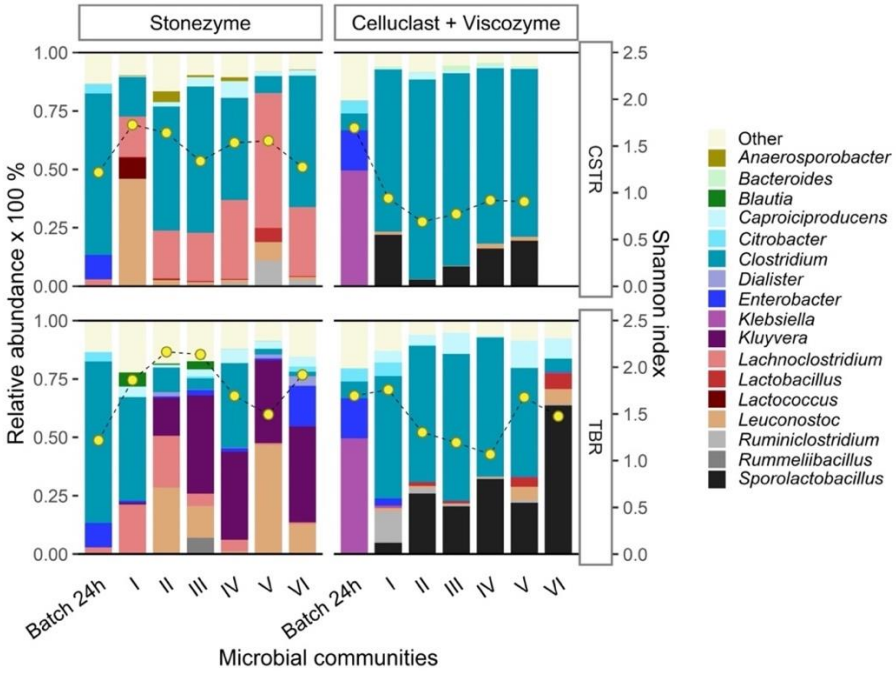

Figure 5.4. Composition of microbial communities in CSTR and TBR systems fed with two different hydrolysates of agave bagasse. Batch 24h refers to the onset of continuous operation. Bars corresponds to relative abundance whereas circles to Shannon index. See Table 5.1 for details of reactors operational conditions.

On the other hand, TBR microbial communities were dominated by microorganisms belonging to *Clostridium* (max relative abundance: 62.9%), *Sporolactobacillus* (max relative abundance: 63.7%), *Lachnoclostridium* (max relative abundance: 22.18%), *Caproiciproducens* (max relative abundance: 11.7%), *Kluyvera* (max relative abundance: 42%), *Leuconostoc* (max relative abundance: 46.8%) genera. However, only a few were consistently found mainly in the TBR configuration: *Kluyvera* (relative abundance: 28.9 ± 16.7%) and *Leuconostoc* (relative abundance: 9.8 ± 14.3%). Nonetheless, in either case, the presence of *Kluyvera* and *Leuconostoc* was

not only associated to the TBR configuration but also to the type of hydrolysate as discussed in section 5.4.4. Moreover, the microbial diversity also changed as function of the reactor configuration. In CSTR systems, the Shannon's diversity index was significatively lower than in TBR systems (1.21 ± 0.38 vs 1.65 ± 0.35, $p < 0.05$). Likewise, the evenness of the microbial community, measured as the Gini coefficient was also found to be lower in the CSTR than in the TBR (0.87 ± 0.06 vs 0.92 ± 0.03, $p < 0.05$). In general, microbial communities of CSTR systems were simpler and uneven than those found in TBR systems.

In general, the sequencing results and statistical analysis revealed that there was a significant effect of the reactor configuration on the composition of microbial communities (Shannon ~ reactor + hydrolysate; $F1,22 = 15.35$, $p < 0.01$). Probably, such changes in microbial communities resulted from intrinsic differences between CSTR and TBR systems. Two main differences can be highlighted: the growth and the control of environmental conditions. CSTR is a suspended-biomass system, where operating conditions (e.g. substrate concentration, pH, and temperature) are homogeneous and relatively simple to control. Moreover, due to the suspended mode of growth, the flow stream (passing through the system) exerts a strict control on microbial communities based on their growth rate [7,37]. In contrast, the TBR is a biofilm system characterized by stratification along the reactor height and within biofilms, where the establishment and development of microbial populations is difficult to predict and control.

Therefore, it is expected that CSTR are characterized by simplified microbial communities since the number of ecological niches is reduced. On the contrary, the stratification of TBR systems is associated to a higher number of ecological niches; therefore, the diversity of microbial communities in TBR is expected to be high. The assessment of microbial diversity and evenness through the Shannon index and Gini coefficient confirmed that microbial communities were more diverse in the TBR than in the CSTR. Nevertheless, the higher diversity of TBR systems compared to CSTR did not lead to better performance. In this regard, previous reports have argued that high-diversity microbial communities are favorable for the functional stability (i.e. H_2 production) by providing a wide reservoir of microbial species that share similar

ecological function but different physiological characteristics that can better support unexpected changes on environmental and operating conditions (pH, temperature, substrate composition, inhibitory substances, etc.) [5,7,38]. Nonetheless, when there is a reliable control on operating conditions, the relevance of microbial diversity seems to decrease, and could even be detrimental for high-performance H_2 production. In such a case, the presence of highly efficient species rather than highly diverse communities should be preferred.

5.4.4 The type of hydrolysate drives the composition and diversity of microbial communities

Microbial communities developed in CSTR systems fed with four different types of hydrolysates are compared in Figure 5.5. In general, results showed that the type of hydrolysate had a significant effect on the diversity of microbial communities (Shannon ~ hydrolysate; $F_{3,24} = 7.39$, $p < 0.01$). Systems fed with hydrolysates prepared with Celluclast, Cellulase, and Celluclast-Viscozyme, were all dominated by microorganisms belonging to the *Clostridium* genus (relative abundances: 7.2–90.8%). In average, the highest *Clostridium* abundances (76.9 ± 6.9%) were found in the system fed with Celluclast-Viscozyme, followed by systems fed with Cellulase (72.2 ± 13.9%) and Cellulase-Viscozyme (67.2 ± 8. %). In contrast, the lowest Clostridium abundances were observed in the system fed with Stonezyme hydrolysates (40 ± 22.7%).

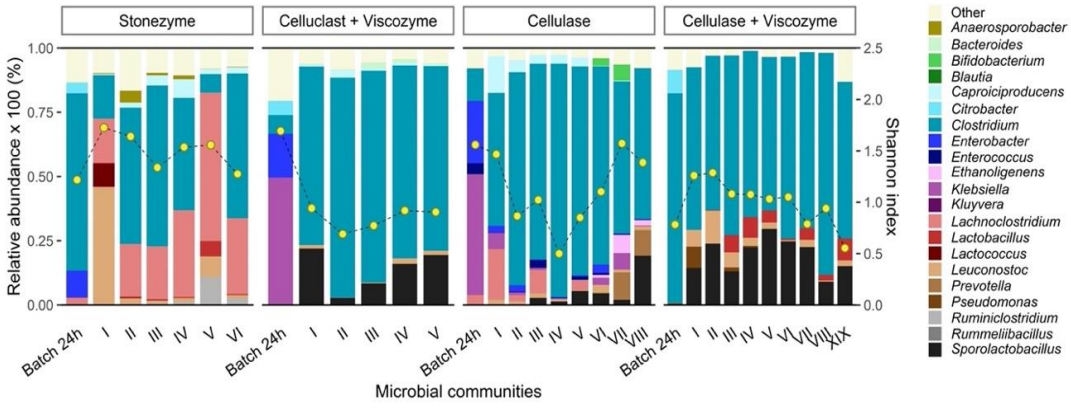

Figure 5.5. Composition of microbial communities developed in CSTR systems fed with four types of hydrolysates of agave bagasse. Batch 24h refers to the onset of continuous operation. Bars corresponds to relative abundance whereas circles to Shannon index. See Table 5.1 for details of reactors operational conditions.

Relevant differences in the microbial community composition were also observed with the *Sporolactobacillus* genus. Systems fed with hydrolysates prepared with Celluclast-Viscozyme and Cellulase-Viscozyme, were characterized by a strong co-dominance of *Sporolactobacillus* (13.7 ± 8.0% vs 19.4 ± 6.7%, respectively). Interestingly, the presence of *Sporolactobacillus* was quite limited in the reactor fed with Cellulase (relative abundance: 4.4 ± 6.2%) while its presence was not detected in the system fed with Stonezyme hydrolysates. In the CSTR fed with Stonezyme hydrolysates, microbial communities showed the most remarkable differences. With this type of hydrolysate, *Clostridium* and *Sporolactobacillus* were found at remarkably lower abundances than in the rest of systems. Moreover, *Lachnoclostridium* co-dominated in all stages of operation (relative abundance: 29.9 ± 15%), being the most abundant genera at some stages (Stage V, up to 57.8%). In general, the diversity and evenness of microbial communities, measured as the Shannon index and the Gini coefficient, were found to be significantly affected by the type of hydrolysate ($p < 0.05$ in both cases). However, differences were observed only when comparing the system fed with Stonezyme hydrolysates versus any of the rest.

Contrary to previous hypothesis [22,37], the presence of *Sporolactobacillus* was not directly associated to high performance H_2 production; this was well illustrated by comparing the performance of systems fed with Celluclast-Viscozyme (up to 13 L H_2/L-d) and Cellulase-Viscozyme (up to 5 L H_2/L-d) hydrolysates. It is rather hypothesized that the appearance of *Sporolactobacillus* was connected to the high proportion of carbohydrates (including xylose and other hemicellulose-related carbohydrates) expected in hydrolysates prepared with Viscozyme. Nevertheless, it is unclear what is the competitive advantage of *Sporolactobacillus* over *Clostridium* on taking the above-mentioned carbohydrates since its use has been also documented for *Clostridium* species (e.g. Refs. [39,40]). Other factors could favor the co-dominance of *Sporolactobacillus*, such as, their ability to produce bacteriocines [41,42], their growth kinetic characteristics, and their possible cooperative relationship with H_2-producing bacteria [43]. On the other hand,

microbial communities developed in the CSTR system fed with Cellulase hydrolysates were dominated by *Clostridium* bacteria (51.8–90.8% of relative abundance), but remarkably low proportions of *Sporolactobacillus* (0.1–5.4% of relative abundance). Still, despite the high dominance of *Clostridium*, this microbial community led to VHPR values of 3.7–11.6 L H_2/L-d, which were among the highest VHPR values in all systems evaluated.

Finally, in the CSTR fed with Stonezyme hydrolysates, microbial communities showed the most remarkable differences. With this type of hydrolysate, microorganisms belonging to the *Clostridium* genus were found at relative abundances of 7.2–62.6%, the lowest values among all CSTR studied. Furthermore, *Leuconostoc* and *Lachnoclostridium* co-dominated at high relative abundances (up to 46 and 57.8%, respectively), being the most abundant genera at some stages (Stages I and V). As stated in section 5.4.2, it is thought that the composition of Stonezyme hydrolysates includes a high ratio of oligomers, which could lead to the selection of microorganisms capable to produce cellulolytic and hemicellulolytic enzymes. In particular, our results clearly showed that the composition of Stonezyme hydrolysates led to more diverse microbial communities, suggesting that such hydrolysates were probably composed by a higher number of carbohydrates and a higher proportion of oligomers in comparison with the three other hydrolysates. Nevertheless, further studies with Stonezyme hydrolysates are necessary to determine what carbohydrates or components are shaping the microbial communities.

5.4.5 Microbial diversity as explanatory factor of H_2 production performance

To investigate the link between community diversity and performance, microbial communities were classified based on their associated VHPR into high performance (VHPR > 8 L H_2/L-d), medium-performance (VHPR = 4–8 L H_2/L-d), and low-performance (VHPR < 4 L H_2/L-d). Interestingly, high-performance and medium-performance H_2-producing systems were both co-dominated by *Clostridium* and *Sporolactobacillus* genera (Figure 5.6). The relative abundance of both genera accounted for more than 90%. As a consequence, medium-performance and high-

performance microbial communities were characterized by relatively low microbial diversity (Shannon index: 0.5–1.68) and an unequal distribution (Gini coefficients: 0.88–0.96). On the contrary, the composition of microbial communities was more diverse (Shannon index: 1.05–2.16) and evenly distributed (Gini coefficients: 0.73–0.95) in low-performance H_2-producing systems (Table 5.3). In specific, *Kluyvera*, *Lachnoclostridium*, and *Leuconostoc* (not observed in high- and medium-performance systems), were present at relative abundances of 0.8–42, 0.6–57.8, and 0.01–46.8%, respectively. In general, Shannon indexes and Gini coefficients confirmed that the diversity of microbial communities was associated to the performance of H_2 production, as well as the type of hydrolysates and substrate.

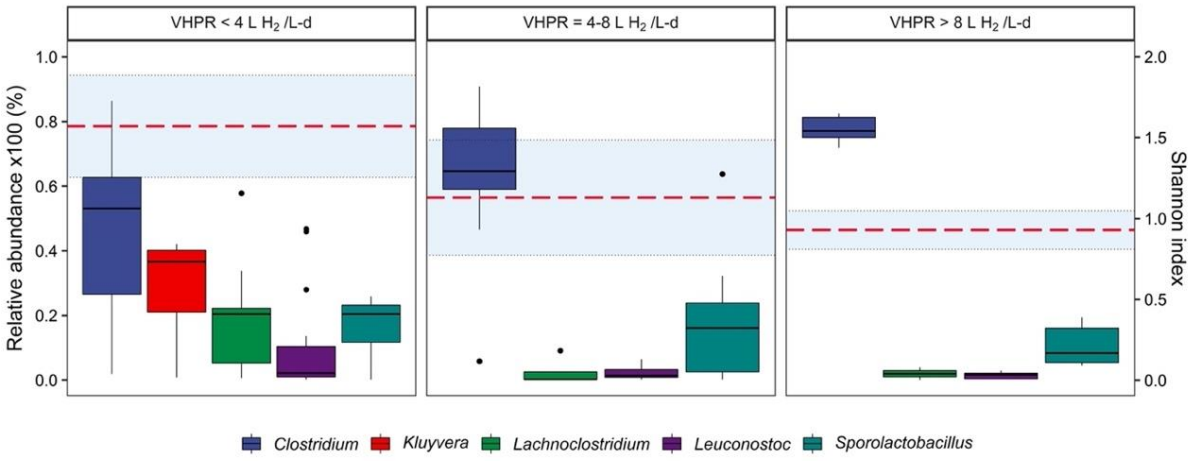

Figure 5.6. Box-plot of main microbial genera in H_2-producing systems fed with hydrolysates of agave bagasse. Microbial communities were classified as function of the achieved VHPR. The dashed line stands for the average Shannon index, while the shadow stands for ±1 standard deviation.

Table 5.3. Shannon indexes and Gini coefficients of microbial communities in systems fed with enzymatic hydrolysates of agave bagasse.

	Type of reactor	Type of hydrolysate	Stage of operation (samples)									
			Batch 24h	I	II	III	IV	V	VI	VII	VIII	IX
Shannon index	CSTR	Celluclast + Viscozyme	1.69	0.94	0.69	0.77	0.92	0.90	-	-	-	-
	CSTR	Stonezyme	1.22	1.73	1.64	1.34	1.54	1.56	1.27	-	-	-
	TBR	Celluclast + Viscozyme	1.69	1.76	1.30	1.19	1.07	1.68	1.48	-	-	-
	TBR	Stonezyme	1.22	1.86	2.16	2.14	1.69	1.49	1.92	-	-	-
	CSTR	Cellulase	1.56	1.47	0.87	1.02	0.50	0.85	1.10	1.57	1.39	-
	CSTR	Cellulase + Viscozyme	0.78	1.26	1.29	1.08	1.08	1.03	1.05	0.79	0.94	0.55
Gini coefficient	CSTR	Celluclast + Viscozyme	0.91	0.88	0.94	0.93	0.90	0.89	-	-	-	-
	CSTR	Stonezyme	0.92	0.83	0.92	0.85	0.89	0.80	0.73	-	-	-
	TBR	Celluclast + Viscozyme	0.91	0.93	0.95	0.94	0.96	0.94	0.91	-	-	-
	TBR	Stonezyme	0.92	0.91	0.88	0.88	0.92	0.90	0.92	-	-	-
	CSTR	Cellulase	0.80	0.86	0.95	0.95	0.95	0.93	0.95	0.93	0.94	-
	CSTR	Cellulase + Viscozyme	0.95	0.96	0.96	0.96	0.95	0.96	0.96	0.96	0.96	0.96

CSTR: Continuous stirred-tank reactor; TBR: Trickling bed reactor.

Following the theory of niches, systems fed with a simple substrate under well controlled and uniform environmental conditions lead to the establishment of a reduced number of niches occupied by the fittest organism from the inoculum. In this regard, low-diverse and uneven microbial communities were expected to appear in CSTR systems. This was the case of CSTR fed with Celluclast-Viscozyme and Cellulase. On the other hand, the establishment of diverse and evenly distributed microbial communities is expected to occur in presence of substrates with more diverse composition of carbohydrates and heterogenous environmental conditions. Such was the case of CSTR and TBR fed with Stonezyme hydrolysates. It is worth to highlight that microorganisms conforming this type of microbial communities are theoretically the most capable to occupy the available niches. However, this is not necessarily related to their capacity to produce H_2. Moreover, due to the diversification of niches (associated to the mode of growth), it is possible that some niches appear for the consumption of H_2. These observations suggest that microbial diversity and evenness should not be considered indispensable features for good H_2 production performance in communities grown under well controlled environments, especially in CSTR systems.

Last but not least important, a regression analysis on the relationship between microbial diversity (Shannon index) and evenness (Gini coefficient) on the performance of H_2-producing systems (VHPR and H_2 yield) was carried out. Among the different relationships, it was revealed that changes of VHPR were significantly affected by the microbial diversity (Shannon index) (Figure 5.7). This finding confirms that the diversity of microbial communities found in H_2-producing systems is a key factor influencing their performance. Contrary to the widespread idea about diversity and performance, an inverse relationship between Shannon index and microbial communities was found and successfully described with a simple exponential model ($\ln \text{VHPR} = 3.02 - 1.35 * \text{Shannon}$, $r^2 = 0.57$, $p < 0.05$). The regression analysis and grouping according to VHPR revealed that the microbial diversity was strongly linked with H_2-producing performance; and low diverse and uneven microbial communities were capable of leading to high-performance H_2 production in systems fed with enzymatic hydrolysates of agave bagasse.

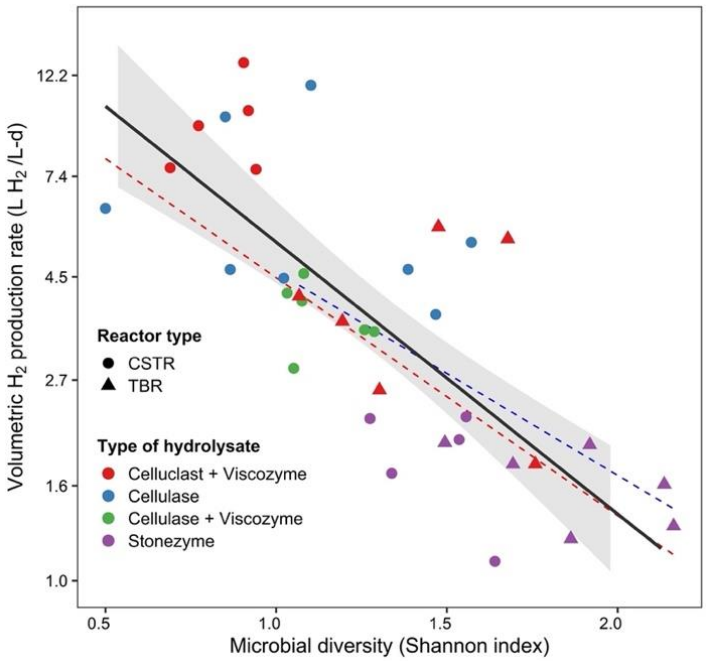

Figure 5.7. Regression analysis on the relationship between microbial diversity (assessed through the Shannon index) and H_2 production performance. Axis *Y* is shown as *ln* transformed to better represent the linear regression. The solid line represents the fitted $VHPR = e^{3.02 - 1.35 * \text{Shannon}}$ (r^2=0.57, p<0.05), while the shaded area stands for the 95% confidence intervals. The blue and red dashed lines represent the regression models for TBR (r^2=0.26) and CSTR (r^2=0.38) systems, respectively.

5.4.6 High performance H_2 production and microbial communities: final remarks

It has been shown that H_2 production from enzymatic hydrolysates of agave bagasse could range from 0.72 to 12.9 L H_2/L-d (Table 5.1). The reasons behind the considerable variability have been thoroughly analyzed. It has been found that the type of reactor, the type of substrate and the organic loading rate are factors with strong effects on the microbial communities and, therefore, on H_2 productivities (sections 5.4.2 and 5.4.5). It was shown that high H_2 production rates (max: 12.9 L H_2/L-d) were attained when microbial communities were relatively simple, co-dominated mainly by *Clostridium* and *Sporolactobacillus*. To sustain simplified communities in the long term, an adequate control of operating conditions is required. It has been previously discussed that short HRT (~6 h) values lead to well-defined H_2-producing microbial communities co-dominated by lactic acid bacteria and H_2-producing bacteria (e.g. Refs. [37, 44]); however, this is only possible when HRT is coupled to the solids retention time, which only occurs in CSTR systems.

Otherwise, when the solids retention time is decoupled from HRT (as it occurs in UASB, biofilm reactors, and others), a higher diversity of microorganisms would be present and it could possibly hinder H_2 production rates and make its control more complicated [7,45,46]. Moreover, it has been also shown that relatively high VHPR values are obtained at high OLR; nevertheless, this relationship largely depends on the type and constituents of hydrolysates. It has been hypothesized that hydrolysates prepared with Celluclast-Viscozyme probably contained a higher proportion of easily degradable sugars which could lead to better performance [16]. In sum, CSTR systems fed with Celluclast-Viscozyme hydrolysates at well-controlled operating conditions (HRT: 6 h, 37 °C, pH 5.5) leads to high performance H_2 production.

5.5 Conclusions

Comprehensive analysis of H_2-producing microbial communities, in two reactor configurations and four different types of enzymatic hydrolysates showed that microbial communities were composed by hydrolysing bacteria (i.e., *Lachnoclostridium*, *Kluyvera* and *Leuconostoc*), dark-fermentation bacteria (i.e., *Clostridium* and *Lachnoclostridium*), and secondary fermenters (i.e., *Sporolactobacillus*, *Lactobacillus*, *Leuconostoc*). The microbial diversity was clearly affected by the reactor configuration; microbial communities were generally more diverse in the TBR than in the CSTR. Such a difference in diversity was associated to the fact that CSTR was consistently better than the TBR in terms of H_2 production. In regard with the type of hydrolysates, the use of Cellulase hydrolysates led to microbial communities dominated by *Clostridium*, reactors fed with Cellulase-Viscozyme and Celluclast-Viscozyme hydrolysates led the co-dominance of *Clostridium* and *Sporolactobacillus*, and reactors fed with Stonezyme led to microbial communities co-dominated by *Clostridium* and *Lachnoclostridium*. In general, it was found that well controlled environments of CSTR systems favored the establishment of low diverse microbial communities composed by *Clostridium-Sporolactobacillus* leading to high-performance H_2 production.

5.6 References

[1] P.C. Hallenbeck, D. Ghosh, Advances in fermentative biohydrogen production: the way forward?, Trends Biotechnol. 27 (2009) 287–97. doi:10.1016/j.tibtech.2009.02.004.

[2] J. De Vrieze, K. Verbeeck, I. Pikaar, J. Boere, A. Van Wijk, K. Rabaey, W. Verstraete, The hydrogen gas bio-based economy and the production of renewable building block chemicals, food and energy, N. Biotechnol. 55 (2020) 12–18. doi:10.1016/j.nbt.2019.09.004.

[3] M.Y. Azwar, M. a. Hussain, A.K. Abdul-Wahab, Development of biohydrogen production by photobiological, fermentation and electrochemical processes: A review, Renew. Sustain. Energy Rev. 31 (2014) 158–173. doi:10.1016/j.rser.2013.11.022.

[4] M. Monti, A. Scoma, G. Martinez, L. Bertin, F. Fava, Uncoupled hydrogen and volatile fatty acids generation in a two-step biotechnological anaerobic process fed with actual site wastewater, N. Biotechnol. 32 (2015) 341–346. doi:10.1016/j.nbt.2014.08.002.

[5] E. Castelló, A.D. Nunes Ferraz-Junior, C. Andreani, M. del P. Anzola-Rojas, L. Borzacconi, G. Buitrón, J. Carrillo-Reyes, S.D. Gomes, S.I. Maintinguer, I. Moreno-Andrade, R. Palomo-Briones, E. Razo-Flores, M. Schiappacasse-Dasati, E. Tapia-Venegas, I. Valdez-Vázquez, A. Vesga-Baron, M. Zaiat, C. Etchebehere, Stability problems in the hydrogen production by dark fermentation: Possible causes and solutions, Renew. Sustain. Energy Rev. 119 (2019). doi:10.1016/j.rser.2019.109602.

[6] C.M. Spirito, H. Richter, K. Rabaey, A.J. Stams, L.T. Angenent, Chain elongation in anaerobic reactor microbiomes to recover resources from waste, Curr. Opin. Biotechnol. 27 (2014) 115–122. doi:10.1016/j.copbio.2014.01.003.

[7] C. Etchebehere, E. Castelló, J. Wenzel, M. del Pilar Anzola-Rojas, L. Borzacconi, G. Buitrón, L. Cabrol, V.M. Carminato, J. Carrillo-Reyes, C. Cisneros-Pérez, L. Fuentes, I. Moreno-Andrade, E. Razo-Flores, G.R. Filippi, E. Tapia-Venegas, J. Toledo-Alarcón, M. Zaiat, Microbial communities from 20 different hydrogen-producing reactors studied by 454 pyrosequencing, Appl. Microbiol. Biotechnol. 100 (2016) 3371–3384. doi:10.1007/s00253-016-7325-y.

[8] L. Cabrol, A. Marone, E. Tapia-Venegas, J.-P. Steyer, G. Ruiz-Filippi, E. Trably, Microbial ecology of fermentative hydrogen producing bioprocesses: useful insights for driving the ecosystem function, FEMS Microbiol. Rev. 41 (2017) 158–181. doi:10.1093/femsre/fuw043.

[9] C.H. Hung, Y.T. Chang, Y.J. Chang, Roles of microorganisms other than Clostridium and Enterobacter in anaerobic fermentative biohydrogen production systems - A review, Bioresour. Technol. 102 (2011) 8437–8444. doi:10.1016/j.biortech.2011.02.084.

[10] J.E. Goldford, N. Lu, D. Bajić, S. Estrela, M. Tikhonov, A. Sanchez-Gorostiaga, D. Segrè, P. Mehta, A. Sanchez, Emergent simplicity in microbial community assembly, Science (80-.). 361 (2018) 469–474. doi:10.1126/science.aat1168.

[11] J. Arreola-Vargas, L.B. Celis, G. Buitrón, E. Razo-Flores, F. Alatriste-Mondragón, Hydrogen production from acid and enzymatic oat straw hydrolysates in an anaerobic sequencing batch reactor: Performance and microbial population analysis, Int. J. Hydrogen Energy. 38 (2013) 13884–13894. doi:https://doi.org/10.1016/j.ijhydene.2013.08.065.

[12] G. Kumar, P. Sivagurunathan, B. Sen, S.H. Kim, C.Y. Lin, Mesophilic continuous fermentative hydrogen production from acid pretreated de-oiled jatropha waste hydrolysate using immobilized microorganisms, Bioresour. Technol. 240 (2017) 137–143. doi:10.1016/j.biortech.2017.03.059.

[13] M. Quéméneur, J. Hamelin, A. Barakat, J.-P. Steyer, H. Carrère, E. Trably, Inhibition

of fermentative hydrogen production by lignocellulose-derived compounds in mixed cultures, Int. J. Hydrogen Energy. 37 (2012) 3150–3159. doi:10.1016/j.ijhydene.2011.11.033.
[14] Z. Liu, C. Zhang, L. Wang, J. He, B. Li, Y. Zhang, X.-H. Xing, Effects of furan derivatives on biohydrogen fermentation from wet steam-exploded cornstalk and its microbial community, Bioresour. Technol. 175 (2015) 152–159. doi:10.1016/j.biortech.2014.10.067.
[15] J. de J. Montoya-Rosales, D.K. Olmos-Hernández, R. Palomo-Briones, V. Montiel-Corona, A.G. Mari, E. Razo-Flores, Improvement of continuous hydrogen production using individual and binary enzymatic hydrolysates of agave bagasse in suspended-culture and biofilm reactors, Bioresour. Technol. 283 (2019) 251–260. doi:https://doi.org/10.1016/j.biortech.2019.03.072.
[16] C. Valencia-Ojeda, J. de J. Montoya-Rosales, R. Palomo-Briones, V. Montiel-Corona, L.B. Celis, E. Razo-Flores, Saccharification of agave bagasse with Cellulase 50 XL is an effective alternative to highly specialized lignocellulosic enzymes for continuous hydrogen production, J. Environ. Chem. Eng. 9 (2021) 105448. doi:10.1016/j.jece.2021.105448.
[17] J. Carrillo-Reyes, A. Tapia-Rodríguez, G. Buitrón, I. Moreno-Andrade, R. Palomo-Briones, E. Razo-Flores, O. Aguilar Juárez, J. Arreola-Vargas, N. Bernet, A.F. Maluf Braga, L. Braga, E. Castelló, L. Chatellard, C. Etchebehere, L. Fuentes, E. León-Becerril, H.O. Méndez-Acosta, G. Ruiz-Filippi, E. Tapia-Venegas, E. Trably, J. Wenzel, M. Zaiat, A standardized biohydrogen potential protocol: An international round robin test approach, Int. J. Hydrogen Energy. 44 (2019) 26237–26247. doi:10.1016/j.ijhydene.2019.08.124.
[18] M. Dubois, K.A.Gilles, J.K.Hamilton, P.A.Rebers, Fred.Smith, Colorimetric Method for Determination of Sugars and Related Substances, Anal. Chem. 28 (1956) 350–356. doi:10.1021/ac60111a017.
[19] APHA/AWWA/WEF, Standard Methods for the Examination of Water and Wastewater, Stand. Methods. (2012). doi:ISBN 9780875532356.
[20] G. Davila-Vazquez, F. Alatriste-Mondragón, A. de León-Rodríguez, E. Razo-Flores, Fermentative hydrogen production in batch experiments using lactose, cheese whey and glucose: Influence of initial substrate concentration and pH, Int. J. Hydrogen Energy. 33 (2008) 4989–4997. doi:10.1016/j.ijhydene.2008.06.065.
[21] J.G. Caporaso, J. Kuczynski, J. Stombaugh, K. Bittinger, F.D. Bushman, E.K. Costello, N. Fierer, A.G. Peña, J.K. Goodrich, J.I. Gordon, G.A. Huttley, S.T. Kelley, D. Knights, J.E. Koenig, R.E. Ley, C.A. Lozupone, D. McDonald, B.D. Muegge, M. Pirrung, J. Reeder, J.R. Sevinsky, P.J. Turnbaugh, W.A. Walters, J. Widmann, T. Yatsunenko, J. Zaneveld, R. Knight, QIIME allows analysis of high-throughput community sequencing data, Nat. Methods. 7 (2010) 335–336. doi:10.1038/nmeth.f.303.
[22] R. Palomo-Briones, E. Trably, N.E. López-Lozano, L.B. Celis, H.O. Méndez-Acosta, N. Bernet, E. Razo-Flores, Hydrogen metabolic patterns driven by Clostridium-Streptococcus community shifts in a continuous stirred tank reactor, Appl. Microbiol. Biotechnol. 102 (2018) 2465–2475. doi:10.1007/s00253-018-8737-7.
[23] C.A. Contreras-Dávila, H.O. Méndez-Acosta, L. Arellano-García, F. Alatriste-Mondragón, E. Razo-Flores, Continuous hydrogen production from enzymatic hydrolysate of Agave tequilana bagasse: Effect of the organic loading rate and reactor configuration, Chem. Eng. J. 313 (2017) 671–679. doi:10.1016/j.cej.2016.12.084.
[24] O. García-Depraect, R. Castro-Muñoz, R. Muñoz, E.R. Rene, E. León-Becerril, I. Valdez-Vazquez, G. Kumar, L.C. Reyes-Alvarado, L.J. Martínez-Mendoza, J. Carrillo-Reyes, G. Buitrón, A review on the factors influencing biohydrogen production from lactate: the key to unlocking enhanced dark fermentative processes, Bioresour.

Technol. 324 (2020) 124595. doi:10.1016/j.biortech.2020.124595.
[25] J. de J. Montoya-Rosales, R. Palomo-Briones, L.B. Celis, C. Etchebehere, E. Razo-Flores, Discontinuous biomass recycling as a successful strategy to enhance continuous hydrogen production at high organic loading rates, Int. J. Hydrogen Energy. 45 (2020) 17260–17269. doi:10.1016/j.ijhydene.2020.04.265.
[26] C. Cisneros-Pérez, J. Carrillo-Reyes, L.B. Celis, F. Alatriste-Mondragón, C. Etchebehere, E. Razo-Flores, Inoculum pretreatment promotes differences in hydrogen production performance in EGSB reactors, Int. J. Hydrogen Energy. 40 (2015) 6329–6339. doi:10.1016/J.IJHYDENE.2015.03.048.
[27] D. Xing, N. Ren, M. Gong, J. Li, Q. Li, Monitoring of microbial community structure and succession in the biohydrogen production reactor by denaturing gradient gel electrophoresis (DGGE), Sci. China Ser. C. 48 (2005) 155. doi:10.1360/04yc0066.
[28] F. Silva-Illanes, E. Tapia-Venegas, M.C. Schiappacasse, E. Trably, G. Ruiz-Filippi, Impact of hydraulic retention time (HRT) and pH on dark fermentative hydrogen production from glycerol, Energy. 141 (2017) 358–367. doi:10.1016/j.energy.2017.09.073.
[29] D.R. Boone, R.W. Castenholz, G.M. Garrity, eds., Bergey's Manual® of Systematic Bacteriology, Springer New York, New York, NY, 2001. doi:10.1007/978-0-387-21609-6.
[30] T.M. Cogan, K.N. Jordan, Metabolism of Leuconostoc Bacteria, J. Dairy Sci. 77 (1994) 2704–2717. doi:10.3168/jds.S0022-0302(94)77213-1.
[31] J. Ravachol, R. Borne, I. Meynial-Salles, P. Soucaille, S. Pagès, C. Tardif, H.-P. Fierobe, Combining free and aggregated cellulolytic systems in the cellulosome-producing bacterium Ruminiclostridium cellulolyticum, Biotechnol. Biofuels. 8 (2015) 114. doi:10.1186/s13068-015-0301-4.
[32] X.Z. Zhang, N. Sathitsuksanoh, Y.H.P. Zhang, Glycoside hydrolase family 9 processive endoglucanase from Clostridium phytofermentans: Heterologous expression, characterization, and synergy with family 48 cellobiohydrolase, Bioresour. Technol. 101 (2010) 5534–5538. doi:10.1016/j.biortech.2010.01.152.
[33] F. Xin, J. He, Characterization of a thermostable xylanase from a newly isolated Kluyvera species and its application for biobutanol production, Bioresour. Technol. 135 (2013) 309–315. doi:10.1016/j.biortech.2012.10.002.
[34] W.J. Choi, M.R. Hartono, W.H. Chan, S.S. Yeo, Ethanol production from biodiesel-derived crude glycerol by newly isolated Kluyvera cryocrescens, Appl. Microbiol. Biotechnol. 89 (2011) 1255–1264. doi:10.1007/s00253-010-3076-3.
[35] H. Ohara, M. Owaki, K. Sonomoto, Xylooligosaccharide fermentation with Leuconostoc lactis, J. Biosci. Bioeng. 101 (2006) 415–420. doi:10.1263/jbb.101.415.
[36] C.A. Contreras-Dávila, V.J. Carrión, V.R. Vonk, C.N.J. Buisman, D.P.B.T.B. Strik, Consecutive lactate formation and chain elongation to reduce exogenous chemicals input in repeated-batch food waste fermentation, Water Res. 169 (2020). doi:10.1016/j.watres.2019.115215.
[37] R. Palomo-Briones, E. Razo-Flores, N. Bernet, E. Trably, Dark-fermentative biohydrogen pathways and microbial networks in continuous stirred tank reactors: Novel insights on their control, Appl. Energy. 198 (2017) 77–87. doi:10.1016/j.apenergy.2017.04.051.
[38] A. Konopka, S. Lindemann, J. Fredrickson, Dynamics in microbial communities: Unraveling mechanisms to identify principles, ISME J. 9 (2015) 1488–1495. doi:10.1038/ismej.2014.251.
[39] Y. Zhu, S.T. Yang, Effect of pH on metabolic pathway shift in fermentation of xylose by Clostridium tyrobutyricum, J. Biotechnol. 110 (2004) 143–157. doi:10.1016/j.jbiotec.2004.02.006.

[40] C. Grimmler, C. Held, W. Liebl, A. Ehrenreich, Transcriptional analysis of catabolite repression in Clostridium acetobutylicum growing on mixtures of d-glucose and d-xylose, J. Biotechnol. 150 (2010) 315–323. doi:10.1016/j.jbiotec.2010.09.938.
[41] S.D. Gomes, L.T. Fuess, T. Mañunga, P.C. Feitosa de Lima Gomes, M. Zaiat, Bacteriocins of lactic acid bacteria as a hindering factor for biohydrogen production from cassava flour wastewater in a continuous multiple tube reactor, Int. J. Hydrogen Energy. 41 (2016) 8120–8131. doi:10.1016/j.ijhydene.2015.11.186.
[42] T. Noike, H. Takabatakea, O. Mizunoc, M. Ohbab, Inhibition of hydrogen fermentation of organic wastes by lactic acid bacteria, Int. J. Hydrogen Energy. 27 (2002) 1367–1371. doi:10.1016/S0360-3199(02)00120-9.
[43] O. García-Depraect, E. León-Becerril, Fermentative biohydrogen production from tequila vinasse via the lactate-acetate pathway: Operational performance, kinetic analysis and microbial ecology, Fuel. 234 (2018) 151–160. doi:10.1016/j.fuel.2018.06.126.
[44] O. García-Depraect, R. Muñoz, E. Rodríguez, E.R. Rene, E. León-Becerril, Microbial ecology of a lactate-driven dark fermentation process producing hydrogen under carbohydrate-limiting conditions, Int. J. Hydrogen Energy. 46 (2021) 11284–11296. doi:10.1016/j.ijhydene.2020.08.209.
[45] S.-Y. Wu, C.-H. Hung, C.-Y. Lin, P.-J. Lin, K.-S. Lee, C.-N. Lin, F.-Y. Chang, J.-S. Chang, HRT-dependent hydrogen production and bacterial community structure of mixed anaerobic microflora in suspended, granular and immobilized sludge systems using glucose as the carbon substrate ARTICLE IN PRESS, (2007). doi:10.1016/j.ijhydene.2007.10.020.
[46] L. Arellano-García, J.B. Velázquez-Fernández, M. Macías-Muro, E.N. Marino-Marmolejo, Continuous hydrogen production and microbial community profile in the dark fermentation of tequila vinasse: Response to increasing loading rates and immobilization of biomass, Biochem. Eng. J. 172 (2021) 108049. doi:10.1016/j.bej.2021.108049.

Chapter 6. *How deep is our knowledge about dark fermentation?*

6.1 General discussion and conclusions

According with the revision about dark fermentation presented in Chapter 1, three main challenges in continuous suspended-biomass systems have been identified for hydrogen production: operational parameters control/optimization, mass transfer conditions and metabolic diversity. The results of the present thesis disclosed that such phenomena are considerably affected by the type and substrate concentration, biomass concentration, and H_2 mass transfer conditions (Figure 6.1).

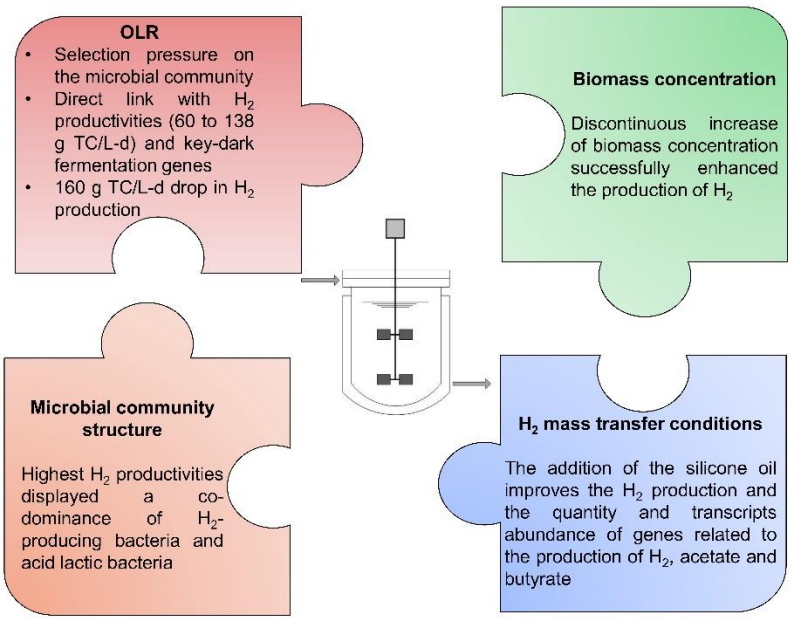

Figure 6.1 Overview of the principal results and conclusions obtained in this investigation.

One important contribution of this thesis was the finding that the OLR performs a selection pressure upon the microbial community and metabolic pathways, whether or not the system was modified by any of the improvement strategies evaluated in this thesis (Chapters 2 to 4). Overall, the Illumina sequencing analysis in systems fed with cheese whey powder (CWP) showed that an OLR $\leq$ 90 g TC/L-d, H_2-producing bacteria from the genera *Clostridium* clearly dominates the microbial community in the systems. In contrast, at the OLR $\geq$ 138 g TC/L-d lactic acid

bacteria (LAB) arose as a co-dominant genus with a maximum relative of abundance of approximately 50% (Figures 2.5, 3.4 and 4.1).

Particularly, the study of the OLR in the systems fed with CWP, showed that this parameter was directly linked to the VHPR and H_2 yield at ≤ OLR 138 g TC/L-d as shown in Chapter 4. In regard the metabolic pathways, the metatranscriptomics analysis revealed a direct relation between the abundance of transcripts of key-dark fermentation genes (e.g. *pfor*, *pfl*, *hydA*, *hycE*) and the H_2 productivities (Figure 4.8). Nevertheless, the OLR of 160 g TC/L-d promoted the drop in VHPR and H_2 yield. This drop in the H_2 productivities possibly is a consequence of a decrease of the abundance and metabolic activity of H_2-production bacteria by the accumulation of H_2, CO_2 and carboxylic acids. The inhibition of H_2-producing bacteria also could favor the abundance and metabolic activity of H_2-consuming bacteria via homoacetogenesis and LAB. This hypothesis was confirmed with the studies of community structure and metatranscriptomics (Figures 4.1 and 4.6). Taking into account such results, it was suggested that at high OLR the increase of homoacetogens and LAB abundance can be associated to three aspects: i) the inhibition of H_2-producing bacteria, that can result when there is a high rate of H_2 production and an inefficient release of H_2 from the fermentation broth to the reactor headspace. These issues lead to the accumulation of dissolved H_2, which inhibits H_2-producing bacteria and, therefore, make an opportunity for LAB to better compete for the substrate uptake, ii) the abundance of substrate, which enhances the competence of LAB and H_2-producing bacteria for substrate, and iii) the accumulation of dissolved CO_2 and H_2 in the fermentation broth, that favors the environmental conditions for the growth of homoacetogens, which consume the dissolved CO_2 and H_2 through the Wood-Ljunhdal pathway.

Interestingly, independently if the system was modified by any of the improvement strategies carried out in this investigation, in all cases when CWP was used as substrate. The maximum VHPRs were reported at the OLR 138 g TC/L-d, displaying a microbial community structure of co-dominance between H_2-producing bacteria (relative abundance between 50 and 75%) and LAB (relative abundance of 15 and 45%). At first this conclusion appears contradictory given that H_2 production is

usually associated with the *Clostridium* genus, and LAB is usually considered a substrate competitor group [1]. Under this panorama, we propose that at the OLR of 138 g TC/L-d there is no apparent inhibition by product accumulation and therefore the abundance of substrate favors the dominance of both bacteria without compromising the dark fermentation performance. An alternative explanation to the co-dominance of LAB and *Clostridium* is the possibility to produce H_2 from the lactate produced by LAB. This process is performed by lactate-fermenting, H_2-producing bacteria (LF-HPB) during a secondary acetate and lactate fermentation to produce butyrate and H_2 [2]. *Clostridium butyricum* is one of the species of *Clostridium* that have been reported as LF-HPB [3,4]. Based on the identification of such bacteria in all the OLR applied (from 60 to 160 g TC/L-d, Figure 4.1), it was hypothesized that in suspended-biomass reactors operated at low HRT (6 h) the secondary fermentation of lactate was possible, improving the production of butyrate and H_2.

Further research work revealed that the interesting dynamics between H_2-producing bacteria and LAB was controlled not only by the OLR but also by the type of substrate as demonstrated in Chapter 5. Specifically, the high-throughput sequencing analysis of the six reactors fed with different enzymatic hydrolysates of agave bagasse at OLR between 40 and 120 g COD/L-d (equivalent to 10 and 65 g TC/L-d), revealed that high-performance and medium-performance H_2-producing systems were both co-dominated by *Clostridium* and LAB (*Sporolactobacillus*) genera; the relative abundance of both genera accounted for more than 90% (Figure 5.6). Moreover, it has been also shown that relatively high VHPR values are obtained at high OLR (from 80 to 120 g COD/L-d); nevertheless, this relationship largely depends on the type and constituents of hydrolysates. We hypothesized that hydrolysates prepared with Celluclast-Viscozyme probably contained a higher proportion of easily degradable sugars which could lead to better dark fermentation performance. It is important to mention, that it was not possible to evaluate OLR greater than 120 g COD/L-d (equivalent to 65 g TC/L-d) with agave bagasse enzymatic hydrolysates, because the concentration of the hydrolysates in terms of COD and TC did not allow it.

In the light of the above results, it was stablished that proper substrate type and OLR in continuous systems is crucial for efficient dark fermentation performance. Nevertheless, the concentration of biomass is another crucial parameter that rules the dark fermentation performance. One of the limitations in the suspended-biomass systems is the difficulty to maintain high biomass concentration at low HRT (6 h) and high OLR. For this reason, the impact of biomass concentration on suspended-biomass reactor was further investigated in Chapter 2. The results demonstrated that the discontinuous increase of biomass concentration successfully enhanced the production of H_2 and carboxylic acids at OLR ranging from 90 to 160 g TC/L-d. At OLR $\leq$ 138 g TC/L-d the VHPR was directly linked with the OLR and biomass concentration. In contrast, at OLR of 160 g TC/L-d a decline in VHPR, H_2 yield and biomass concentration was observed. Interestingly, on such OLR with the discontinuous biomass increase strategy, it was possible to reach VHPR of 17 L H_2/L-d with a controlled biomass concentration of 11 g VSS/L. Despite the positive effect of increasing and controlling the biomass concentration in suspended-biomass reactors, it was proposed that the increase of the VHPR produced an increment of the concentration of dissolved H_2 and CO_2 that might have undesirable consequences on the H_2 productivities, boosting the homoacetogenesis and lactic acid production pathways.

In alignment with these ideas, the impacts of the H_2 mass transfer rate on dark fermentation performance, metabolic pathways and microbial community structure were further investigated in chapters 3 and 4. For such attempt, two-phase partitioning reactors using silicone oil as an organic extractive phase, were assessed with the objective to reduce the concentration of H_2 and CO_2 in the fermentation broth. The results demonstrated that the addition of the silicone oil improves the H_2 and carboxylic acids productivity at OLR (from 60 to 160 g TC/L-d). It was hypothesized, that the extractive phase increases the global mass transfer area in the reactor, causing a dramatic reduction in the concentration of H_2 and CO_2 in the fermentation broth, enhancing the metabolic pathways with highest dark fermentation performance. The metatranscriptomics analysis confirms that the addition of silicone oil at both OLR of 138 and 160 g TC/L-d improves the quantity

and transcripts abundance of genes related to the production of H_2, acetate and butyrate as shown in Chapter 4.

Beyond the impacts of type and substrate inlet concentration, biomass concentration, and H_2 mass transfer conditions on dark fermentation performance, the present thesis approached the emergent concern to study dark fermentation at a much deeper level through the use of omics sciences (i.e. metatranscriptomics, metaproteomics, metabolomics, among others). Overall, the combination of experimental results (e.g. VHPR, carboxylic acids production, biomass concentration) with advanced molecular tools (e.g. qPCR and metatranscriptomics) is an excellent approach for obtaining solid and deeper conclusions about the microbial community structure and function from dark fermentation systems. As demonstrated in Chapter 4, the effect of the OLR and the addition of silicone oil can be correlated to a modification in the VHPR, carboxylic acids production, abundance of H_2-producing bacteria and H_2-consuming bacteria (measured by the *hydA* and *fthfs* gene through PCR, respectively), and abundance of transcripts of the genes related to H_2 production (e.g. *pfor, pfl, hydA, fdh*), lactate production and consumption (e.g. *ldh*) and homoacetogenesis (e.g. *fthfs*). Notwithstanding that metatranscriptomics is not a precise estimation of metabolic activity, it is a closer approximation of metabolism than 16S rRNA genome-based predictions that have been reported previously for dark fermentation investigations.

The consumption of H_2 and CO_2 via homoacetogenesis have been reported experimentally and theoretically in dark fermentation systems [1,5,6]. On one hand, the experimental data that estimates the homoacetogenesis pathway is very limited and do not replicate the hydraulic regimes of dark fermentation continuous systems. On the other hand, the theoretical homoacetogenesis estimation by the mass balance described by Arooj et al. [7], consider that H_2 is only produced through the acetate and butyrate pathways, nevertheless, do not contemplate the production of H_2 via the lactate-acetate pathway and via oxidation of NADH. Also, such theoretical estimation does not contemplate the production of other compounds (e.g. ethanol) aside of acetate in the homoacetogenesis pathway. Therefore, the evaluation of homoacetogenesis by the metatranscriptomics analysis is another important

contribution of this thesis. In general, the metatranscriptomics analysis (Chapter 4) reveals that the genes that carried out the homoacetogenesis pathway are active in all the OLRs evaluated and in all the stages with and without silicone oil as an extractive organic phase. In particular, the metatranscriptomics uncovers the direct relationship between the OLR and the abundance of homoacetogenesis genes. This results evidence that homoacetogenesis is a concomitant phenomenon on H_2 production in suspended-biomass reactors.

6.2 Perspectives

Traditionally, the research of dark fermentation has concentrated on the study and optimization of operational parameters (pH, temperature, OLR, type of substrate) to enhance the H_2 productivities in terms of VHPR and H_2 yield. For example, it has been demonstrated that H_2 production in suspended-biomass reactors at HRT of 6 h, 37 ºC and 300 rpm achieves VHPR of 26 L H_2/L-d with model substrates (e.g. cheese whey powder) [8,9]. The use of non-model substrates (e.g. lignocellulosic residues) in dark fermentation process has been extensively studied in recent years. In our research group a positive relationship between carbohydrates/COD loading rate and VHPR was observed in CSTR systems using agave bagasse hydrolysates prepared with commercial enzymes without a previous step of pretreatment of the agave bagasse (chapter 5). However, with this strategy it has not been possible to evaluate OLRs higher than 120 g COD/L-d. For the above reason, it is necessary to further pretreat the agave bagasse in order to increase the concentration of carbohydrates/COD released in a subsequent enzymatic hydrolysis, and therefore assess OLR beyond 120 g COD/L-d. The use of ionic liquids as pretreatment stands out as a worthy option. Previous studies have evaluated the enzymatic saccharification of agave bagasse pretreated with different ionic liquids. These investigations have reported an increase in total carbohydrates up to 6.3 times compared to the substrate without pretreatment [10].

In recent years, a second wave of investigation dedicated to the study of microbial communities with the objective to dilucidate more information about the dark fermentation. Overall such investigations, showed that the diversity and structure of

the microbial community plays a crucial role in the dark fermentation performance [11]. In particular, the use of high-throughput technologies (e.g. 16S rRNA sequencing) allowed to describe the microbial community assembly at a very good definition [12]. Nevertheless, to elucidate the dark fermentation pathway it is necessary to include of the omics sciences to the analysis (e.g. proteomics, transcriptomics, metabolomics, metagenomics), in combination with the high-throughput technologies and microorganisms quantification techniques (e.g. qPCR, flow cytometry). To the best of my knowledge, omics sciences such as proteomics and metabolomics is an unexplored field in dark fermentation; whereas, transcriptomics and metagenomics has been poorly investigated.

Studies with the objective to enhance the VHPR and H_2 yield also have been carried out in the recent years. The increase of biomass concentration (Chapter 2) and the use of two-phase partitioning reactors (Chapters 3 and 4) were strategies evaluated in this thesis that successfully increased H_2 productivities in continuous suspended-biomass reactors. Other strategies such as, gas sparging, modification of stirring speed, bioaugmentation, biomass immobilization, have been successfully implemented to enhance the production of H_2 [13–16]. However, all these strategies focused to enhance the production of H_2 leaving in second place the production of value-added short-carboxylic carboxylic acids such as lactate, acetate, butyrate, and even the production of medium-chain carboxylic acids (e.g. valerate, caproate) in a secondary fermentation. The stimulation/presence of homoacetogens at high OLR ($\geq$ 138 g TC/L-d) was one of the main results obtained in this investigation (chapter 4). Nevertheless, the use of biomass with high abundance and activity of homoacetogens for syngas fermentation has been poorly studied. The syngas is a mixture of CO, CO_2 and H_2 that can be used as a feedstock to produce chemicals. In syngas fermentation, microorganisms catalyze the syngas to a wide range of carboxylic acids and alcohols. Ethanol and acetate are the easiest compound to produce. Nonetheless, upgrading such biomass it is possible to produce longer-chain acids (e.g. butyrate, valerate, caproate) by the chain-elongation of the acetate and ethanol produced from the fermentation of syngas. Therefore, a foreseen way forward in the field is the development of a sequential system for the production of

H_2, short-chain carboxylic and medium-chain carboxylic acids. The implementation of this system consists of two continuous reactors. In the first reactor, the dark fermentation process will be carried out with the production of H_2, CO_2, and short-chain carboxylic acids at OLRs where homoacetogenic bacteria are naturally present. In the second reactor, the syngas fermentation will be performed using the H_2 and CO_2 produced in the first reactor and the selected and enriched autotrophic biomass from the first reactor as a source of inoculum. This second reactor is expected to produce acetate and ethanol without the fed of an organic substrate, as well as butyrate, valerate, caproate by the chain-elongation process.

Derived from the observations of this thesis that the highest VHPR presents a microbial structure co-dominated between H_2-producing bacteria and LAB, and considering the results previously reported in the literature [2,4], it is hypothesized that the lactic acid produced by LAB can be used by *Clostridium* species for the production of butyrate and H_2 in suspended-biomass reactors operated at low HRT (6 h). In fact, this phenomenon has been recently reported and documented in batch dark fermentative reactors. However, the study of lactate to enhance the production of H_2 in continuous reactors has been barely studied. Hence, the operation of continuous suspended-biomass reactors using lactate as a substrate, alone and/or in combination with an organic substrate (e.g. cheese whey powder, enzymatic hydrolysates), could be one strategy to study the effect of lactate in dark fermentation systems.

6.3 References

[1] E. Castelló, A.D. Nunes Ferraz-Junior, C. Andreani, M. del P. Anzola-Rojas, L. Borzacconi, G. Buitrón, J. Carrillo-Reyes, S.D. Gomes, S.I. Maintinguer, I. Moreno-Andrade, R. Palomo-Briones, E. Razo-Flores, M. Schiappacasse-Dasati, E. Tapia-Venegas, I. Valdez-Vázquez, A. Vesga-Baron, M. Zaiat, C. Etchebehere, Stability problems in the hydrogen production by dark fermentation: Possible causes and solutions, Renew. Sustain. Energy Rev. 119 (2019). doi:10.1016/j.rser.2019.109602.

[2] O. García-Depraect, E. León-Becerril, Fermentative biohydrogen production from tequila vinasse via the lactate-acetate pathway: Operational performance, kinetic analysis and microbial ecology, Fuel. 234 (2018) 151–160. doi:10.1016/j.fuel.2018.06.126.

[3] O. García-Depraect, R. Muñoz, E. Rodríguez, E.R. Rene, E. León-Becerril, Microbial ecology of a lactate-driven dark fermentation process producing hydrogen under

carbohydrate-limiting conditions, Int. J. Hydrogen Energy. 46 (2021) 11284–11296. doi:10.1016/j.ijhydene.2020.08.209.
[4] O. García-Depraect, R. Castro-Muñoz, R. Muñoz, E.R. Rene, E. León-Becerril, I. Valdez-Vazquez, G. Kumar, L.C. Reyes-Alvarado, L.J. Martínez-Mendoza, J. Carrillo-Reyes, G. Buitrón, A review on the factors influencing biohydrogen production from lactate: the key to unlocking enhanced dark fermentative processes, Bioresour. Technol. 324 (2020) 124595. doi:10.1016/j.biortech.2020.124595.
[5] G. Henderson, S.C. Leahy, P.H. Janssen, Presence of novel, potentially homoacetogenic bacteria in the rumen as determined by analysis of formyltetrahydrofolate synthetase sequences from ruminants, Appl. Environ. Microbiol. 76 (2010) 2058–2066. doi:10.1128/AEM.02580-09.
[6] L. Fuentes, R. Palomo-Briones, J. de Jesús Montoya-Rosales, L. Braga, E. Castelló, A. Vesga, E. Tapia-Venegas, E. Razo-Flores, C. Ecthebehere, Knowing the enemy: homoacetogens in hydrogen production reactors, Appl. Microbiol. Biotechnol. (2021). doi:10.1007/s00253-021-11656-6.
[7] M. Arooj, S. Han, S. Kim, D. Kim, H. Shin, Continuous biohydrogen production in a CSTR using starch as a substrate, Int. J. Hydrogen Energy. 33 (2008) 3289–3294. doi:10.1016/j.ijhydene.2008.04.022.
[8] G. Davila-Vazquez, C.B. Cota-Navarro, L.M. Rosales-Colunga, A. de León-Rodríguez, E. Razo-Flores, Continuous biohydrogen production using cheese whey: Improving the hydrogen production rate, Int. J. Hydrogen Energy. 34 (2009) 4296–4304. doi:10.1016/j.ijhydene.2009.02.063.
[9] C.B. Cota-Navarro, J. Carrillo-Reyes, G. Davila-Vazquez, F. Alatriste-Mondragón, E. Razo-Flores, Continuous hydrogen and methane production in a two-stage cheese whey fermentation system, Water Sci. Technol. 64 (2011) 367–374. doi:10.2166/wst.2011.631.
[10] J.A. Pérez-Pimienta, J.P.A. Icaza-Herrera, H.O. Méndez-Acosta, V. González-Álvarez, J.A. Méndoza-Pérez, J. Arreola-Vargas, Bioderived ionic liquid-based pretreatment enhances methane production from: Agave tequilana bagasse, RSC Adv. 10 (2020) 14025–14032. doi:10.1039/d0ra01849j.
[11] C. Etchebehere, E. Castelló, J. Wenzel, M. del Pilar Anzola-Rojas, L. Borzacconi, G. Buitrón, L. Cabrol, V.M. Carminato, J. Carrillo-Reyes, C. Cisneros-Pérez, L. Fuentes, I. Moreno-Andrade, E. Razo-Flores, G.R. Filippi, E. Tapia-Venegas, J. Toledo-Alarcón, M. Zaiat, Microbial communities from 20 different hydrogen-producing reactors studied by 454 pyrosequencing, Appl. Microbiol. Biotechnol. 100 (2016) 3371–3384. doi:10.1007/s00253-016-7325-y.
[12] A. Cabezas, J.C. de Araujo, C. Callejas, A. Galès, J. Hamelin, A. Marone, D.Z. Sousa, E. Trably, C. Etchebehere, How to use molecular biology tools for the study of the anaerobic digestion process?, Rev. Environ. Sci. Bio/Technology. 14 (2015) 555–593. doi:10.1007/s11157-015-9380-8.
[13] G. Dreschke, S. Papirio, G. d'Ippolito, A. Panico, P.N.L. Lens, G. Esposito, A. Fontana, H2-rich biogas recirculation prevents hydrogen supersaturation and enhances hydrogen production by Thermotoga neapolitana cf. capnolactica, Int. J. Hydrogen Energy. 44 (2019) 19698–19708. doi:10.1016/j.ijhydene.2019.06.022.
[14] R. Palomo-Briones, J. de J. Montoya-Rosales, E. Razo-Flores, Advances towards the understanding of microbial communities in dark fermentation of enzymatic hydrolysates: Diversity, structure and hydrogen production performance, Int. J. Hydrogen Energy. 46 (2021) 27459–27472. doi:10.1016/j.ijhydene.2021.06.016.
[15] P. Sivagurunathan, G. Kumar, P. Bakonyi, S.H. Kim, T. Kobayashi, K.Q. Xu, G. Lakner, G. Tóth, N. Nemestóthy, K. Bélafi-Bakó, A critical review on issues and overcoming strategies for the enhancement of dark fermentative hydrogen production

in continuous systems, Int. J. Hydrogen Energy. 41 (2016) 3820–3836. doi:10.1016/j.ijhydene.2015.12.081.
[16] A. Marone, G. Massini, C. Patriarca, A. Signorini, C. Varrone, G. Izzo, Hydrogen production from vegetable waste by bioaugmentation of indigenous fermentative communities, Int. J. Hydrogen Energy. 37 (2012) 5612–5622. doi:10.1016/j.ijhydene.2011.12.159.

About the Author

José de Jesús Montoya Rosales (Atolinga, Zacatecas, 1993) received his bachelor degree in Environmental Engineering from The Unidad Profesional Interdisciplinaria de Ingeniería Campus Zacatecas – Instituto Politécnico Nacional in 2016, with the thesis: "Biogas production in a continuous biorreactor with pretreated bean Straw with the fungus *pleurotus ostreatus".* With such thesis he won the first place in the national contest clean energies bachelor's level in the "26th National Thesis Competitions 2015-2017" granted by the Secretaría de Energía (Energy department of México). From January to February of 2016, he carried out an academic stay at The University of Queensland, Australia, in The School of Civil Engineering under the supervision of Dr. Denys Villa Gómez.

His Master of Science degree in Environmental Sciences was granted in 2018 from the Instituto Potosino de Investigación Científica y Tecnológica A.C.(IPICYT) with the thesis "Hydrogen production in a percolator filter reactor: Evaluation of agave bagasse hydrolysates obtained with commercial enzymes". In August of 2018, he started his doctoral studies on the theme "Study of critical factors in dark fermentation to increase hydrogen production in continuous reactors". The M.Sc. and Ph.D. studies were done under the supervision of Dr. Elías Razo Flores.

Scientific articles

Published

- José de Jesús Montoya-Rosales, Rodolfo Palomo-Briones, Lourdes B. Celis, Claudia Etchebehere, Luis F. Cházaro-Ruiz, Vladimir Escobar-Barrios, Elías Razo-Flores. 2022. **Coping with thermodynamic inhibition in dark fermentation using a two-phase partitioning bioreactor**. Chemical Engineering Journal. 445, 136749 (IF=16.744).

- Laura Fuentes, Rodolfo Palomo-Briones, José de Jesús Montoya-Rosales, Lucía Braga, Elena Castelló, Alejandra Vesga, Estela Tapia-Venegas, Elías Razo-Flores, Claudia Ecthebehere. 2021. **Knowing the enemy: homoacetogens in hydrogen production reactors**. Applied Microbiology and Biotechnology. 105, 8989–9002 (IF=5.560).

- Casandra Valencia-Ojeda, José de Jesús Montoya-Rosales, Rodolfo Palomo-Briones, Virginia Montiel-Corona, Lourdes B. Celis, Elías Razo-Flores, 2021. **Saccharification of agave bagasse with Cellulase 50 XL is an effective alternative to highly specialized lignocellulosic enzymes for continuous hydrogen production**. Journal of Environmental Chemical Engineering. 9 (4), 105448. (IF=7.968)

- Rodolfo Palomo-Briones, José de Jesús Montoya-Rosales, Elías Razo-Flores, 2021. **Advances towards the understanding of microbial communities in dark fermentation of enzymatic hydrolysates: Diversity, structure and hydrogen production performance**. International Journal of Hydrogen Energy. 46 (54), 27459-27472. (IF=7.139)

- José de Jesús Montoya-Rosales, Rodolfo Palomo-Briones, Lourdes B. Celis, Claudia Etchebehere, Elías Razo-Flores, 2020. **Discontinuous biomass recycling as a successful strategy to enhance continuous hydrogen production at high organic loading rates.** International Journal of Hydrogen Energy. 45 (35), 17260-17269. (IF=7.139)

- J.J. Montoya-Rosales, M. Peces L.M. González-Rodríguez, F. Alatriste-Mondragón, D. K. Villa-Gómez, 2020. **A broad overview comparing a fungal, thermal and acid pre-treatment of bean straw in terms of substrate and anaerobic digestion effect**. Biomass and Bioenergy journal. 142, 105775. (IF=5.774)

- Montoya-Rosales, J. de J., Olmos-Hernández, D.K., Palomo-Briones, R., Montiel-Corona, V., Mari, A.G., Razo-Flores, E., 2019. **Improvement of continuous hydrogen production using individual and binary enzymatic hydrolysates of agave bagasse in suspended-culture and biofilm reactors**. Bioresour. Technol. 283, 251–260. (IF=11.889).

- Villa-Gomez, D.K., Becerra-Castañeda, P., Montoya-Rosales, J de J., González-Rodríguez, L.M., 2019. **Anaerobic digestion of bean straw applying a fungal pre-treatment and using cow manure as co substrate.** Environmental Technology. 41 (22), 2863-2874 (IF=3.247)

In preparation

- José de Jesús Montoya-Rosales et al. 2022. **Microbial community structure and function in two-phase partitioning dark fermentation reactors at high organic loading rate**. *Environmental Science and Technology.* In preparation

Popular scientific articles

- José de Jesús Montoya-Rosales, Elías Razo-Flores, 2022. **Let´s make a cake from garbage: The dark fermentation process to produce hydrogen.** Frontiers for young minds. Accepted for publication.